West Central Kansas GMD1 Model

Kansas Water Office Contract 14-116

Funded by the

Kansas Water Office (Kansas Water Plan)

and

Western Kansas Groundwater Management District # 1

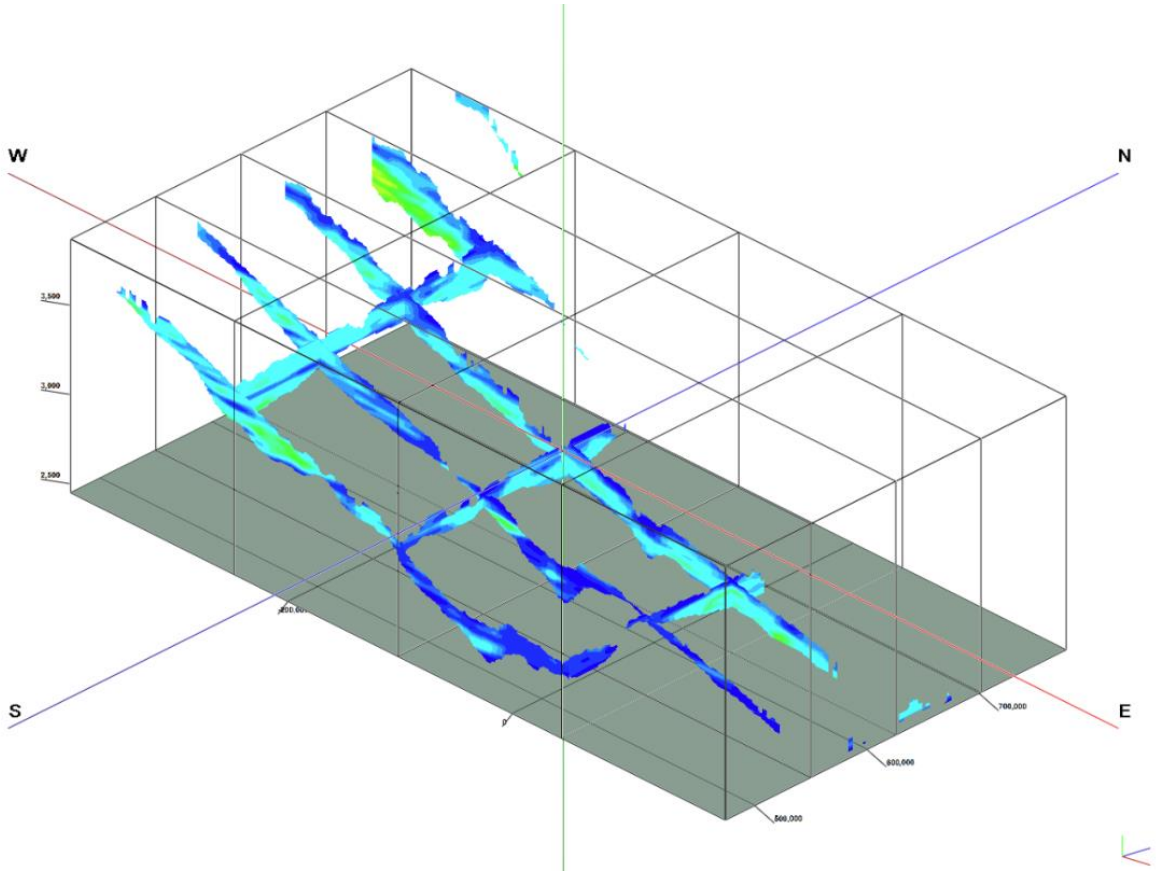

Brownie Wilson, Gaisheng Liu, Geoff Bohling, Donald Whittemore, and James Butler, Jr.

Kansas Geological Survey Open File Report 2015-33

GEOHYDROLOGY

KANSAS GEOLOGICAL SURVEY
The University of Kansas

West Central Kansas GMD1 Model

Kansas Water Office Contract 14-116

This project was funded by the

Kansas Water Office (Kansas Water Plan)
and
Western Kansas Groundwater Management District # 1

Kansas Geological Survey Open File Report 2015-33

Kansas Geological Survey, Geohydrology Section
University of Kansas, 1930 Constant Avenue,
Lawrence, KS 66047
http://www.kgs.ku.edu/

Disclaimer

The Kansas Geological Survey does not guarantee this document to be free from errors or inaccuracies and disclaims any responsibility of liability for interpretations based on data used in the production of this document or decisions based thereon.

TABLE OF CONTENTS

INTRODUCTION

Western Kansas Groundwater Management District No. 1 (GMD1) was formally established in 1973 and was the first of five such local management districts in Kansas authorized under the Groundwater Management District Act of 1972. Overlying portions of five counties in west-central Kansas, GMD1's official purpose is to promote the better use of groundwater, collect and disseminate research information, and work congruently for better water management.

GMD1 was one of the first areas developed for groundwater in Kansas with the first irrigation well being drilled in 1907. As such, it has one of the largest densities of vested water rights, those that precede the 1945 Kansas Water Appropriation Act, in the state. The Ogallala portion of the High Plains aquifer (HPA) is the primary water source for virtually all water uses. Like much of western Kansas, GMD1 has experienced declining water tables and reductions in historically limited streamflows. Today, most of the district contains fewer than 40 ft of saturated thickness. However, there are two areas where the thickness of the Ogallala is at or more than 100 ft. One area is in the southern portion of Wallace County, and the other is in a north-south trending trough in Scott County.

Project Objective

The Kansas Water Office (KWO) and GMD1 contracted with the Kansas Geological Survey (KGS) in January of 2013 to develop a numerical groundwater model for the GMD1 area. The primary objective of the model is to better understand the hydrologic system and water table changes occurring in the underlying HPA. The model will be used to simulate future water use and management scenarios to estimate their effects on the HPA in this region.

The project period covered January 2013 through the summer of 2015. The calibrated transient model was completed in July 2015. This final report was completed in August 2015.

Model Oversight

As part of the model development process, GMD1 formed a Model Advisory Committee (MAC) to oversee the initial phases of the project. The MAC met approximately three times a year in Scott City, and the meetings included conference calls and Internet-based PowerPoint presentations viewed by all individuals invited to the meeting. Members of the MAC included staff from the KWO, the Topeka/Manhattan headquarters and Garden City field office of the Kansas Department of Agriculture, Division of Water Resources (KDA-DWR), GMD1 manager and board members, and several individual members of the district representing irrigation and municipal water supply interests. During the model's development, several agencies had key staffing changes, specifically the GMD1 manager and KWO's primary point of contact for the project.

The KGS presented updates throughout the model's creation at various county-based meetings, GMD1's annual meetings, the Governor's 50 Year Water Vision meetings, and regular GMD1 board meetings. The KGS made the final model available for review to the KDA-DWR.

DESCRIPTION OF STUDY AREA AND GENERAL MODEL SETUP

The study area includes the area of GMD1 in west-central Kansas and extends roughly six miles beyond the extent of the district in all directions (fig. 1). The total area covered by the model is a little over 6,438 square miles and includes a portion of eastern Colorado. Groundwater-based irrigation is the primary use of water, although the HPA is also the source of municipal water supplies for the county seats of Sharon Springs, Tribune, Leoti, Scott City, and Dighton. The entire GMD1 boundary and the majority of the active area of the model lie within the newly designated Upper Smoky Hill Regional Planning Area for the Kansas Water Authority and Kansas Water Plan.

Previous Geohydrologic Studies

Several KGS bulletins report on the geology and groundwater resources of the model area. McLaughlin (1943) for Hamilton and Kearny counties, Latta (1944) for Finney and Gray counties, and Waite (1947) for Scott County all contain information concerning predevelopment conditions, those before widespread groundwater development occurred. Later bulletins provide additional early time period data and descriptions of the HPA in Prescott (1951) for Lane County, Prescott et al. (1954) for Wichita and Greeley counties, and Hodson (1963) for Wallace County. Finally, Krieger (1957) included parts of counties along Ladder Creek in northern sections of the model area. All of these publications provided well records and lithologic logs used to construct and calibrate the model.

The U.S. Geological Survey (USGS) report by Boettcher (1964) provides information about the geology and groundwater resources of eastern Cheyenne and Kiowa counties in the Colorado portion of the HPA in the model area. Other publications that cover regional aspects of the geohydrology of the model area include Gutentag et al. (1984).

Although a past study by the USGS (Luckey et al., 1986) involved simulating groundwater flow across the whole HPA in the United States, the cell size used was 10 mi on a side (100 mi^2), which is much too coarse to be of value for simulating future water use and management scenarios on the GMD1 scale. No previous numerical modeling projects have been conducted specifically over the GMD1 area.

Physiographic Setting

The vast majority of the active area of the model lies within the High Plains physiographic region. Much of the High Plains region is characterized by flat to gently rolling, eastward sloping uplands. Shallow depressions/playas are common features. Ladder and Whitewoman creeks are the principal drainage paths, both containing relatively small but pronounced valleys. Portions of southern Gove, northeast Finney, and northernmost Lane and southern Ness counties in the model domain are in the Smoky Hills region where the HPA has been eroded away, often exposing the underlying chalk formations, which provide abrupt and scenic valleys.

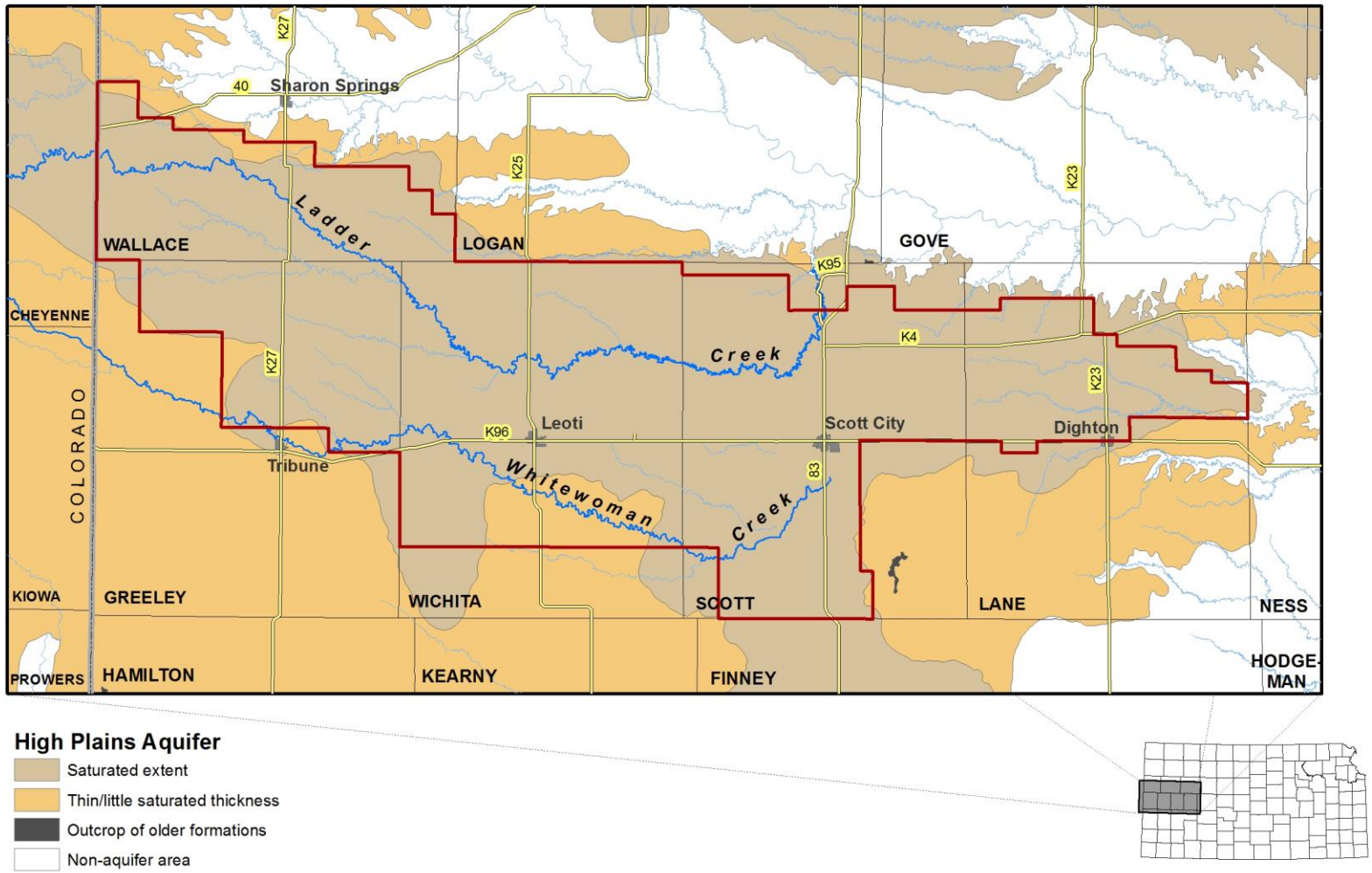

Figure 1. Map of GMD1 model area in Kansas and Colorado. The red line indicates the district boundaries of GMD1.

Model Design

This project used MODFLOW-NWT, modeling software developed by the USGS that is based on a finite-difference approximation of the flow equation (Harbaugh et al., 2000; Niswonger et al., 2011). MODFLOW is one of the most widely used groundwater flow models in the world. It can be used to simulate the effects of many processes, such as areal recharge, stream-aquifer interactions, drains, evapotranspiration, and pumping. MODFLOW-NWT is a special formulation of MODFLOW that was developed to more accurately represent drying and rewetting of unconfined aquifers, which is particularly suitable for the simulated conditions in GMD1.

Input files for the MODFLOW-NWT model were created with assistance from scripts written in Matlab (http://www.mathworks.com/). The model was run by entering the executable file in a Matlab command window. Model simulation results were processed by Matlab scripts and then imported into Excel and GIS software to produce various graphs.

The model uses uniform and equally spaced square cells, 0.5 x 0.5 miles in size (0.25 mi^2). There are 116 rows and 222 columns resulting in 25,752 individual model grid cells (fig. 2). The grid was designed to perfectly align with model cells used in the Modflow-based groundwater flow model for GMD3 in southwest Kansas, developed by the KGS in 2010 (Liu et al., 2010). The GMD1 model uses one convertible layer that allows both confined and unconfined properties of the aquifer to be simulated, depending on water levels. The streamflow-routing package (SFR in MODFLOW) was used to compute stream-aquifer interactions (Prudic et al., 2004) by subdividing streams into a series of segments and reaches.

Time-varying specified-head boundaries are located along the edges of the model where the HPA is present (fig. 2). The head values for these boundaries are determined by a spatial and temporal interpolation of the water-level observations from nearby wells. Drain cells are specified for the small tributary creeks, into which groundwater might discharge especially during the early period (1940s to 1950s). Water in these creeks typically flows out of the active model area. For the drain cells, water from the aquifer can discharge to the surface depending on water-table elevations. If the water levels drop below the land surface, this connection is broken and the drains become inactive (e.g., a spring becomes dry after the water table falls below the spring bed). The lower boundary of the model is the top of the Permian and Cretaceous bedrock (mainly shale) that has much lower permeability than the HPA and is treated as a no-flow boundary. The upper boundary of the model is specified as the land surface where water may enter or leave the aquifer through areal recharge, evapotranspiration, and stream-aquifer interactions.

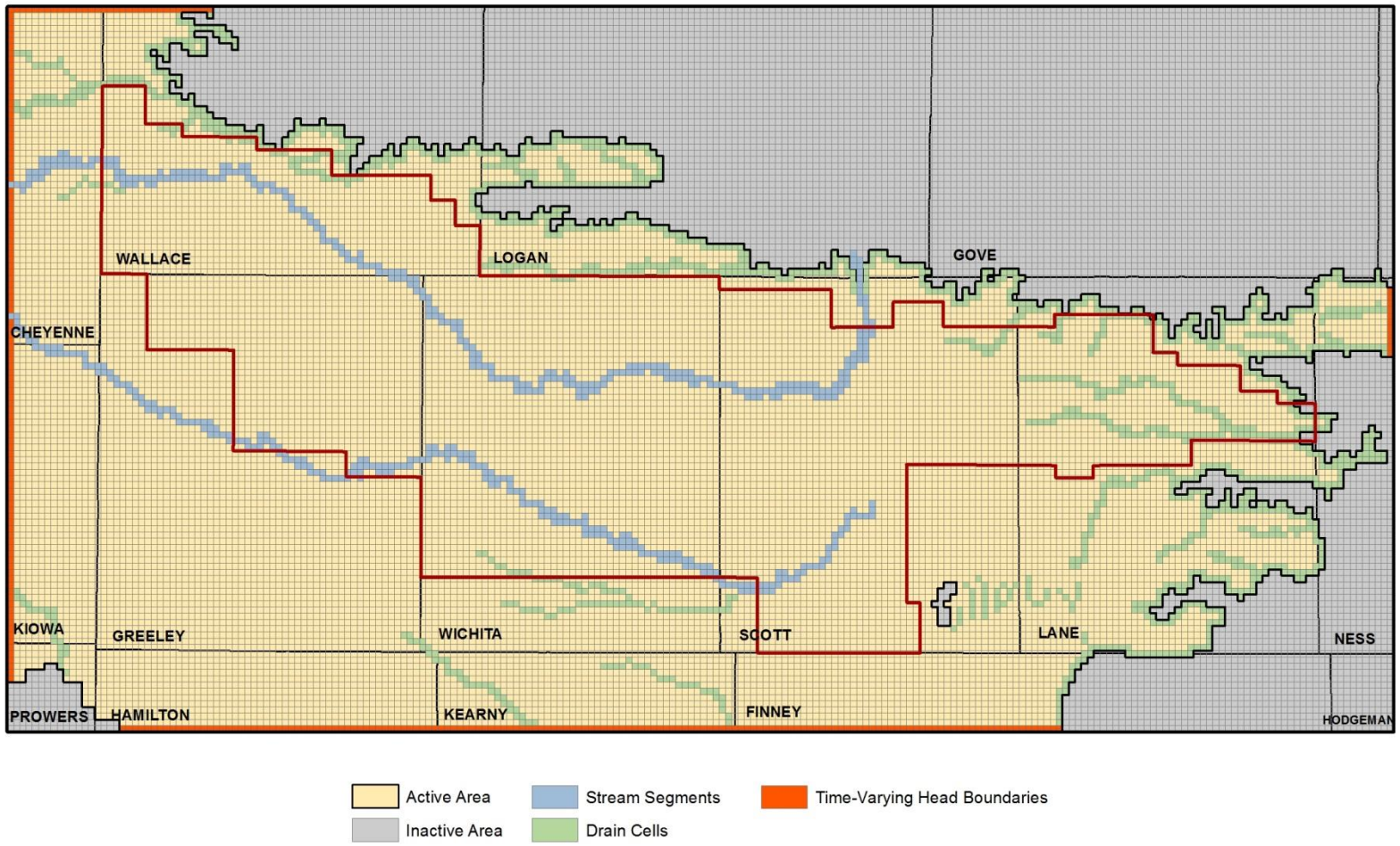

Figure 2. Model boundaries, grid cells, active area, and special model cells.

The modeling work was divided into two major steps. First, a steady-state simulation was generated for the predevelopment period before 1947. Data used for predevelopment simulation were typically from 1944–1946, during which large-scale, intensive pumping activities were not present over most of GMD1 (in certain cases additional data representing the early 1950s were also used to fill in spatial data gaps). Second, a transient simulation was conducted for the period between 1947 and 2014 to replicate the historic evolution of the groundwater system and stream-aquifer interactions. The predevelopment step established the initial conditions for the subsequent transient simulation.

The model takes advantage of detailed information from the KGS HyDRA program, in which thousands of lithologic logs have been collected and their entries transcribed and categorized into common groups. Based on the lithologic categorizations, three-dimensional grids of hydraulic conductivity and specific yield were developed. In each time step, the model's vertically averaged hydraulic conductivity and specific yield values are dynamically assigned depending on where water-table elevations occur within the three-dimensional grid. More than 2,700 lithologic logs were used in this process.

The model was calibrated to match predevelopment water-levels and long-term hydrographs of selected wells, especially the water-level change over time. Low flow conditions in Ladder and Whitewoman creeks (average flows between January and March, during which surface runoff contributions are typically a small component of the total streamflow) were also used to assist in the calibration process. The recharge-precipitation relationship, the delay characteristics between water infiltrating below the land surface and reaching the water table, the lagged release of water storage from dewatered sediments, hydraulic conductivity, and specific yield are all treated as calibration parameters due to their relatively large uncertainties and high impacts on model results.

Active and Inactive Areas

Most groundwater models of this type include "active" and "inactive" areas. The actual groundwater flow calculations are only conducted within the active cells. In this study, the extent of the HPA in and around GMD1 represents the active area. "Inactive" cells are those where the HPA is not present, that are disconnected from the GMD1 area (such as the northern extents of Logan and Gove counties), or that have a substantial area of bedrock outcroppings such as occurs in northeast Prowers County, Colorado. The number of active cells in the model is 17,177, giving a total active model area of 4,294 square miles, a little over 66% of the model domain (fig. 2).

REVIEW AND SETUP OF DATA PARAMETERS

Land Use/Land Cover

The USGS's 2011 National Land Cover Database shows that cropland is the primary land-cover type over the model area and even more so within the active area of the model (fig. 3). Grassland, the next most common cover classification, is most prevalent along Ladder and Whitewoman creeks and virtually the entire northern and eastern border of the model's active area.

Precipitation and Temperature Data

Monthly precipitation and temperature data were downloaded from the PRISM Climate Group at Oregon State University (http://prism.oregonstate.edu) in April 2013. PRISM provides raster-based grids (roughly 4 x 4 km) for the entire continental United States, and the data compare very favorably with similar precipitation-based data processing undertaken in past KGS activities (Wilson and Bohling, 2003; Wilson et al., 2008; and Liu et al., 2010).

The monthly PRISM grids for each year from 1944 to 2013 were processed to compute the annual average, minimum, and maximum precipitation and temperature for each year along with averages for the "summer" period (April to September) and the "winter" period (October to March). The "summer" and "winter" periods represent the irrigation and non-irrigation seasons, respectively. The output for each of these processing steps was a new raster-based grid, which was then overlain on the model area and the values assigned to each of the model cell centers.

The average annual precipitation over the model area from 1944 to 2013 is 18.52 inches with the majority of that falling during the months of April to September (fig. 4). The highest precipitation year was 1951 followed closely by 1993, with 26.21 and 25.69 inches, respectively, and the lowest year of precipitation was 1956 during the drought of the 1950s with only 8.8 inches. The maximum average winter temperature fluctuates around 53 degrees F with the lowest maximum temperatures occurring in 1993. These two climatic parameters are used to estimate historic and future groundwater pumping, described in later sections of this report.

Spatial patterns in the normal precipitation (average precipitation over the period of the last full three decades, 1981 to 2010) computed from the PRISM monthly data are similar to those at the state-wide level (fig. 5). Typically, the area has a pronounced west-to-east gradient with precipitation levels lower along the western and southwestern edges of the model area and increasing eastward to their maximum levels, reflective of the pattern across the state.

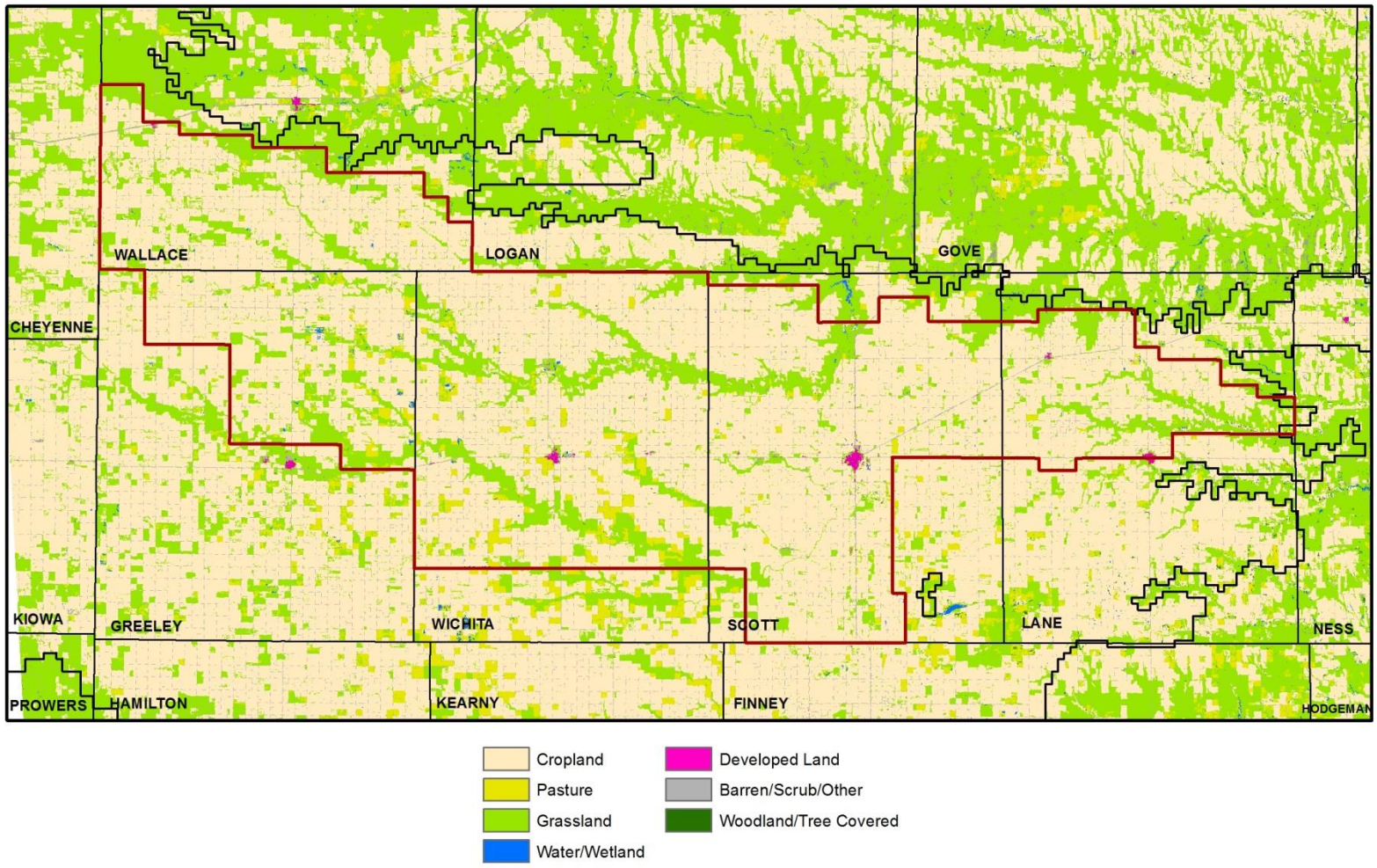

Figure 3. Land use/land cover classifications in the model area, 2011. The black line represents the active area of the model.

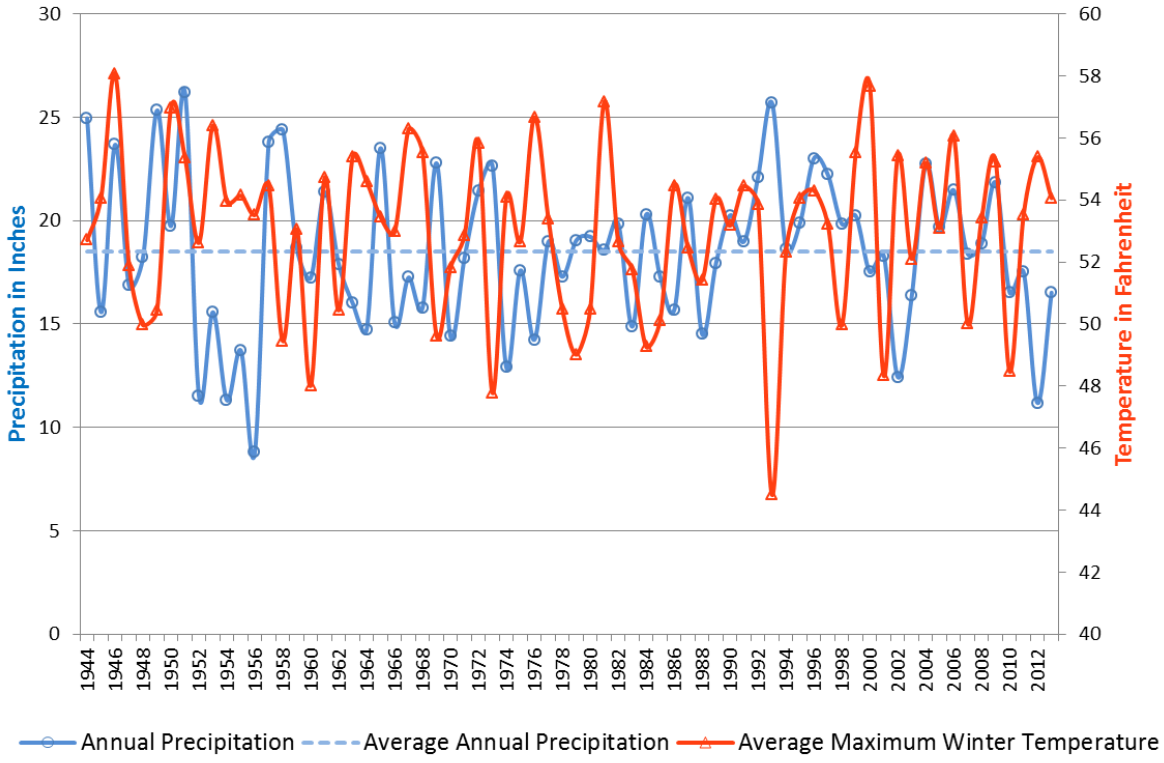

Figure 4. Average annual precipitation and average maximum "winter" temperature.

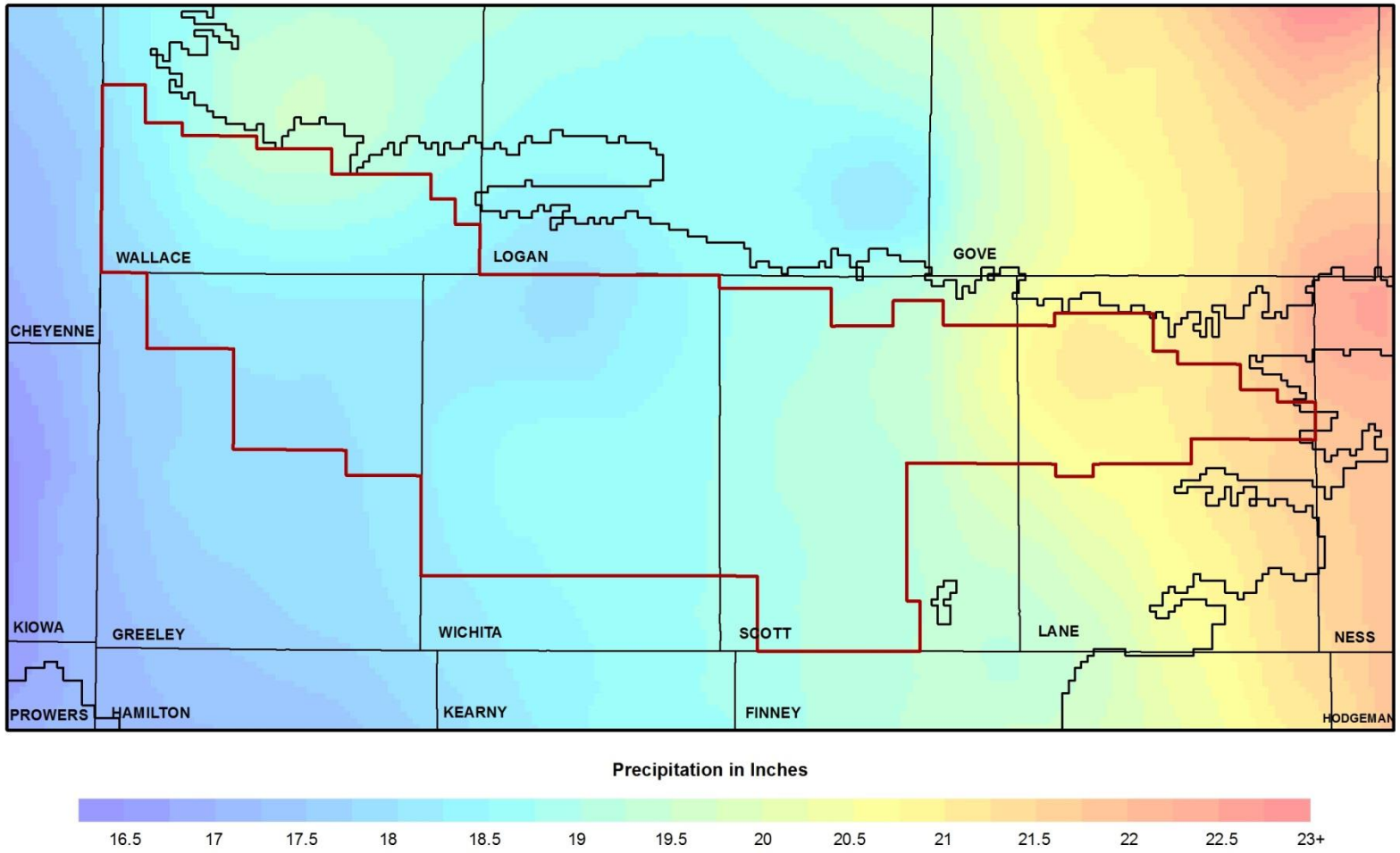

Figure 5. Computed PRISM Normal Precipitation (average for 1981 to 2010) by model cell.

Geology and Lithology

Geologic formations at or near the surface across the model area are sedimentary in nature and typically range in age from Late Cretaceous to recent. The oldest of these exposed at the surface is the Carlile Shale overlain by the Fort Hays Limestone Member of the Niobrara Chalk, generally found in western portions of Ness County and southern Gove County. Moving westward, the area becomes overlain by unconsolidated sediments primarily from the Ogallala Formation of the HPA, belonging to the Neogene System, and undifferentiated Pleistocene deposits, mainly loess and recent alluvial deposits (fig. 6). The Ogallala and undifferentiated Pleistocene deposits, which consist of clay, silt, sand, and gravel, accumulated as an apron of clastic (particulate) sediments that were eroded from the uplifting Rocky Mountains and carried eastward by streams (Ludvigson et al., 2009). Eolian (wind deposited) sand dunes are not common but can be found in southeast Scott and southwest Lane counties along with a small area several miles north of Tribune. The northern and eastern boundaries of the active model area coincide with Ogallala/late Cretaceous outcrops. The core areas of the model are concentrated over the thicker portions of the unconsolidated sediments that overlie the bedrock (fig. 7).

Aquifer Characteristics

The HPA is the principal aquifer in the area and provides water for almost all uses within the active area of the model. Although groundwater is found in the alluvial deposits of Ladder and Whitewoman creeks, as a sole-source water supply these deposits are limited to relatively small yields. The intent of this project is to simulate groundwater conditions in the unconsolidated material and no distinction is made between the HPA and alluvial deposits.

Cretaceous-aged formations underlie the HPA but are not considered in this study. The Niobrara Formation is a water-bearing formation but is not considered a principal source because the water typically is found in fractured limestone or in dissolved solution openings and thus can be highly variable in terms of availability. The Graneros Shale, Greenhorn Limestone, and Carlile Shale are found below the Niobrara but are generally of very low permeability and yield little water. The Dakota aquifer system is water bearing and underlies the entire model area. However, given its depth and higher salinity, only 13 water-right wells have been developed in the Dakota in recent years (3 in Lane, 8 in Scott, and 1 in Wichita) and account for less than one percent of the total overall average use of their respective counties (Whittemore et al., 2014). All water-level and water-right data known to be associated with Cretaceous strata were removed before calculations and simulations were performed for the model.

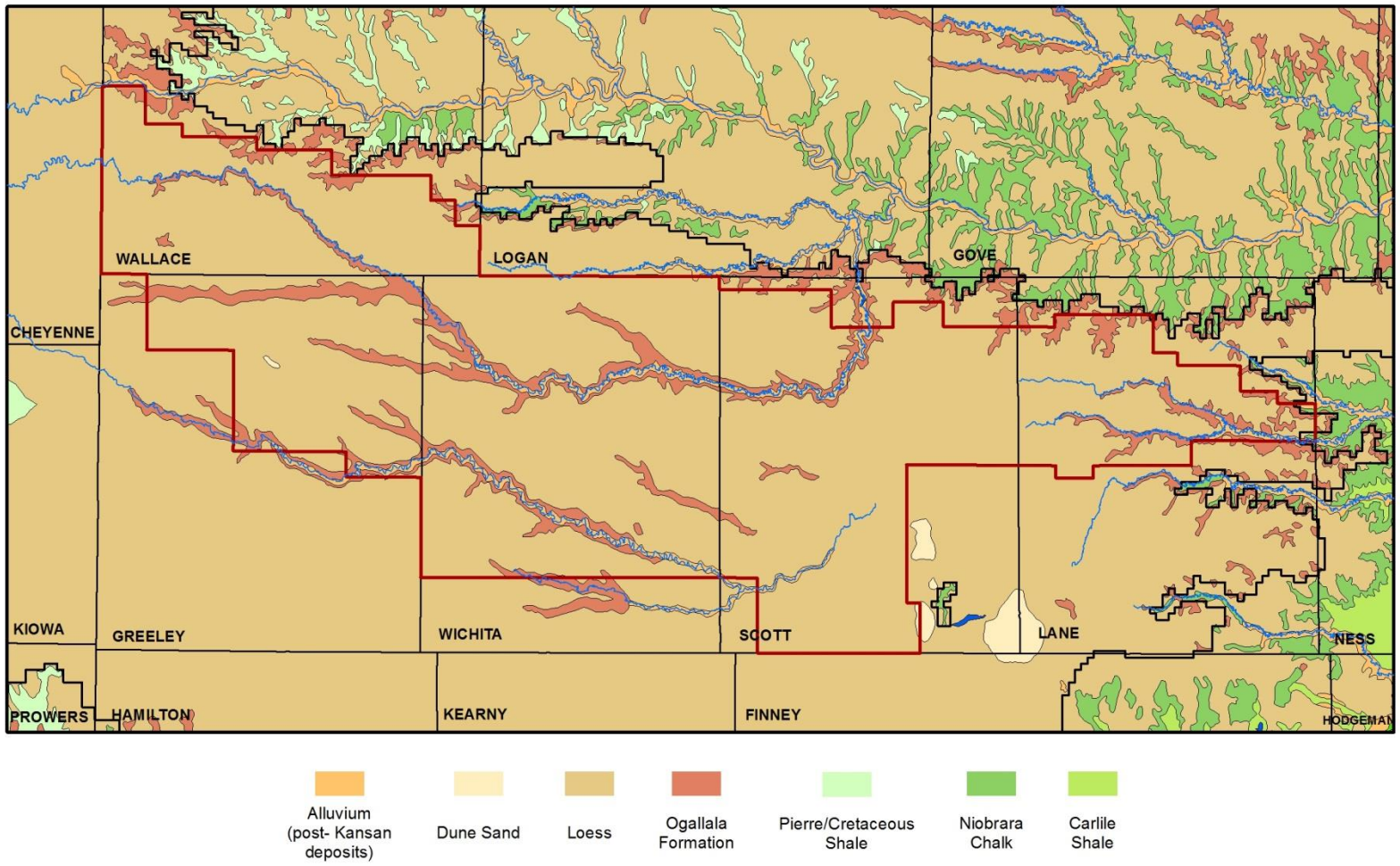

Figure 6. Surficial Geology.

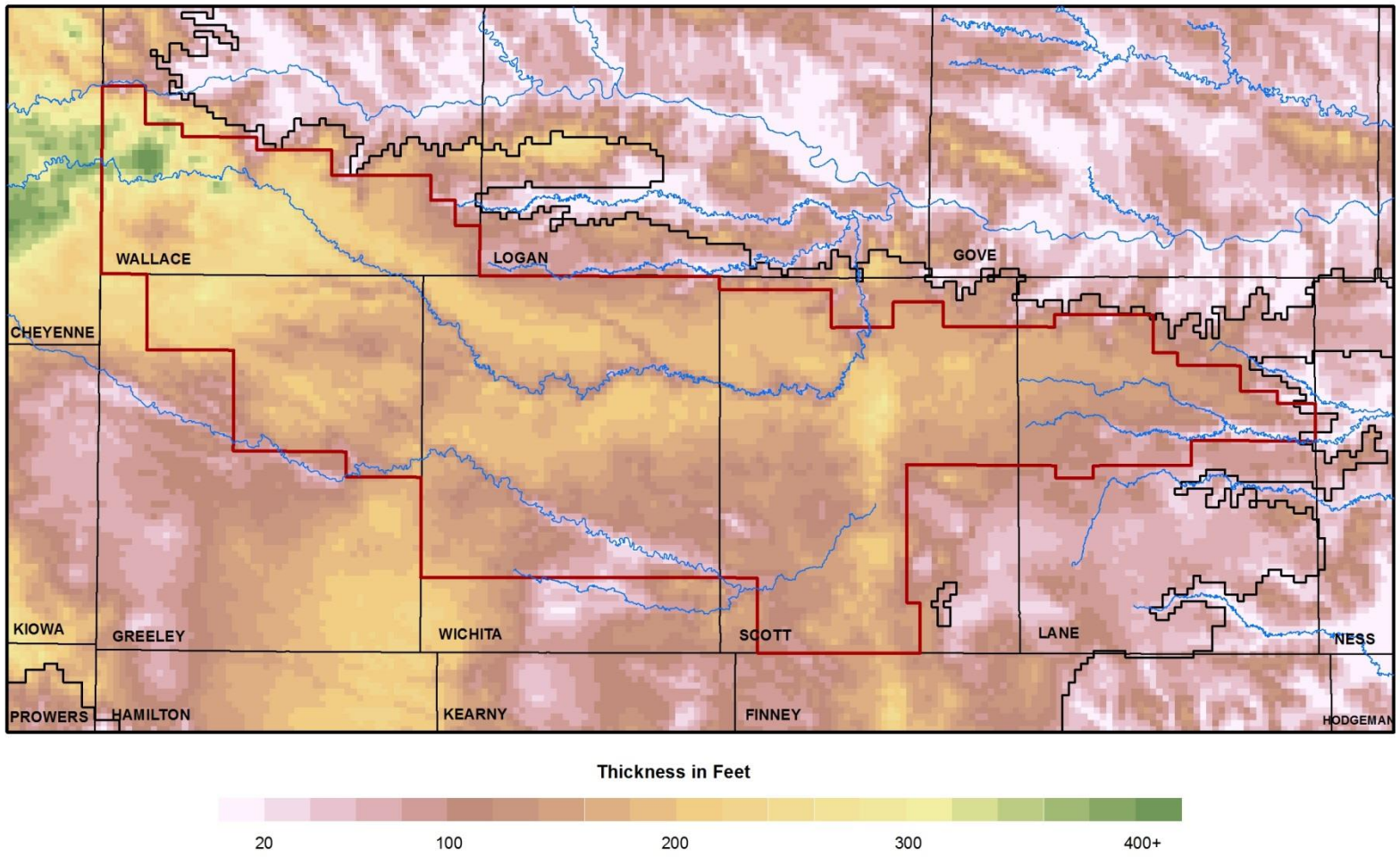

Figure 7. Thickness of unconsolidated sediments.

Bedrock Surface.

Data for the bedrock surface were obtained by updating a previous bedrock study by Macfarlane and Wilson (2006). In this study, lithologic logs were obtained from water well completion records, county geologic bulletins, and geophysical logs stored at the KGS, along with additional data from the USGS and the Henkle Drilling and Supply Company in Garden City, Kansas. Additional logs were obtained from water well completion records submitted since the completion of MacFarlane and Wilson (2006) and well records from other geologic bulletins.

The bedrock elevation well points were interpolated to form a continuous raster-based surface (fig. 8). The model cells were overlain on the interpolated surface and the average bedrock elevation within each model cell computed. In 21 model cells, the bedrock elevation was manually adjusted to be at least 10 ft below the land surface. These cells were mostly found along the fringes of the active area, outside of the GMD1 boundaries, where the model's 0.5 x 0.5 mile grid size was too coarse to adequately capture the local elevation changes interpolated from sparse bedrock points.

The bedrock surface elevation follows the same general slope as the land surface, with highs located along the western edge of the model and lower values to the east. Bedrock highs are concentrated in Cheyenne County, Colorado, with the lowest bedrock elevations found along the eastern edge of the model's active area in Ness County. The depth to bedrock ranges from near the land surface to more than 400 ft in southwestern Wallace County and southeast Cheyenne County, Colorado. The average depth to bedrock across the model area is approximately 147 ft below the land surface.

A three-dimensional version of the bedrock surface (fig. 9) facilitates visualization of the bedrock topography. An area of particular surface undulation is described by Boettcher (1964) in southwestern Wallace County and southeast Cheyenne County, Colorado, where a rolling erosional drainage pattern was formed on the surface of the Pierre Shale before the Ogallala Formation was deposited. The other topographical bedrock feature of prominence is the north-south trending Scott County trough that is thought to have formed prior to the Tertiary depositional events during a period of folding followed by a period of erosion in which all the Upper Cretaceous sediments were removed (Waite, 1947).

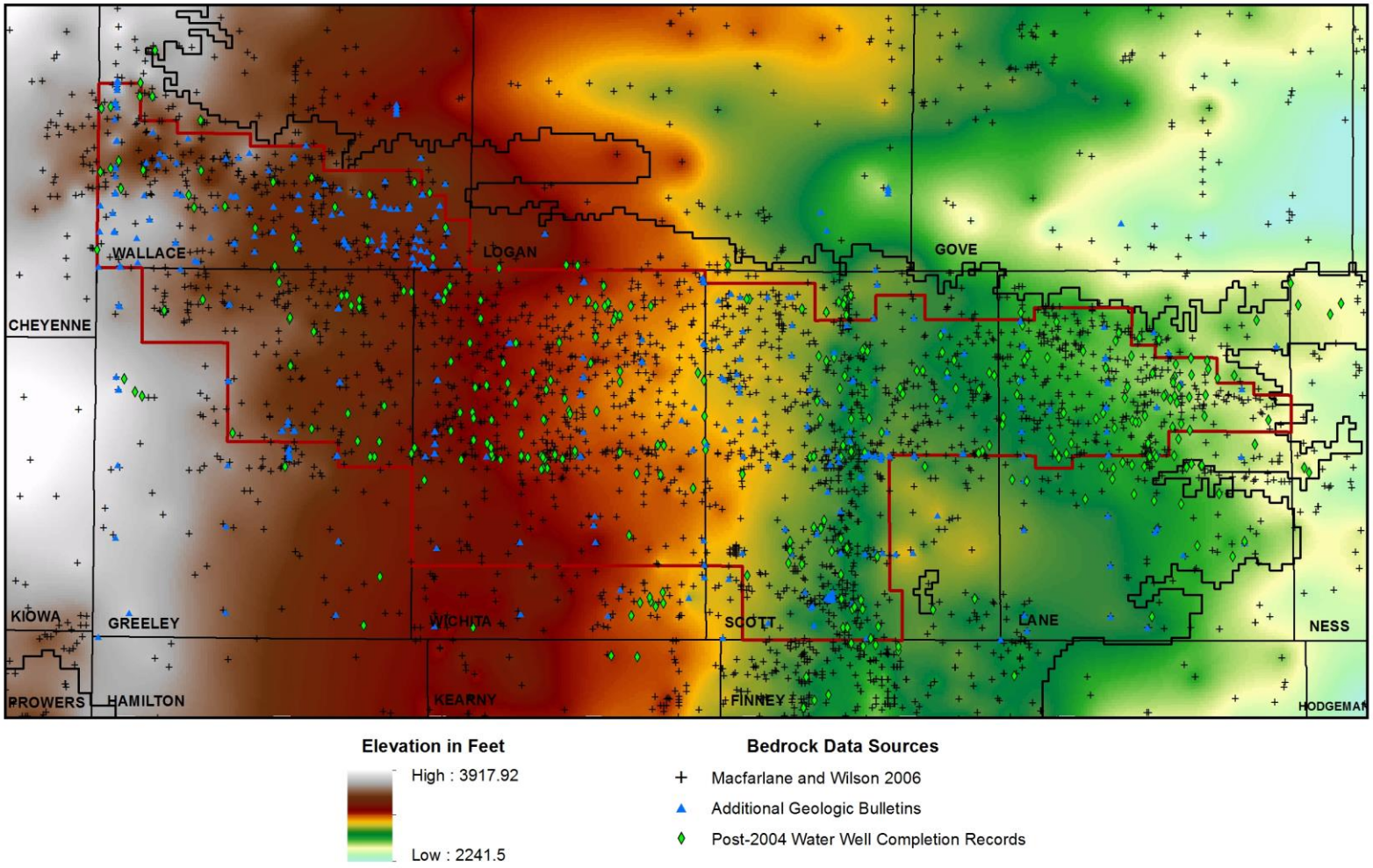

Figure 8. Elevation of the bedrock surface interpolated from well logs.

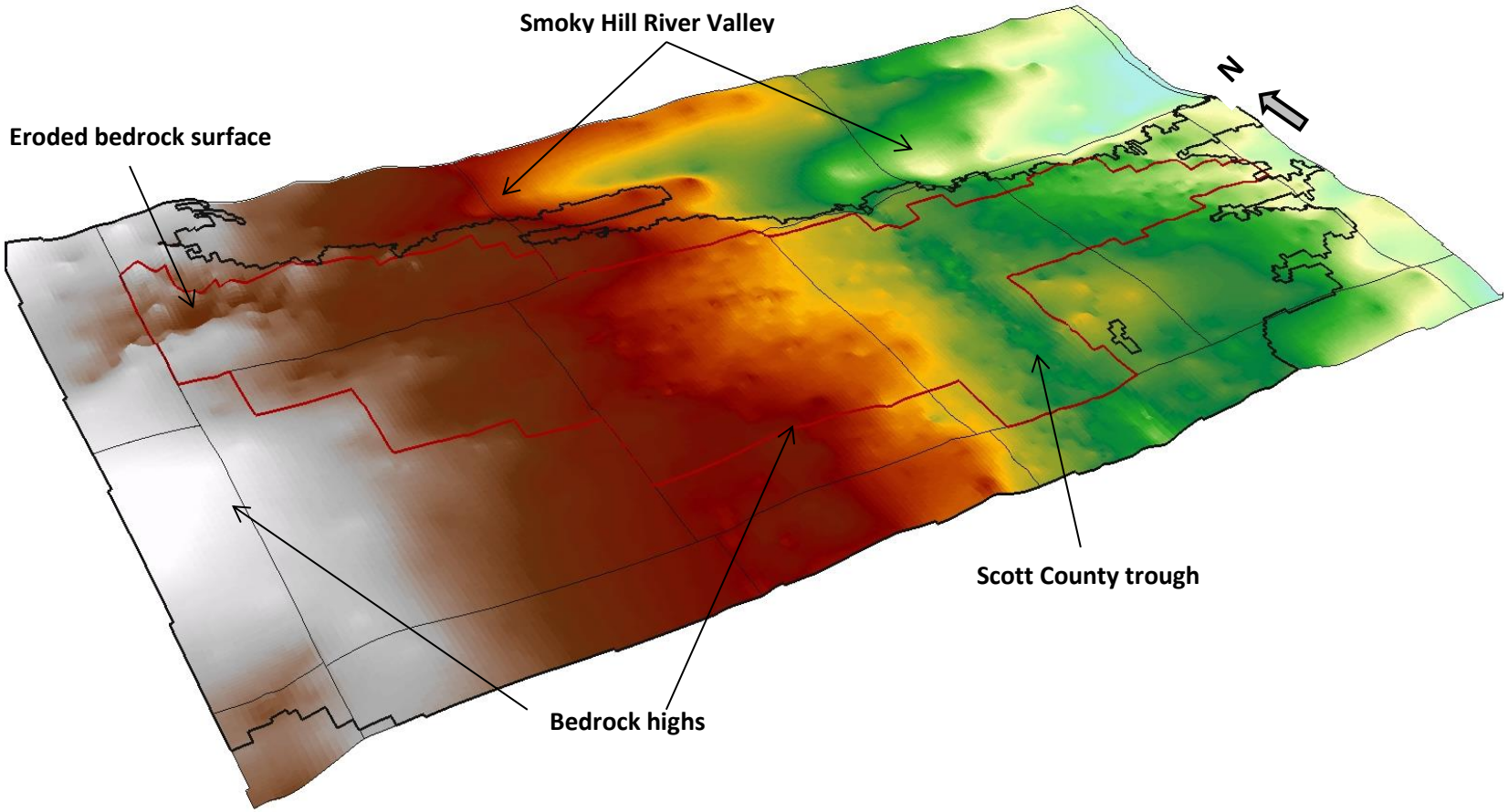

Figure 9. Three-dimensional view of the interpolated bedrock surface, looking northeast (see fig. 8 for color scale).

Lithologic Classifications

The KGS has established methods to extract and categorize information from drillers' logs with the most recent process known as the Hydrostratigraphic Drilling Record Assessment (HyDRA). Lithologic descriptions and interval depths have been transcribed and stored in Oracle, an enterprise-level relational database management system, from which they are further categorized into similar descriptive groupings. The HyDRA process is unique in comparison to past lithologic categorization activities (Macfarlane et al., 2005; Macfarlane and Schneider, 2007; Liu et al., 2010) in that it applies an automated quality-control measure to filter out potentially marginal well logs before interpolating the lithology category proportions from the wells to a 3D grid. For this project, MODFLOW accesses the HyDRA processed grids to compute the aquifer's vertically averaged hydraulic conductivity (K) and specific yield (SY) values for each model cell, based on where the model's ` water level for that particular time step falls within the three-dimensional space.

The quality of lithologic data provided through drillers' logs is known to vary substantially in terms of detail and usefulness in describing the subsurface. Figure 10 compares an example of a high-quality well log to an example of a marginal one. A quick and automated process to filter out marginal well logs was tested in Scott County, where more than 913 well logs were manually reviewed and subjectively graded and categorized for quality as "Excellent," "Good," "Fair," and "Poor" based on the level of vertical detail and the descriptions within each interval.

The average interval thickness of each log was then compared against the subjective grading categories. It was found that when averaging the overall thickness used to describe the lithology intervals, selecting logs with an average thickness of 20 ft or less isolated the majority of "Excellent" and "Good" logs from "Fair" and "Poor" groupings (fig. 11). Although this 20 ft average thickness excluded some "Excellent" logs and did not completely eliminate "Poor" logs, this filter can be readily applied to thousands of logs where manual grading is not practical. Using this approach, a total of 2,216 of 2,757 well logs were selected from the model's active area for further processing (fig. 12).

With the majority of marginal wells culled out of the GMD1 active area, the descriptions for each lithology interval were assigned to 71 standardized lithology codes. The standardized lithologies, in turn, were further categorized into groups representing the overall permeability and specific yield of the aquifer (table 1) from which values for K and SY can be assigned. In some cases, an individual lithology interval may have multiple lithology codes. In these cases, the percentage contribution of each lithology is assigned according to rules based on the number of lithologies in the interval and their order of appearance in the description.

Initially, the same five lithologic groupings as used in the GMD3 model (Liu et al., 2010) were applied to this project. However discussions with irrigators suggested that the water bearing units of the HPA in the western portions of GMD1 were exceptionally coarse with layers composed almost solely of gravel deposits. This area of Wallace County specifically is known to have groundwater supplies in deeper and thicker saturated intervals, with present-day transmissivities that allow well yields on the order of thousands of gallons per minute. Consequently, the permeability categories were expanded to seven to isolate lithologic descriptions with only gravel intervals and combinations of gravels with sand (table 1).

With the lithologic groupings in place, HyDRA segments each lithologic well location into 10-ft intervals starting from the interpolated predevelopment water table (described in the next section of this report) to bedrock. The proportion of each of the seven K lithology categories occurring within each 10-ft interval was estimated based on the driller's log. The seven category proportions in the 10-ft intervals were then interpolated into a three-dimensional grid across the model's active area, so that each grid cell (2,640 x 2,640 x 10 ft) contains a set of values representing the category proportions within that cell. A summary representation of this information, the proportion-weighted average K category, is shown in fig. 13. A special program was written to intersect MODFLOW-formatted water table and bedrock elevation grids with the three-dimensional proportional grids and then write out the vertically averaged K and SY values to MODFLOW-formatted grid files, based on the category proportions within the intersected grid cells and the K and SY values assigned to each category.

(a)

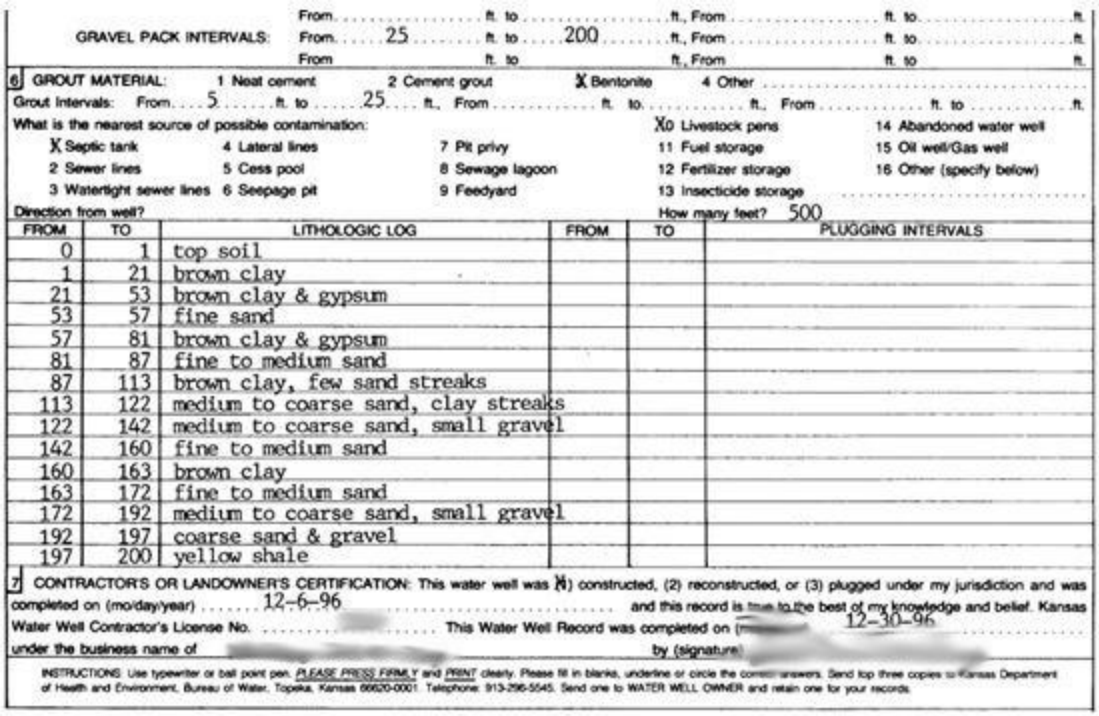

GRAVEL PACK INTERVALS: From ..... ft. to ..... ft., From ..... ft. to ..... ft.
From 25 ft. to 200 ft., From ..... ft. to ..... ft.
From ..... ft. to ..... ft., From ..... ft. to ..... ft.

6 GROUT MATERIAL: 1 Neat cement 2 Cement grout X Bentonite 4 Other .....
Grout Intervals: From 5 ft. to 25 ft., From ..... ft. to ..... ft., From ..... ft. to ..... ft.

What is the nearest source of possible contamination:
X Septic tank 4 Lateral lines 7 Pit privy X Livestock pens 14 Abandoned water well
2 Sewer lines 5 Cess pool 8 Sewage lagoon 11 Fuel storage 15 Oil well/Gas well
3 Watertight sewer lines 6 Seepage pit 9 Feedyard 12 Fertilizer storage 16 Other (specify below)
Direction from well? 13 Insecticide storage .....
How many feet? 500

FROM	TO	LITHOLOGIC LOG	FROM	TO	PLUGGING INTERVALS
0	1	top soil			
1	21	brown clay			
21	53	brown clay & gypsum			
53	57	fine sand			
57	81	brown clay & gypsum			
81	87	fine to medium sand			
87	113	brown clay, few sand streaks			
113	122	medium to coarse sand, clay streaks			
122	142	medium to coarse sand, small gravel			
142	160	fine to medium sand			
160	163	brown clay			
163	172	fine to medium sand			
172	192	medium to coarse sand, small gravel			
192	197	coarse sand & gravel			
197	200	yellow shale			

7 CONTRACTOR'S OR LANDOWNER'S CERTIFICATION: This water well was (1) constructed, (2) reconstructed, or (3) plugged under my jurisdiction and was completed on (mo/day/year) 12-6-96 and this record is true to the best of my knowledge and belief. Kansas Water Well Contractor's License No. ..... This Water Well Record was completed on (mo/day/yr) 12-30-96
under the business name of [redacted] by (signature) [redacted]

INSTRUCTIONS: Use typewriter or ball point pen. PLEASE PRESS FIRMLY and PRINT clearly. Please fill in blanks, underline or circle the correct answers. Send top three copies to Kansas Department of Health and Environment, Bureau of Water, Topeka, Kansas 66620-0001. Telephone: 913-296-5545. Send one to WATER WELL OWNER and retain one for your records.

R
E/W
SEC.
¼
¼
¼

(b)

GRAVEL PACK INTERVALS: From ..... ft. to ..... ft., From ..... ft. to ..... ft.
From 20 ft. to 75 ft., From ..... ft. to ..... ft.
From ..... ft. to ..... ft., From ..... ft. to ..... ft.

6 GROUT MATERIAL: 1 Neat cement 0 2 Cement grout 20 3 Bentonite 4 Other .....
Grout Intervals: From 0 ft. to 20 ft., From ..... ft. to ..... ft., From ..... ft. to ..... ft.

What is the nearest source of possible contamination:
1 Septic tank 4 Lateral lines 7 Pit privy 10 Livestock pens 14 Abandoned water well
2 Sewer lines 5 Cess pool 8 Sewage lagoon 11 Fuel storage 15 Oil well/Gas well
3 Watertight sewer lines 6 Seepage pit 9 Feedyard 12 Fertilizer storage 16 Other (specify below)
Direction from well? South 13 Insecticide storage .....
How many feet? 60

FROM	TO	LITHOLOGIC LOG	FROM	TO	LITHOLOGIC LOG
0	20	Clay			
20	185	Sand and gravel with clay streaks			

7 CONTRACTOR'S OR LANDOWNER'S CERTIFICATION: This water well was (1) constructed, (2) reconstructed, or (3) plugged under my jurisdiction and was completed on (mo/day/year) 7/3/87 and this record is true to the best of my knowledge and belief. Kansas Water Well Contractor's License No. [redacted] This Water Well Record was completed on (mo/day/yr) 9/28/87
under the business name of [redacted] by (signature) [redacted]

INSTRUCTIONS: Use typewriter or ball point pen. PLEASE PRESS FIRMLY and PRINT clearly. Please fill in blanks, underline or circle the correct answers. Send top three copies to Kansas Department of Health and Environment, Bureau of Water Protection, Topeka, Kansas 66620-7320. Telephone: 913-862-9360. Send one to WATER WELL OWNER and retain one for your records.

R
E/W
SEC.
¼
¼
¼

Figure 10. Example driller logs in GMD1 of (a) excellent quality and (b) poor quality.

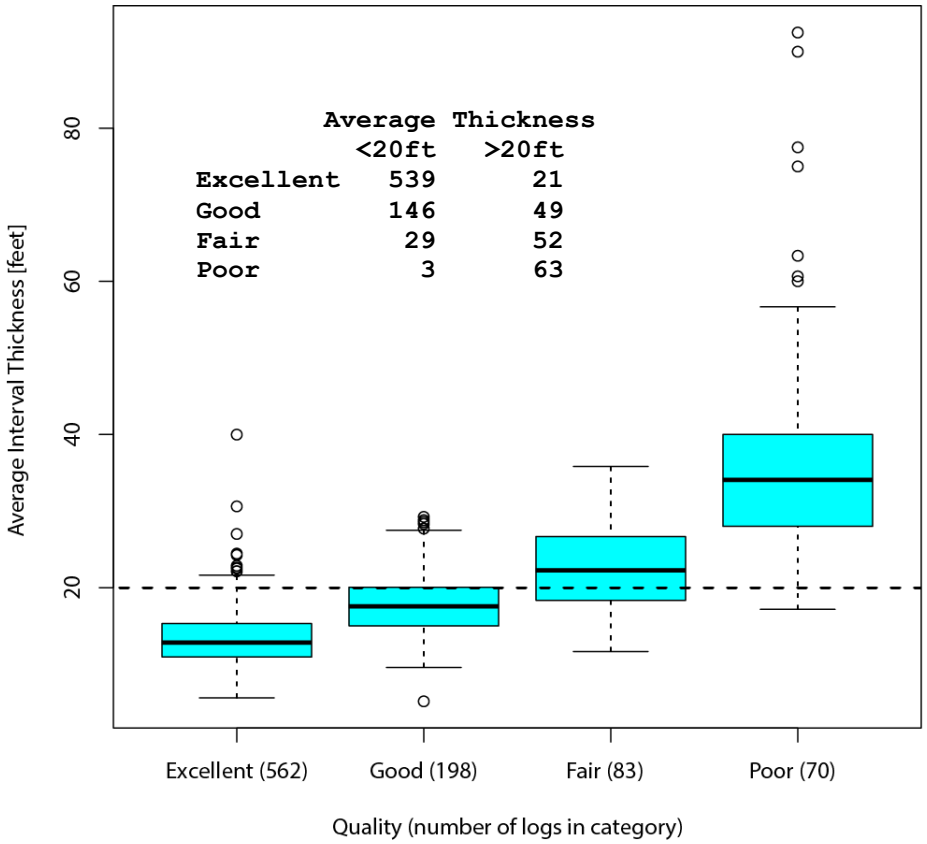

Figure 11. Distribution of the four lithologic grading classifications of drillers' logs in Scott County in relation to a 20-ft average interval thickness. Lower and upper box limits are the 25th and 75th percentiles, the heavy line in the box is the median, whiskers extend to the most extreme points within 1.5 times the interquartile range (75th percentile minus 25th percentile) beyond box limits, and more extreme points are plotted individually.

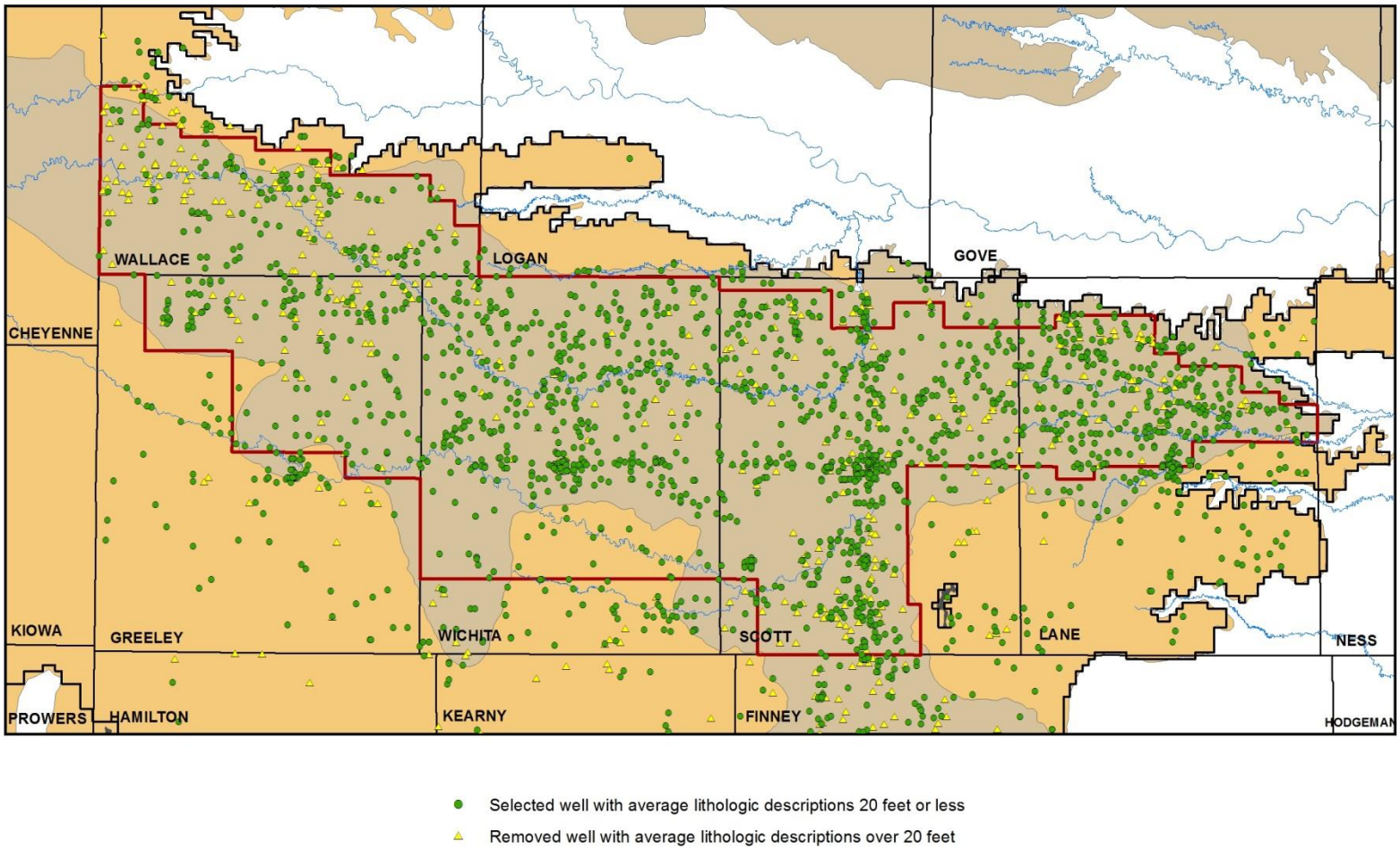

Figure 12. Distribution of lithologic logs based on an average 20-ft interval for lithology classifications.

Table 1. Standardized lithologies and hydraulic conductivity (K) in feet-per-day and specific yield (SY) categories with calibrated representative estimates.						
Category 1 K = 4.0e-6 SY = 0.05	**Category 2 K = 2.0e-3 SY = 0.05**	**Category 3 K = 0.02 SY = 0.05**	**Category 4 K = 50 SY = 0.25**	**Category 5 K = 145 SY = 0.26**	**Category 6 K = 200 SY = 0.20**	**Category 7 K = 400 SY = 0.15**
shale clay coal bedrock red bed rock siltstone	fine silty clay fine to medium silty clay silty clay medium silty clay fine to coarse silty clay medium to coarse silty clay fine sandy clay fine to medium sandy clay medium sandy clay sandy clay fine to coarse sandy clay medium to coarse sandy clay coarse sandy clay clayey silt fine silt silt top soil overburden marl calcified material (limestone/caliche)	fine sandy silt fine to medium sandy silt medium sandy silt sandy silt fine to coarse sandy silt medium to coarse sandy silt coarse sandy silt gravelly clay sandstone	clayey sand fine silty sand fine to medium silty sand silty sand medium silty sand fine to coarse silty sand medium to coarse sandy silt coarse silty sand unknown cemented sand and/or gravel fine sand fine to medium sand	sand medium sand fine to coarse sand fine to medium coarse sand medium to coarse sand coarse sand clayey gravel silty gravel	fine sand and gravel fine to medium sand and gravel medium sand and gravel sand and gravel fine to coarse sand and gravel medium to coarse sand and gravel coarse sand and gravel fine to coarse sandy gravel	fine gravel fine to medium gravel medium gravel gravel fine to coarse gravel medium to coarse gravel coarse gravel

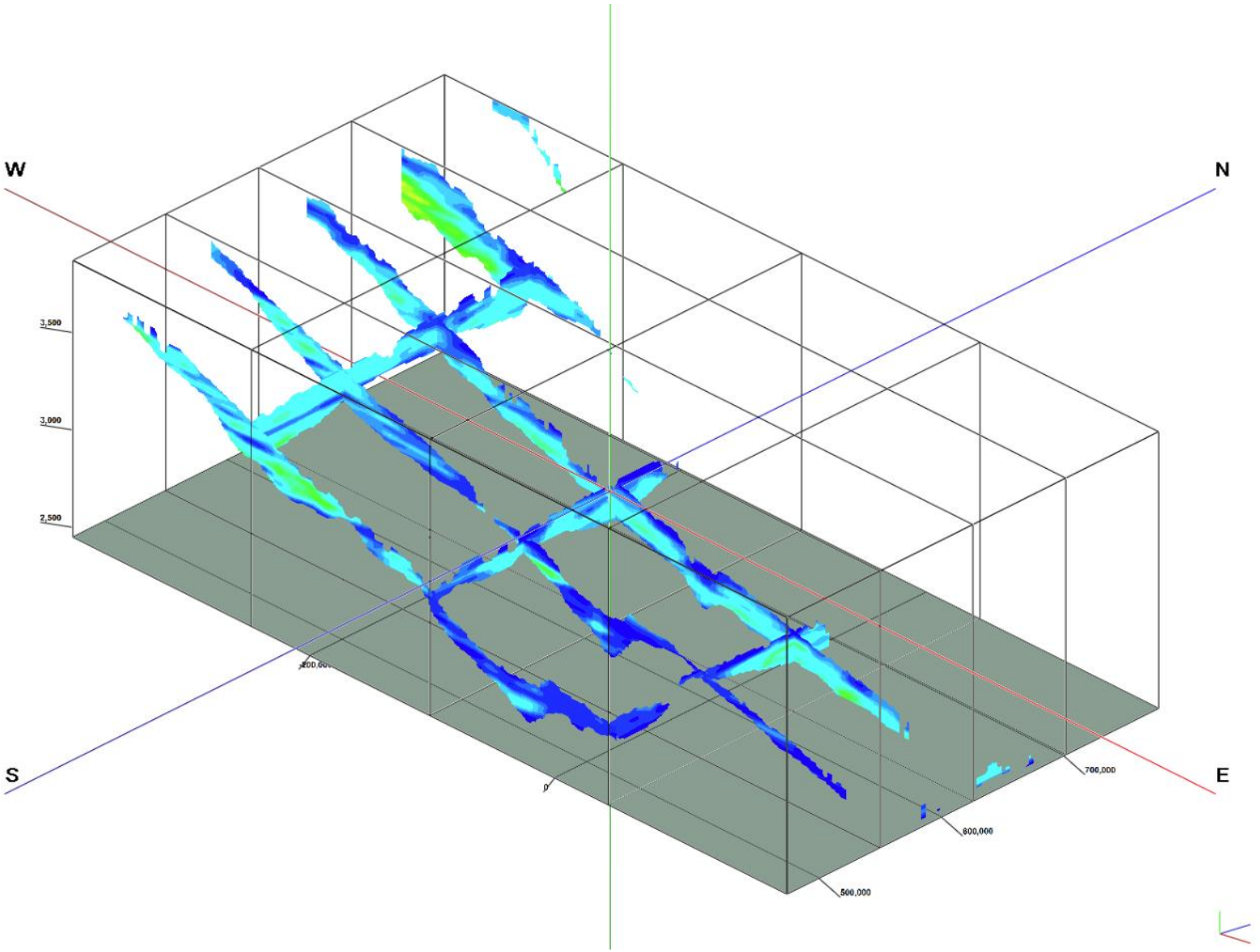

Figure 13. Proportion-weighted average K category in cross sections of the 3D grid. The dark blue colors indicate lower K classes whereas light green to yellow represent higher K classes.

Water Levels

Estimates of the predevelopment water table were compiled primarily from the "Well Records" listing of county-based geologic bulletins. Most of the depth-to-water measurements in these reports were made from the mid-1930s to 1952. Figure 14 shows that the geologic bulletin-based wells are spatially distributed across the entire extent of GMD1. Water levels taken from the Wallace County bulletin (Hodson, 1963) are typically from 1957 to 1960 with the majority of the wells being located just to the north of the GMD1 boundary. A series of wells in south-east Scott County were coded as being in the Niobrara only. Given that the listed source material consisted of "Sands and Gravel" and the listed water levels fell in line with other surrounding well measurements, it was assumed they were likely screened across the entire interval and were kept in the data set.

Predevelopment isolines from a USGS map product (Becker, 1999) were clipped to represent conditions in Kiowa County, Colorado, where no point-based records could be obtained. The earliest available water-level measurements (1954 to 1959) from the USGS's National Water Information System (NWIS) were downloaded to represent conditions in Cheyenne County, Colorado.

Given the lack of any predevelopment water-level measurements or estimates for Ness County, static water levels from Water Well Completion Records (WWC5) were used. Since 1974, Kansas drilling companies have been required by state law to submit a WWC5 form when a water well is drilled, reconstructed, or plugged. The activity dates for the 16 WWC5 records used run from 1979 to the early 1990s, with five occurring after 2000. The aquifer here is relatively thin with little groundwater development, so water levels are assumed to be static.

The predevelopment water-table elevation data sources described above were interpolated together to form a continuous 1,320 x 1,320-ft gridded surface. The model cells were overlain on the gridded surface and the average predevelopment water-table elevation within each model cell computed. In a few areas outside the GMD1 boundaries where the aquifer is particularly thin (e.g., western Greeley County and southern Lane County), the predevelopment water table was manually adjusted to be at least 5 ft above the bedrock surface.

Like the bedrock surface, the predevelopment water-table elevation follows the same general slope as the land surface, trending from highs along the western edge of the model to lows in the east. The overall predevelopment depth-to-water varies across the model's active area (fig. 15). The stream valleys of Ladder and Whitewoman creeks typically have predevelopment water levels within 50 ft of the land surface as does the southern extent of the north-south trough in Scott County (near the aptly named town of Shallow Water, Kansas). The average predevelopment depth-to-water across GMD1 is estimated to be approximately 90 ft.

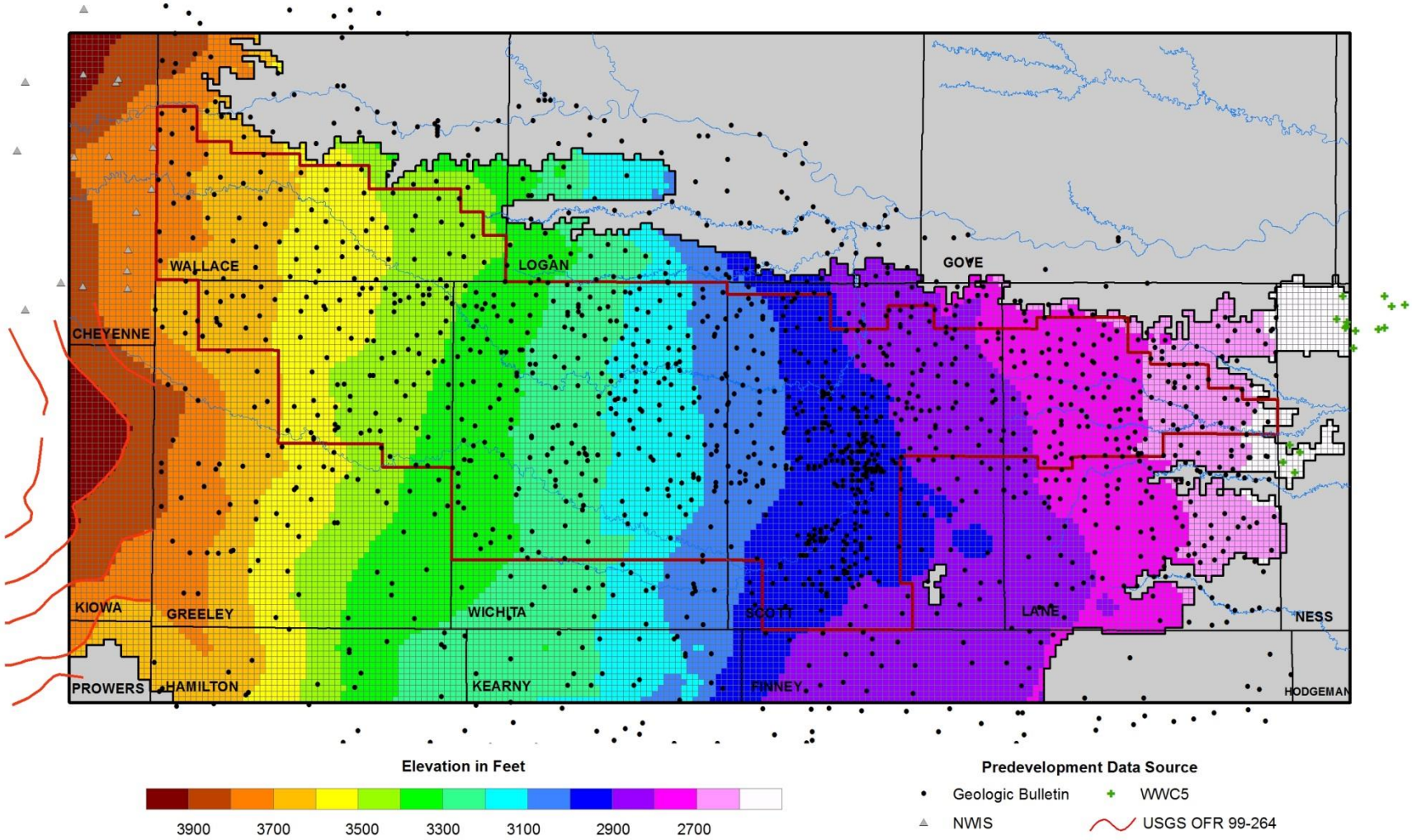

Figure 14. Interpolated predevelopment water table.

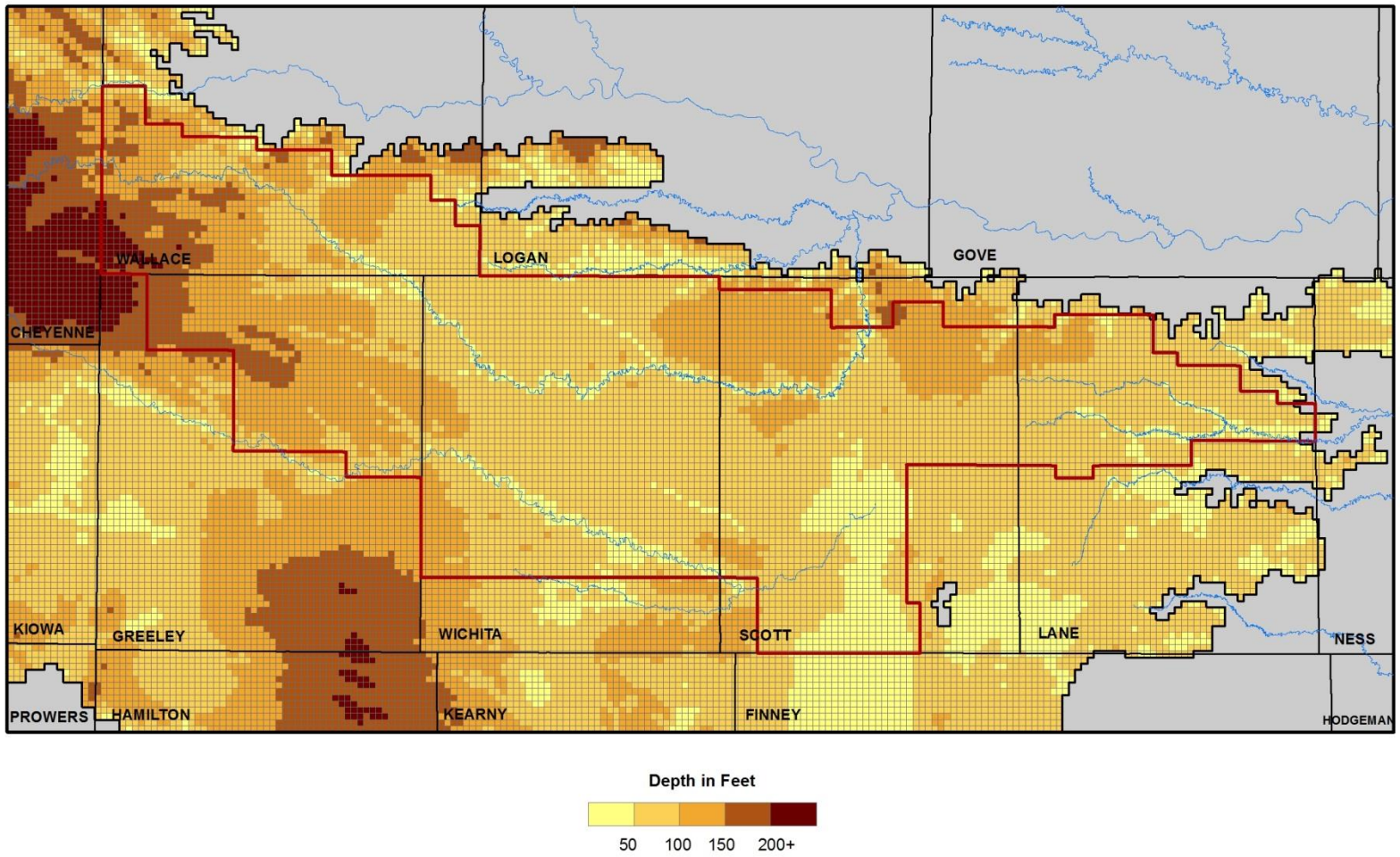

Figure 15. Interpolated predevelopment depth to water.

The average predevelopment saturated thickness within the GMD1 boundary is 75 ft, with the deeper bedrock areas in Wallace County, portions of Wichita County, and the Scott County trough being notable areas of thicker saturations (fig. 16). Most of Lane County typically had predevelopment saturated thicknesses around 53 ft. Higher bedrock elevations just outside the GMD1 boundaries in southern Greeley, southeast Scott, and southern Lane counties keep the saturated thickness relatively thin in those areas.

Water-level measurements after the predevelopment period vary greatly both in terms of the number of wells measured and their spatial distribution (fig. 17). Depth-to-water measurements for the Kansas portion of the model were obtained from the Water Information Storage and Retrieval Database (WIZARD). The majority of these records from 1996 to present were obtained as part of the annual Kansas Cooperative Water Level Program, operated by the KGS and KDA-DWR. Colorado-based measurements were downloaded from the NWIS.

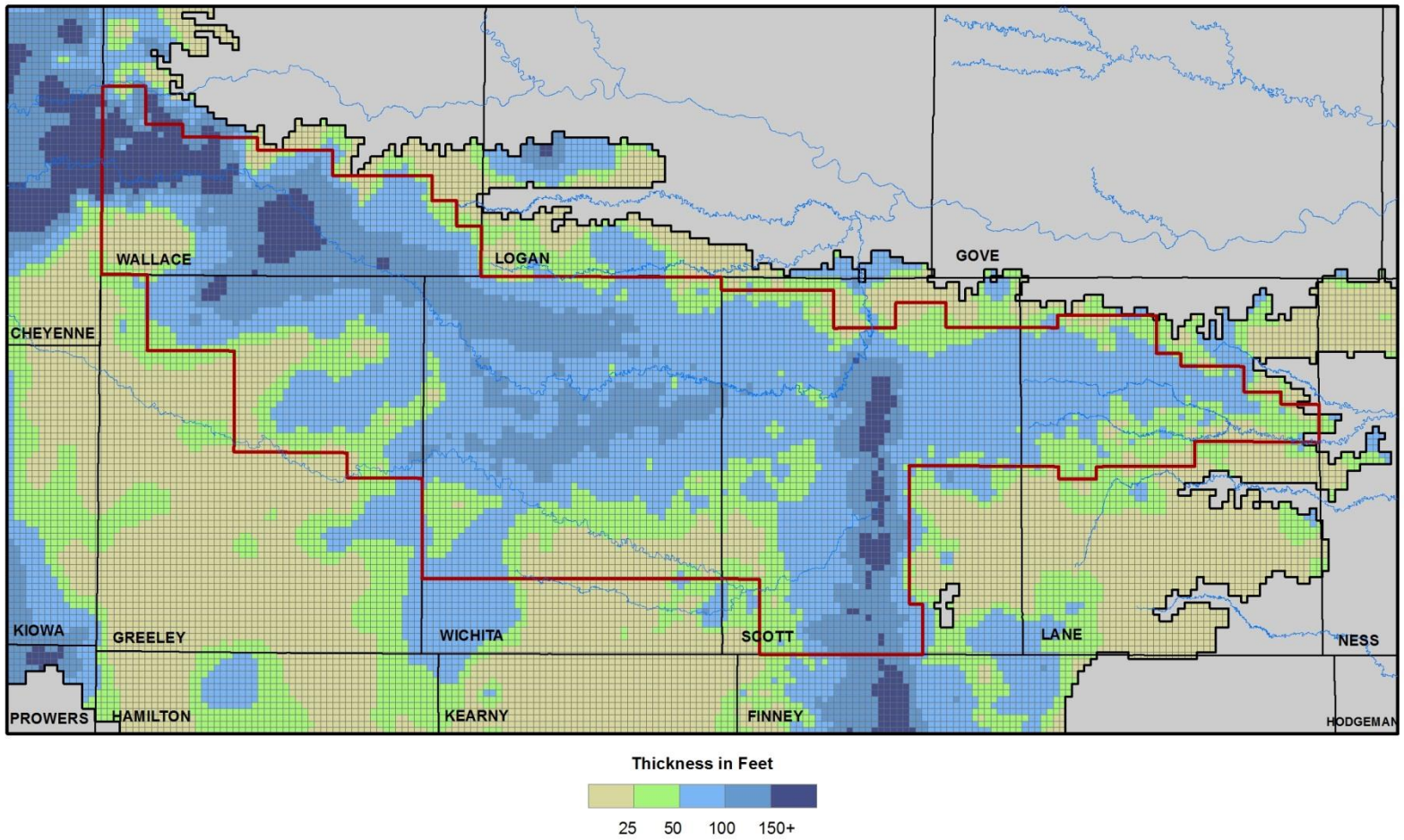

Figure 16. Interpolated predevelopment saturated thickness.

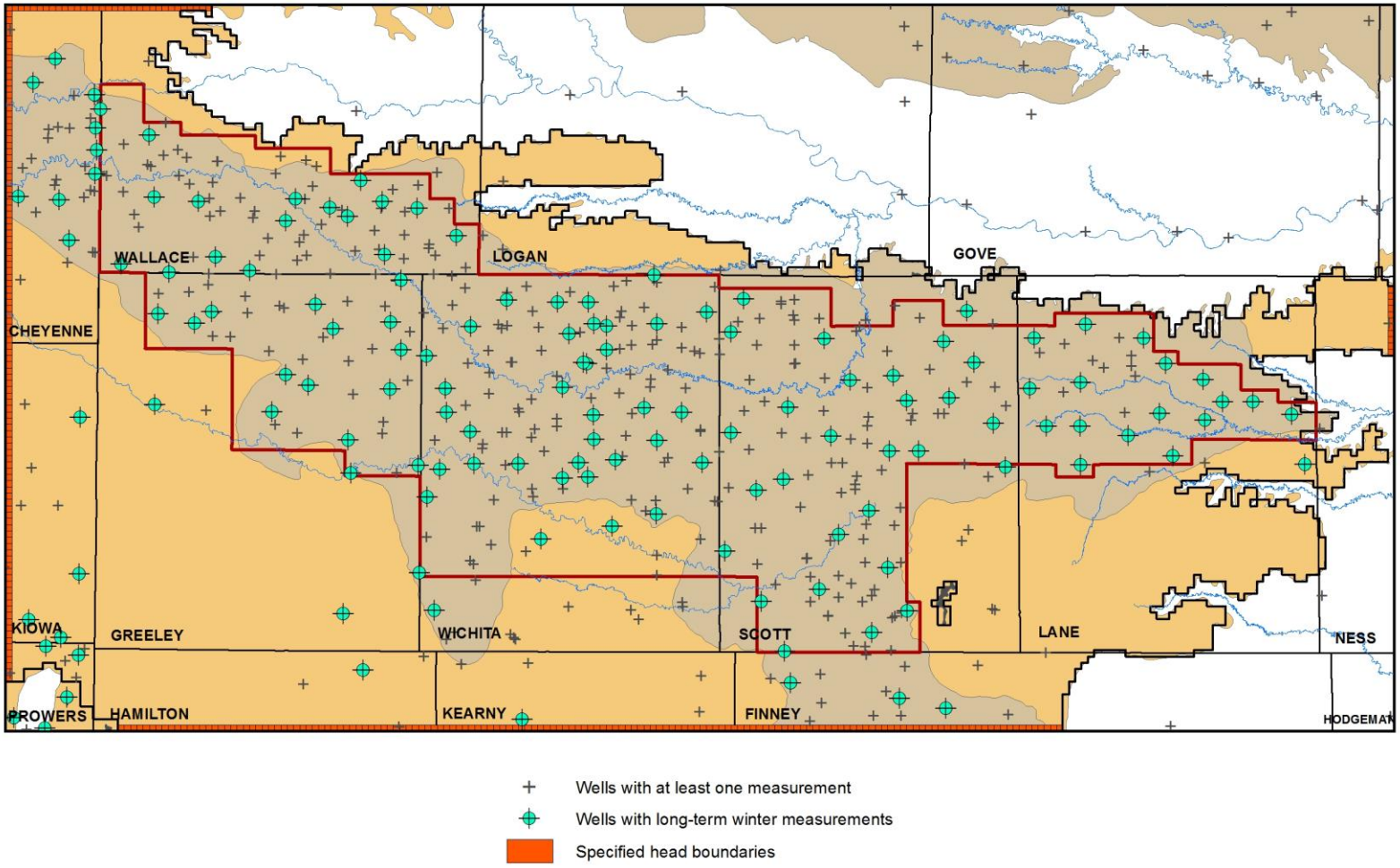

Figure 17. Distribution of water-level measurement wells.

Water-level measurements with special status codes indicating the value may not reflect normal conditions (e.g., the well was being pumped) were removed. At any given well, "winter" measurements, those taken between December 1 and April 15, were averaged to represent a single value for the year. Since the inception of the Kansas Cooperative Network, more than 80 percent of the measurements for a given well are taken in the month of January. The number of wells and their spatial extent across the model area are relatively low between predevelopment and the middle 1960s. From 1966 to 1984, more than 250 wells were measured over the winter months, and roughly 180 wells were measured in the winter months from 1985 to present (fig. 18). At the time of this report, 2011 was the most recent year of water-level data from the NWIS for wells in the Colorado portion of the model area.

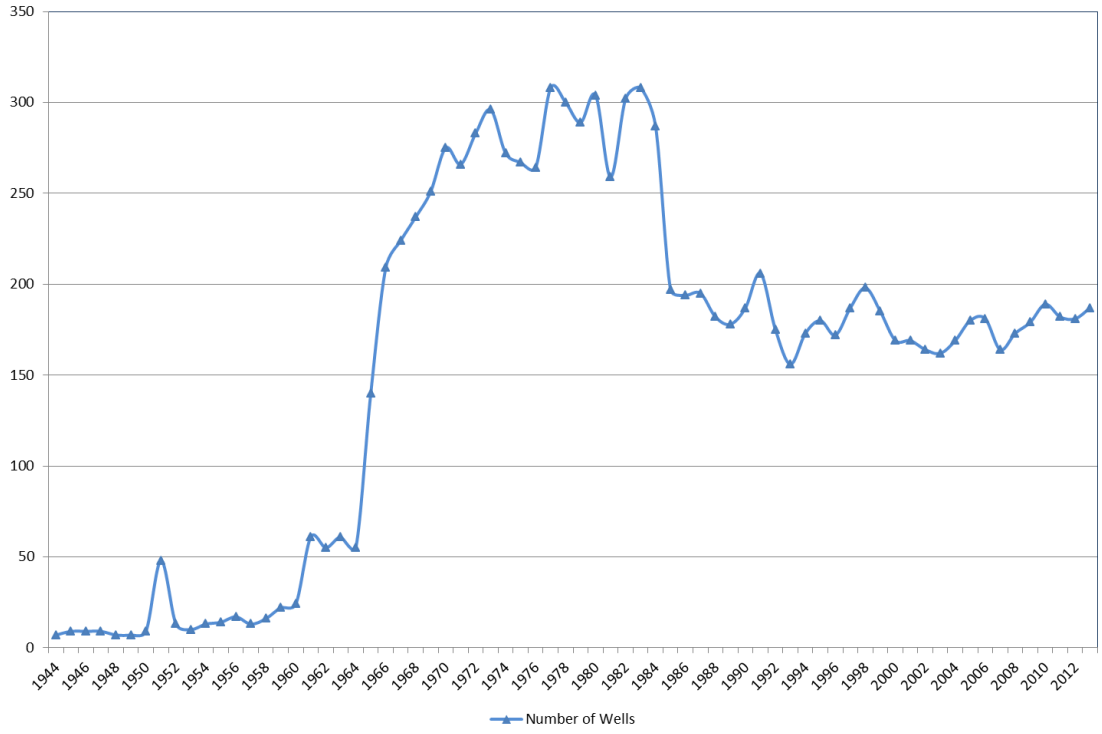

Figure 18. Number of wells in the model domain with "winter" (December 1 to April 15) measurements.

To compare with predevelopment conditions, all winter 2011 water levels were used to interpolate the water table and, in turn, the saturated thickness (fig. 19). In 2011, the saturated thickness across GMD1 averages just over 30 ft. The thickest saturated portions of the HPA in the model are found in Wallace County, Kansas, and Cheyenne County, Colorado, and along the Scott County trough, where the saturated thicknesses are near or more than 100 ft. The eroded bedrock surface in Wallace County has a significant effect on the availability of groundwater. A small area just south of Weskan, Kansas, has present-day thicknesses ranging from 150 to 200 ft, but within a few miles of this area, increases in the bedrock elevation combined with past water-level declines have resulted in saturated thickness at or close to zero.

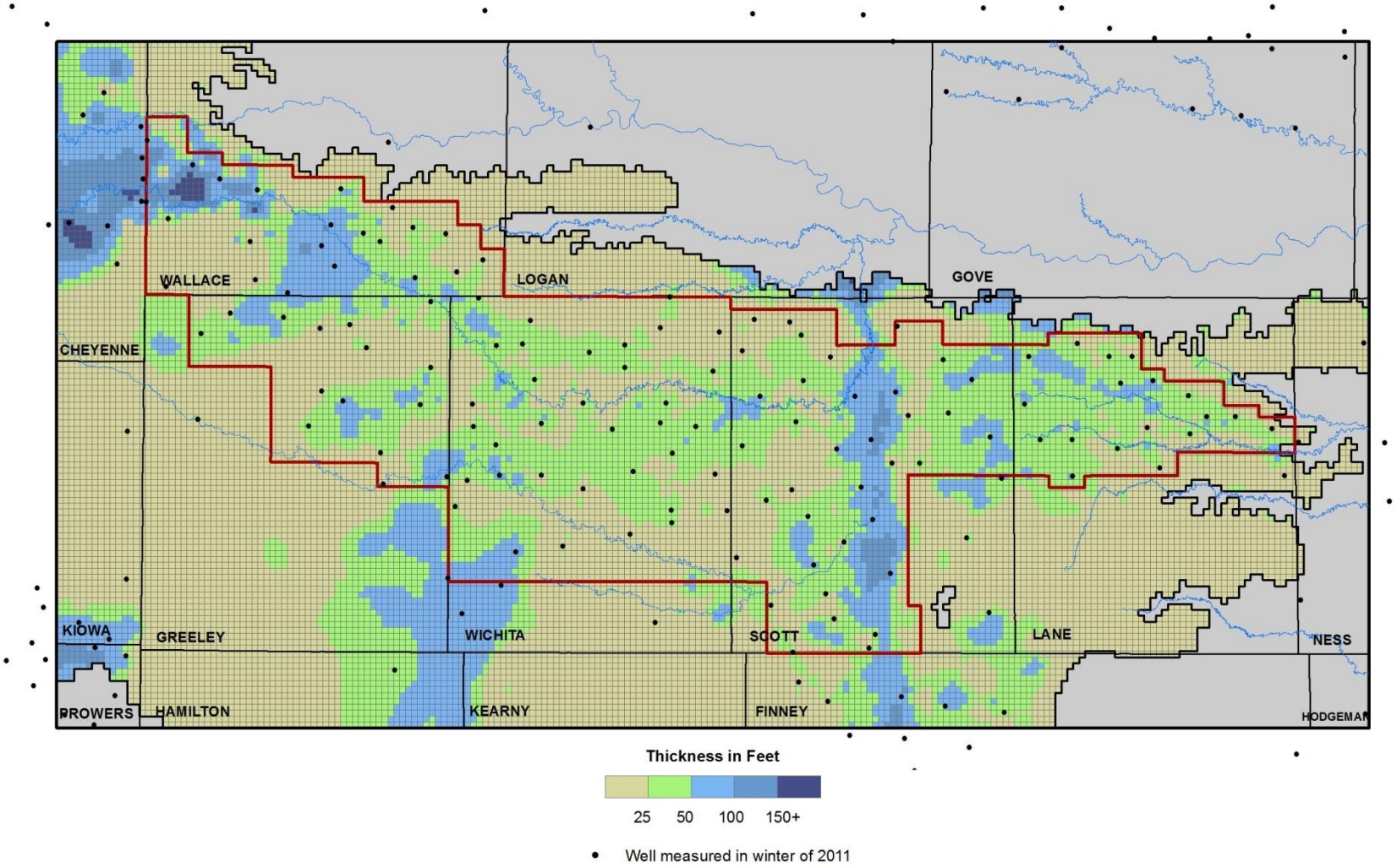

Figure 19. Interpolated 2011 saturated thickness.

Boundary Conditions

The model uses time-varying specified head boundaries along the northwest, western, and southern edges of the active area and where the HPA extends beyond the eastern edge of the model in Ness County (fig. 17). Specified head boundary cells are important elements to numerical models as they allow water to move in and out of the active area. Given that head boundaries in the model are not located along natural or known hydrologic boundaries, setting appropriate head values for them is challenging, especially in areas lacking data.

Starting with the interpolated predevelopment water levels, each time-varying head cell was reviewed in relation to well measurements taken over the transient period. More than 600 wells were measured sometime during the transient period. However, only 122 of them contain long histories of consistent measurements taken in the winter months (fig. 17). In cases where these wells are located in or near the head-boundary cells, the water-level trends shown in the measurement histories were applied to the head-boundary cells, starting at predevelopment.

Measurements from wells without long-term, winter-based measurements were still used when possible. Many of these wells had numerous measurements from 1966 to 1984. If these wells fell within any head-boundary cells, then their water levels were transferred to the head-boundary cells and linear regression equations were established with those water levels and the predevelopment estimate to fill in the transient period of record. If the wells were located near but not in the head-boundary cells, the water levels were still transferred to the head-boundary cells but only after making slight subjective adjustments based on the predevelopment water-level gradient. This process of filling in the holes with nearby data and using regression equations to fill in the temporal gaps worked well where data records are present. The process is very subjective in areas with little to no data, such as along the thinly saturated areas of the HPA, namely along all of Kiowa and Prowers counties in Colorado, and Hamilton, Kearny, and Ness counties in Kansas.

Stream Characteristics and Flow

Ladder Creek and Whitewoman Creek are the primary stream courses running through the model area (fig. 20). Ladder Creek, which used to be called Beaver Creek, enters the model area from Cheyenne County, Colorado, crosses the core of the model's active area, and turns north in Scott County where it flows into Scott County Lake and then the Smoky Hill River. Whitewoman Creek also enters the model area from Cheyenne County, crosses the bedrock highs of Greeley County, into the thicker portions of the unconsolidated sediments of eastern Greeley and western Wichita counties, over bedrock highs south of Leoti, and ending in the Scott Basin, a large depression southeast of Scott City. Both streams have historically been intermittent, although Prescott et. al., (1954) reported that springs in central Wichita County once provided enough water for permanent flow in Ladder Creek. Today, both streams are ephemeral with water typically only being found during and after heavy rainfall events.

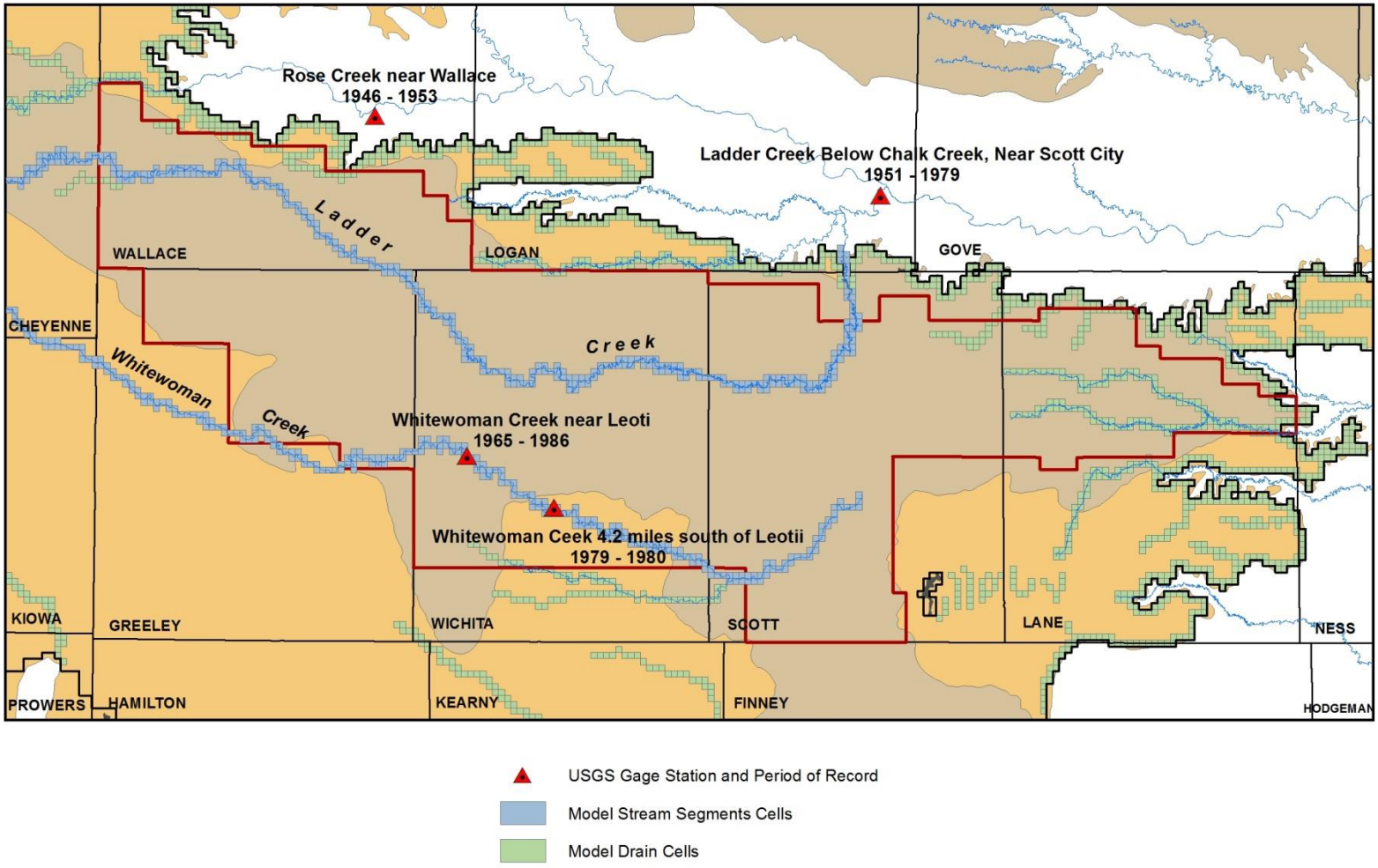

Figure 20. Model stream and drain cells and USGS stream gaging stations.

Stream Channel Characteristics

This project uses the Stream package for MODFLOW, which requires all surface water courses to be broken down into individual segments and reaches. A "segment" is a longer portion of the stream, which in turn is further divided into "reaches" that represent each portion of a stream segment within individual model cells. The model uses four stream segments (Ladder Creek above Scott County Lake, Scott County Lake itself, Ladder Creek downstream of the lake, and Whitewoman Creek) with a total of 787 reaches. Figure 21 shows an example of the segment/reach division.

Both Ladder and Whitewoman creeks have pronounced channels with defined bluffs and banks. The stream segments were measured at various spots across the model area, and 15 ft was used to represent their widths. Streambed elevations were obtained by determining where land surface contours (10-ft intervals) from 7.5-minute USGS topographic maps crossed the stream channel. Of the 309 model cells that comprise Ladder Creek, 175 of them (or roughly 57%) had elevation contours crossing the channel. For Whitewoman Creek, 160 (or roughly 62%) of the 259 stream cells had crossing topographic contours. For stream cells without crossing topographic contours, elevations were interpolated between cells with assigned elevations based on the overall change in elevation and length of the particular stream segment.

Depending on how the streams meander over the model's 0.5 x 0.5 mile grid, the streambed elevations in relation to the bedrock elevations may not be properly represented in the model. Reaches 2 and 4 of segment 2 in fig. 21 are both located in a model cell where the stream segment is located directly adjacent to the valley wall. This particular model cell is considered a "stream" cell even though the cell is dominated by upland topography. As such, the estimated bedrock elevations for this cell are substantially above the streambed, causing computational errors in the model. A total of 14 model stream cells had bedrock elevations estimated to be above the streambed elevations. The bedrock elevations for these cells were lowered to 0.1 ft below the streambed.

Figure 22 illustrates the streambed elevation in relation to the bedrock for the model stream cells. Within the model's active area, Ladder Creek typically is associated with thicker areas of aquifer. Not until it reaches areas along the Scott/Logan county line does the streambed come in close contact with the underlying bedrock. Whitewoman Creek crosses areas where the underlying bedrock rises and falls, in particular the very thinly saturated areas of southern Wichita County.

Gaged Streamflow

Mean monthly streamflow records were obtained from the USGS's NWIS for all gaging stations in the model area. Ladder Creek was gaged about 20 miles north of Scott City from 1951 to 1979. Whitewoman Creek was gaged from 1965 to 1986 roughly seven miles west of Leoti and then very briefly in 1979 four miles south of the town. Over the period of record for the gages, streamflow averaged less than one cubic foot per second. The starting input streamflow where Ladder and Whitewoman creeks enter the model along its western edge is zero. The gaged data that are available are used as a measure of the aquifer's baseflow contribution occurring during winter periods of the model (gaged flow in summer months is much more significantly affected by surface runoff from precipitation events).

Stream Drains

Much of the northern and eastern extent of the model's active area is marked by a boundary where the headwaters from numerous small tributaries have cut short, deep, and often rugged canyons into the aquifer. The numerous springs in this area can largely be attributed to gravity-based discharge from the HPA and in some cases the underlying Cretaceous formations. Some of the larger springs in northern Scott County were actually developed for public use during predevelopment times as the yields ranged from a few up to 400 gallons per minute (Waite, 1947). Today most of the springs no longer receive discharge from the aquifer as declining water tables have broken or limited hydrologic connections to these stream channels.

To simulate this interaction, MODFLOW's drain boundary conditions were used. As the name implies, drain boundaries allow water to discharge from the aquifer when the water levels are at or above the drain elevations. Unlike stream cells where flow can be into or out of the aquifer, drains only allow flow in one direction, discharge out of the aquifer. If water tables decline enough, the connection is broken and water will no longer discharge out of the system; this condition occurred in the model during the 1960s when pumping began to intensify and the rate of water-table decline accelerated. Drain model cells were established all along the northern and eastern boundaries of the model's active areas to simulate the headwaters of the numerous ephemeral streams (fig. 20). Drains were also added in areas of Dry Lake in southeast Scott and southwest Lane counties and along the Smoky Hill River (Wallace County), Chalk Creek (Logan County), Wild Horse Creek (Prowers County), and the various stream forks of Walnut Creek (Lane County).

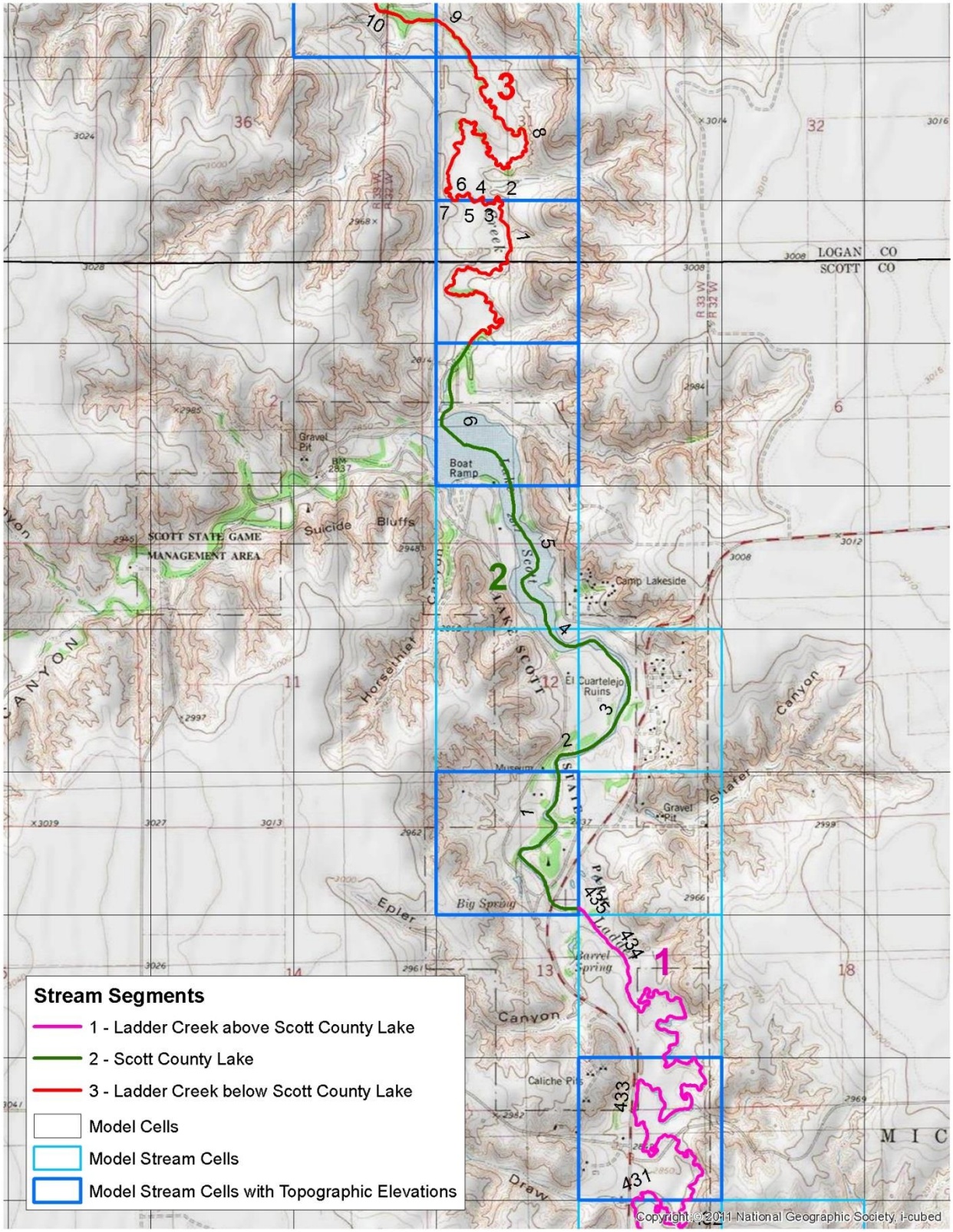

Figure 21. Selected area of the model showing stream segment and reach designations along Ladder Creek near Scott County Lake.

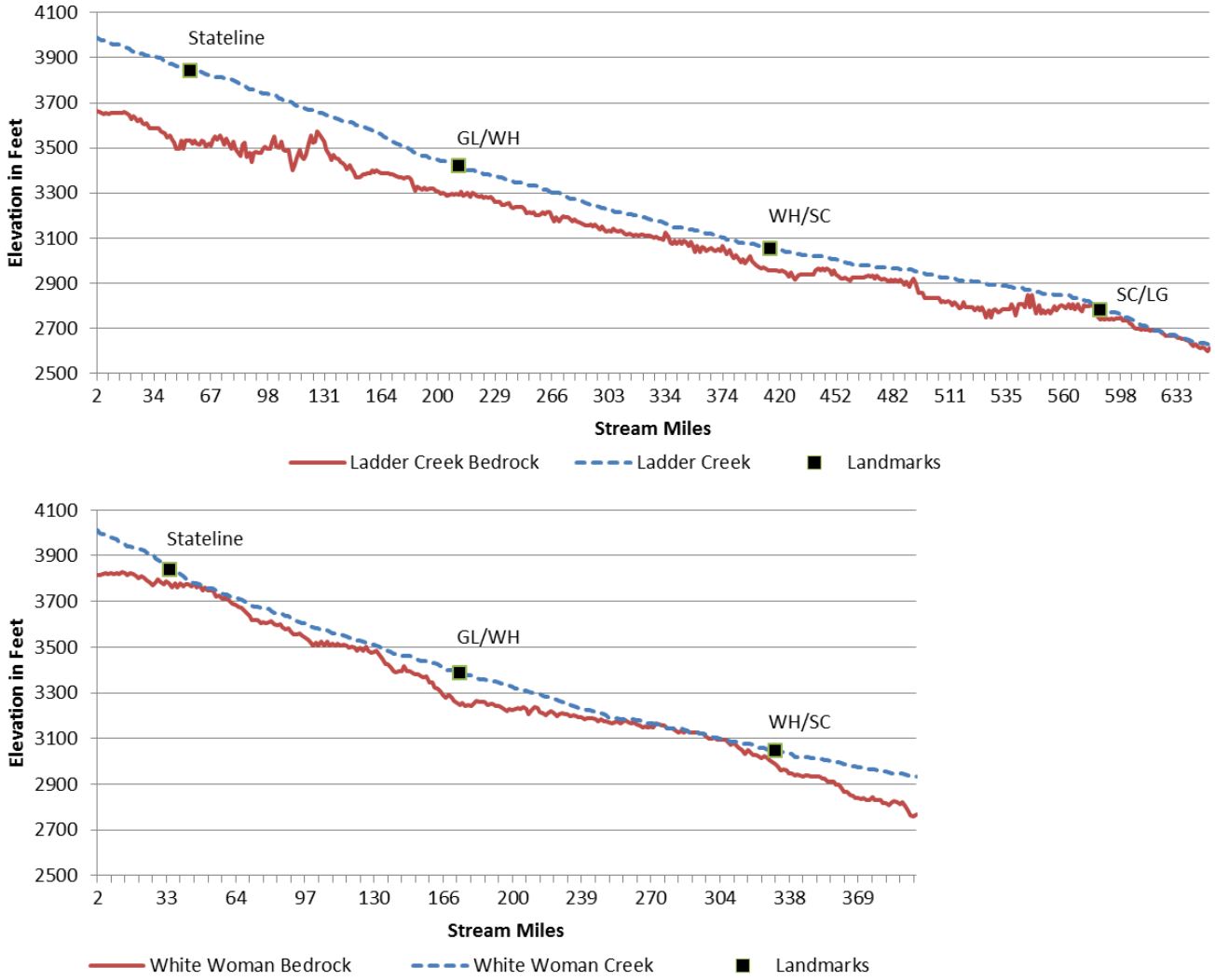

Figure 22. Estimated elevation for the streambed and bedrock for Ladder and Whitewoman creeks. The landmarks mark the Colorado-Kansas line and county boundaries. GL = Greeley County, WH = Wichita County, SC = Scott County, LG = Logan County.

Water Right Development

In the United States, regulation of groundwater has traditionally been left to the states. All of the states north, south, and west of Kansas follow some version of appropriation doctrine (first in time, first in right) involving water-right permits or certificates. Water rights in Kansas are highly regulated in terms of how much water can be used annually and where that water is applied. Kansas is also one of the few states that maintain a self-reporting water-use program. A substantial amount of Kansas water-right data is online. Colorado-based water-right data are also available online. The KGS has a strong working knowledge of the Kansas water-right system, including the intricacies of the underlying data structure and the business rules used to represent the data. Water-right data from Colorado are not as well known nor is Colorado's own adaptation of the appropriation doctrine, although its overlying permitting process follows the spirit of the Kansas system.

Kansas

Water rights in Kansas are dynamic entities whose characteristics can change over time. The authorized quantities and water-right locations used in the model represent conditions as of October 3, 2013. Data were accessed from the Water Information Management and Analysis System (WIMAS). The vast majority of water rights in the model area are groundwater based (fig. 23). Within the model's active area are 2,529 unique appropriated and vested water rights. The vast majority of these, 97 percent, are authorized for groundwater-based irrigation (table 2). Although some surface-water-based appropriations exist, most have been limited by water availability and are insignificant relative to the total authorized quantities. None of the surface-based water rights have had significant levels of reported water use for decades and, as such, are not considered in the GMD1 model. The few groundwater-based water rights (26 in total) known to be screened solely in aquifer units other than the HPA, such as the Dakota, were also removed from consideration.

Table 2. Total authorized quantity, in acre-feet, for appropriated and vested water rights, by use made of water and source of supply for the Kansas portion of the GMD1 model active area
Represents conditions as of October 3, 2013

	Domestic	Industrial	Irrigation	Municipal	Recreation	Stockwater	Other
Surface	0	0	1,524.0	0	1,062.0	0	204.6
Ground	8.89	545.89	731,960.8	4,973.8	419.0	12,879.78	0
Total	8.89	545.89	733,484.8	4,973.8	1,481.0	12,879.78	204.6

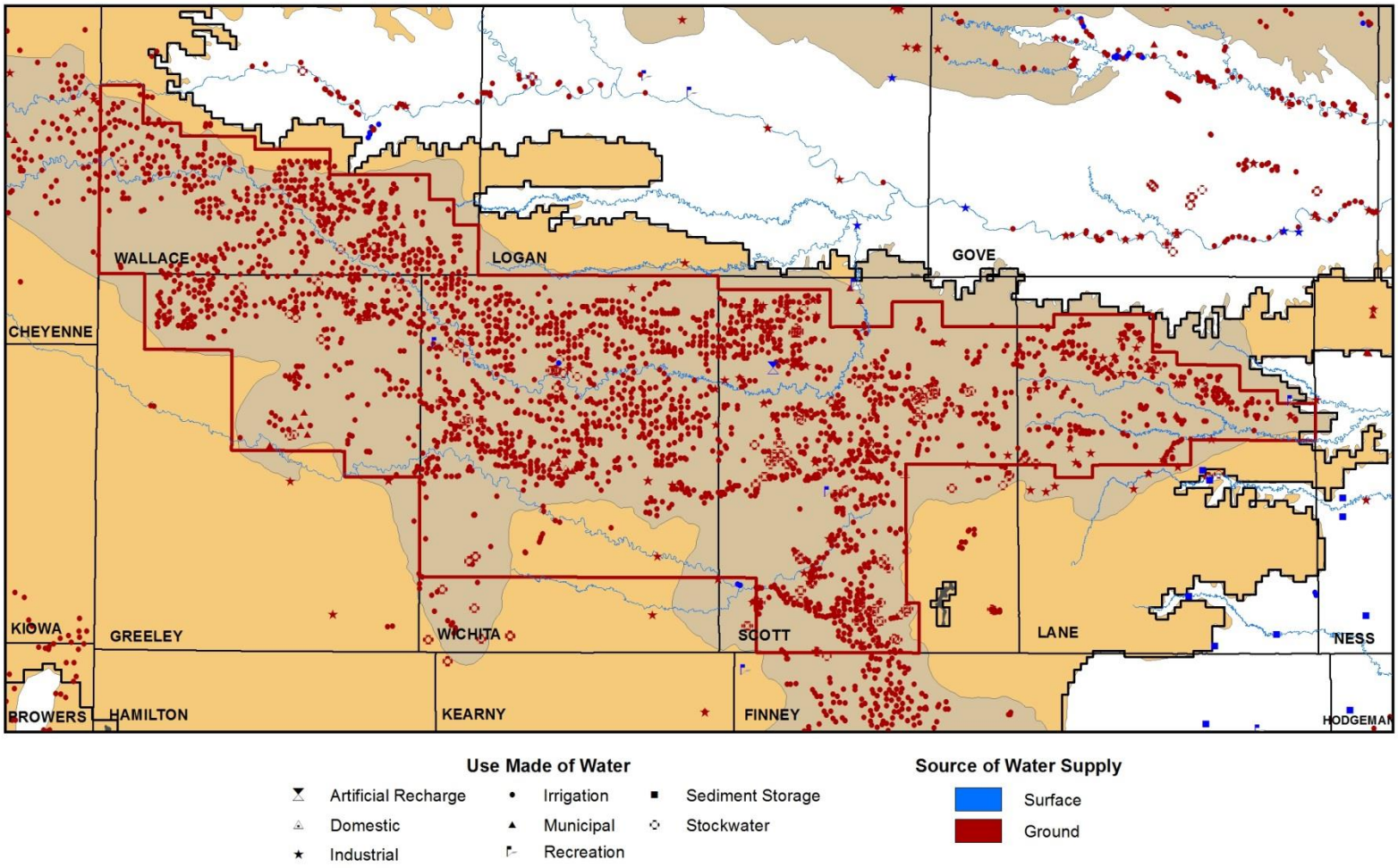

Figure 23. Water-right distribution in Kansas and Colorado.

The WIMAS database only stores a water right's authorized quantity as of the present. Although quantity values can change as a water right goes through the certification process or by other administration actions (generally becoming less), the historic trends used in the model are based on the appropriated quantity values at the time of the download (10/03/2013) and in relation to the priority date of the water right.

A common complexity with Kansas water-right quantities is that the annual appropriation can be associated with the water right itself (regardless of how many uses or points of diversion it might have), with the water right's uses of water, or with the water right's multiple points of diversion. Because the points of diversion for a particular water right could be located across multiple model cells, the total annual authorized quantities for water rights that had their appropriations stored by the water right or use made of water were divided equally among the water right's point(s) of diversion. Each point of diversion would then have an associated quantity that when added with the other points of diversion under the water right would equal the total quantity authorized. If the quantity was already stored by the point of diversion, it remained unchanged.

The trend in authorized quantity over time, based on priority dates, in the active portion of the model's area (fig. 24) is characteristic of much of western Kansas. Kansas water law started with the passage of the 1945 Water Appropriation Act. Water users in place before that time could apply for a "vested" water right. Water rights issued after 1945 are referred to as "appropriated" rights. The number of water rights started increasing in the late 1960s and leveled out by the mid-1970s/early 1980s.

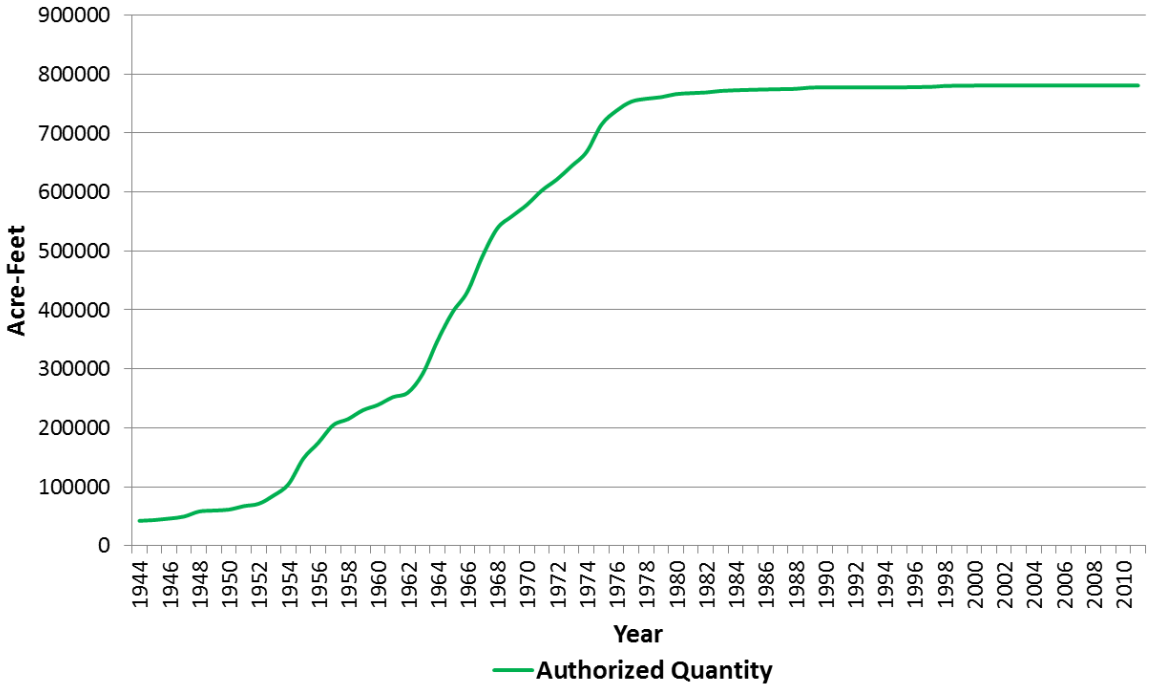

Figure 24. Total authorized quantity of Kansas groundwater-based water rights in the model's active area.

Estimation of Historic Water Use

Although Kansas water-use reports go back to 1958, actual water usage across large areas was probably much higher than these reports would indicate, since it wasn't until 1978 that water rights were required to be obtained before diverting water for beneficial use. Even then, it wasn't until the early 1980s that water-right holders were required to submit annual water-use reports and not until 1987 that the KDA-DWR had the regulatory authority to fine water-right holders for lack of submission or knowingly falsifying reports. The Water Use Program of the Kansas Water Office was initiated in 1990. Now operated through the KDA-DWR, this program provides quality control and assurance for the submitted water-use reports. As such, reported water-use records were only downloaded from 1990 to 2012 (at the time of the model development, 2012 was the most recent year available for access as the 2013 reports were still under review).

In order to estimate historical pumping levels before 1990, linear regression equations were first determined based on the ratio of water use/authorized quantity versus precipitation between 1990 and 2012, similar to past KGS modeling projects (Whittemore et al., 2006: Wilson et al., 2008). However, as was seen in the GMD3 model (Liu et al. 2010), the R-squared value (percentage of total variation in water use/authorized quantity accounted for by the regression) based on precipitation alone was very low. Several attempts were made to improve correlations using a variety of selected subsets of water use against multiple independent climatic variables. However, none ever achieved R-squared values above 0.2.

A primary reason why linear regression of the water use/quantity ratio against annual precipitation failed may be that water use from 1990 to 2012 shows a notable declining trend while the authorized quantity, precipitation, and temperature exhibit little to any trend over the same time period. Many factors control changes in water use that are unrelated to precipitation, such as the economics of fuel costs and crop prices, which may account for these observations. However, it is likely the declining trend in reported water use is primarily the result of reduced water availability, although the improvement in the accuracy of metered use also contributed to the decline.

A solution was to add water-level measurements as another independent variable to represent changing conditions in the aquifer. A query of water levels showed that 29 wells have been measured virtually every winter from 1980 to 2012 (fig. 25). The average depth to water for all these wells was used as another independent variable. A simple linear trend starting from the predevelopment water table for the cells overlying these wells to 1980 was used to estimate water levels from 1947 to 1979.

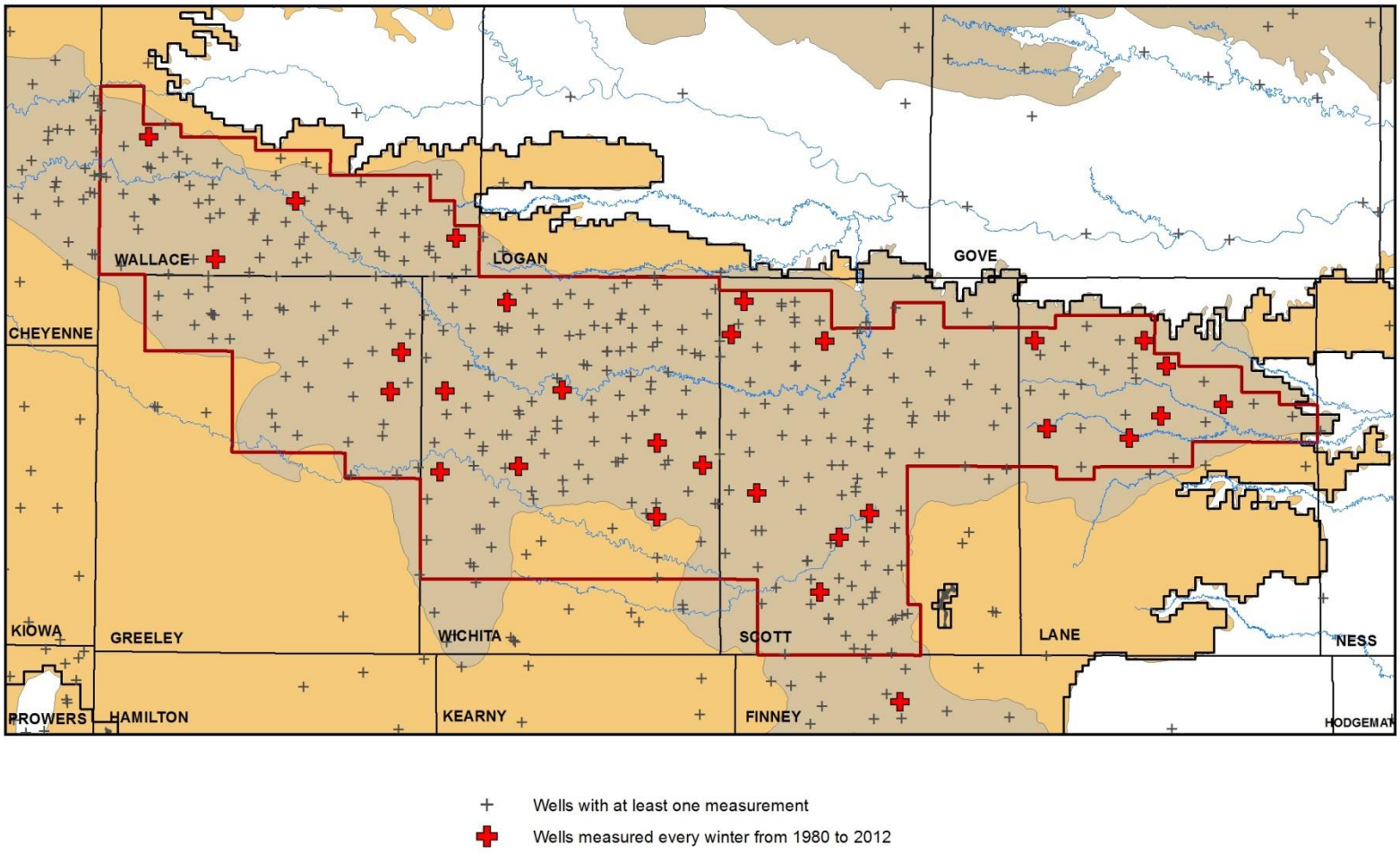

Figure 25. Selected wells with water-level measurements taken every year, 1980 to 2012.

Various iterations found the ratio of water use/authorized quantity against the annual precipitation, average maximum monthly winter temperature, and the average depth-to-water from selected monitoring wells from 1992 to 2012 yielded an R-squared value of 0.819. Figure 26 shows variations in the independent variables. The resultant R-squared value indicates that almost 82 percent of the variation of groundwater pumping in the Kansas portion of the model can be statistically explained by variations in annual precipitation, maximum winter temperatures, and changes in the depth to water.

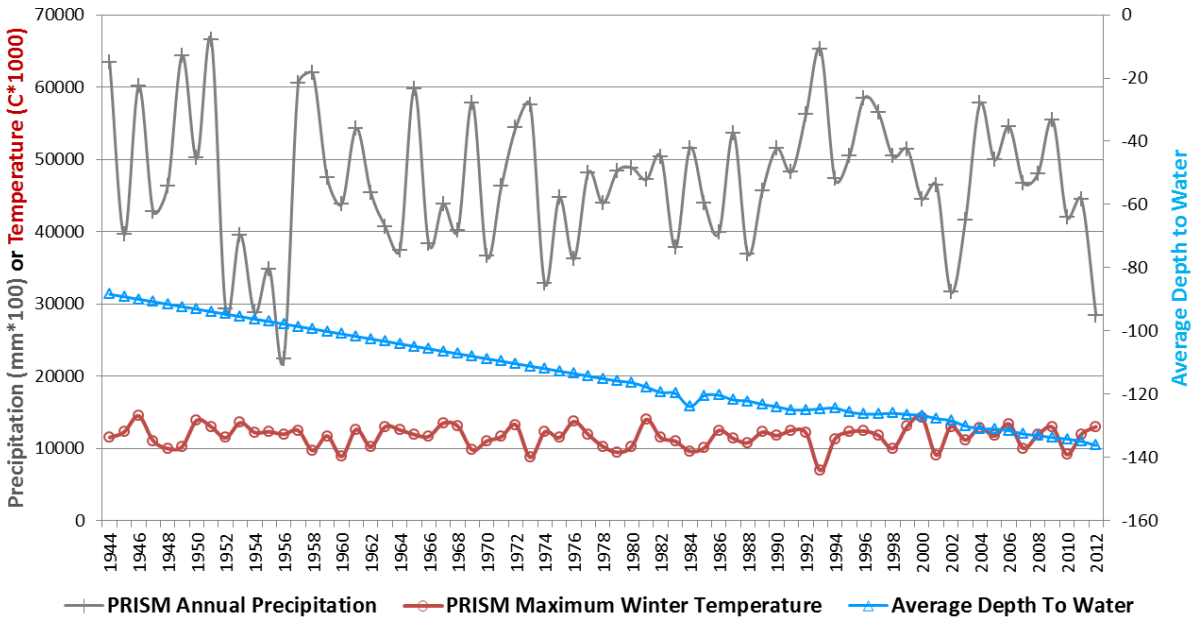

Figure 26. Independent variables used to regress the ratio of water use/authorized quantity.

Figure 27 shows the results of the regression-based water-use estimates against the authorized quantity and the 1990–2012 reported water use. The ratio of water use/authorized quantity is computed for every model cell for a given year based on variations in the annual precipitation, average maximum monthly winter temperature, and the average depth to water, represented as a negative number, at the start of each year for 29 selected monitoring wells. That ratio is then multiplied against the authorized quantity for a given year to yield an estimate of the amount of water used. The transient model uses the regressed water use from predevelopment until 1989, the actual reported water-use data for 1990–2012, and regressed water use for years going forward after 2012.

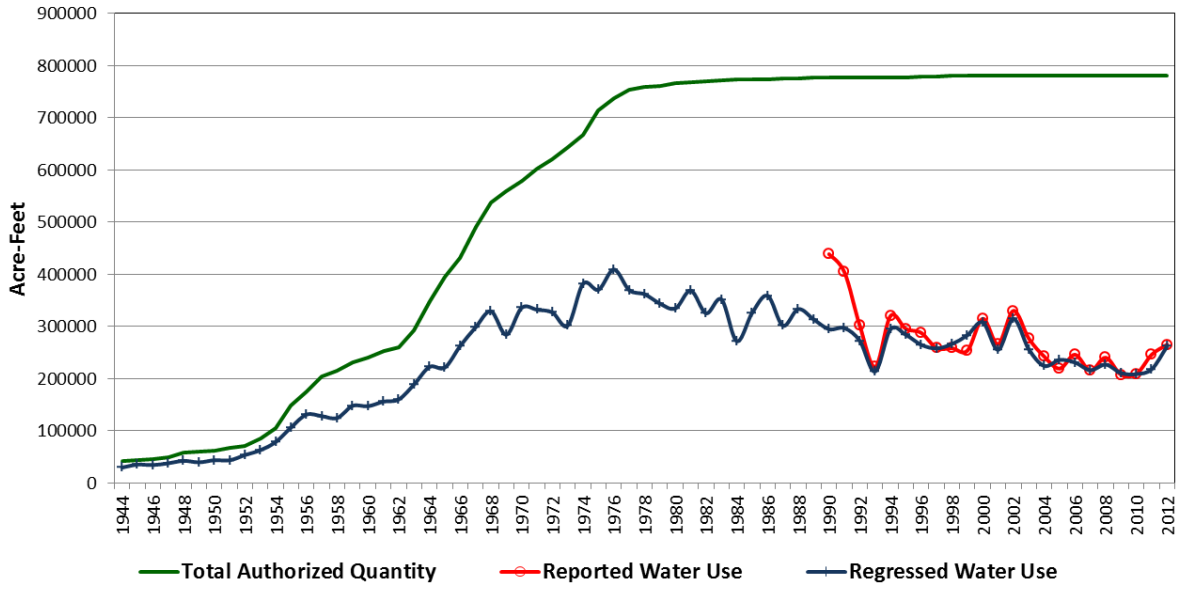

Figure 27. Total authorized quantity, regressed water use, and reported water for the Kansas portion of the model.

Colorado

The Colorado Decision Support System (CDSS), developed by the Colorado Water Conservation Board and Colorado Division of Water Resources, provides GIS-ready information about groundwater diversions. For this project, well application data were downloaded from the CDSS interactive mapping application in the area and further processed to produce information similar to that provided on the Kansas side of the model. The Colorado data are likely based on complex underlying information, similar to the Kansas water-right data, but we do not know all the complexities associated with the Colorado data. Consequently, the processing results should be viewed with a certain level of caution.

The CDSS records contain information related to permit numbers, annual permitted quantities, use(s) of water, well characteristics, aquifer sources, and dates of use. To isolate only active, large-capacity wells, the CDSS data were queried to select only "Constructed" wells or those listed with "Permit Issued" or "Permit Extended" statuses with irrigation, industrial, or municipal uses of water. Records listed as being plugged, associated with expired permits, or screened in the Dakota were deleted.

Some CDSS records contained null permitted quantity values even though the well appeared to be active. In these cases, other information associated with each record was used to estimate a reasonable permitted amount. For example, the permitted acres, if provided, were multiplied by 2 acre-ft. This is similar to the maximum appropriated quantity allowed in Wallace County, Kansas. If only a pumping rate was listed, this value was multiplied by 1,440 minutes per day for 90 days. As a last resort, the permitted quantities were estimated by identifying possible places of use from aerial photographs and applying a 2 acre-ft per acre permit quantity.

Likewise, most CDSS records contained a record listing the first date water was used. Well construction date, permit issued date, or a representative date based on other surrounding permitted wells were all used as proxies to fill in missing values.

Estimation of Historic Water Use

Given the lack of any organized water-use data in Colorado (like most western states), the regression equation used to estimate water use in Kansas (based on annual precipitation, maximum monthly winter temperature, and average depth to water) was applied to model cells in Colorado against the Colorado permitted quantities. As a means of comparison, the regressed water usage for the 77 permits in Cheyenne County was compared against 77 water rights in Wallace County, Kansas, that were close to Cheyenne County and distributed over a similar-sized area. Figure 28 illustrates permitted quantities in Colorado similar to appropriated quantities in Kansas both in terms of absolute volumes and trends for the 77 water rights in each of the counties.

Regressed water usage is also very comparable between the two areas, although the Colorado estimated use data exhibit the same notable declining trend that is observed across GMD1 as a whole in contrast to the generally constant use for the selected water rights in Wallace County. In reality, the water usage in Cheyenne County is likely more similar to Wallace County given the aquifer there is quite viable in terms of water availability, with present-day flow rates still being measured in the thousands of gallons per minute. If needed, a future enhancement to the model might be to de-trend the groundwater pumping in Cheyenne County, Colorado, to match patterns seen in Wallace County, Kansas.

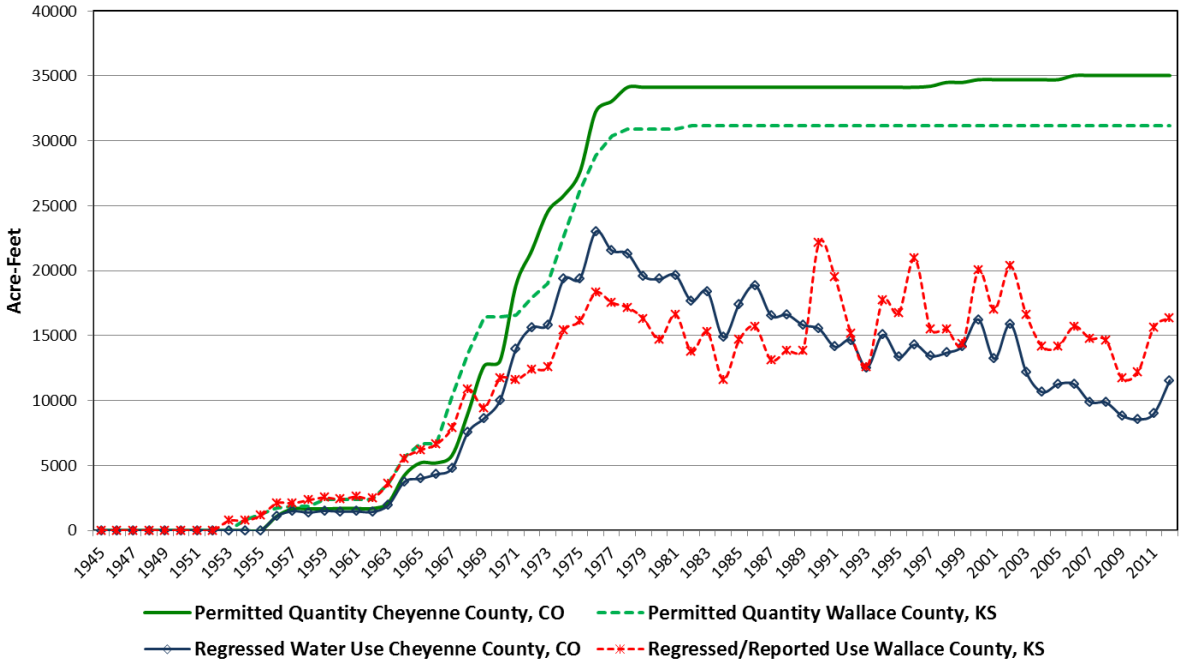

Figure 28. Total quantity and regressed water usage from the 77 water right or permitted wells in Cheyenne County, Colorado, and 77 selected similar wells in Wallace County, Kansas.

Irrigation Return Flow

A certain amount of water applied by irrigation systems makes its way back to the aquifer in the form of irrigation return flow. The rate of this aquifer recharge is determined by a variety of factors, one of which is the efficiency of the irrigation system. Irrigation system types were added to KDA-DWR water-use reports in 1991. County reviews of the reported irrigation systems from 1991 to 2012 across the model area show flood systems to be the most common type of system used in the early 1990s, with a shift to more efficient systems over time. Figures 29 to 31 show the trends in reported system types for Wallace, Wichita/Kearny, and Lane/Ness counties. As farming operations have improved with technological advancements, so have irrigation efficiencies, thus reducing the amount of return flow over time.

The irrigation return-flow percentages (relative to the total irrigation water pumped) used in the GMD3 model (Liu et. at., 2010) were assigned to the system types reported in the GMD1 water-use data. In order of decreasing return-flow percentages, those are the following: flood irrigation 25%, center pivot and flood 17%, center pivot 9%, sprinkler other than center pivot 9%, center pivot with low energy precision applicators (LEPA) 7%, and subsurface drip (SDI) in combination with other type 4%.

The average return-recharge percentage was then computed in each county for each year of 1991 to 2012 based on the number of each system type and its assigned return-flow percentage. It was assumed that flood irrigation was the only system type in use prior to 1955. Between 1955 and 1991, a smooth transition from flood to center pivot types for each county area was then applied. The total return-flow percentage averaged as a whole for each county shows a spatial pattern of increasing efficiencies moving from east to west across the model area (fig. 32). Water use occurring within these county areas is multiplied by the average return-flow percentage to determine the total amount of water returning to the aquifer. This return flow is treated separately from natural recharge in the model.

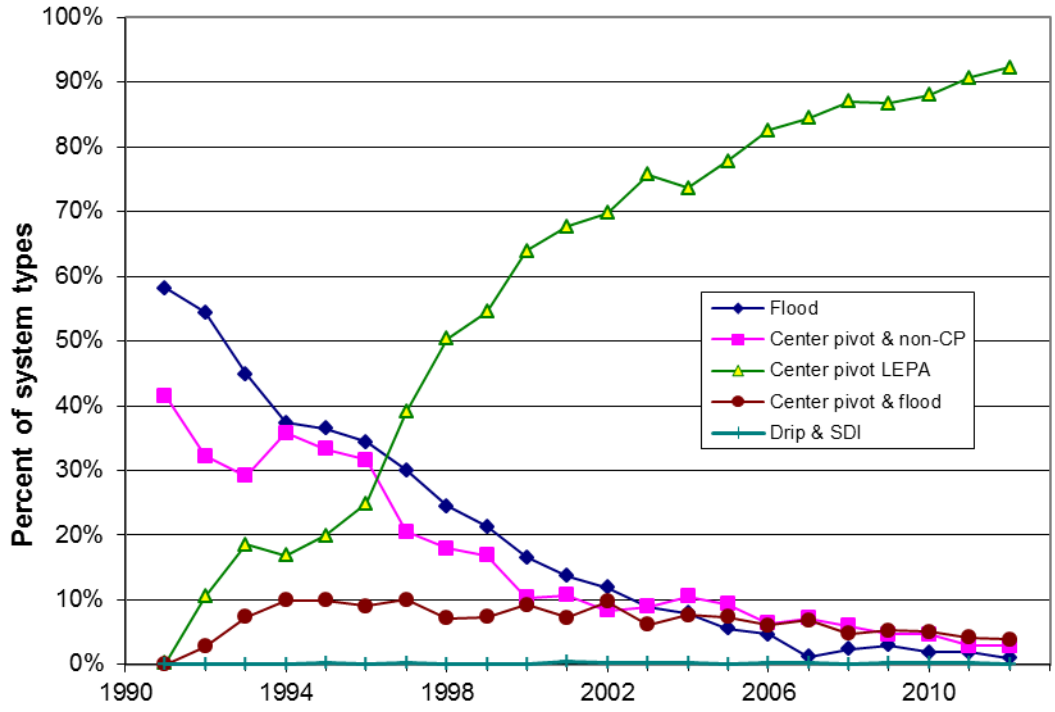

Figure 29. Reported irrigation system types, Wallace County GMD1 model area, 1990 to 2012.

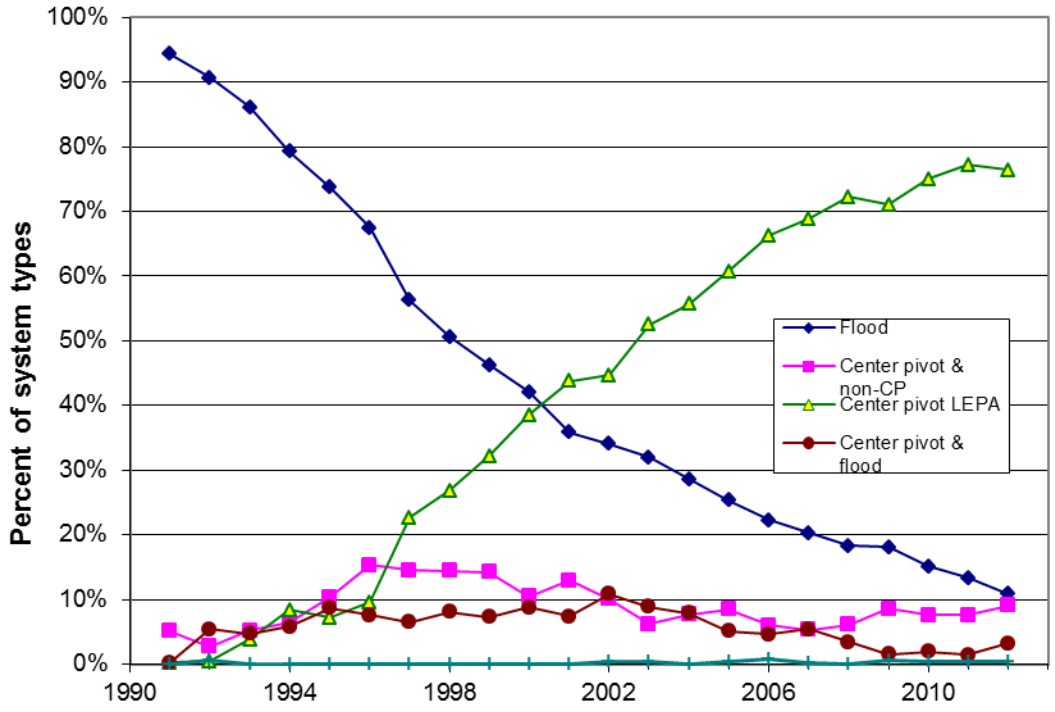

Figure 30. Reported irrigation system types, Wichita/Kearney counties GMD1 model area, 1990 to 2012.

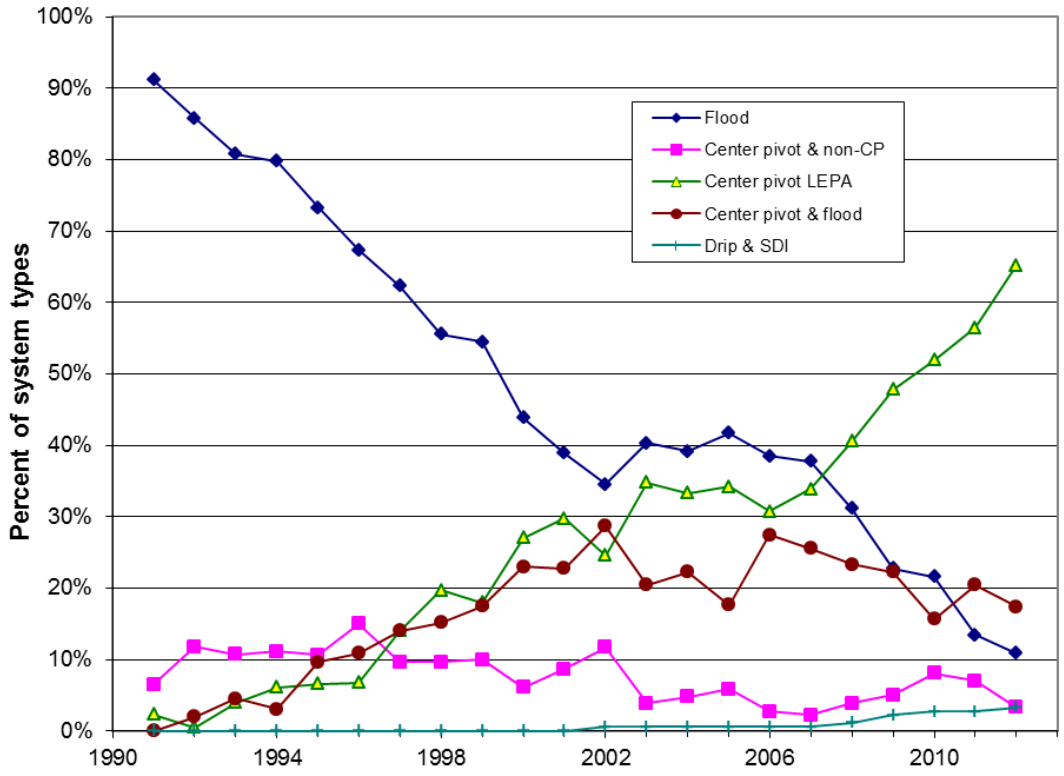

Figure 31. Reported irrigation system types, Lane/Ness counties GMD1 model area, 1990 to 2012.

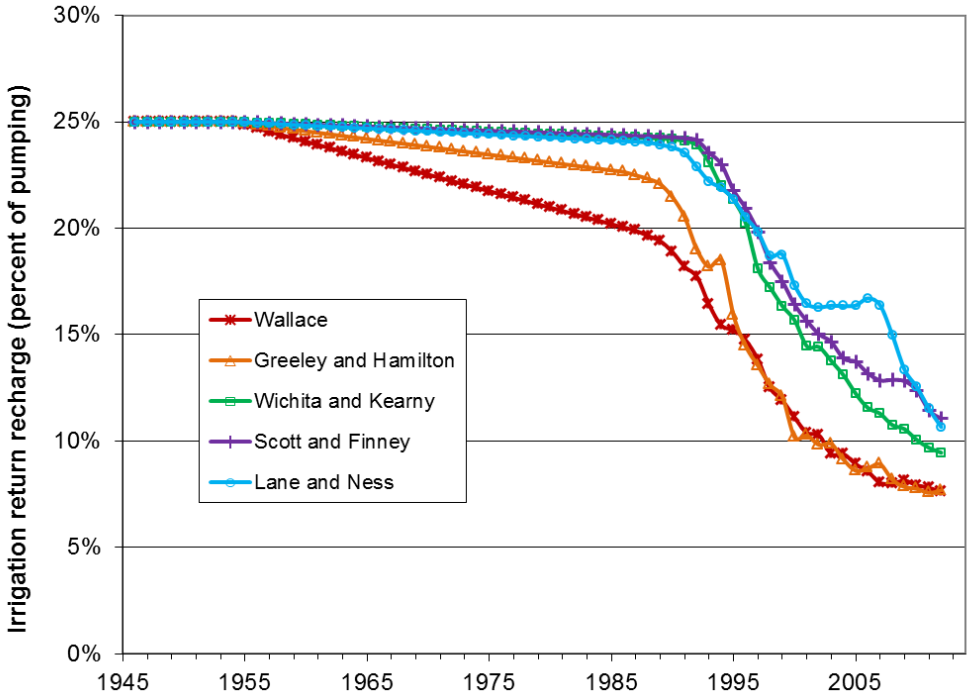

Figure 32. Average percentage of irrigation return flows by county, 1945 to 2012.

MODEL CALIBRATION AND SIMULATION

Like past KGS modeling projects, the GMD1 model is divided into two major simulation periods, a steady-state predevelopment period during which water levels remain relatively stable and a transient period during which groundwater development increases and water levels change over time. The predevelopment simulation establishes the conditions from which the subsequent transient model starts.

The major data sources for the predevelopment period cover the years 1944 to 1946. The average monthly Palmer Drought Severity Index for climatic division 4 (west-central Kansas) over this period was 1.71, which is in the range for slightly wet conditions (near normal is -0.5 to 0.5). Contrary to the term and implied conditions during "predevelopment" (a period of time representing the aquifer before it was extensively developed), the GMD1 model includes a relatively small but concentrated area of pumping, primarily in south-central Scott County. Given the high water availability, irrigation wells started appearing here in 1910, and by the 1940s, 129 wells were in operation irrigating an average of roughly 18,000 acres a year (Waite, 1947).

The transient period simulates groundwater conditions from predevelopment to 2013, during which time groundwater pumping increased, producing sizable water-level declines. The transient period is based on six-month time steps—a "summer" or growing season from April to September and a "winter" period representing the months of October to March. This project uses several techniques during the transient phase that have not previously been used by the KGS, specifically functions that estimate the travel time of surface-based recharge through the vadose zone, lagged drainage from dewatered sediments, and modifications to how the hydraulic conductivity and specific yields are calculated from detailed lithology logs.

Model Characteristics

Predevelopment pumping

Waite (1947) described irrigation-based groundwater development from 1910 to the mid-1940s and suggested it formed a region of decline that significantly altered the configuration of the water table. To replicate this, the steady-state or predevelopment model uses a pumping file. Both present-day active and inactive vested water rights, those permitted water rights that had verified water uses in place before the 1945 Kansas Water Appropriation Act, were queried from the WIMAS data. Point density functions show a large concentration of these in the area described by the Scott County geologic bulletin (fig. 33).

Two-thirds of the vested water rights' present-day authorized quantity was assumed to represent predevelopment pumping. Given the lack of any over-riding state or local water law and the readily accessible water supply, it was thought historic pumping would be higher than most water rights, where reported use is typically between 50 and 60 percent of the allocation.

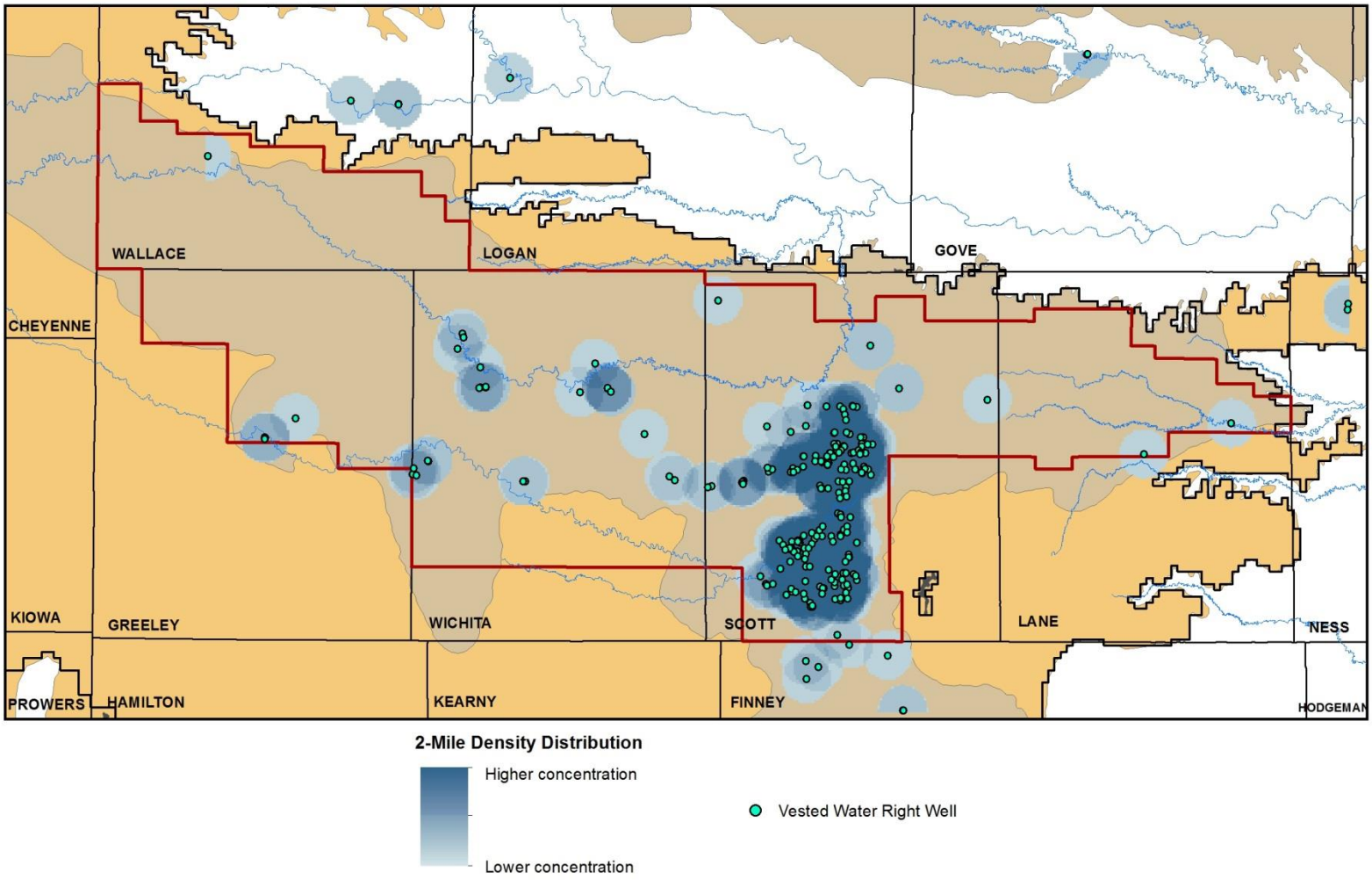

Figure 33. Distribution of Kansas vested water rights in the model's active area.

For the vested rights that today are listed as inactive, the model used the average authorized quantity of other active vested rights of similar uses of water to represent a past quantity (authorized quantity in WIMAS is only valid as of the date of the download and historic quantity values are not maintained). A total of 30,196 acre-ft was initially used to represent predevelopment pumping. Initial predevelopment simulation results suggested this estimate was too high and should be more in the range of 25% of the authorized quantities (based on comparing simulated to observed water levels). Pumping values at this level totaled 10,870 acre-ft, which falls into the range of water usage Waite (1947) estimated based on energy records (electricity and natural gas usage) from 1938 to 1945. Those estimates ranged from 9,400 acre-ft to 24,700 acre-ft with an average of 16,463 acre-ft.

Transient Pumping and Irrigation Return Flows

The "Water Right Development" section of the report describes how groundwater pumping is determined for both the Kansas and Colorado portions of the model. The reported and regressed water usages are for an annual basis. For the model's six-month time steps, all irrigation usage was assigned to the "summer" period representing conditions from April to September. All other groundwater usage was proportioned with 60 percent occurring in the summer period and 40 percent occurring during the winter period. Irrigation return flows were added to the overall recharge input file used by the model for the summer period.

Stream Characteristics

Ladder and Whitewoman creeks are simulated in this project as rectangular channels with an underlying streambed. The streambed widths were measured from aerial photographs at various locations and a representative value of 15 ft used throughout the model area. The streambed thickness is assumed to be 1 ft with a streambed conductivity of 0.01 ft/day. The limited streamflow data available from USGS gages at Ladder Creek below Chalk Creek near Scott City and Whitewoman Creek near Leoti were used in calibrating the stream-aquifer interactions.

Drains

Drains are used along most of the northern and eastern extent of the model's active area where the headwaters for numerous tributaries have cut into the HPA. Drains allow water to discharge from the aquifer based on water-table elevations relative to the drain cell's elevation. The drain elevation for each drain cell was set to 20 ft below its land surface elevation to represent the erosional channels of ephemeral streams. Drains were found to be important for lowering the simulated water levels to produce a better agreement with observed water levels during the predevelopment period. The impact of drains diminishes with time during the transient phase as the water table declines with the intensifying pumping.

Evapotranspiration

Evapotranspiration (ET) from groundwater was only considered in the alluvial valleys of Ladder and Whitewoman creeks where the water table is close to the land surface. The maximum ET rate at the land surface and the extinction depth were estimated to be 4 in/yr and 5 ft, respectively. When the depth to water is between the land surface and extinction depth, the ET rate is linearly interpolated based on the depth to water relative to the extinction depth.

Time-Varying Specified-Head Boundaries

Time-varying specified-head boundaries are used for active model cells along the western and southern extent of the model's active area. Time-varying specified heads were established based on a time- and labor-intensive process of reviewing each model cell in relation to any surrounding water-level measurement. Water-level trends shown in the measurement history of wells were applied to the head-boundary cells.

Precipitation Recharge

Precipitation-based recharge was calculated based on the power-function used in the GMD3 model (Liu et. al., 2010),

$$R = \begin{cases} 0, & P < P_0 \\ a\left(P - P_0\right)^b, & P \geq P_0 \end{cases},$$

where R is precipitation recharge to groundwater, P is precipitation at a given model cell and six-month time step, P_0 is threshold precipitation above which groundwater recharge occurs, and a and b are the coefficients of the power function. The precipitation recharge calculated above represents the amount of infiltration through the surface soil of non-irrigated lands. The enhancement to precipitation recharge in irrigated fields is computed as an additional source of recharge water as discussed in the next section.

The model divides the recharge-precipitation power functions into three zones (fig. 34) and two time periods (summer and winter). Recharge in the main aquifer generally averages less than half an inch per year while the stream channels of Ladder and Whitewoman creeks along with the Scott County depression have higher recharge rates, accounting for enhanced recharge that occurs during runoff events. The actual recharge rate varies for each model cell as the precipitation amounts change between different cells and time steps. For the same precipitation, the recharge rate is higher in the non-growing season than in the growing season as surface evapotranspiration is much more significant in the growing season (higher temperature and more consumptive use by plants). The power-function parameters P_0, a, and b are calibrated by matching observed water levels and streamflows to simulated values.

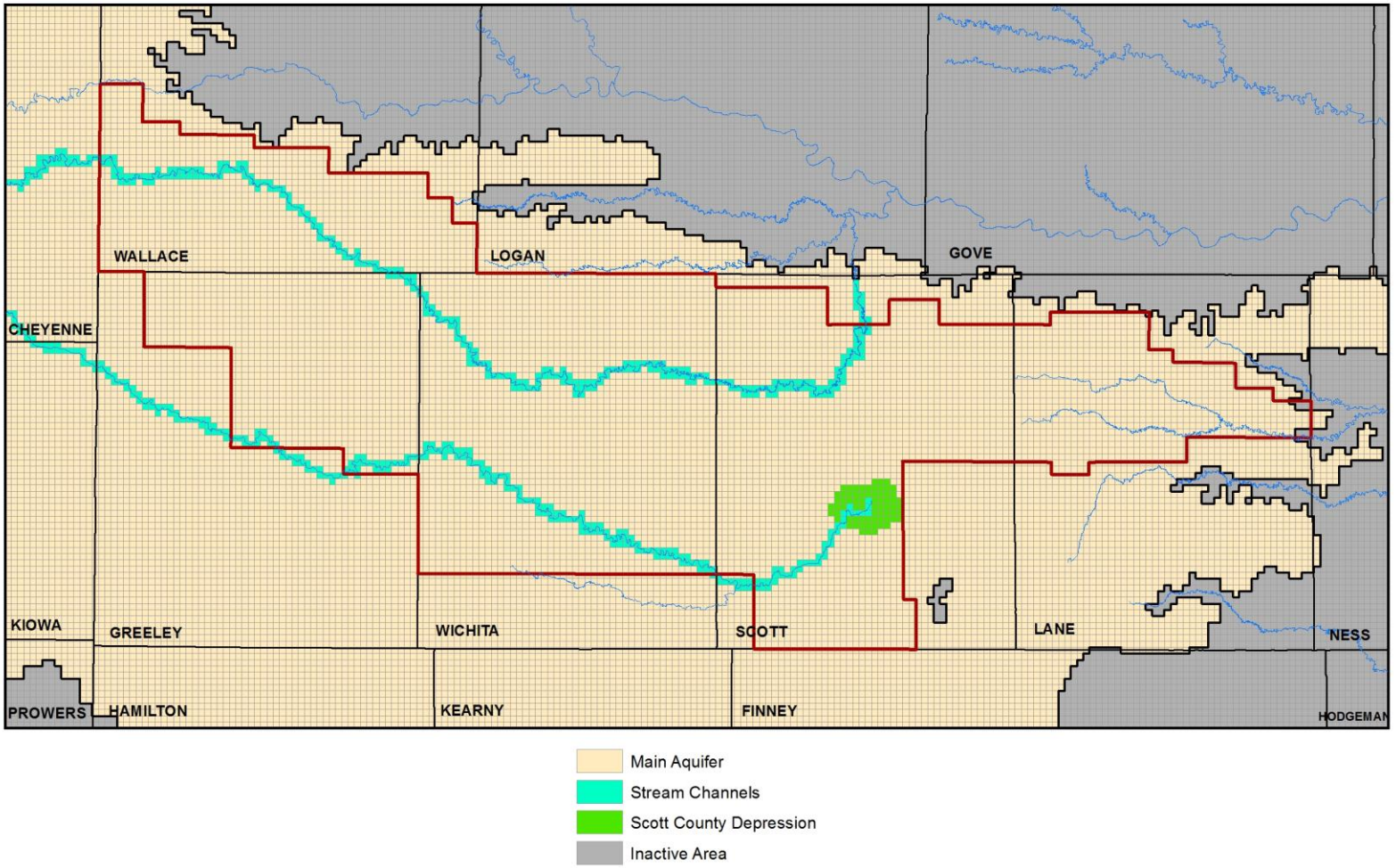

Figure 34. Recharge zones for precipitation-based recharge.

Irrigated Land Fractions

Precipitation-based recharge was enhanced for the model cells under irrigation since infiltration rates are higher when precipitation falls on irrigated soil that is already at or near saturation. In past KGS modeling projects, this adjustment was only used within model cells containing irrigation points of diversion. In reality, irrigation water is applied to field boundaries that can cross into model cells that do not contain pumping wells. For this project, field-irrigated enhanced recharge is based on where water is estimated to be applied, commonly referred to as the place of use.

KDA-DWR water-use reports contain information about the total number of acres irrigated each year; however, the location of the field boundaries is unknown. Each water right's permit or certificate specifies the authorized place(s) of use and, for irrigation uses, the authorized boundaries are categorized by 40-acre Public Land Survey System (PLSS) tract(s). The total net (referred to as "additional") acres for each 40-acre tract was summed and joined to a GIS layer representing 40-acre PLSS boundaries to spatially map the authorized places of use across the model area.

Figure 35 shows the distribution of 40-acre tracts symbolized by the total net acres authorized and represents conditions as of May 20, 2014. The average acres authorized under each 40-acre tract is 36.96. For a tract with 40 acres (or more), it is assumed the entire tract is irrigated. For tracts with less than 40 acres, irrigation is authorized within that tract but the exact location and field boundaries can only be determined by looking at the original water-right permit or certificate on file with the KDA-DWR. Like annual quantities, authorized place(s) of use are only maintained for present conditions.

A single water right often has multiple places of use, whereas a single place of use can be authorized under multiple water rights. Water rights in the model domain were grouped based on how they overlap each other by point(s) of diversion or place(s) of use. The earliest priority date within the water-right group was assumed to represent the first point in time irrigation water was applied to the 40-acre places of use authorized under the group. It was assumed the senior water right covered all the acres listed under the 40-acre tracts and the junior water rights in the group did not add any additional acreage.

To estimate the place-of-use data in Colorado, the circular field boundaries created by center pivots were identified on aerial photographs and then subjectively associated with the nearest permitted well. The date of first use associated with the wells was then assigned to the place of use. A few of the mapped pivot circles had no apparent well associated with them. For these places of use, the average date of first use for the Colorado data set, 1970, was used.

The Kansas 40-acre place-of-use tracts and the Colorado mapped pivot circles were then merged with the model cells and the percentage overlap computed. The enhancement of precipitation recharge by agricultural irrigation is computed by multiplying the precipitation recharge for non-irrigated land by a constant factor for the irrigated acreage in each cell over time, based on the priority date (or in Colorado, the date of first use) of the most senior water right. That factor is set to 1.0 based on the previous model study in southwest Kansas by Liu et al. (2010). Because the enhanced precipitation recharge by irrigation is added to precipitation recharge computed using the calibrated precipitation-recharge curve (assuming no irrigation), the total precipitation recharge in the irrigated fields is twice that if the fields were not irrigated.

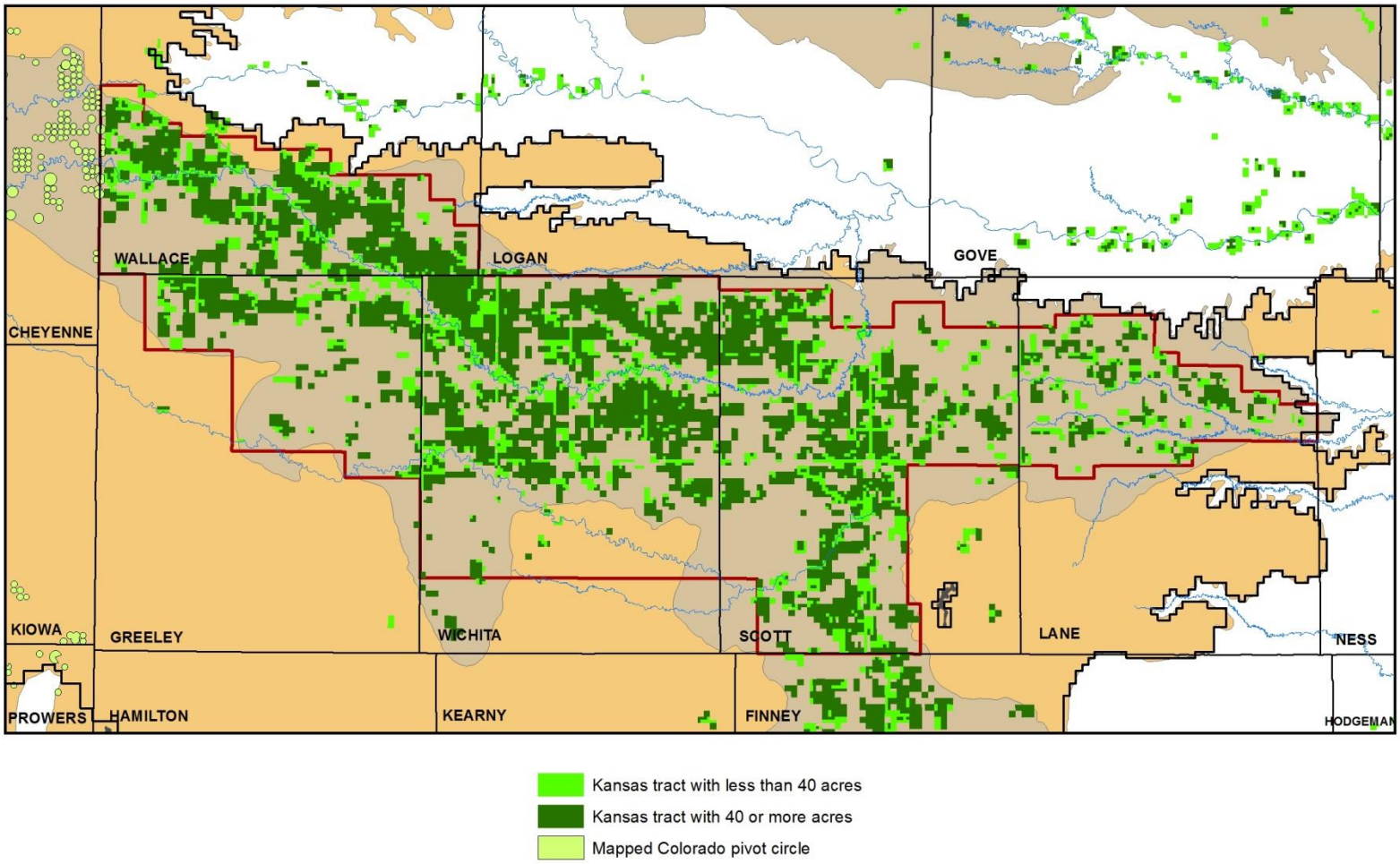

Figure 35. Authorized places of irrigation use as of May 20, 2014.

Delayed Recharge

Traditional groundwater models developed by the KGS and others assume that land-surface-based recharge reaches the water table within the same model time step. In reality, however, the downward movement of water can take a much greater period to reach the underlying aquifer, depending on the depth to the water table and the material of the vadose zone through which the water must travel. For precipitation-based recharge, seasonal fluctuations over time are likely smoothed out during the lengthy transit of water through a thick vadose zone, so that the actual recharge at the water table may be treated more appropriately as a constant rather than a temporally varying quantity. For the irrigation return flow, due to its large variation with time (largest in the 1970s–1980s when flood irrigation peaked), the timing of recharge at the water table could be significantly misrepresented if the travel of that water through the vadose zone is not adequately captured by the model.

A review of long-term hydrographs across the model area reveals that numerous wells share a similar pattern as illustrated in fig. 36 for selected wells from each of the five counties in GMD1. Winter measurements show an early period of higher rates of water-level declines in the 1970s and 1980s that began to slow during the 1990s only to accelerate again in the 2000s. Although there are wells in the region that do not exhibit this pattern, the trend is fairly persistent in hydrographs across GMD1 (along with areas in Northwest Kansas GMD4). The same trend can be seen in fig. 37, in which the average water-level change from 1970 to 2012 is plotted for all available winter depth-to-water measurements regardless of a well's observation history or duration. Precipitation patterns over the same time period show no trend (although drier conditions are prevalent starting in 2010) while pumping volumes (estimated and reported) show a notable decline since the 1970s. This implies the rate of aquifer recharge in the 1990s may be higher than that in the previous years so that the rate of water-table decline is smaller during that time compared to the rest of the period.

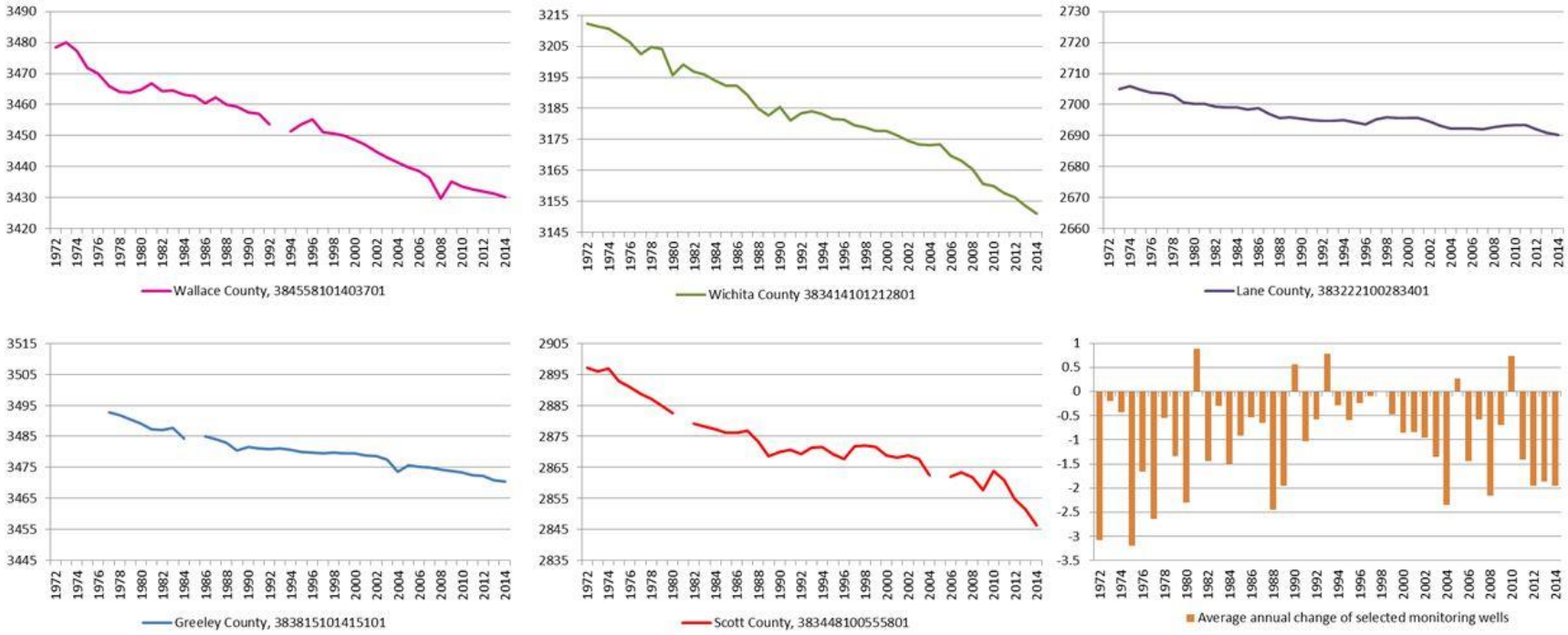

Figure 36. Water-table elevation hydrographs of selected wells and their average water-level change in GMD1.

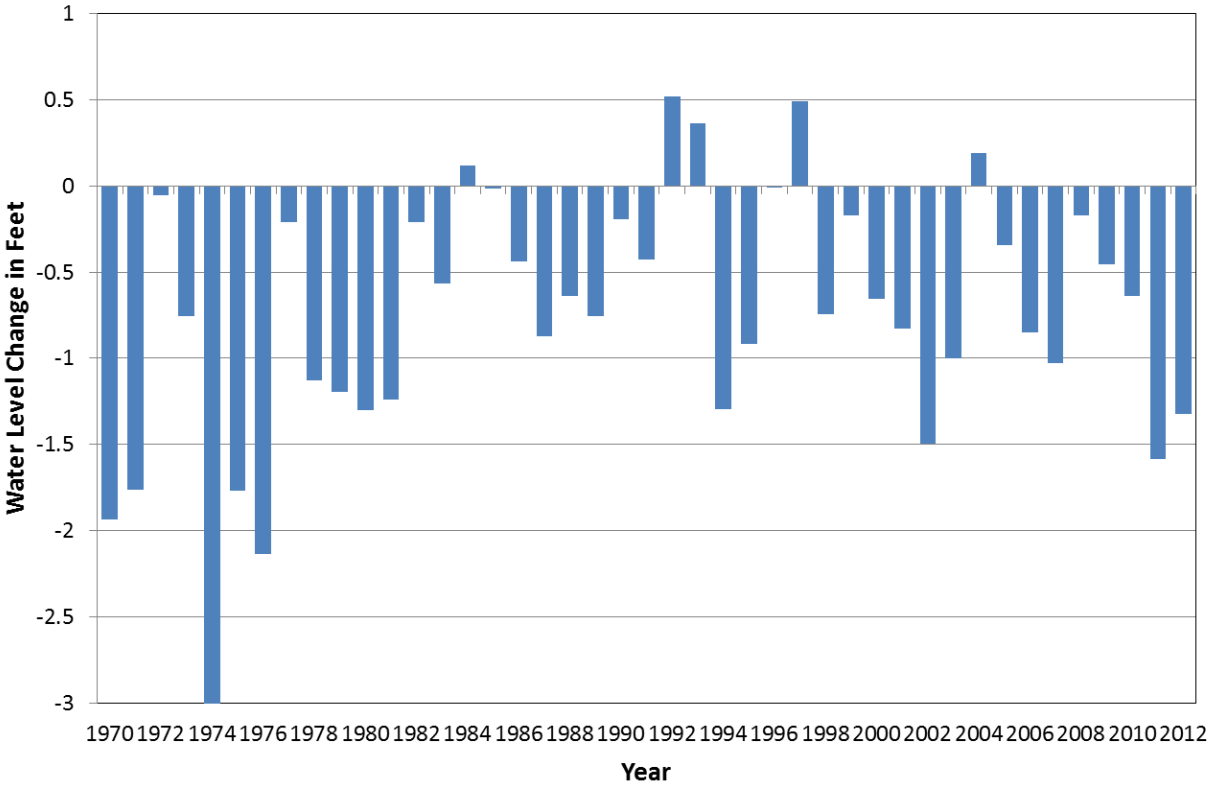

Figure 37. Annual water-level change based on all available winter water-level measurements in GMD1.

Interpretation of the hydrographs from the continuously recorded water levels collected by the index wells in Thomas County and Scott County suggests that inflows to these sites, at least temporarily, are greater than originally thought (Butler et. al., 2015). The source of this additional recharge is yet to be determined. At the time of this report, the two most likely sources for this inflow are thought to be 1) water temporarily held by less permeable layers below which water levels had declined, that eventually drains under the force of gravity, and 2) return flow from decades-old irrigation application that finally reaches the water table.

These additional inflows to the aquifer likely combine with each other and have varying time constraints in terms of their influence and duration. Slow drainage from fine-grained sediments introduced by declining water tables would be a one-time event spread over a given period as eventually the mass of water in question, which is not replenished, reaches the water table. Return flows from historic (and less efficient) water irrigation practices would also be considered temporary given the declining trend in pumping volumes and ever increasing irrigation efficiencies.

The consistent patterns in water-level changes shown in figs. 36 and 37, as well as the results from the index wells in Thomas County and Scott County (Butler et. al., 2015), led this project to develop a new recharge approach that does not make the traditional assumption of instant recharge from the land surface to the water table. Instead, we considered the travel of water

that must take place in the vadose zone before water-table recharge occurs. A key component to this concept is that the irrigation return flows from past and less efficient irrigation systems, along with precipitation-based recharge and enhanced recharge from irrigated lands, is delayed based on the ever-increasing vertical distance surface recharge water must travel to reach the water table. This would help explain the slowing rates of water-level declines in the 1990s as the majority of irrigation return flows from past water usage starts to reach the water table during that time. As pumping volumes decrease and irrigation systems become more efficient, less and less water enters the subsurface, resulting, at least temporarily, in accelerated water-level declines in later years, even if pumping was reduced by a moderate amount.

To simulate the vertical movement of water through the vadose zone, all surface-based recharge, either from precipitation over a non-irrigated area, enhanced precipitation over irrigated lands, or irrigation return flows, is assumed to move down through the vadose zone at a constant velocity and diffusivity (diffusivity describes how water molecules spread out about the average velocity and is illustrated in fig. 38). This movement can be expressed by the following function:

$$R(z,t) = \frac{R_0}{2\sqrt{\pi Dt}} \exp\left(-\frac{(z-ut)^2}{4Dt} \right),$$

where R(z,t) is the recharge rate (L) at time t and depth z in the vadose zone resulting from a recharge event at the surface R_0 (L). The parameters *u* (L/T) and *D* (L^2/T) are the velocity and diffusivity of water movement in the vadose zone, respectively, both of which are dependent on properties of vadose zone materials and are determined by model calibration in this work. R_0 includes precipitation recharge, precipitation recharge enhancement by irrigation in the irrigated lands, and the irrigation return flows and is computed for each model cell and six-month time step. For water-table depth L and model time step t_L, the amount of water that has reached the water table from R_0 is calculated as

$$R_T = \int_0^{t_L - t_0} R(L,t) u dt,$$

where R_T is water-table recharge from R_0, and t_0 is the time step at which R_0 is computed. To compute the total water-table recharge from the surface at a given time step, the model considers R_0 over all previous time steps that have $R_T > 0.0001 R_0$ (i.e., time step t_0 is included in the calculation if greater than 0.01% of surface recharge R_0 reaches the water table). The water that enters the water table from R_0 during a given time step is the difference between the R_T computed at the end of that step and the R_T computed at the beginning of that step.

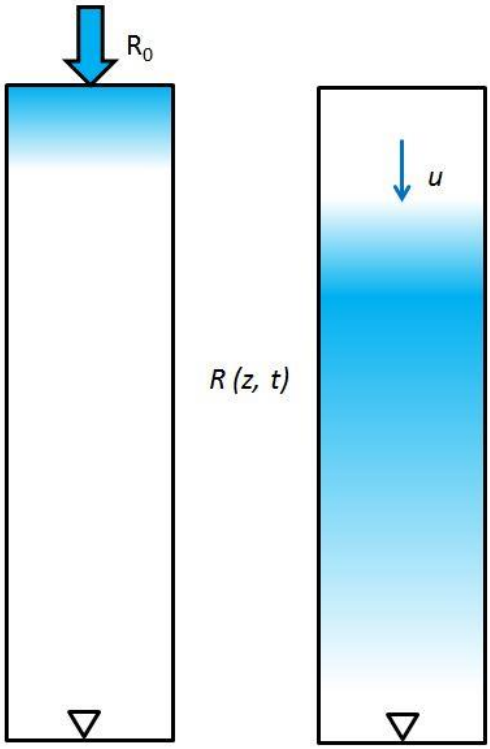

Figure 38. Schematic of the movement of surface recharge in the vadose zone.

Lagged Drainage from Dewatered Sediments

As the water table declines, the previously saturated material composing the aquifer still retains some water that is held in place by capillary forces. Part of this water will eventually drain down to the water table. This phenomenon is different from perched water, where some volume is being held up by an underlying aquitard. Here, both high and low permeability units become exposed as the water table drops and those units still retain water. Over time, a portion of that held water drains out under the influence of gravity. The amount of water being held and how readily it drains out depends on the material in question. The lower-permeability materials typically have finer grain sizes and can hold significantly more water after the water table falls and it will take a much longer time for that water to drain out than from the higher-permeability sediments.

For this modeling work, the lagged drainage of water after the water table fall is simulated with the following function:

$$W(t) = cd\exp\left(-d(t-t^*)\right), \quad t>t^*$$

where W(t) is the amount of water draining out at time t, t* is the time when the water table falls below the geological unit, c is the total amount of water for delayed drainage per unit volume of dewatered sediment, and d is the exponential decay coefficient (the later, the smaller the amount of drainage).

Figure 39 shows the curves of lagged drainage for seven different geological units (see table 1 for the detailed information about each categorical unit). Sand and gravel layers (categories 5–7) drain quickly and do not hold a significant amount of capillary water. Silt and clay layers (categories 1–4) can hold a sizable amount of water, however, because of the small pore space and may retain the vast majority of it for decades or centuries

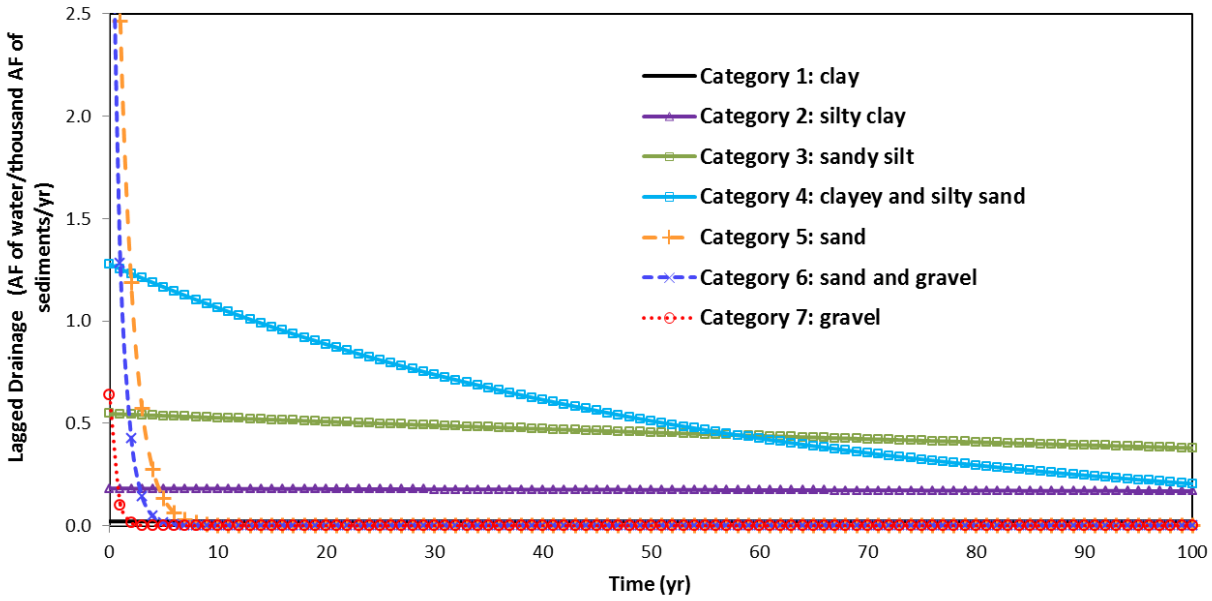

Figure 39. Lagged drainage of water for different geological units.

Hydraulic Conductivity and Specific Yield

As described earlier, the code developed for the HyDRA project has been used to develop a three-dimensional grid describing the proportional distribution of seven different categories of the material composing the aquifer throughout the model domain, based on drillers' logs contained in the WWC5 database and other sources. A special program was developed to allow water levels generated for each time step in MODLFOW to intersect with this three-dimensional grid to compute proportion-weighted averages of K and SY in each cell of the two-dimensional flow model.

For the predevelopment K calculation, the effective K for each model cell is the proportion-weighted vertical average of the category-specific K values, based on the category proportion occurring between the predevelopment water level and bedrock in that model cell. During the transient portion of the model, two water levels are associated with each model cell, representing the start and end water levels at each transient time step, with the average K computed from the average of the two water levels to bedrock.

Calculations for SY follow a similar approach. However, two different vertically averaged SY values are computed, one representing the interval between the upper and lower water levels (the depth interval through which the water table is moving during that model time step) and one representing the interval between the lower water level and bedrock. The MODFLOW model uses the former SY value for simulation at each transient step.

Figure 40 shows the HyDRA lithology-based estimated K for the interval between the predevelopment water levels to the bedrock surface based on the estimates of K for each of the standardized lithologies listed in table 1. The average K across GMD1 was approximately 70 ft/day with the highest estimates originating from the coarse gravel deposits found mostly in Wallace County. Similarly, fig. 41 illustrates the HyDRA-estimated SY from the predevelopment water table to the bedrock surface based on the estimates of SY for each of the standardized lithologies listed in table 1. Note that although gravels such as those in Wallace County have a higher K value, they have a lower calibrated value of specific yield (the amount of water that can be readily pumped out) than the sands throughout the district. The lower SY for gravels can potentially be caused by poorer sorting of gravels (deposited in a higher-energy environment) than that of sands (deposited in a lower-energy environment). In addition, the simulated water-level changes that have been lower than the observed values in this area of Wallace County could be due to less-than-ideal model representation of bedrock conditions. Finally, fig. 12 illustrates numerous drillers' logs did not meet the average 20-ft interval for lithology classifications and thus were removed from consideration. Future enhancements to the model would be to further review the quality of these logs for possible inclusion to the HyDRA process along with similar lithologic classifications in the Colorado side of the model.

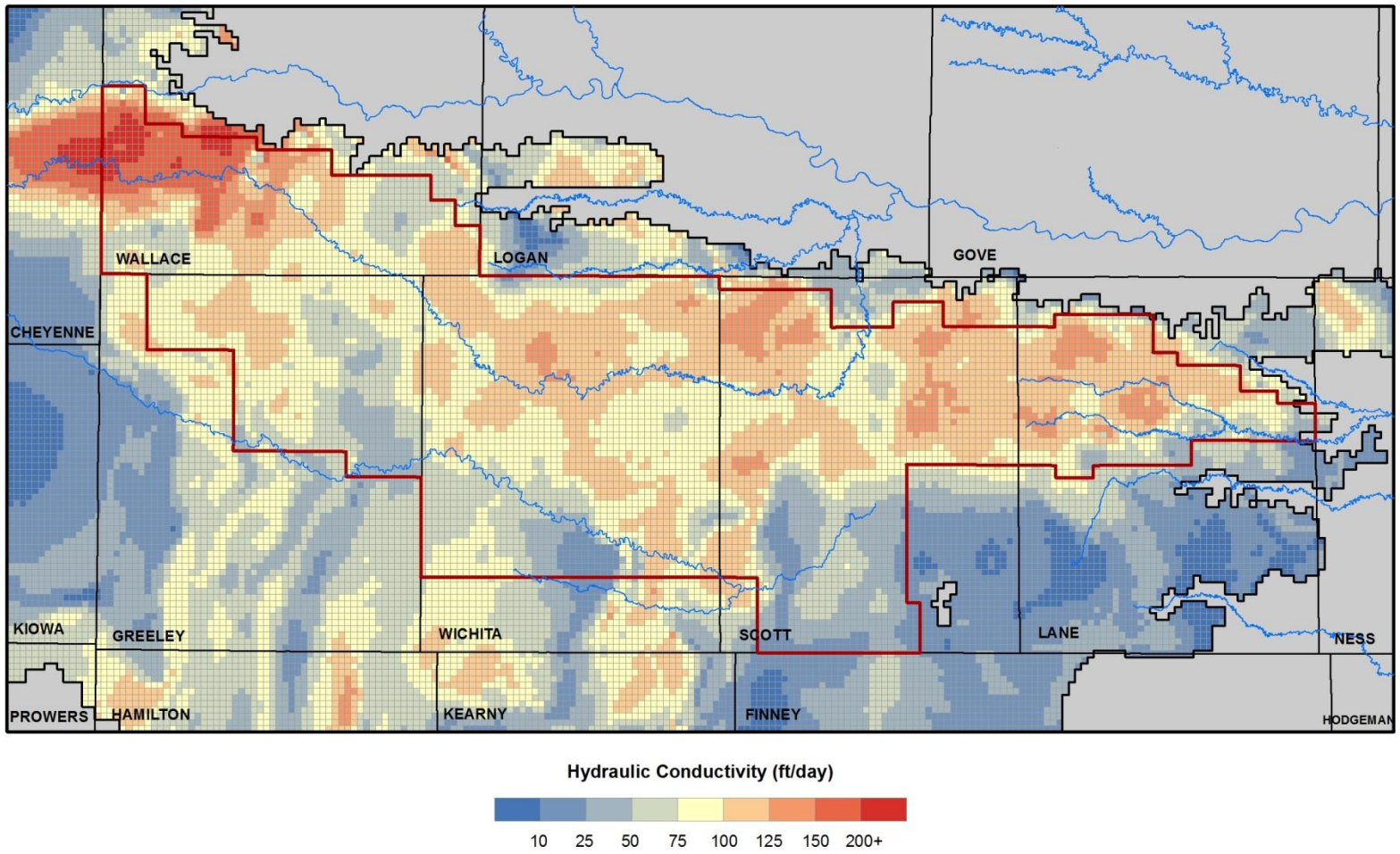

Figure 40. Vertically averaged K based on seven calibrated HyDRA lithologic classifications for the interval between the predevelopment water table and the bedrock surface.

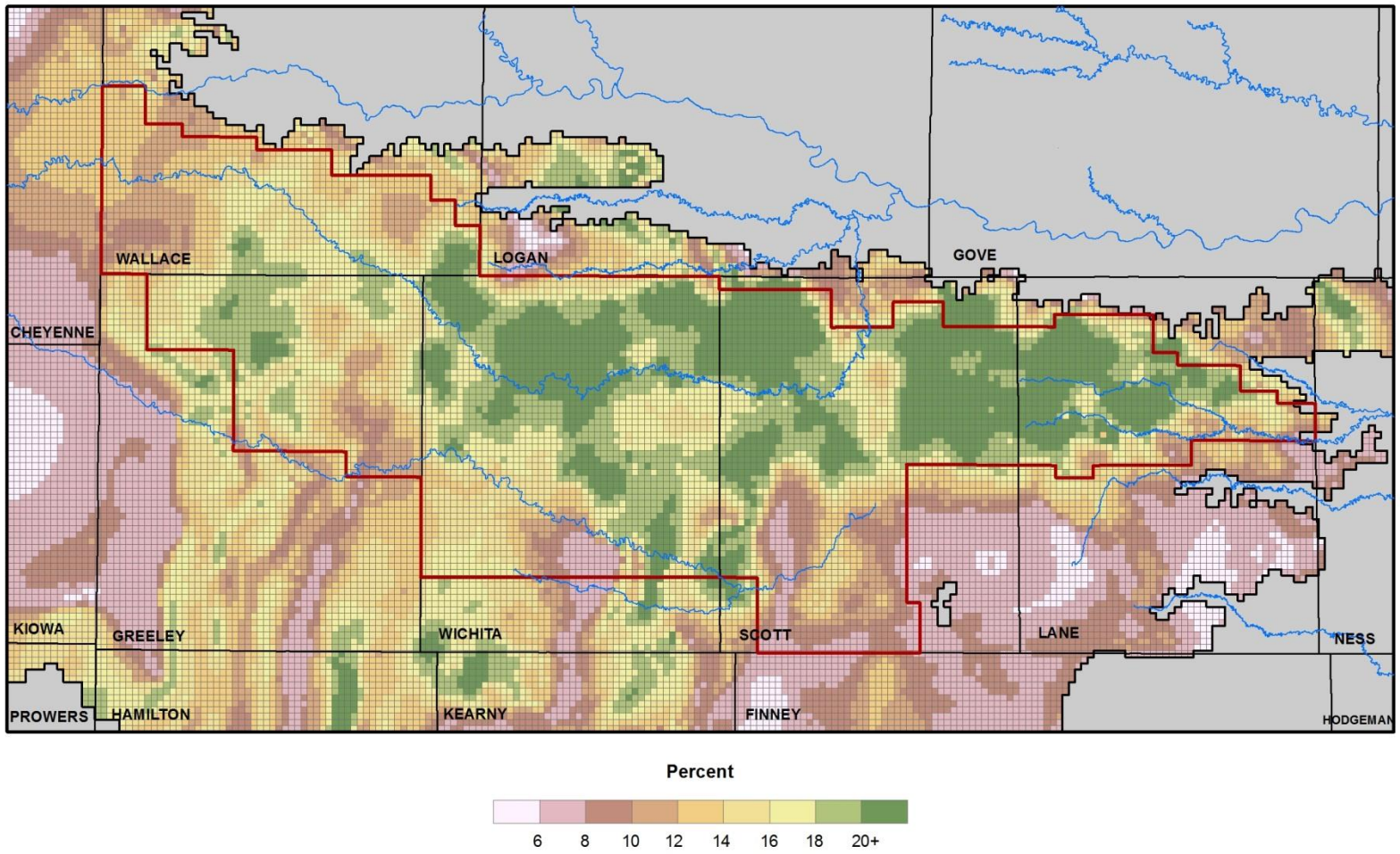

Figure 41. Vertically averaged SY based on seven calibrated HyDRA lithologic classifications between the predevelopment water table and bedrock.

Model Calibration

Because of our imperfect understanding of the hydrologic conditions in the field, some model parameters, especially those that are key contributors to aquifer budget calculations (e.g., aquifer K and SY, recharge rate), need to be adjusted so that the simulated results match with observed data to the best extent possible. This process is generally referred to as model calibration. For GMD1 model calibration, data for comparison with the simulated results include 1) water levels for a number of wells in the active model area from predevelopment to January 2014 and 2) streamflows for Ladder and Whitewoman creeks. For the wells that have multiple water levels during the transient period, the first value (i.e., the water-table elevation) is directly used in model calibration; for the subsequent years, the change between consecutive measurements is used instead. The water-level change provides a more sensitive indicator of aquifer response to different hydrologic processes during the transient simulation. The model parameters whose values were adjusted during calibration are 1) the threshold precipitation P_0 for recharge and power function coefficients a and b for all three recharge zones, 2) the velocity and diffusivity of water movement in the vadose zone, 3) the lagged drainage function coefficient c and d for all seven lithological categories, and 4) the hydraulic conductivity and specific yield for seven lithological categories. The calibration process was performed with the parameter estimation program (PEST; Doherty, 2004).

The delayed surface recharge and lagged drainage calculations significantly increased the computer run time. A MODFLOW run from predevelopment to January 2014 without these calculations took 15–20 minutes to complete; however, when the delayed surface recharge and lagged drainage were calculated for every six-month step, a predevelopment–2014 run took more than 20 hours. To significantly reduce the computer run time, the delayed surface recharge was calculated once every three years and the lagged drainage once every 10 years. By simplifying the delayed recharge and drainage calculations, the MODFLOW run time was reduced to 2.5 hours. The shortened time was necessary for PEST to perform the calibration successfully as hundreds of MODFLOW simulations are typically involved in a single PEST run.

The total number of calibrated parameters is much higher than that in previous KGS modeling projects due to the expansion of the lithological categories and incorporation of the delayed surface recharge and lagged drainage calculations. This, along with the fact that each MODFLOW simulation took a longer time to complete, significantly increased the PEST run time. As a result, the final PEST calibration run required a total of 305 MODFLOW runs and took nearly a month to complete. Note that after the model was calibrated, each future scenario simulation only took several hours.

Figure 42 shows the calibrated precipitation recharge curves for different recharge zones. For a given precipitation amount, precipitation recharge is much lower in the main aquifer than in the stream channels and Scott County depression. Note that in the non-growing season, the threshold precipitation at which water starts to infiltrate through the top soil (i.e., recharge starts) is lower, resulting in a larger recharge rate than that in the growing season for the same precipitation amount. The recharge rate is similar between the stream channels and the Scott County depression (identical in the non-growing season), indicating that these two zones can probably be joined together to form a single recharge zone without a significant loss of model accuracy.

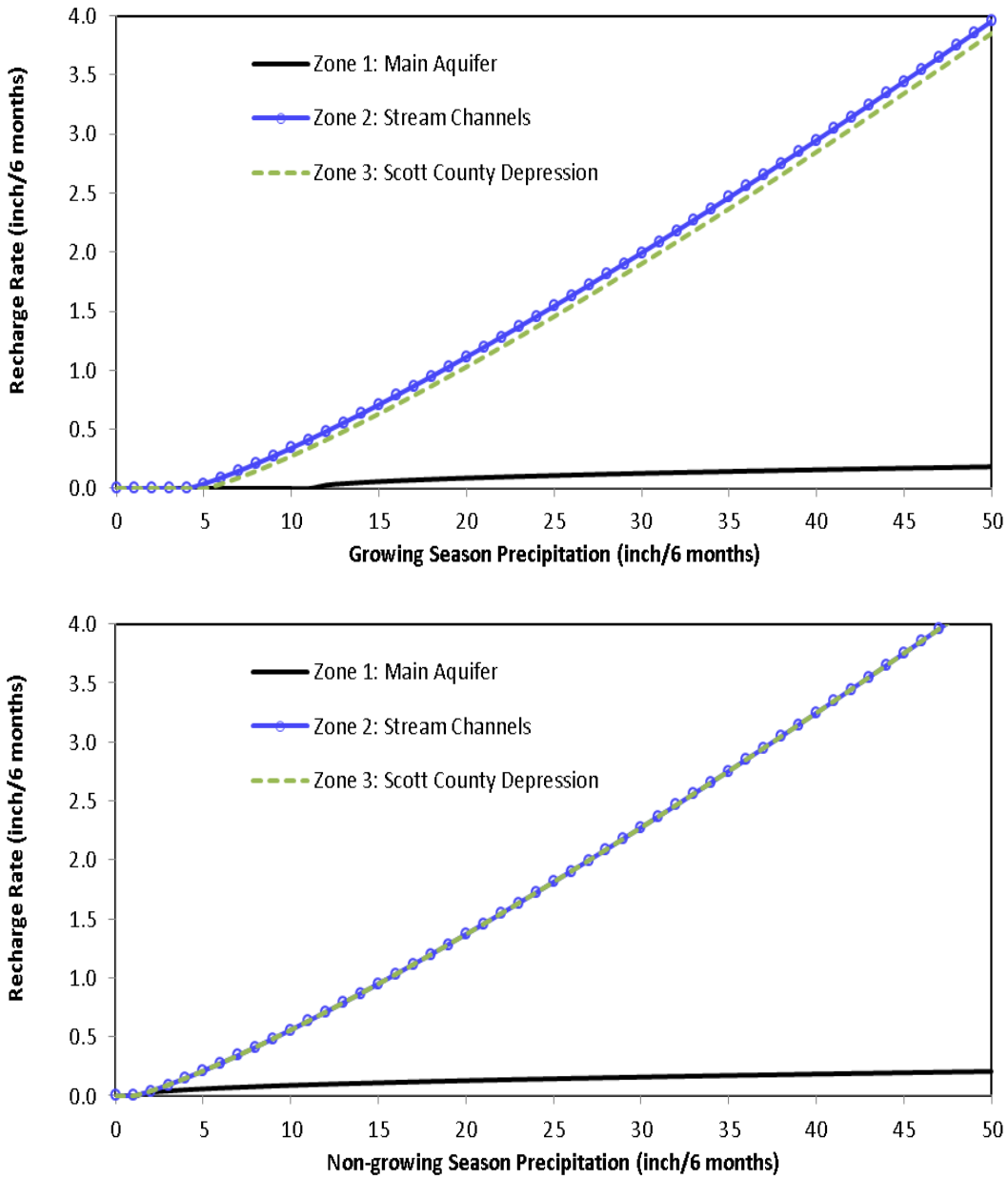

Figure 42. The calibrated precipitation recharge curves for different recharge zones in the growing (top chart) and non-growing (bottom chart) seasons. Precipitation recharge curves are essentially identical for zones 2 and 3 in the non-growing season (overlapping curves).

The calibrated velocity and diffusivity of water movement in the vadose zone are 9.4 ft/year and 0.01 ft^2/year, respectively. This indicates that in predevelopment time when the average depth to water was 90 ft, it took about 9.6 years for the main portion of surface recharge to reach the water table. In 2011, when the average depth to water increased to 135 ft, the average travel time of surface recharge to the water table increased to 14.4 years. Table 1 lists the calibrated values of K and SY, and fig. 39 shows the calibrated lagged drainage curves for each of the seven lithological categories.

Figure 43 shows the simulated versus observed heads from the PEST calibration. These heads are the first water levels recorded at each well. Most of these head measurements are for the predevelopment period. If predevelopment data are not available, the earliest water-level records from the transient period were used. As the figure illustrates, the simulated heads align very well with the observed values. Figure 44 shows the simulated versus observed transient water-level changes from the PEST calibration. Water-level changes were computed by subtracting the later water levels from their corresponding earlier values, so that positive values indicate a decline of water table with time. Figure 45 shows the simulated versus observed streamflows during winter time (average for January through March) at Ladder and Whitewoman creeks.

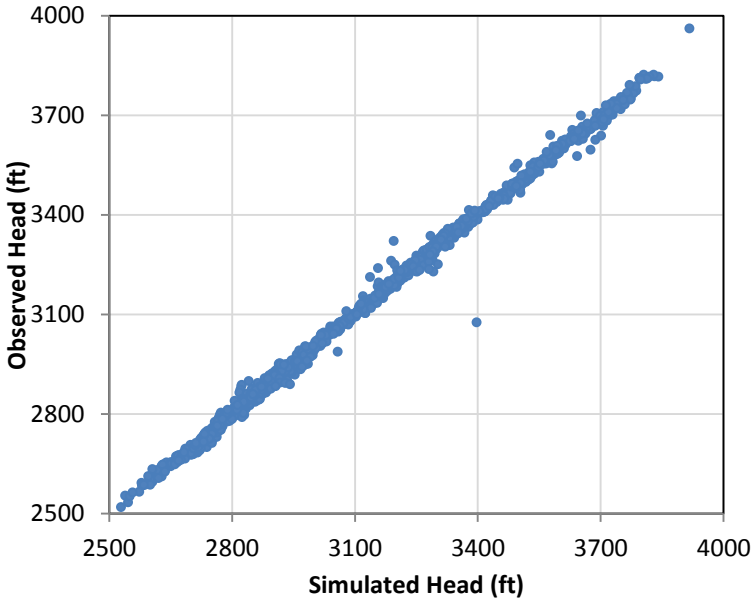

Figure 43. Observed versus simulated heads from the calibrated model. These are the water levels directly used in PEST calibration. Values plotted here are only for the first water levels recorded at each well. Predevelopment water levels, if available, are treated as the first water-level record at the wells. If predevelopment water levels are not available, the earliest water-level records in the transient period are used.

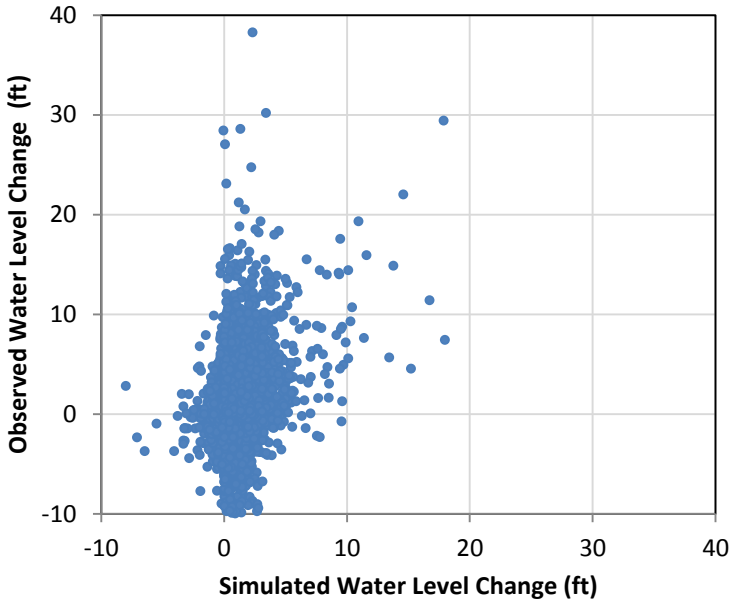

Figure 44. Observed versus simulated water-level changes from the calibrated transient model. Water-level changes are computed between two adjacent winter water-level measurements (separated by one or more years for each well).

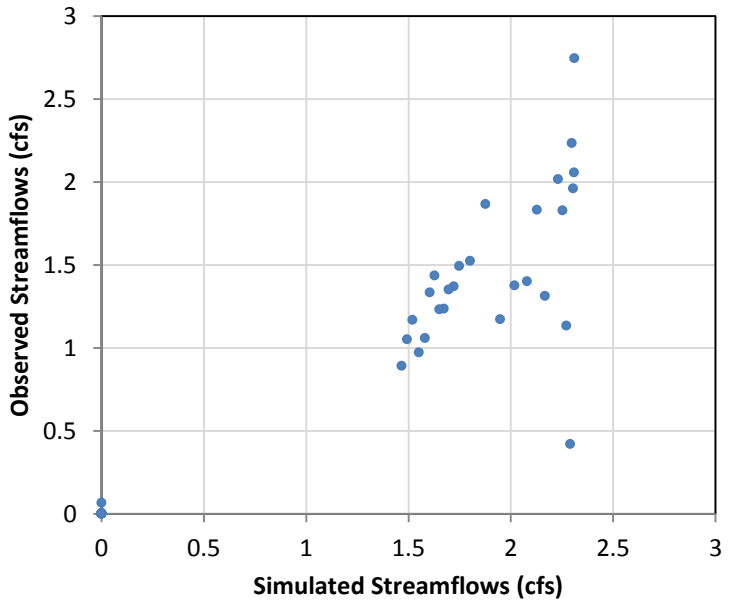

Figure 45. Observed versus simulated streamflows from the calibrated model.

Table 3 lists the mean residual, mean absolute residual, and root mean square of residuals of the PEST calibration data targets. The mean residual is given as the mean of observed minus simulated values, whereas the mean absolute residual is the mean of the absolute values of observed minus simulated values. The mean residuals for both the starting water level at each well and the water-level change during the transient period are very small, indicating the model provides a very good match for the overall water-table conditions between predevelopment and 2014 across the entire district. The simulated streamflow is also a very accurate representation of the gaged data during the winter period.

Table 3. Mean residuals, mean absolute residuals, and root mean square of residuals for model calibration targets.

	Number of data	Mean residual	Mean absolute residual	Root Mean Square of residuals (RMS)
Water level (ft)	1,544	-0.17	10.76	16.81
Transient water-level change (ft)	8,940	-0.0009	1.75	3.24
Streamflow (ft^3/sec)	48	-0.23	0.30	0.48

Sensitivity Analysis

Table 4 lists the sensitivities of different model parameters during model calibration. The relative sensitivity of a parameter *p* is computed as (Liu et al., 2010)

$$RS_p = \sqrt{\frac{1}{N}\sum_{i=1}^{N}\left(\frac{\partial d_i}{\partial p/\acute{p}}\right)^2}$$

where ∂p is the small perturbation around the calibrated parameter value $\acute{p}$; ∂d_i is the change in the model-simulated groundwater level or streamflow at observation *i,* and *N* is the total number of observation data points used in the sensitivity calculation. In table 4, p11 and p14 are the threshold precipitation for recharge to start during the growing and non-growing seasons in the main aquifer, respectively, and p12 and p13 are the precipitation recharge power function coefficients for the main aquifer. Similarly, p21 through p24 and p31 through p34 are the precipitation recharge parameters defined for the stream channels and Scott County depression, respectively. The parameters vel and dif are the velocity and diffusivity of water movement in the vadose zone. Parameters g11 and g12, g21 and g22 through g71 and g72 are the hydraulic conductivity and specific yield for the first, second, through seventh lithological category, respectively. Parameters c11 and c12, c21 and c22 through c71 and c72 are the lagged drainage function coefficients for the first, second, through seventh lithological category, respectively. Overall, all calibrated parameters have similar relative sensitivities, indicating that they have similar impacts on the statistical agreement between the model-simulated water levels and streamflows and the observed values.

Table 4. Relative sensitivities of different model parameters during the PEST calibration.					
Parameter	**Relative Sensitivity**	**Parameter**	**Relative Sensitivity**	**Parameter**	**Relative Sensitivity**
p11	0.11	p21	0.12	p31	0.12
p12	0.09	p22	0.12	p32	0.12
p13	0.13	p23	0.16	p33	0.13
p14	0.10	p24	0.15	p34	0.13
vel	0.09	g21	0.12	g41	0.12
dif	0.12	g22	0.12	g42	0.12
g11	0.12	g31	0.12	g51	0.09
g12	0.15	g32	0.12	g52	0.14
g61	0.12	c11	0.12	c31	0.12
g62	0.12	c12	0.12	c32	0.12
g71	0.13	c21	0.12	c41	0.12
g72	0.12	c22	0.12	c42	0.12
c51	0.11	c61	0.12	c71	0.12
c52	0.12	c62	0.12	c72	0.12

Transient Model Results

Water Levels

Figures 46 to 48 show a series of comparisons of the simulated groundwater elevations from the calibrated model in relation to interpolated observed data for the years of predevelopment, 1974, 1984, 1994, 2004, and 2014. The contour maps (top) are an indication of flow directions and water-level gradients while the cell-based shaded maps (bottom) show absolute differences between the simulated and observed water levels. In all years, the majority of the GMD1 area has model-estimated water levels within 25 ft of observed values. Although there are local mismatches in certain areas, the simulated water levels agree well with the observed values throughout the transient period.

Figures 49 to 51 compare the model's simulated water-level changes between predevelopment and 1974, subsequent 10-year intervals up to 2014, and predevelopment to 2014 with interpolated observed changes for the same intervals. Similar to the water-table elevation maps, the overall agreement between the simulated and observed changes is good across the core area of GMD1 with some areas having local mismatches. The largest discrepancy is found in southwestern Wallace County, especially in the later years of the transient period. As outlined in earlier sections of this report, bedrock elevations here are highly variable. It is thought the aquifer is becoming compartmentalized at the local level. As water levels fall below bedrock elevations, the aquifer units become isolated at the local level as lateral inflows are essentially cut off, a behavior not simulated during the model's transient phase. Further improvement in this area may be possible by using a finer grid to better represent these compartmentalized systems and additional lithologic logs to better define the aquifer properties.

Figure 52 plots monitoring well locations, labeled by the row and column of the model cell in which each well is located, that were used in the model calibration. The hydrographs for these wells are plotted in figs. 53 to 59. The transient model best matches simulated and observed water levels through the heart of GMD1, with water levels often within 20 ft of each other. There are examples of wells where the simulated values over- or underestimate the observed water levels; however, in most cases, they still mimic the same trends. The wells in the northwest corner of the district (southwest Wallace County) have the greatest disagreement. The well located in model cell row 21, column 23 shows that water-level declines have been accelerating in recent years, an indication that the aquifer here is becoming isolated as water levels fall below surrounding bedrock highs.

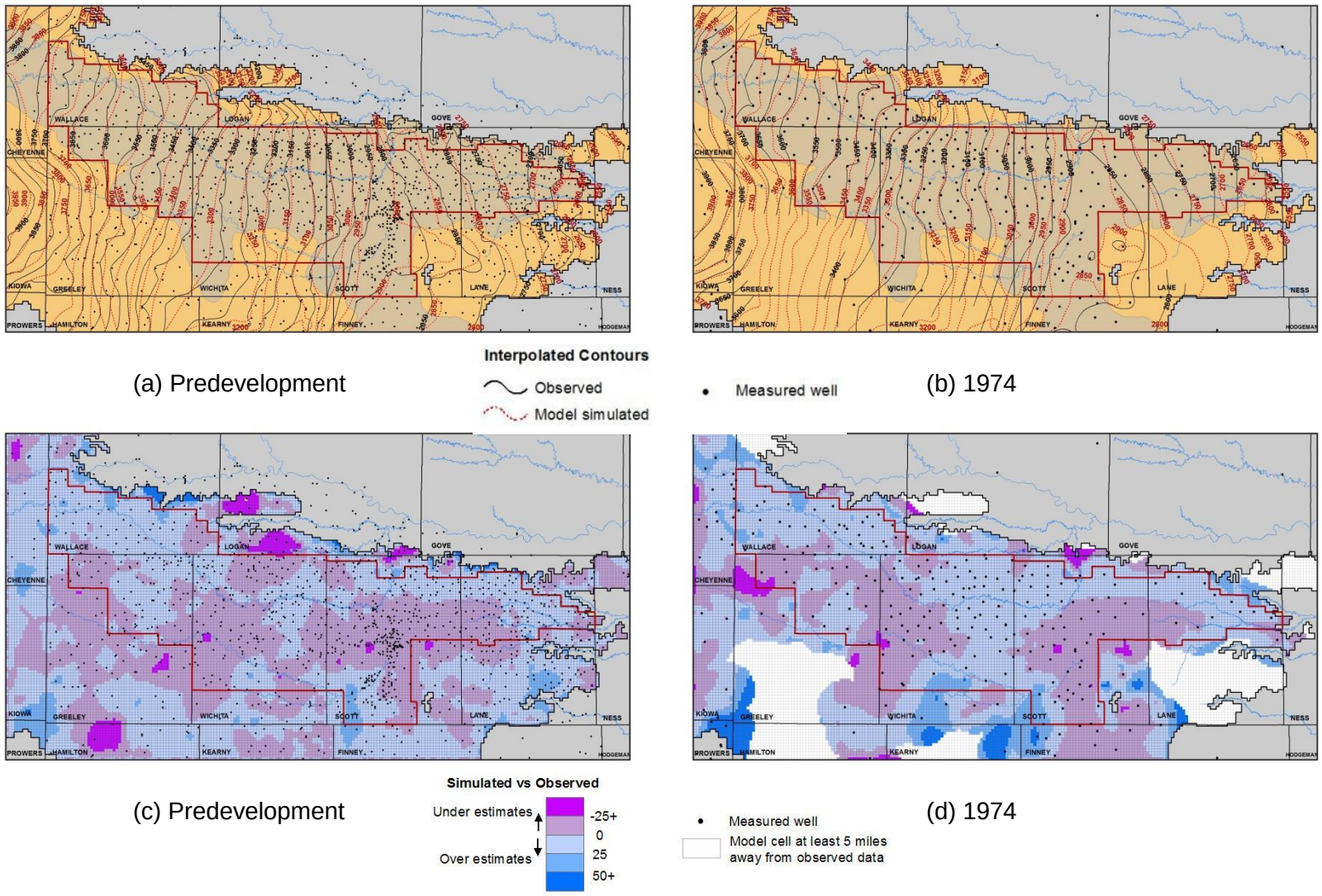

Figure 46. Comparison of simulated versus observed water levels, predevelopment and 1974.

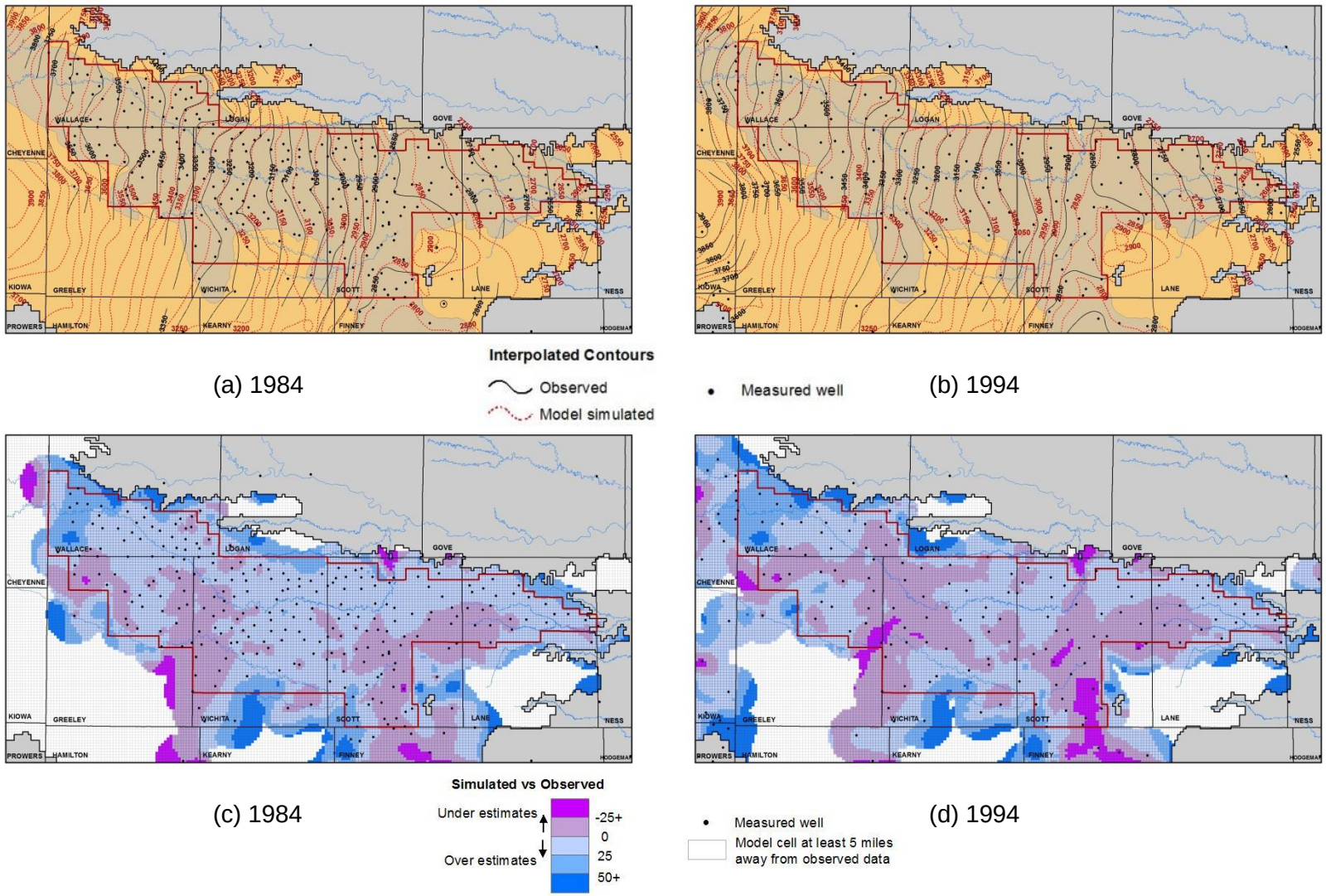

Figure 47. Comparison of simulated versus observed water levels, 1984 and 1994.

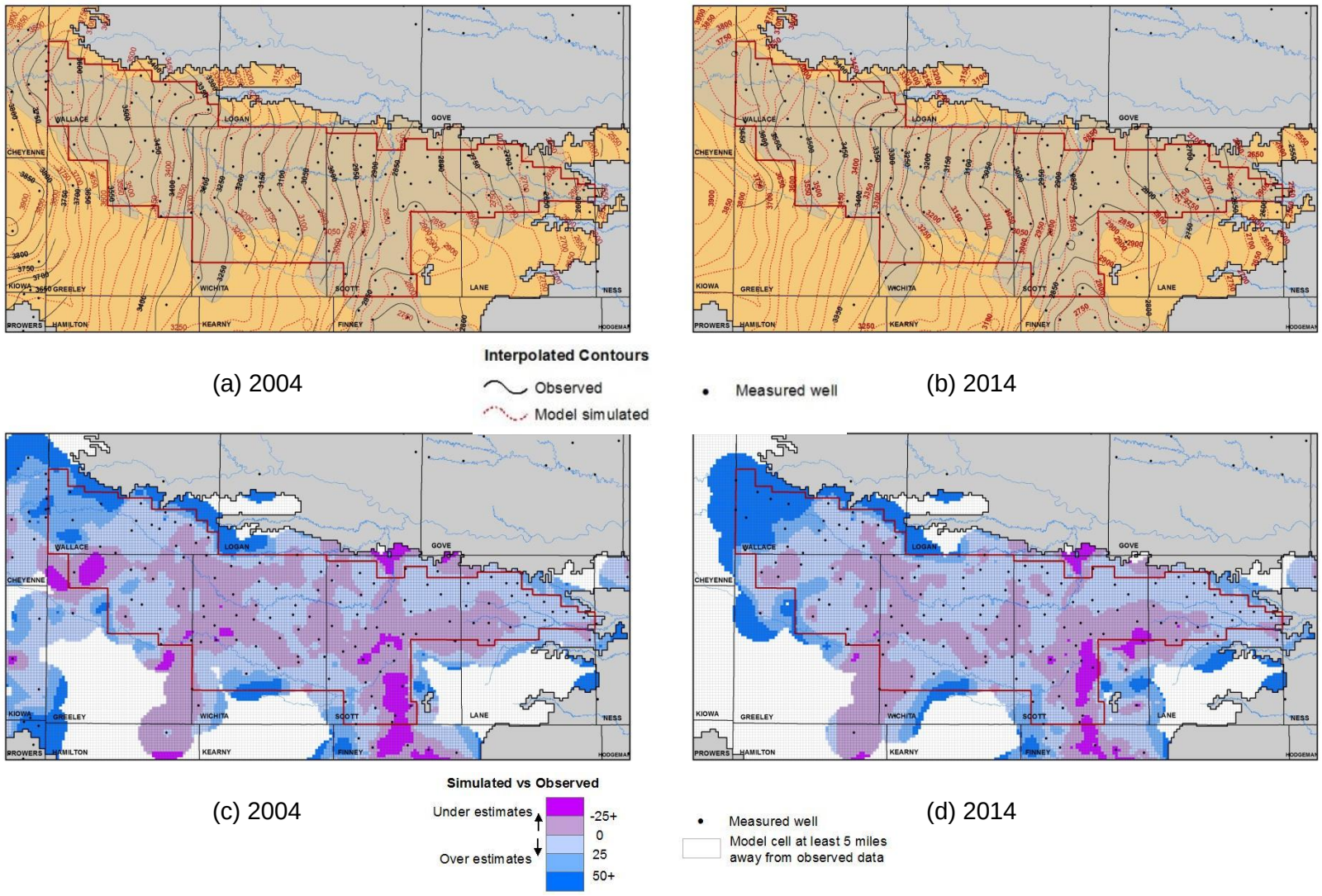

Figure 48. Comparison of simulated versus observed water levels, 2004 and 2014.

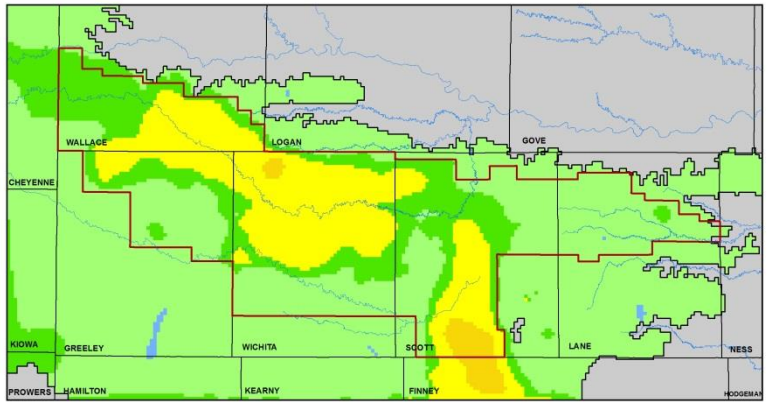

(a) Simulated predevelopment to 1974

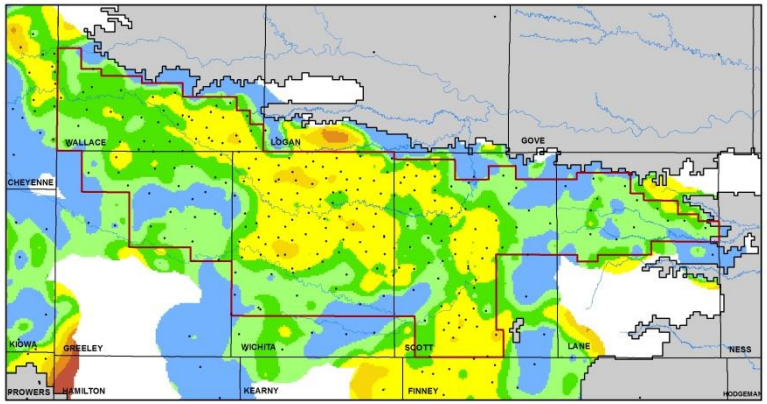

(b) Observed predevelopment to 1974

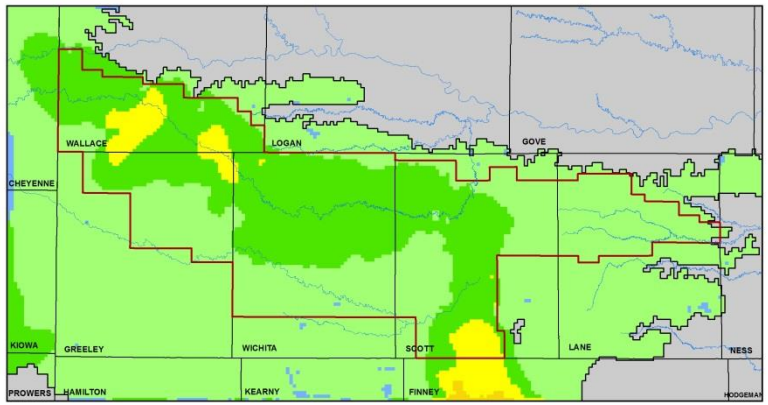

(c) Simulated 1974 to 1984

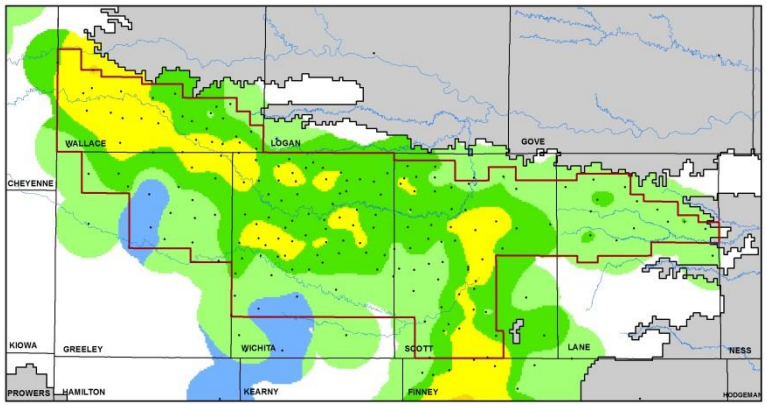

(d) Observed 1974 to 1984

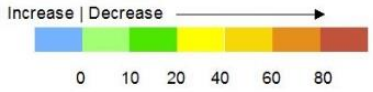

Figure 49. Simulated versus observed water-level changes for the intervals predevelopment to 1974 and 1974 to 1984.

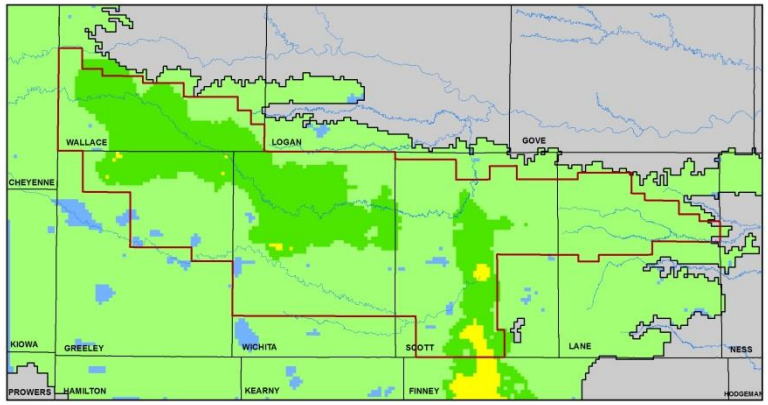

(a) Simulated 1984 to 1994

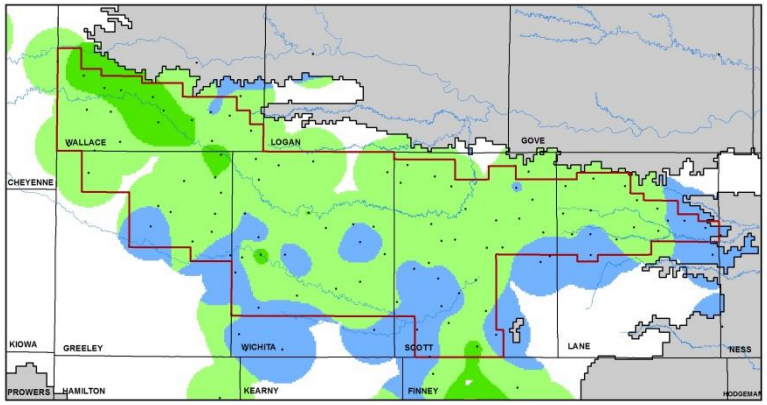

(b) Observed 1984 to 1994

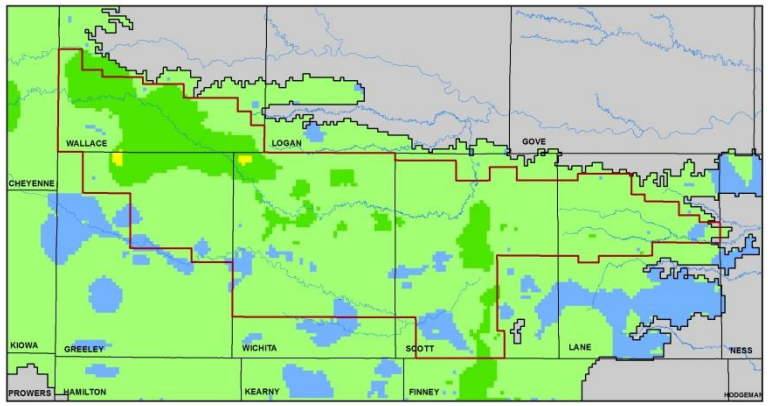

(c) Simulated 1994 to 2004

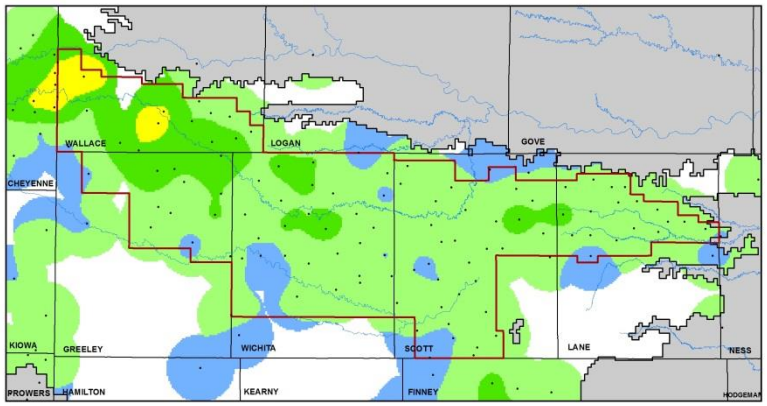

(d) Observed 1994 to 2004

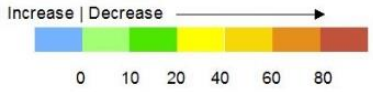

Figure 50. Simulated versus observed water-level changes for the intervals 1984 to 1994 and 1994 to 2004.

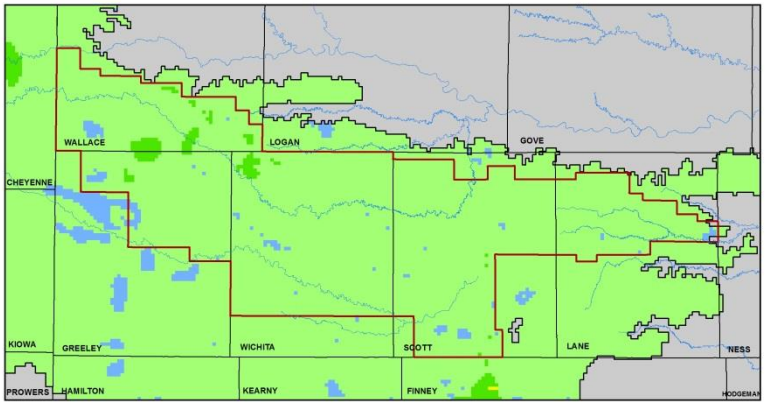

(a) Simulated 2004 to 2014

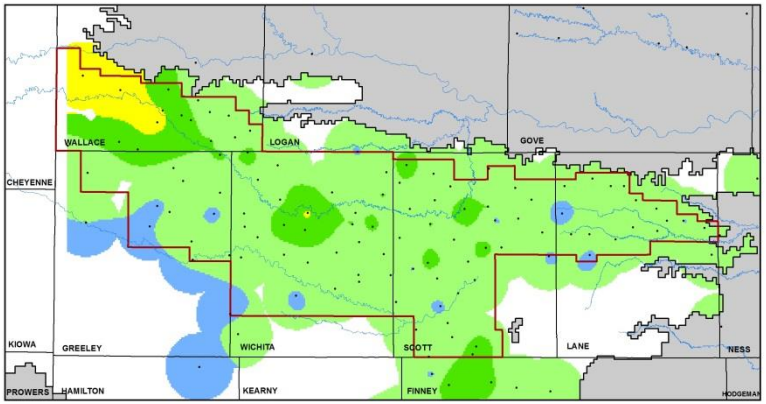

(b) Observed 2004 to 2014

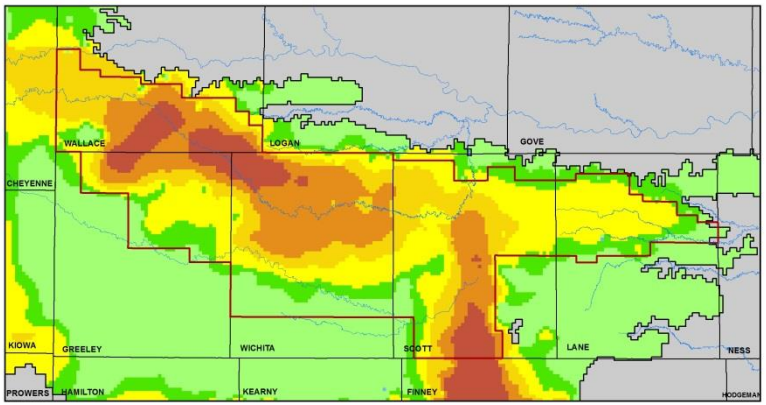

(c) Simulated predevelopment to 2014

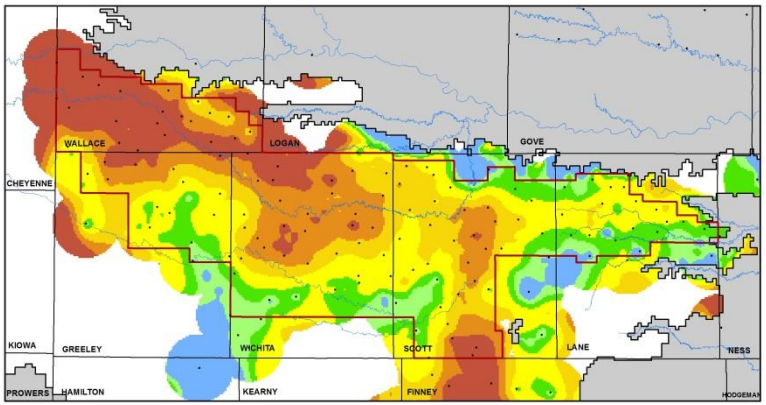

(d) Observed predevelopment to 2014

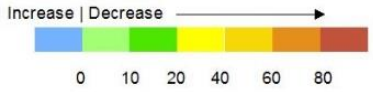

Figure 51. Simulated versus observed water-level changes for the intervals 2004 to 2014 and predevelopment to 2014.

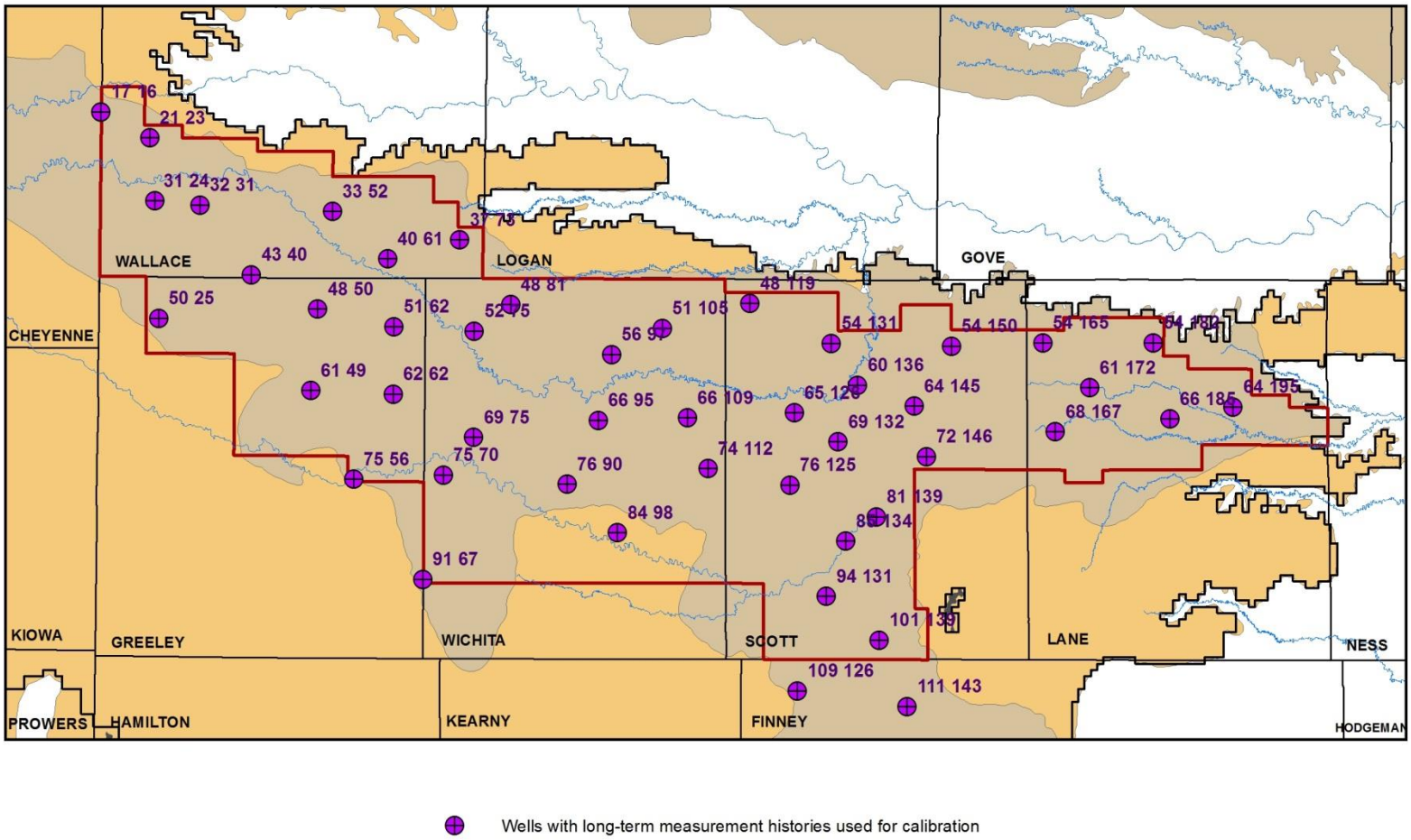

Figure 52. Wells with long-term measurement histories used for model calibration, labeled by row and column of the model cell in which each well is located.

Figure 53. Simulated versus observed well hydrographs, Wallace County.

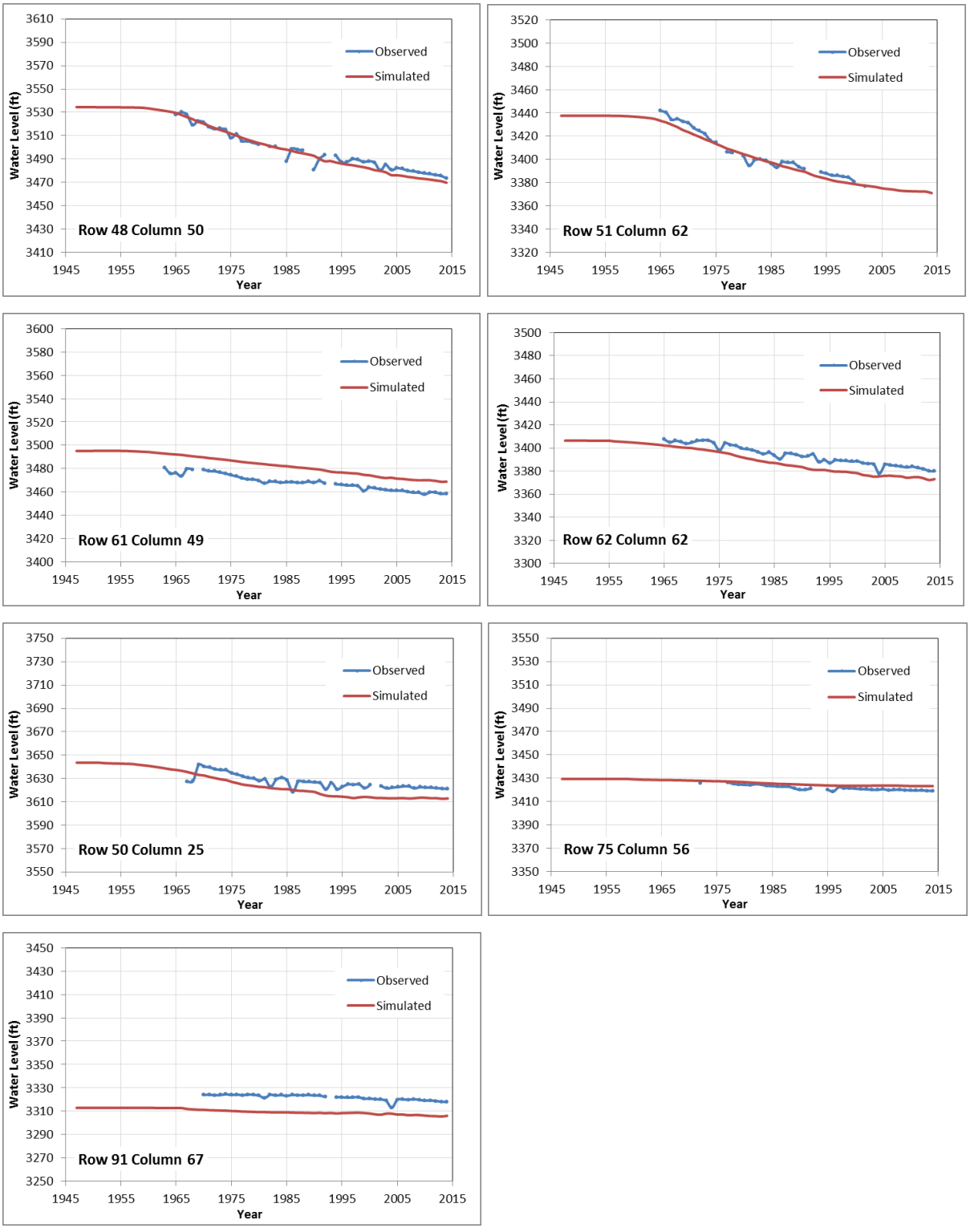

Figure 54. Simulated versus observed well hydrographs, Greeley County.

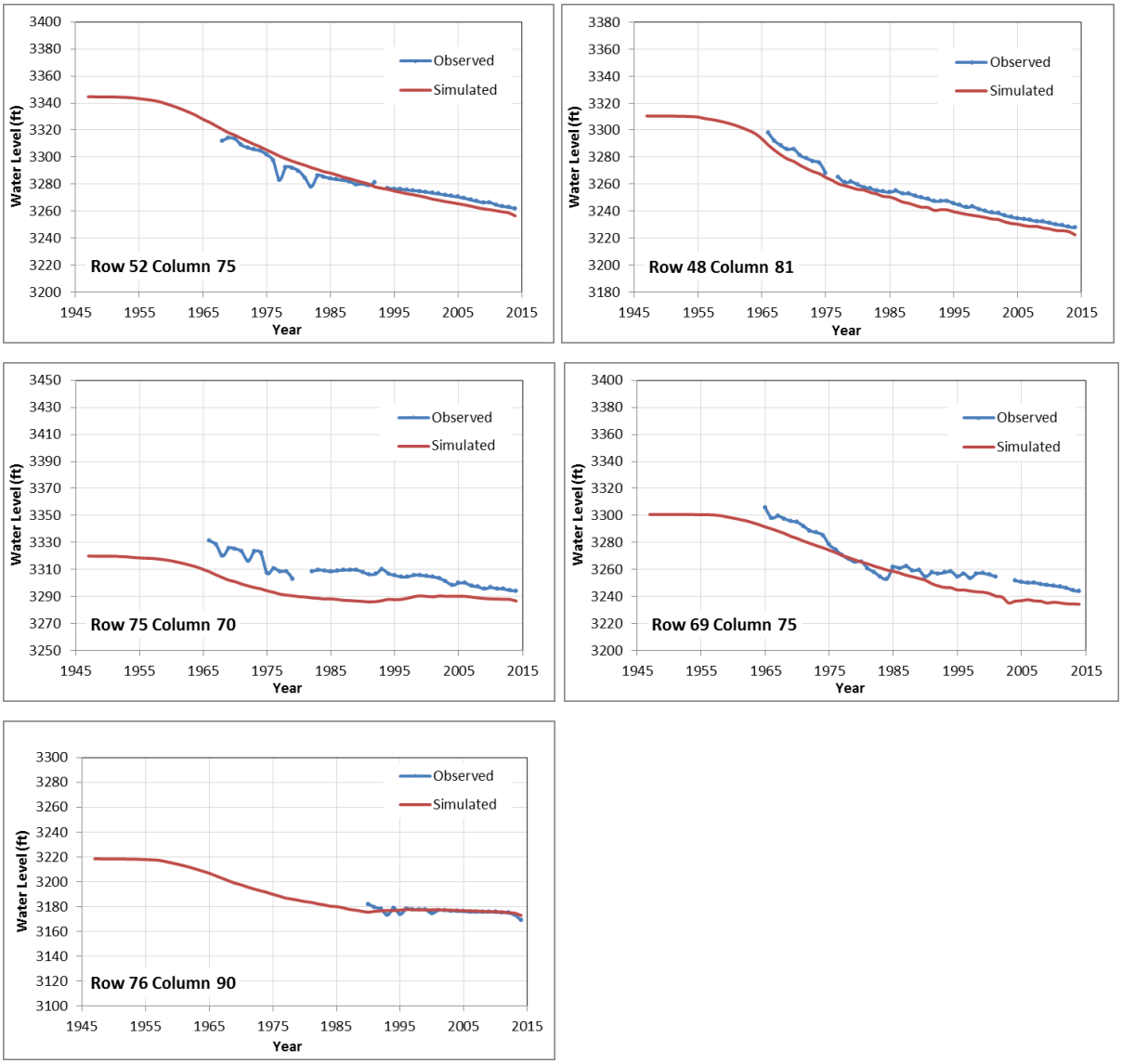

Figure 55. Simulated versus observed well hydrographs, western Wichita County.

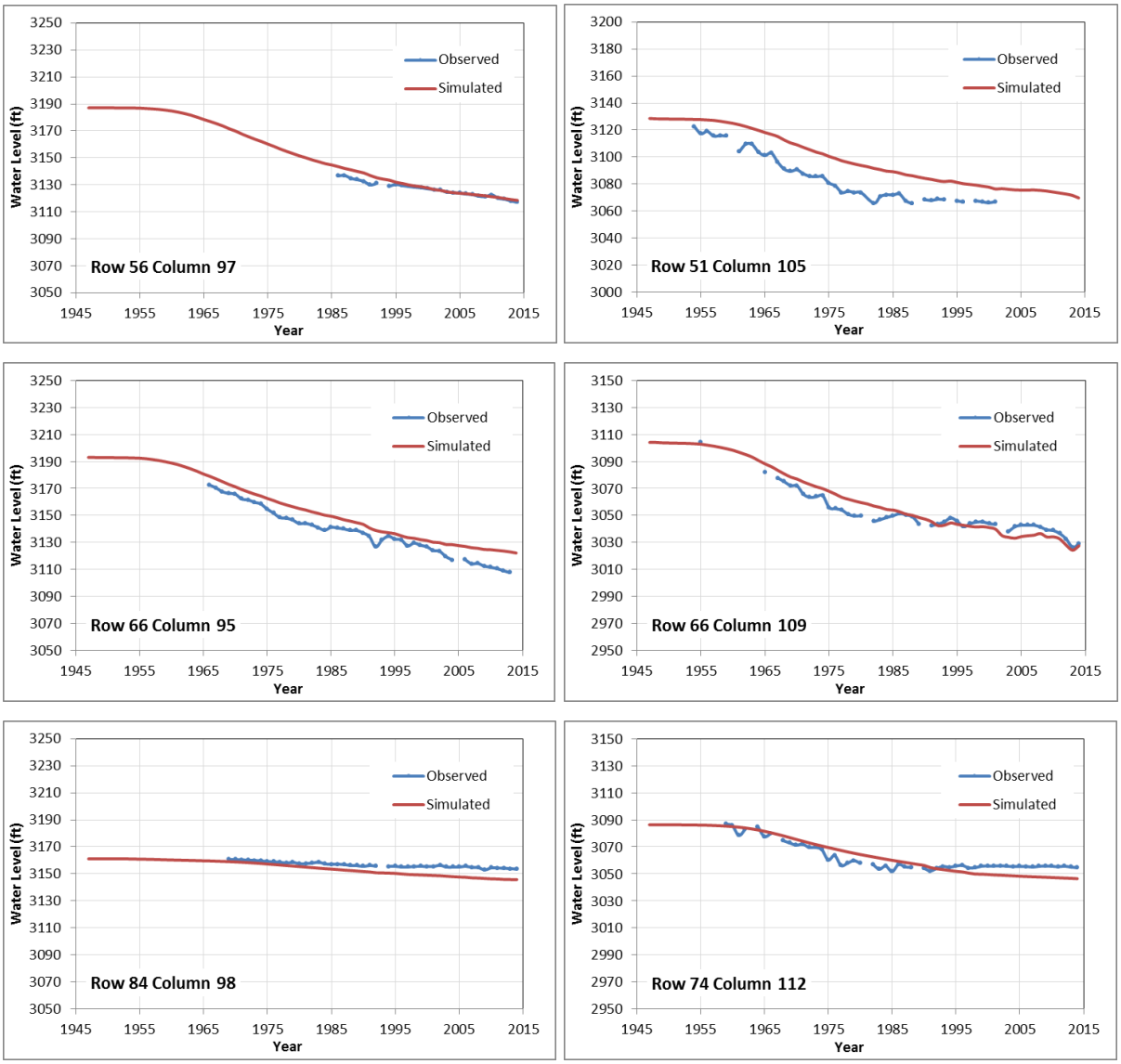

Figure 56. Simulated versus observed well hydrographs, eastern Wichita County.

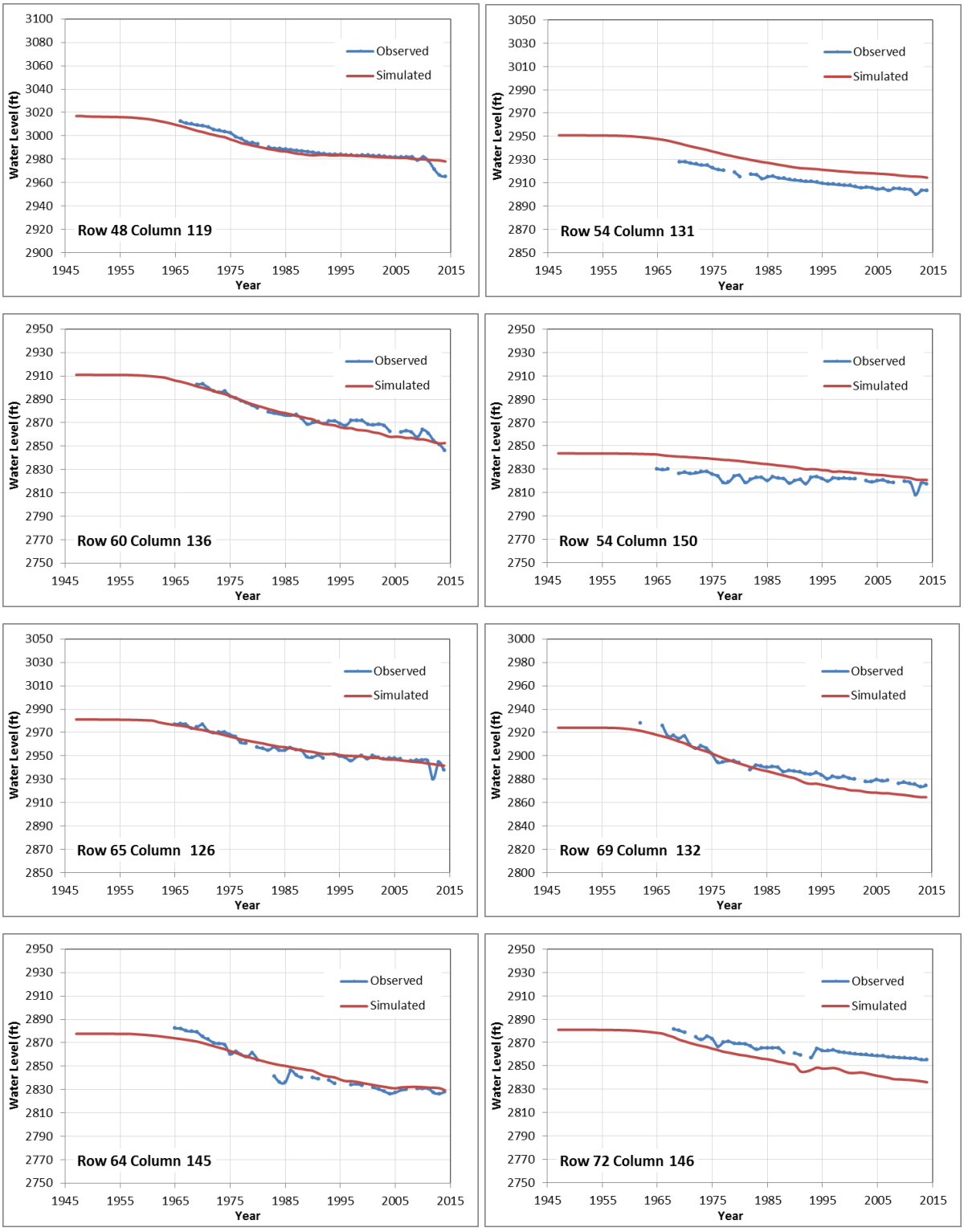

Figure 57. Simulated versus observed well hydrographs, northern Scott County.

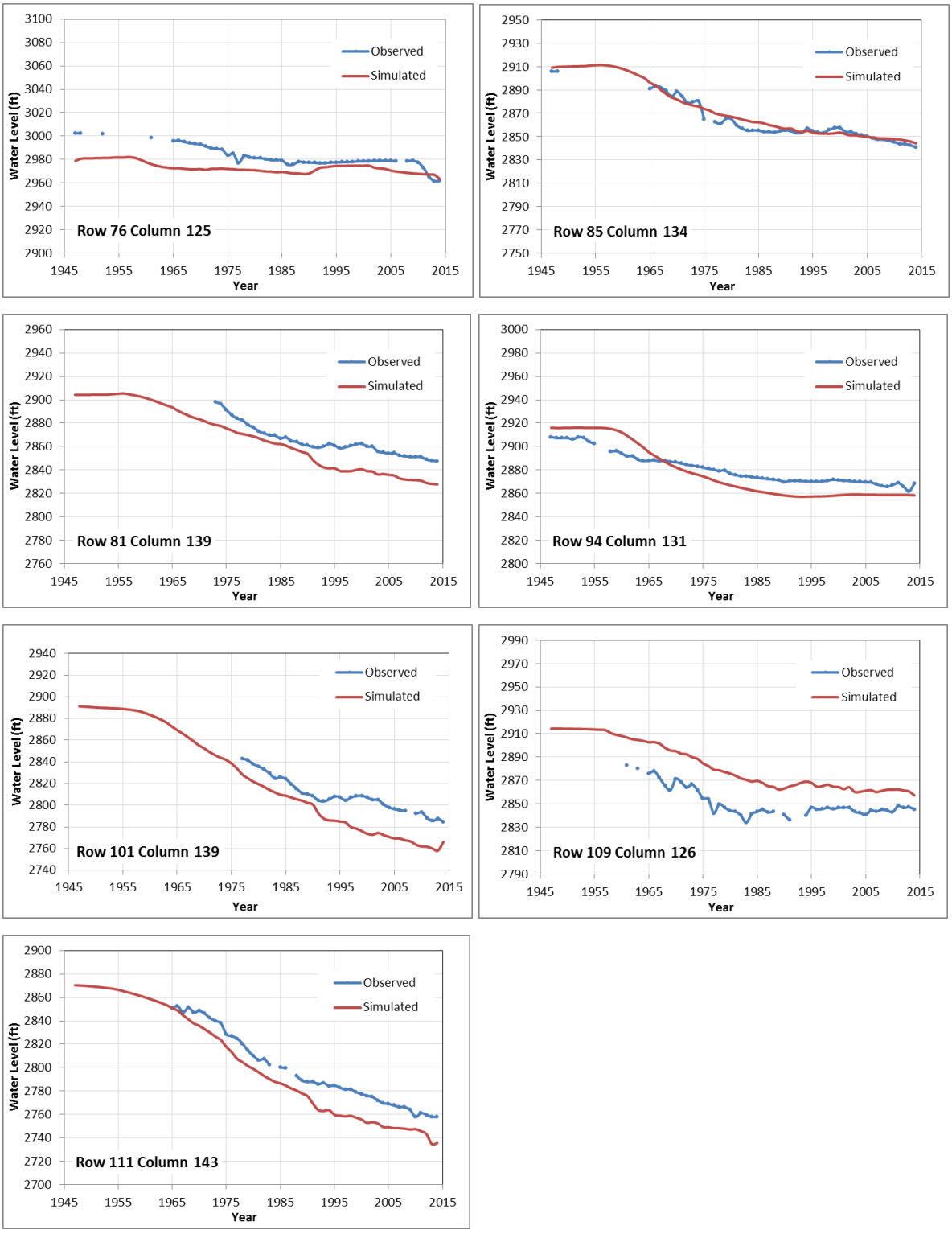

Figure 58. Simulated versus observed well hydrographs, southern Scott and northern Finney counties.

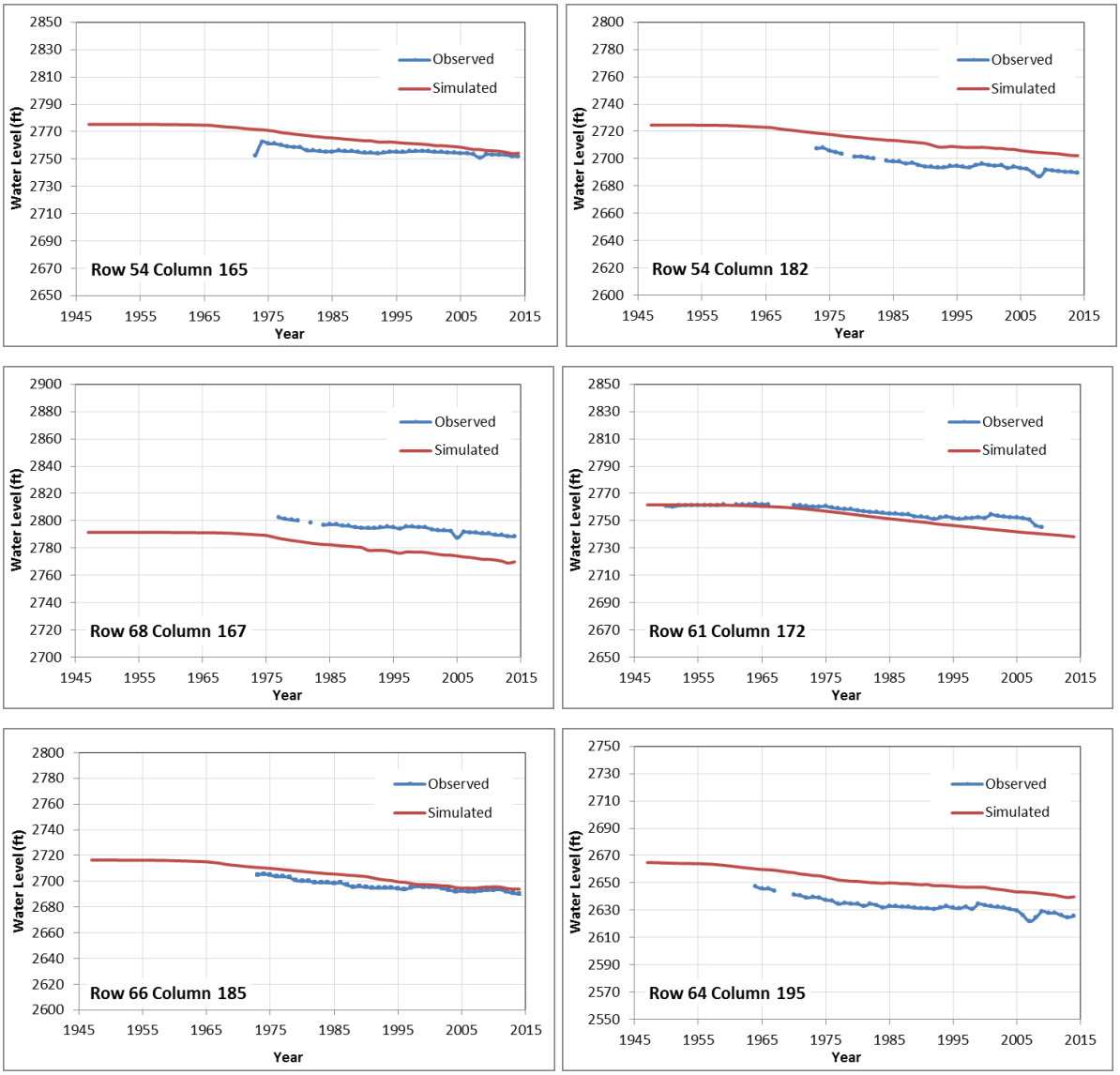

Figure 59. Simulated versus observed well hydrographs, Lane County.

Streamflow

The transient model was also calibrated to the limited amount of streamflow data available for the Ladder and Whitewoman creek gages. The model only simulates the stream-aquifer interactions and does not take into account surface runoff from precipitation events. Figure 60 plots the model simulated versus observed values for Ladder Creek averaged between January and March when base flow is likely the primary contributor to streamflow. The gage on Whitewoman Creek did not record any January streamflow during its operational time span from 1967 to 1985, a condition replicated by the model.

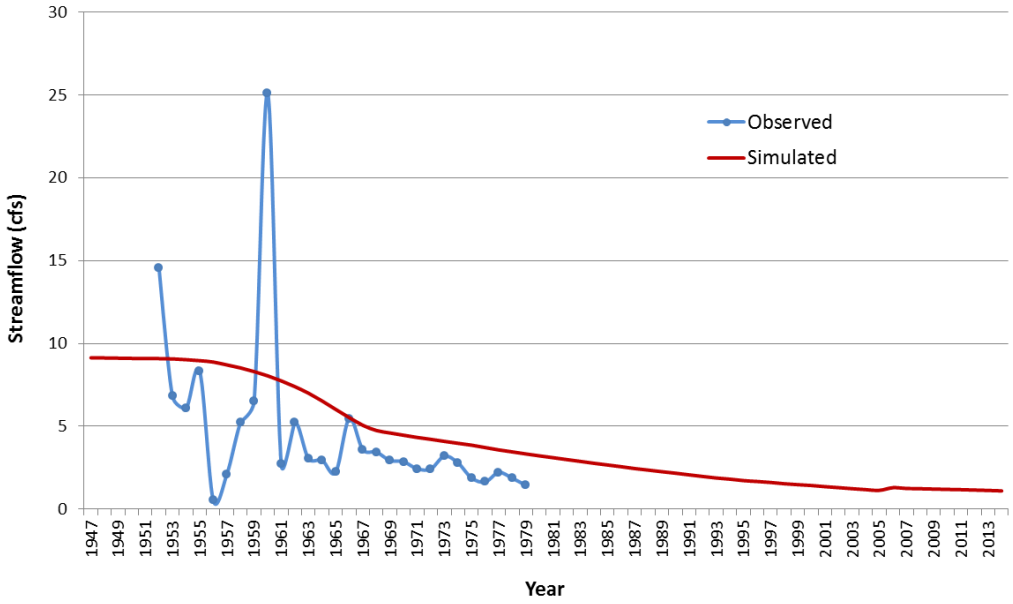

Figure 60. Simulated versus observed January–March average streamflow at the Ladder Creek gage.

Model Budgets

Figure 61 shows the groundwater budget over the transient period, including the net storage, flow across head boundaries, well pumping (wells in the legend), evapotranspiration (ET) loss, total areal recharge, drain cell loss, and stream leakage. Positive values indicate inflows of water to the aquifer system (recharge and lateral flow from the head boundaries), and negative values reflect outflows from the aquifer.

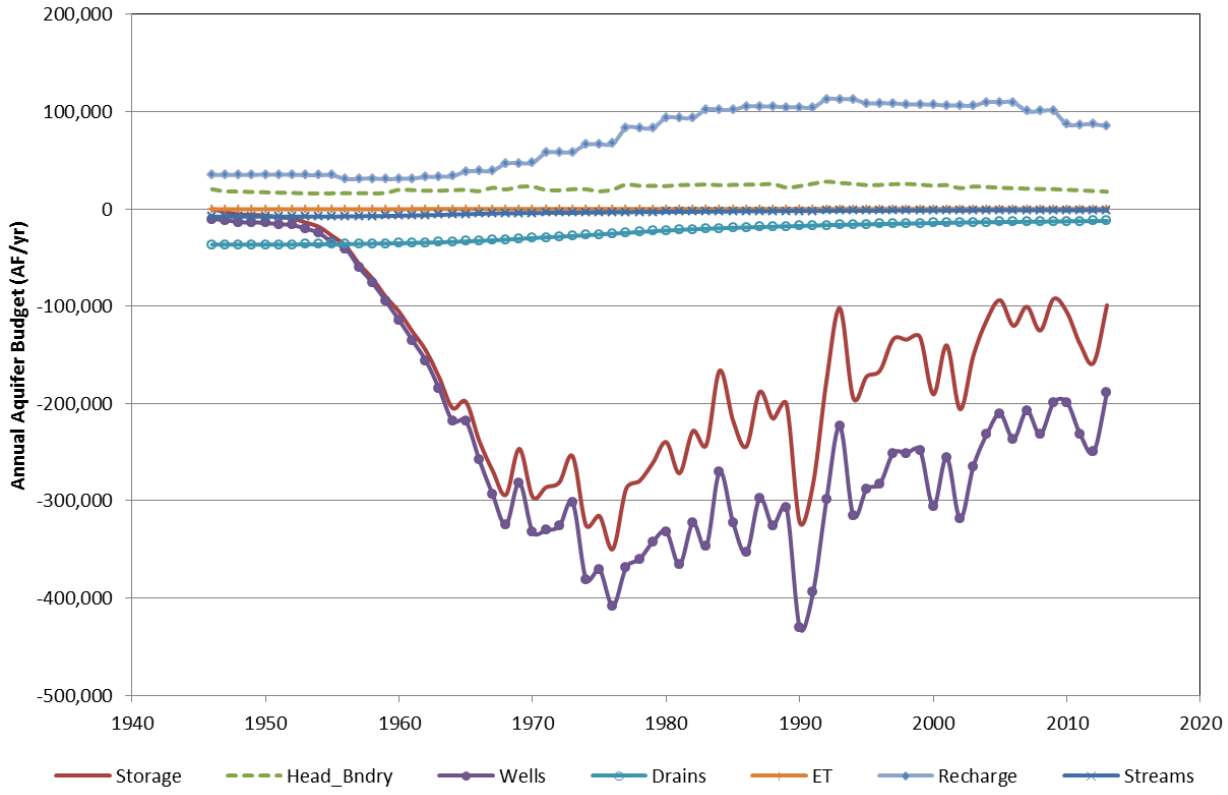

Figure 61. Annual aquifer budget from the calibrated model.

Recharge is the largest component of inflows to the aquifer and represents the sum of precipitation-based recharge, irrigation return flows, and lagged storage releases from low-permeable units. Figure 62 plots the various recharge components originating from the land surface. Precipitation recharge is generated by the recharge curves described earlier in this report and represents the amount of new water entering the aquifer system from both the upland areas of the aquifer and the higher rates of recharge for stream channels and the Scott County depression. Recharge from irrigation return flows represents the amount of pumped irrigation water that infiltrates past the root zone of the irrigated crops, eventually reaching the water table. As the number of water rights and pumping volumes increase during the 1960s and 1970s, so does the amount of return flows. As water usage declines and irrigation systems become more and more efficient, the amount of return flow declines. The final component is the amount of water coming from enhanced precipitation-based recharge occurring over irrigated fields.

Compared to the precipitation recharge calculated under no irrigation, the irrigation-enhanced precipitation recharge is relatively small because 1) irrigation enhancement to precipitation recharge only occurs during the growing season while the precipitation recharge calculated under no irrigation includes both the growing and non-growing seasons and 2) the acreage of irrigated lands is much smaller than the active model area (fig. 35). Therefore, although irrigation doubles the precipitation recharge in the irrigated fields during the growing season, the amount of irrigation-enhanced precipitation recharge is small when compared to the overall precipitation recharge over the entire active model area.

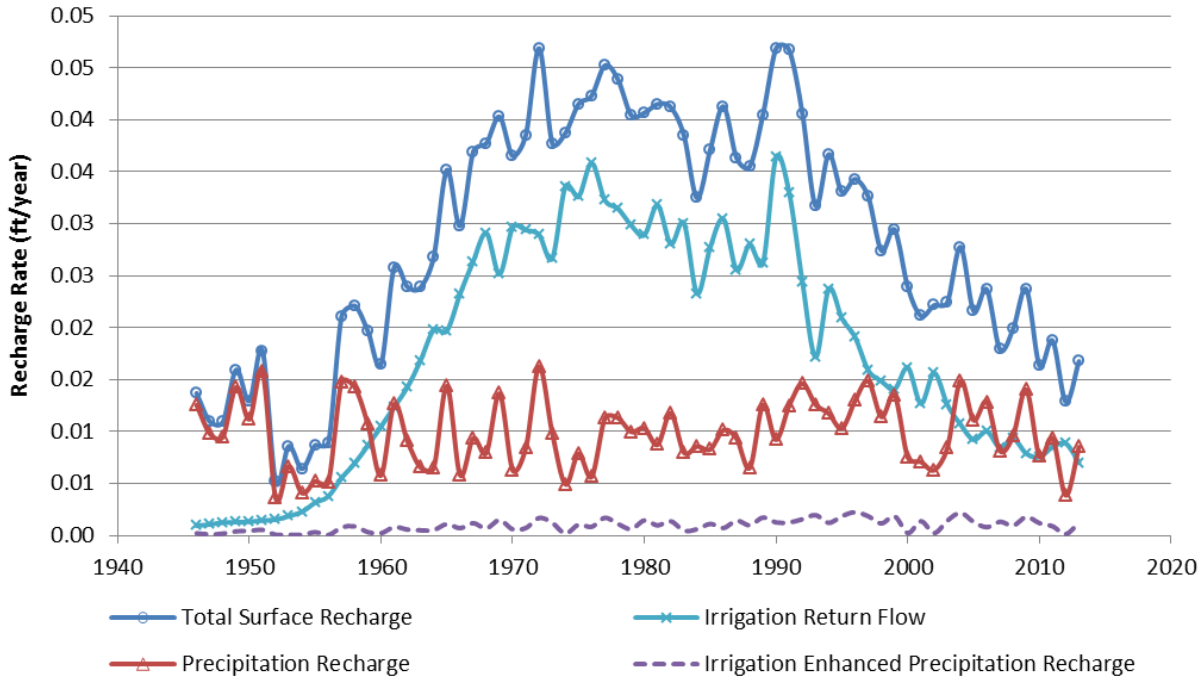

Figure 62. Land-surface-based recharge components.

Each of the land-surface recharge components is subject to the model's delay function, and the total amount of water in each time step is tracked. Figure 63 illustrates the total amount of water derived from surface recharge that actually reaches the ever-changing water table, termed "water-table recharge." The total amount of water-table recharge substantially increases during the 1970s and 1980s as the majority of the return flows from decades-earlier irrigation applications finally reaches the saturated portions of the aquifer. The water-table recharge becomes the largest in the 1990s and stays high through most of the 2000s. With the decline in irrigation return flows (starting in the early 1990s), the water-table recharge significantly declines in the last several years of the transient simulation. The average rate at which the surface recharge reaches the water table, represented by the olive-green line, is 0.31 inches a year over the entire transient period and active model area (the rate would be much higher if only considering the last three decades and irrigated fields).

Figure 64 plots the amount of lagged drainage of water released from partially dewatered sediments. The total recharge to the water table is the sum of the lagged storage release and the delayed recharge from the surface. Given that lagged drainage only occurs when a water

table declines below various units of the aquifer, the delayed storage releases do not start to reach the water table until the mid-1960s. As the sediments above the water table become more dewatered with time and the rates of groundwater-level declines begin to decrease, the amount of water released from lagged storage gradually starts to decline after it peaks around the late 1970s. The rate of lagged storage release is much smaller (about 0.02 inches per year) than the delayed recharge from the surface. The average rate of recharge from all sources (precipitation, enhancement by irrigation, return flows, and lagged storage release) during the transient period averages 0.33 inches a year (0.027 ft/year in fig. 64), which is in line with most recharge estimates for the Ogallala portion of the HPA. However, the average rate of recharge from all sources during the last three decades (1984–2014) is substantially greater, 0.46 in/year (0.039 ft/year), than during the entire transient period.

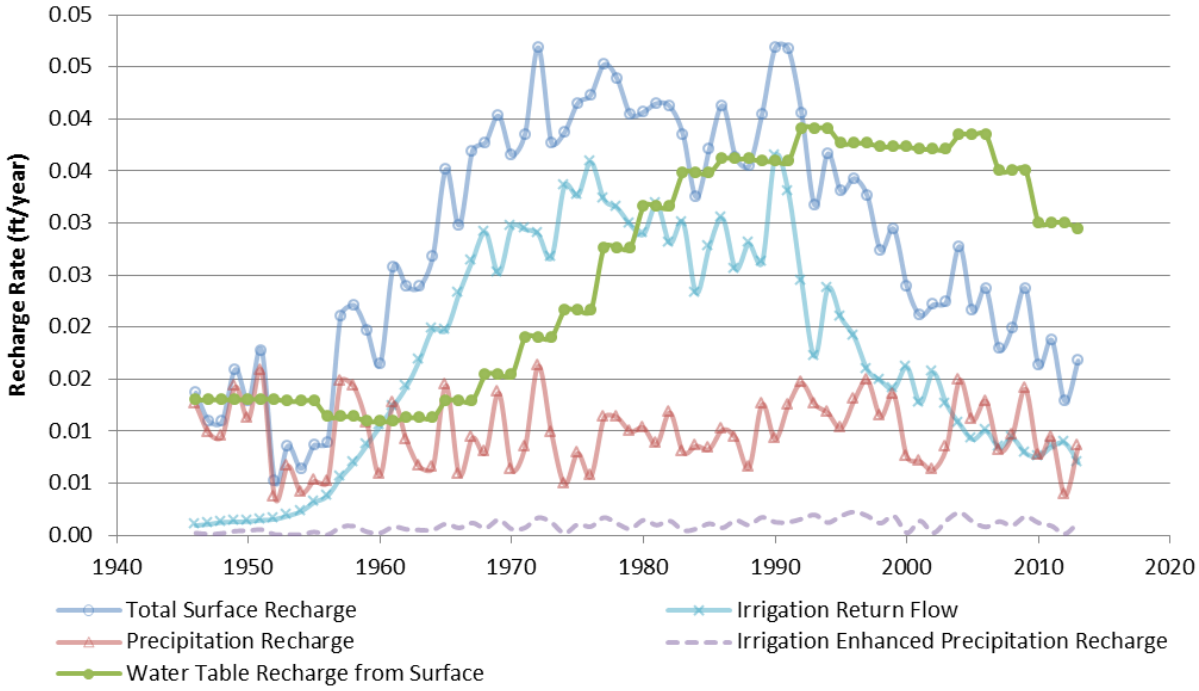

Figure 63. Total delayed recharge reaching the water table from the surface.

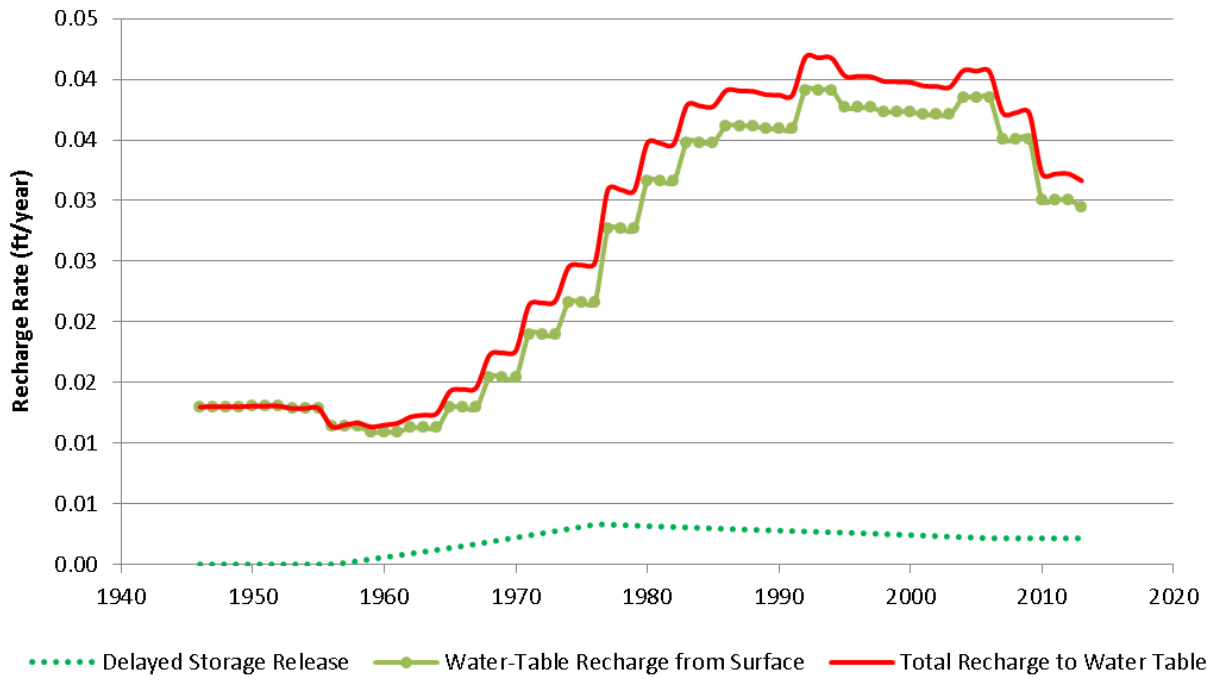

Figure 64. Lagged storage release and the total amount of recharge to the water table.

Groundwater pumping (identified as "Wells" in fig. 61) represents the largest outflow from the aquifer. Annual groundwater usage continually increased from predevelopment to its maximum levels in the mid-1970s to early 1980s and has been gradually decreasing since then. The total amount of water reaching the water table is slowed by the model's delayed recharge functions and does not peak until the 1990s. The delayed recharge starts to decline in the late 2000s.

Lateral flow of groundwater in and out of the model (head boundary component of the budget) is a little above zero. The largest volume of water enters the model through the western head boundaries from Colorado. Water flows laterally following the general west-to-east gradient and exits the model primarily through the drain cells present along the eastern edge of the active area. Declining water levels have reduced the amount of water flowing out of the drain cells and have also reduced baseflow contributions to Ladder and Whitewoman creeks to near zero in recent years.

The amount of water lost from the aquifer directly to ET by model cells located in the stream valleys is negligible. Note that the model only accounts for the amount of water moving from the aquifer to the atmosphere through the ET process. ET loss of precipitation at the land surface is not explicitly simulated by the model; instead, it is indirectly taken into account by the calibrated precipitation recharge relation (only a small part of the precipitation becomes recharge to aquifer). The ET loss of irrigation water is also indirectly considered through different efficiencies assigned to different irrigation system types in the calculation of irrigation return flows.

Figure 65 plots the cumulative change in the model's groundwater budget. Aquifer storage is calculated for each model step based on the simulated water levels and calibrated specific yield

values for the different HyDRA lithology groups. The computed total predevelopment aquifer storage within the active area of the model is 22,151,620 acre-ft. The net effect of pumping relative to other model components produces an estimated 164,089 acre-ft average annual loss of storage. The simulated storage in 2014 is 10,993,589 acre-ft, which represents about half of the predevelopment value. For active model cells within GMD1, the computed storage was reduced from about 15,158,000 acre-ft in predevelopment time to 5,978,000 acre-ft in 2014, a decrease of about 60 percent.

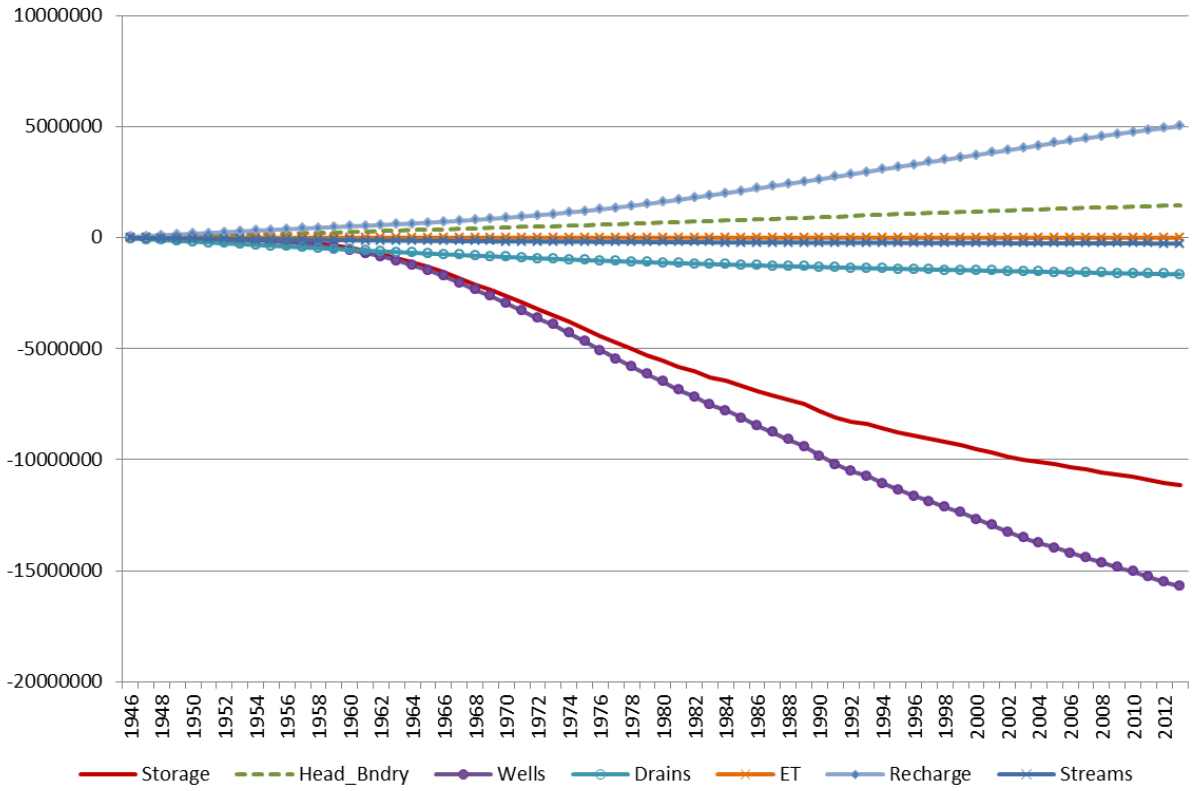

Figure 65. Accumulated groundwater budget.

Figure 66 plots the spatial patterns in the simulated aquifer storage for predevelopment time, 1974, 1994, and 2014. Storage is computed based on the water level for a given year in relation to the calibrated specific yield values for the different standardized lithologies groups categorized by HyDRA. The largest loss in storage occurs along the Greeley/Wallace county line, northern Wichita County, and around Scott City, Kansas. As would be expected, the model estimates that the greatest present-day (2014) storage occurs in the greater saturated thickness area formed by the deep bedrock elevations of southwest Wallace County and the north-south trough in Scott County.

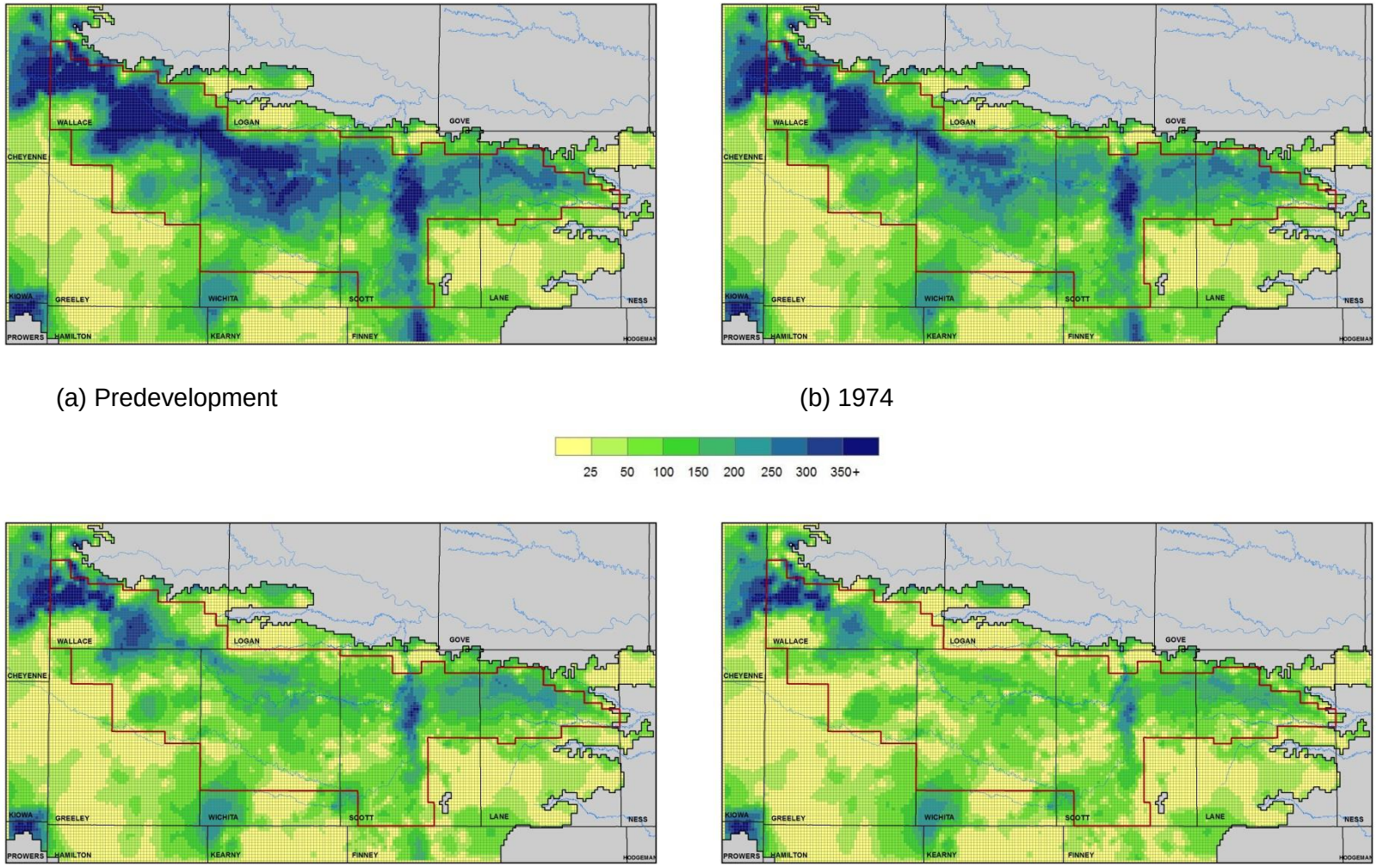

(a) Predevelopment

(b) 1974

(c) 1994

(d) 2014

Figure 66. Spatial distribution of simulated aquifer storage (in 100 acre-ft) for different model times.

MODEL SCENARIOS

One of the important uses of a calibrated groundwater model is to assess the future responses of an aquifer to different water resources management and climatic scenarios. Three basic scenarios were considered in this study:

1) No change in water-use policy.
2) All irrigation wells shut off within GMD1.
3) Pumping for all GMD1 irrigation wells reduced by 20%.

In all three scenarios, the calibrated model is run from 2014 to 2080 with a repeat of the 1947 to 2013 climatic conditions. Groundwater pumping outside the GMD1 district boundary is assumed to continue into the future as usual. The irrigation system types are assumed to be the same as for 2013. For the specified head boundaries, the average water-level change over the last 10 years is used to project future water levels on these boundaries until a minimum saturated thickness of 10 ft is reached.

In the first scenario, assuming there is no change in the water-use policy, future irrigation pumping is driven by current (2013) water rights, with aquifer-imposed reductions in areas where the irrigation demands cannot be fully met due to the diminishing groundwater yields. In the second scenario, all irrigation pumping is shut off in GMD1, while non-irrigation pumping (industrial, municipal, and other uses) continues as normal. This scenario offers some insights into how the aquifer would recover with time without any future irrigation pumping. In the third scenario, irrigation pumping is reduced by 20% across the GMD1 district. This scenario explores whether a relatively modest reduction in irrigation pumping could significant affect the future of groundwater supply in the area.

No change in water-use policy

This scenario uses the regression equation determined in the transient model calibration to compute the ratio of water use/authorized quantity, assuming there is no change in future water-use policy. For a given future year, the ratio is dependent on annual precipitation, maximum winter temperature, and the depth to water table at that year. The ratio is then converted into the actual water-use demand by multiplying it by the present-day (2013) authorized quantity. Considering that in some areas the aquifer may not be able to fully meet the water-use demand as a result of the ever-declining water table, the regression-based water use is checked against aquifer transmissivity dynamically calculated for the pumping well location for that year. If the transmissivity is calculated to be less than 1,000 ft^2/d (a saturated thickness of 10 ft for sand with K 100 ft/d), pumping is assumed to be not viable and the water use is adjusted to be zero.

Note that during MODFLOW runs, the MODFLOW-NWT program further reduces well pumping in a model cell when the water level is below 5% of the cell thickness. The pumping reduction by MODFLOW-NWT is not significant during the transient model calibration, but becomes increasingly larger in the future scenario simulations. The final adjusted pumping data (after both transmissivity check and MODFLOW-NWT reduction) are used in aquifer budget calculations for both the transient calibrated model and all future scenarios.

Figure 67 shows the annual aquifer budget for the no change in future water use scenario. Groundwater pumping, primarily caused by agricultural irrigation, continues to be the most significant driver of aquifer budget balance. The total water-table recharge, including both the delayed surface recharge (i.e., the water that has moved from surface recharge down to the water table) and lagged drainage release (fig. 68), is not sufficient to balance the pumping from the aquifer. As a result, the HPA aquifer continues to lose water out of its storage (annual storage budget is negative through most years). The other budget items such as ET, flow across head boundaries, drains, and streams, are relatively small and appear to balance each other out in the model-wide aquifer budget calculation. Note that despite annual fluctuations, future pumping remains at about the 2013 level for the next 10 years or so. After that, the pumping amount decreases substantially to approximately two-thirds of the 2013 level by the early 2030s and then continues to decline gradually over the remaining future years. At the end of the simulation (2080), the pumping amount decreases to about a third of the 2013 level.

Figure 68 shows the contributions of the water-table recharge from delayed surface recharge and lagged drainage from partially dewatered sediments after water-table decline. The lagged drainage from dewatered sediments is much smaller than the recharge from the surface. Figure 69 shows different surface recharge components. Consistent with past irrigation practices, the irrigation return flow was more significant than precipitation recharge between 1960 and 2000. As irrigation system efficiency improves and less water is available for supporting future pumping, the amount of irrigation return flow has continuously decreased since the 1990s (the declining trend continues into the future). On the other hand, precipitation recharge remains fairly constant despite the annual fluctuations. The slow movement of water through the vadose zone has delayed the arrival of the irrigation return flow at the water table; however, by 2013, the majority of that water has arrived at the saturated portion of the aquifer. Due to the continuation of irrigation return flow and lagged drainage from dewatered sediments (albeit at a level lower than that in the transient model), the water-table recharge in 2080 is about 30% higher than the natural recharge rate during the predevelopment period.

Figure 70 shows the simulated head changes for selected intervals for the no change in future water use scenario. Most of the district will continue to see a certain amount of water-level decline with the most significant declines in Wichita and Scott counties. Figure 71 displays the simulated aquifer storage at selected years for the no change in future water use scenario. The most significant storage left in GMD1 occurs in portions of southern Wallace County, where spatial variations are also very high (aquifer storage can vary dramatically within a short distance).

The detailed county budgets for the no change in future water use scenario are shown in Supplement A.

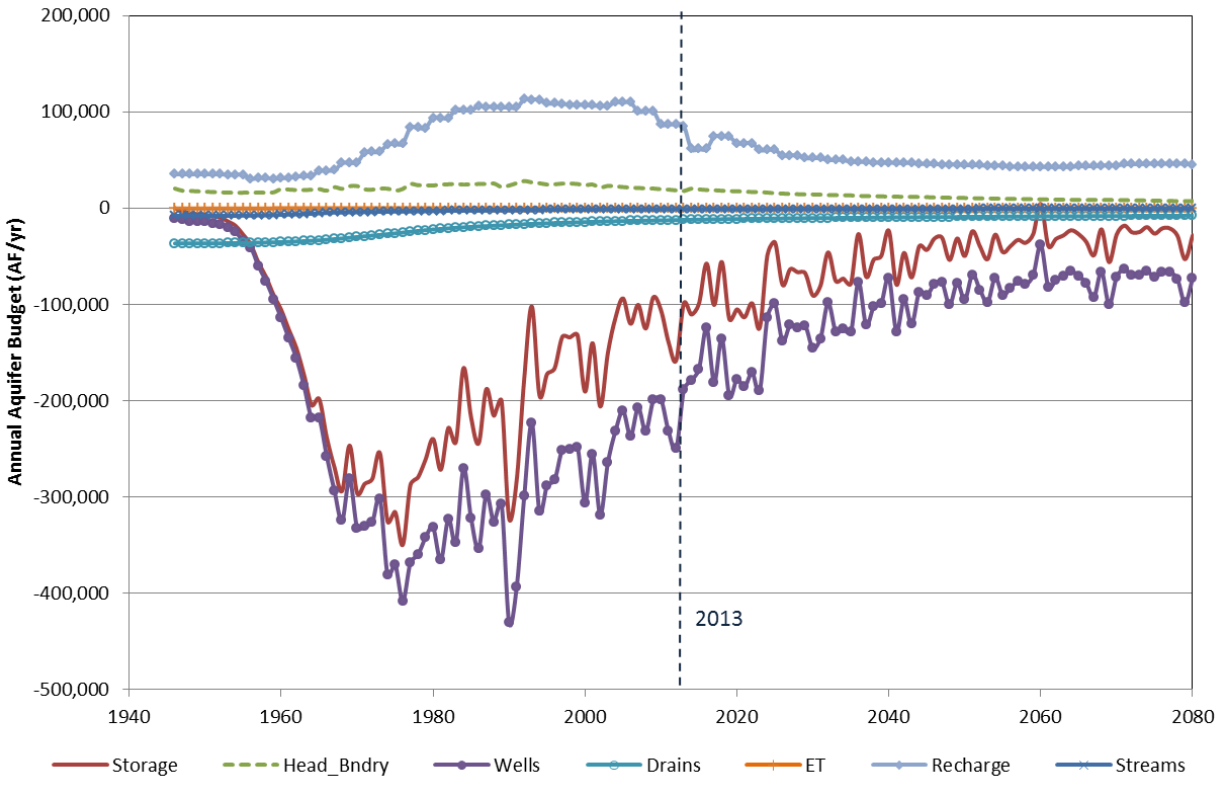

Figure 67. Annual aquifer budget for the no change in future water use scenario. The calibrated model budget (predevelopment to 2013) is also plotted for comparison.

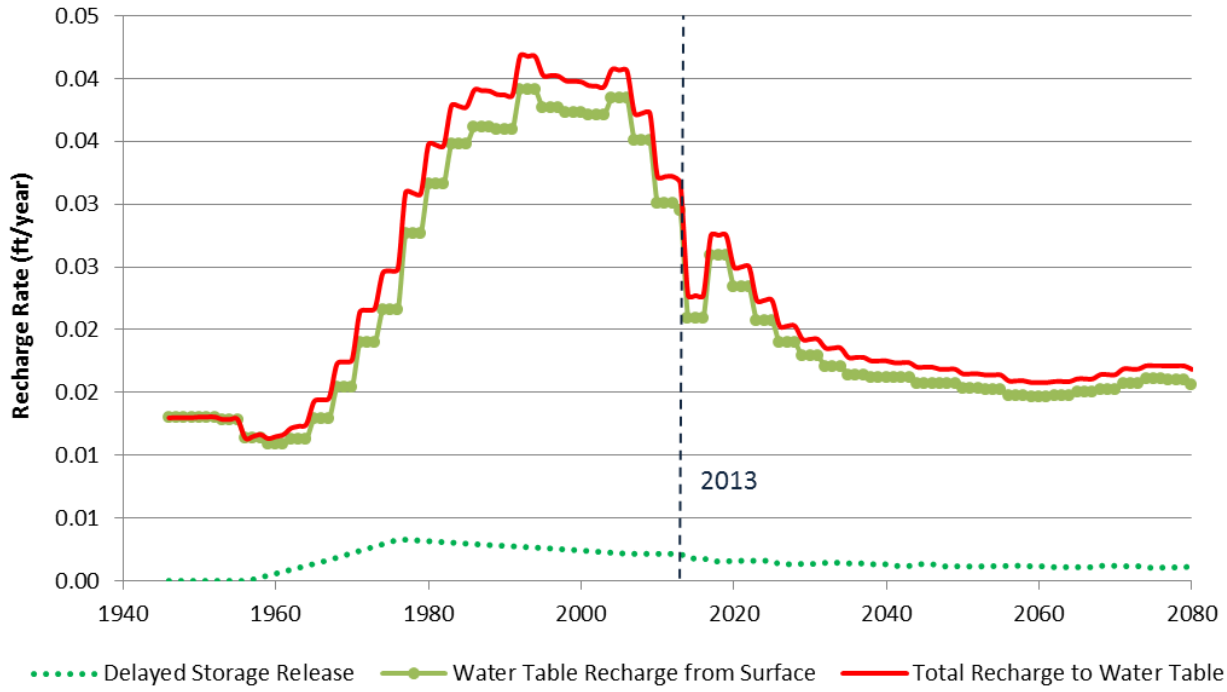

Figure 68. Water-table recharge for the no change in future water use scenario.

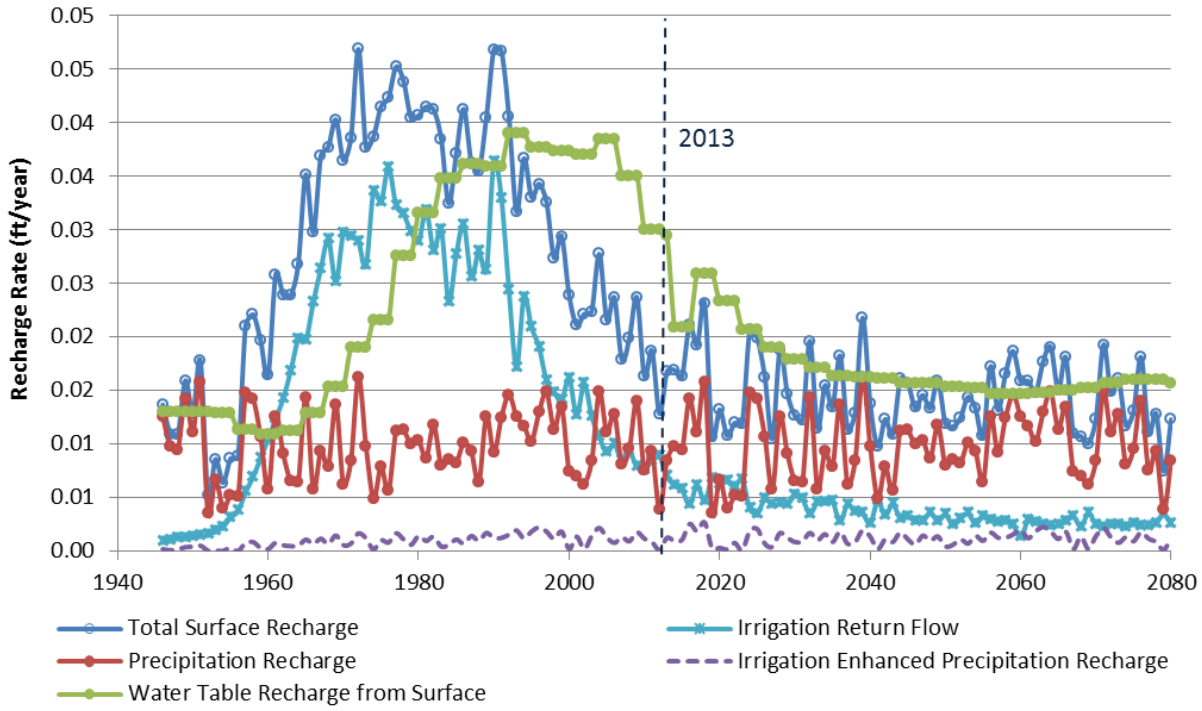

Figure 69. Different surface recharge components for the no change in future water use scenario. The delayed surface recharge (listed as “Water Table Recharge from Surface”) is also plotted for comparison.

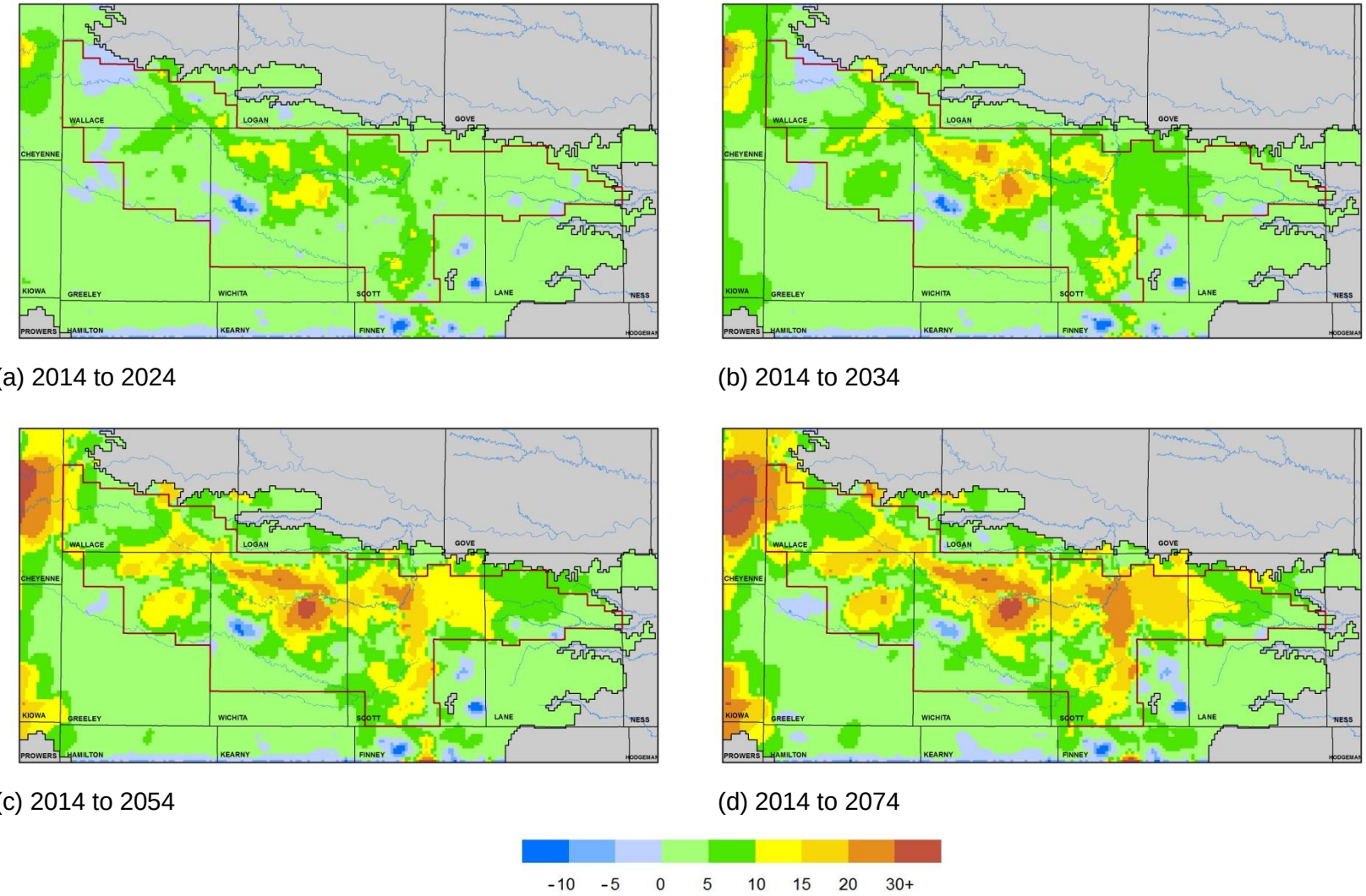

(a) 2014 to 2024

(b) 2014 to 2034

(c) 2014 to 2054

(d) 2014 to 2074

Figure 70. Simulated water-level change, in feet, for the no change in future water use scenario. Positive numbers indicate water-table decline.

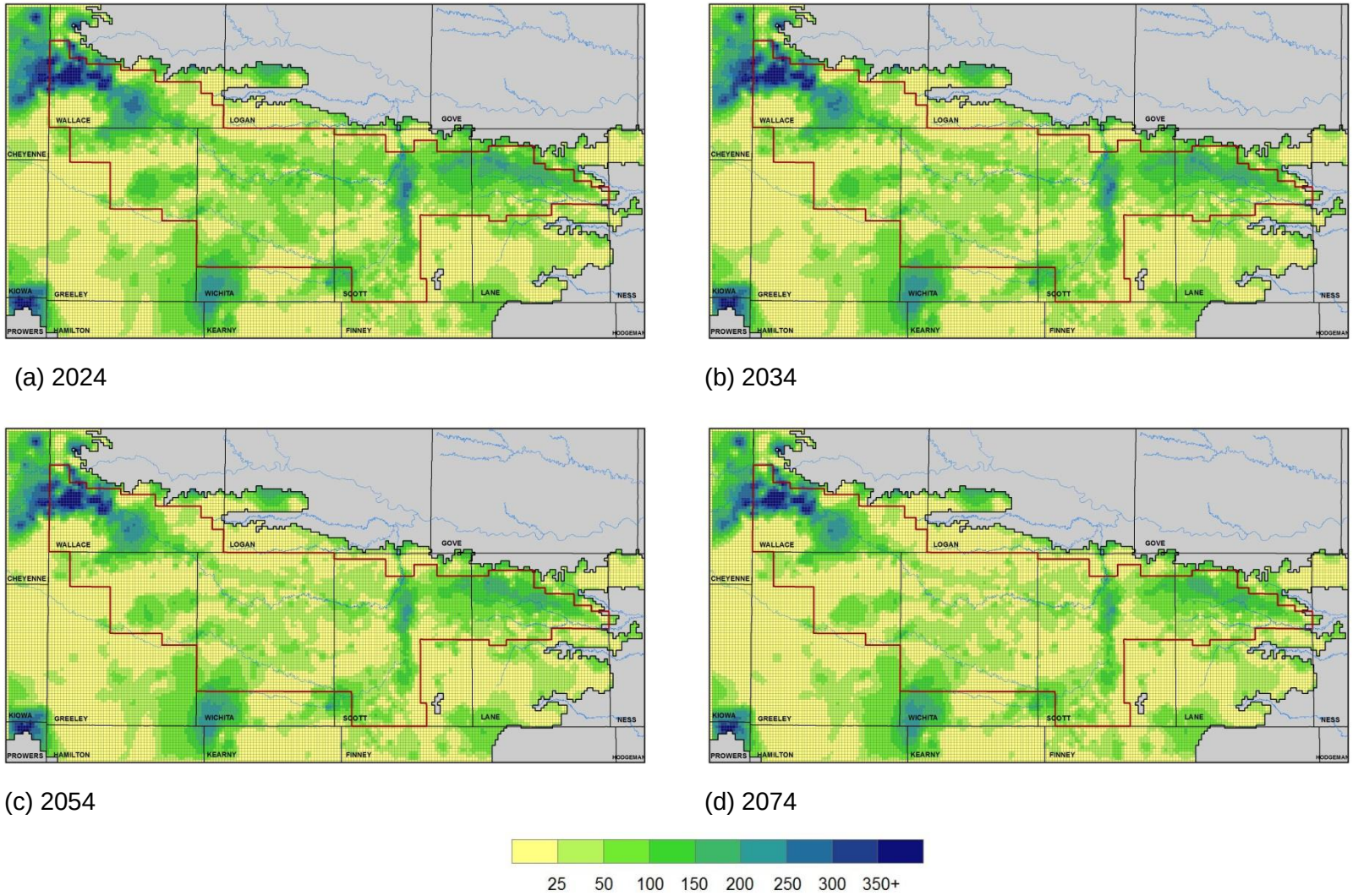

(a) 2024

(b) 2034

(c) 2054

(d) 2074

Figure 71. Spatial distribution of simulated aquifer storage (in 100 acre-ft) for the no change in future water use scenario.

All irrigation wells shut off within GMD1

In this scenario, all of the irrigation pumping wells are shut off within GMD1, while pumping outside the GMD1 boundary continues as normal. The non-irrigation wells, such as those for municipal and stockwater uses, within GMD1 also continue to pump as normal. This scenario is a hypothetical one and is only used to explore how the aquifer would recover if future irrigation pumping, the district's largest user of water, were to be stopped.

Figure 72 shows the annual aquifer budget for the no irrigation pumping scenario. After irrigation pumping is turned off in GMD1, the total pumping from the aquifer is significantly reduced. The sum of pumping outside GMD1 and non-irrigation pumping within GMD1 is about 25,000 acre-ft, which remains nearly constant with time. The delayed recharge of surface recharge and lagged drainage produces a relatively large increase in annual storage in the first couple decades. The annual rate of storage change becomes very small after the irrigation return flow has all entered the saturated zone. The cumulative result causes a substantial recovery in aquifer storage for about 20 years after 2013. After that, the storage recovery becomes very small.

Figure 73 displays the contributions of lagged drainage and delayed surface recharge to the recharge at the water table for the no irrigation pumping in GMD1 scenario. As the water table does not decline, future lagged drainage is smaller than that in the no change in water-use policy scenario. Figure 74 shows the different surface recharge components for the scenario. After the irrigation pumping is turned off, irrigation return flow becomes zero, which results in a smaller amount of delayed recharge from the surface.

Figure 75 shows the simulated water-level changes at selected year intervals for the no irrigation pumping in GMD1 scenario. Most of the district sees a rise of water levels (blue colors) due to cessation of irrigation pumping. Some areas continue to see a small level of water-level decline (green colors) due to lateral aquifer flow within the model and a small amount of non-irrigation pumping. Figure 76 shows the simulated storage at selected years for the no irrigation pumping in GMD1 scenario. Overall, aquifer storage increases slowly after the irrigation wells are turned off.

The detailed county budgets for the no irrigation pumping in GMD1 scenario are shown in Supplement B.

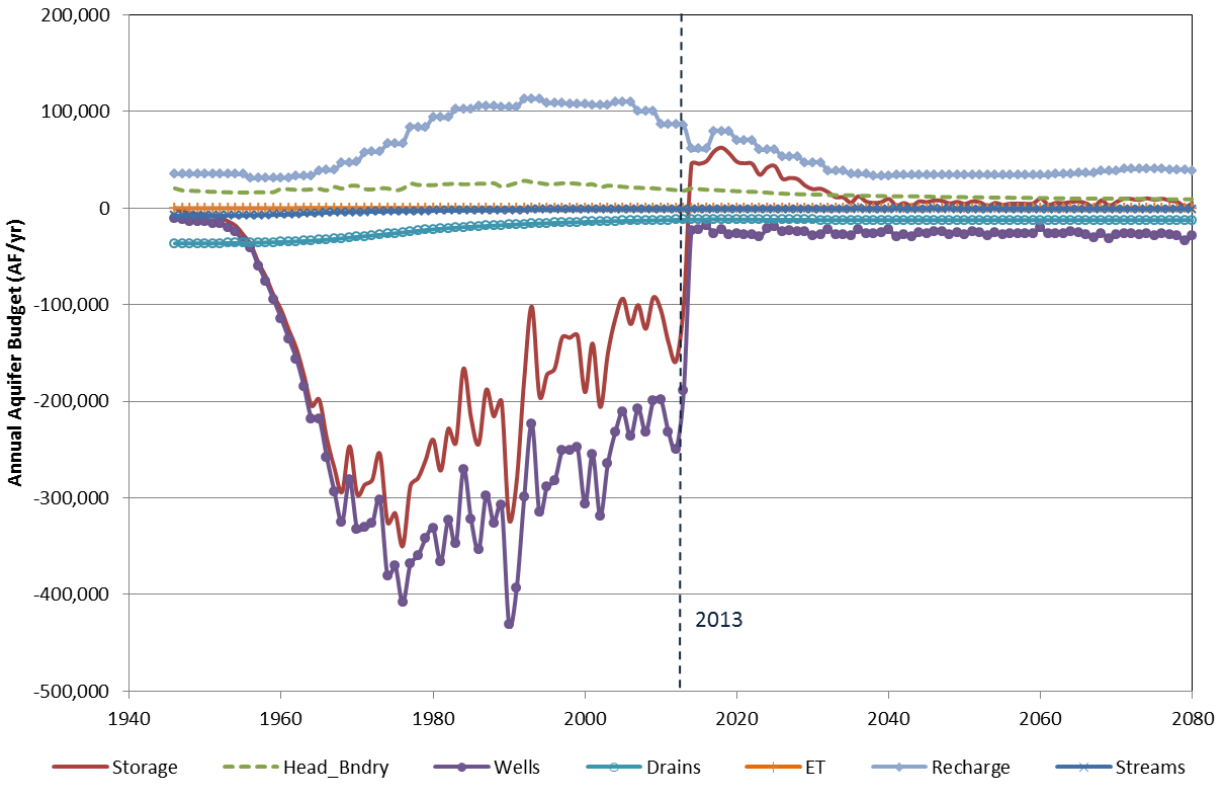

Figure 72. Annual aquifer budget for the no irrigation pumping in GMD1 scenario.

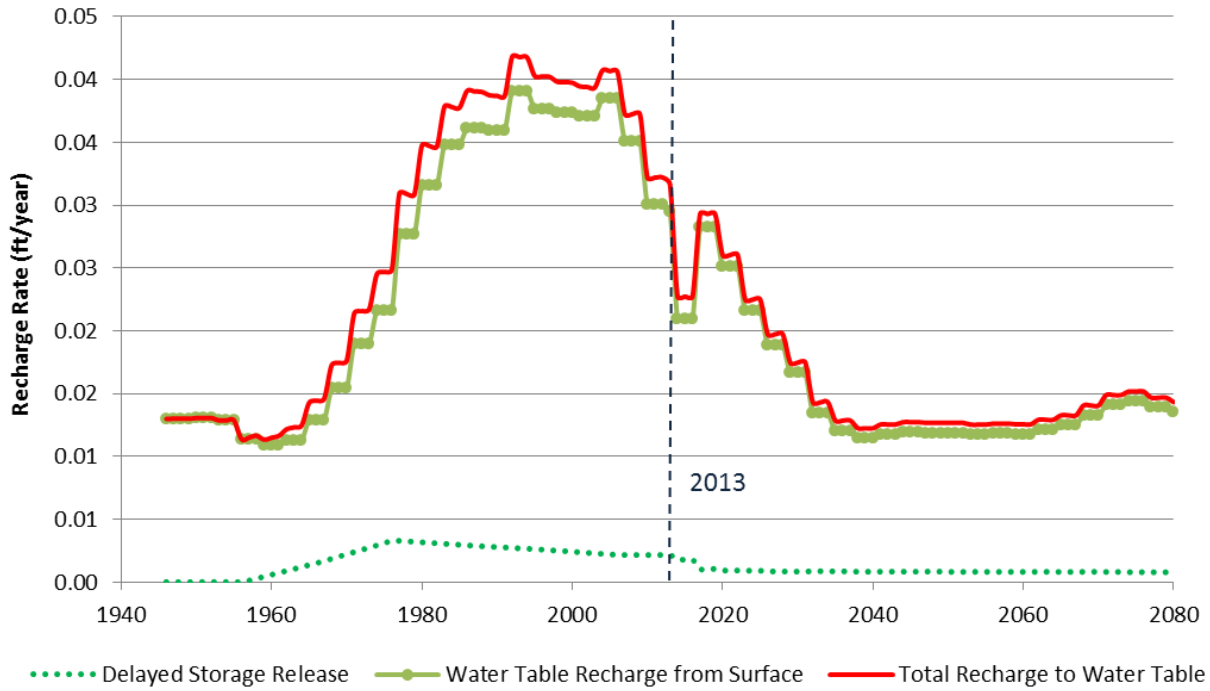

Figure 73. Water-table recharge for the no irrigation pumping in GMD1 scenario.

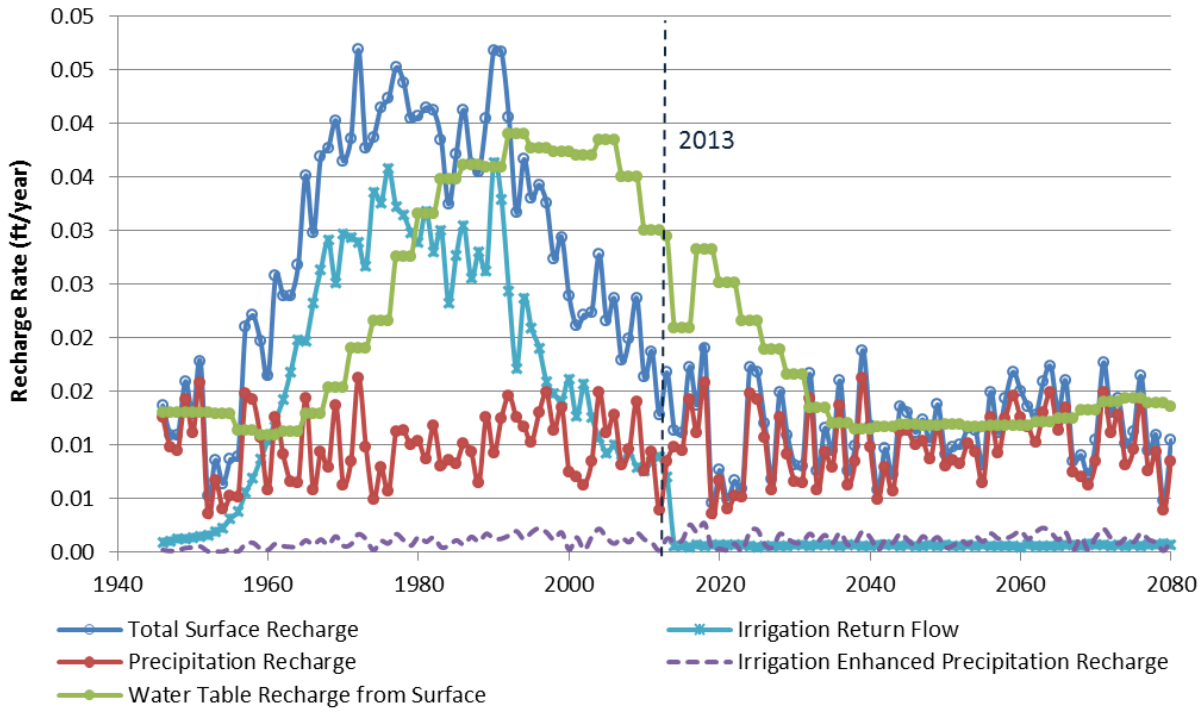

Figure 74. Different surface recharge components for the no irrigation pumping in GMD1 scenario.

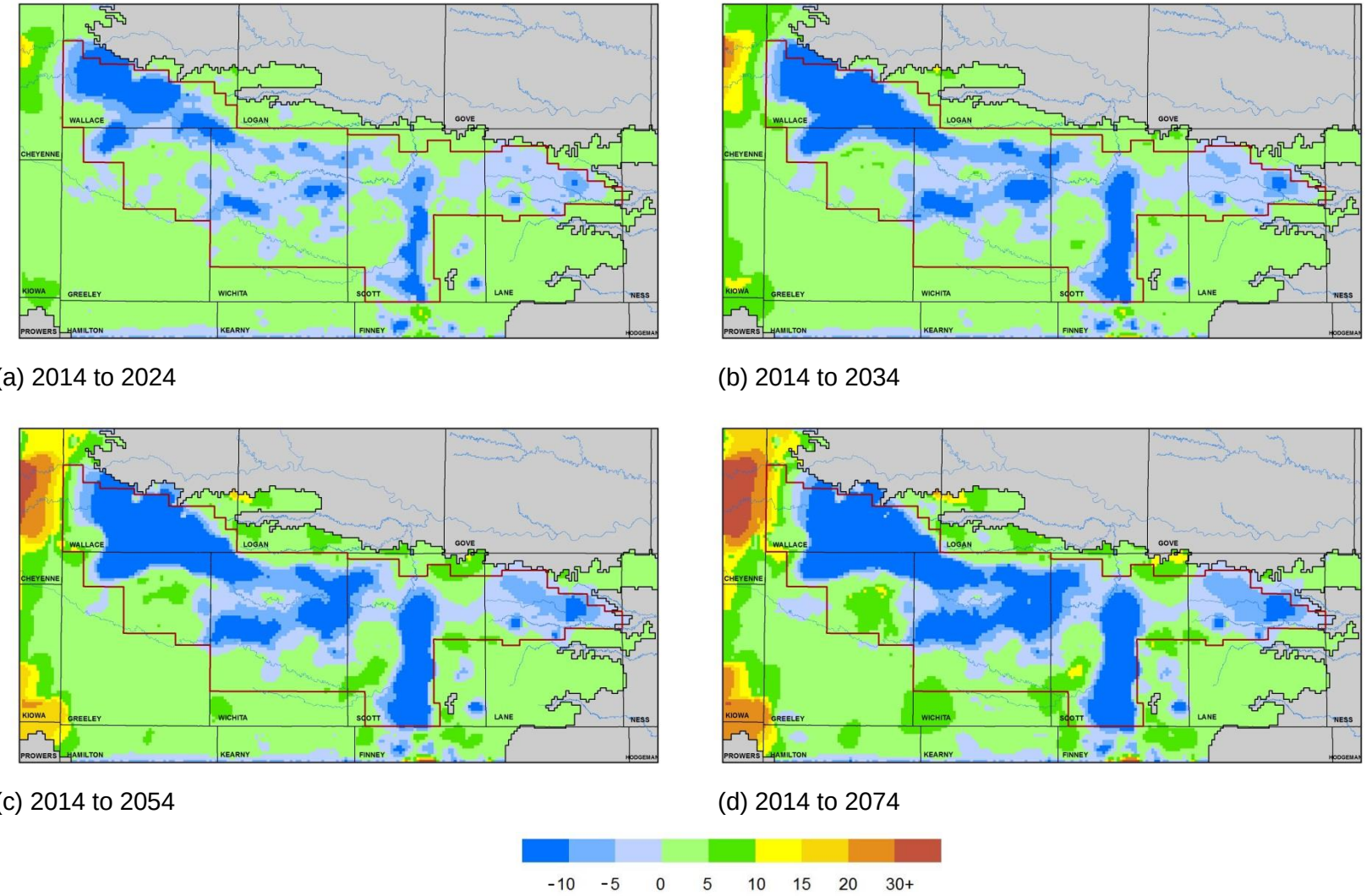

(a) 2014 to 2024

(b) 2014 to 2034

(c) 2014 to 2054

(d) 2014 to 2074

Figure 75. Simulated water-level change, in feet, for the no irrigation pumping in GMD1 scenario.

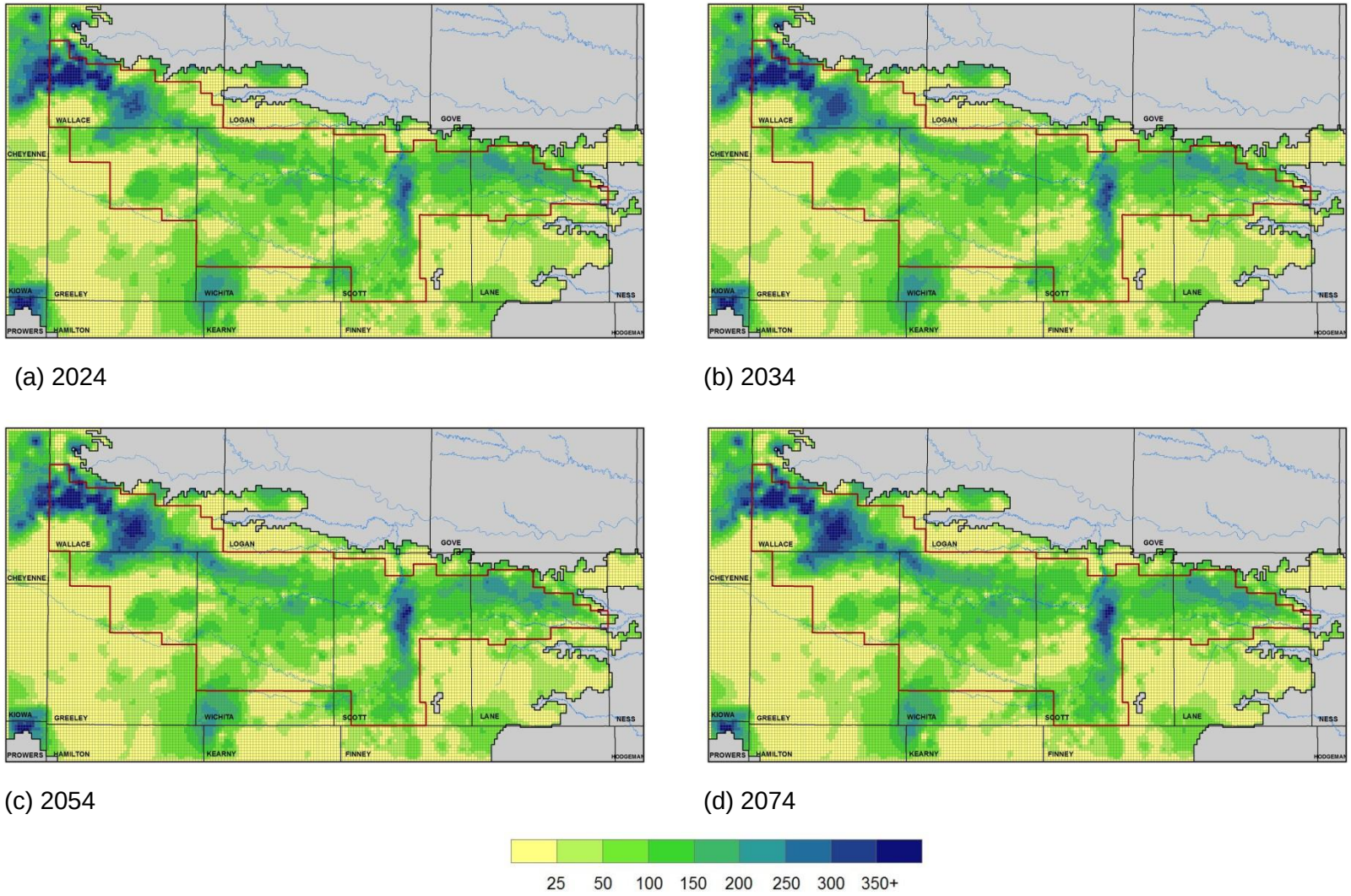

(a) 2024

(b) 2034

(c) 2054

(d) 2074

Figure 76. Spatial distribution of simulated aquifer storage (in 100 acre-ft) for the no irrigation pumping in GMD1 scenario.

Pumping for all GMD1 irrigation wells reduced by 20%

In this scenario, future irrigation pumping in GMD1 is reduced by 20% while the pumping outside GMD1 and non-irrigation pumping across the entire active model area continue as normal. This scenario simply reduced the amount of irrigation pumping used in the no change in future water use scenario by 20%. This reduction was only applied to irrigation pumping in GMD1.

Similar to the no change in water use policy scenario, all well pumping (including the 20% reduced irrigation pumping in GMD1 and continuous pumping for areas outside GMD1 and nonirrigation uses scenario) is further checked dynamically against the transmissivity calculated for each model cell and pumping season. If the computed transmissivity is less than 1000 ft^2/d, the pumping rate is changed to zero. During the MODFLOW run, the MODFLOW-NWT also reduces well pumping if the saturated thickness is below 5% of the cell thickness.

Figure 77 shows the annual aquifer budget for the 20% irrigation pumping reduction scenario. Compared to the no change in water-use policy scenario, the overall aquifer pumping is reduced, and the aquifer storage depletion is smaller. Figure 78 shows the contribution of lagged drainage and delayed surface recharge for this scenario, and fig. 79 displays the different surface recharge components.

Figure 80 shows the simulated head changes at selected year intervals for the 20% GMD1 irrigation pumping reduction scenario. Similar to the no change in water-use policy scenario, most of the district continues to have water-level declines, but the rates of declines are smaller. Figure 81 displays the simulated storage at selected years for the 20% GMD1 irrigation pumping reduction scenario. The detailed county budgets for the 20% GMD1 irrigation pumping reduction scenario are shown in Supplement C.

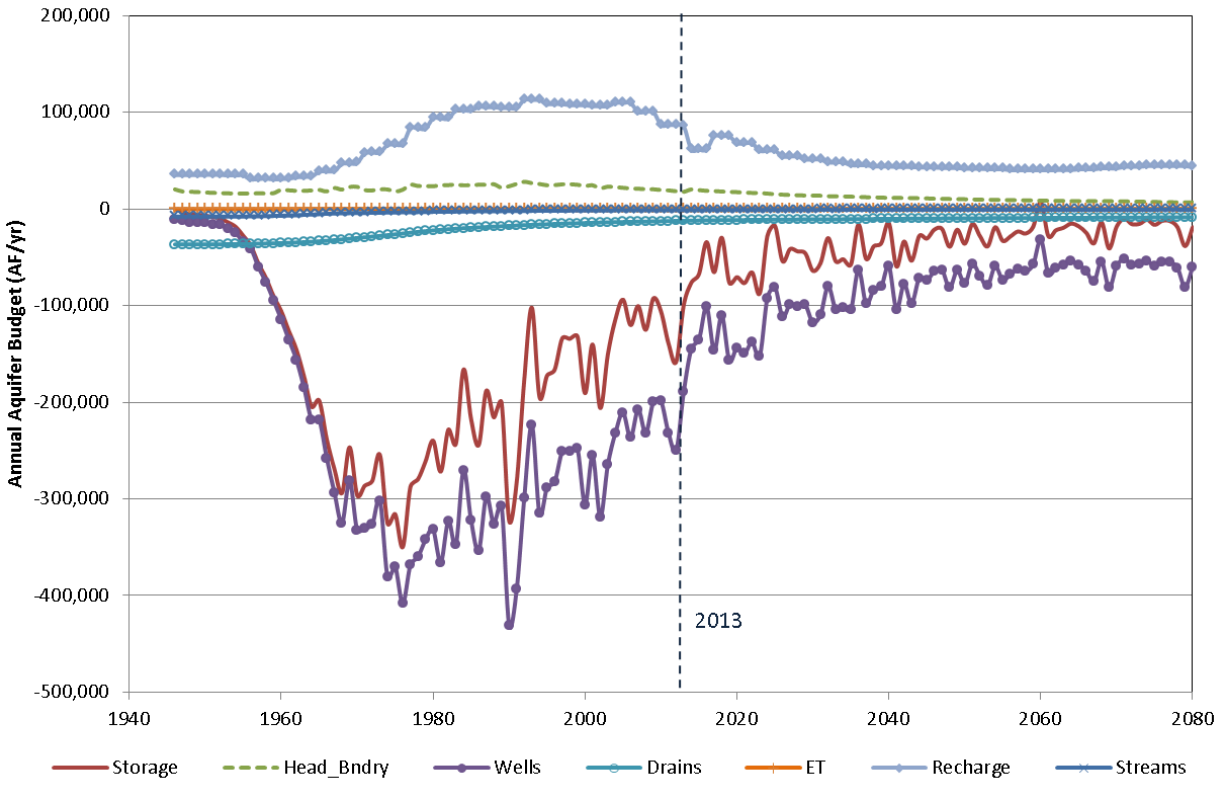

Figure 77. Annual aquifer budget for the 20% irrigation pumping reduction scenario.

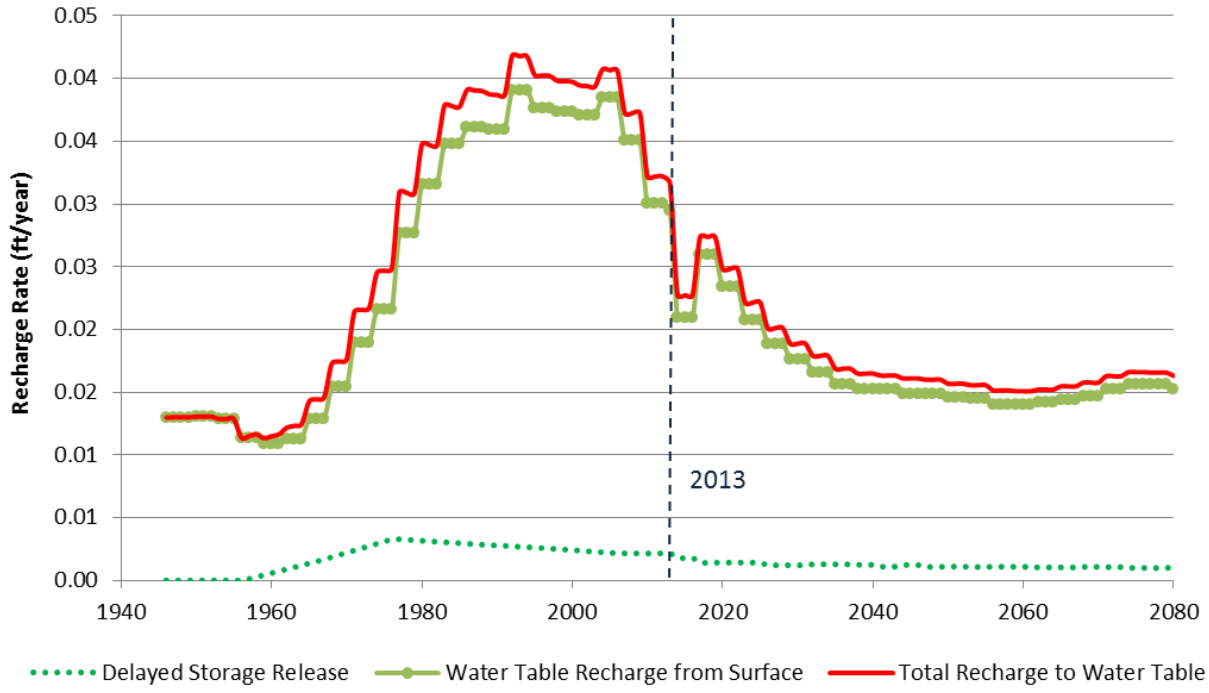

Figure 78. Water-table recharge for the 20% irrigation pumping reduction scenario.

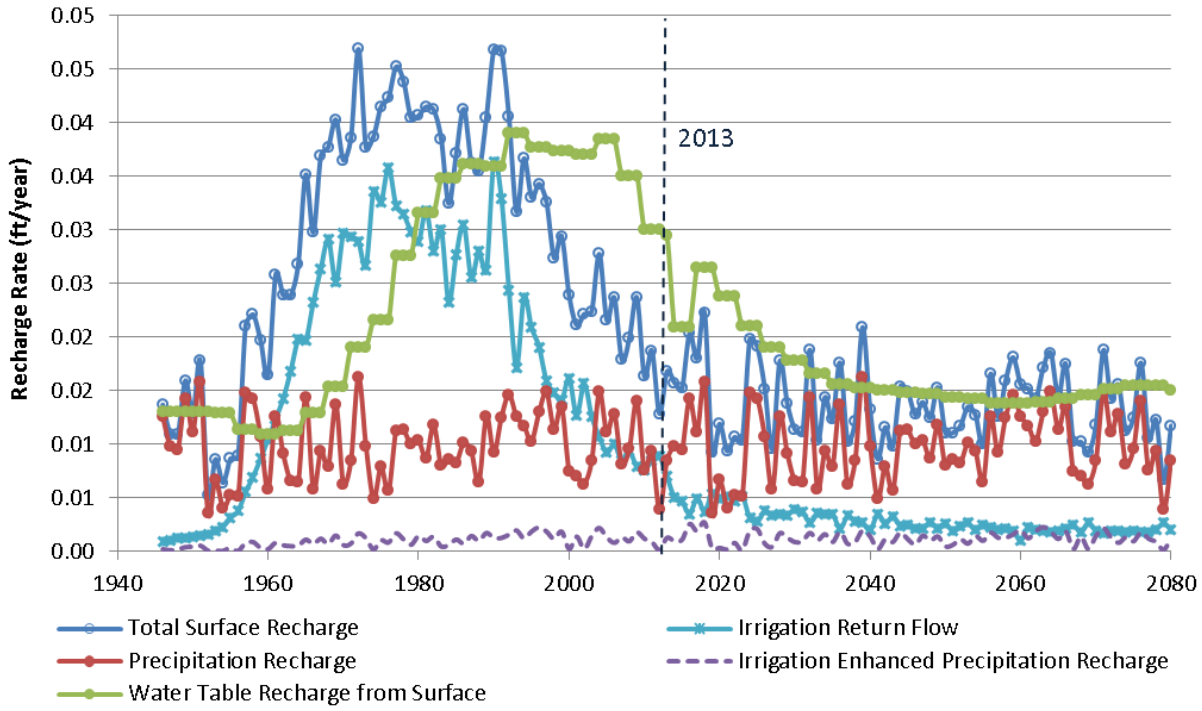

Figure 79. Different surface recharge components for the 20% irrigation pumping reduction scenario.

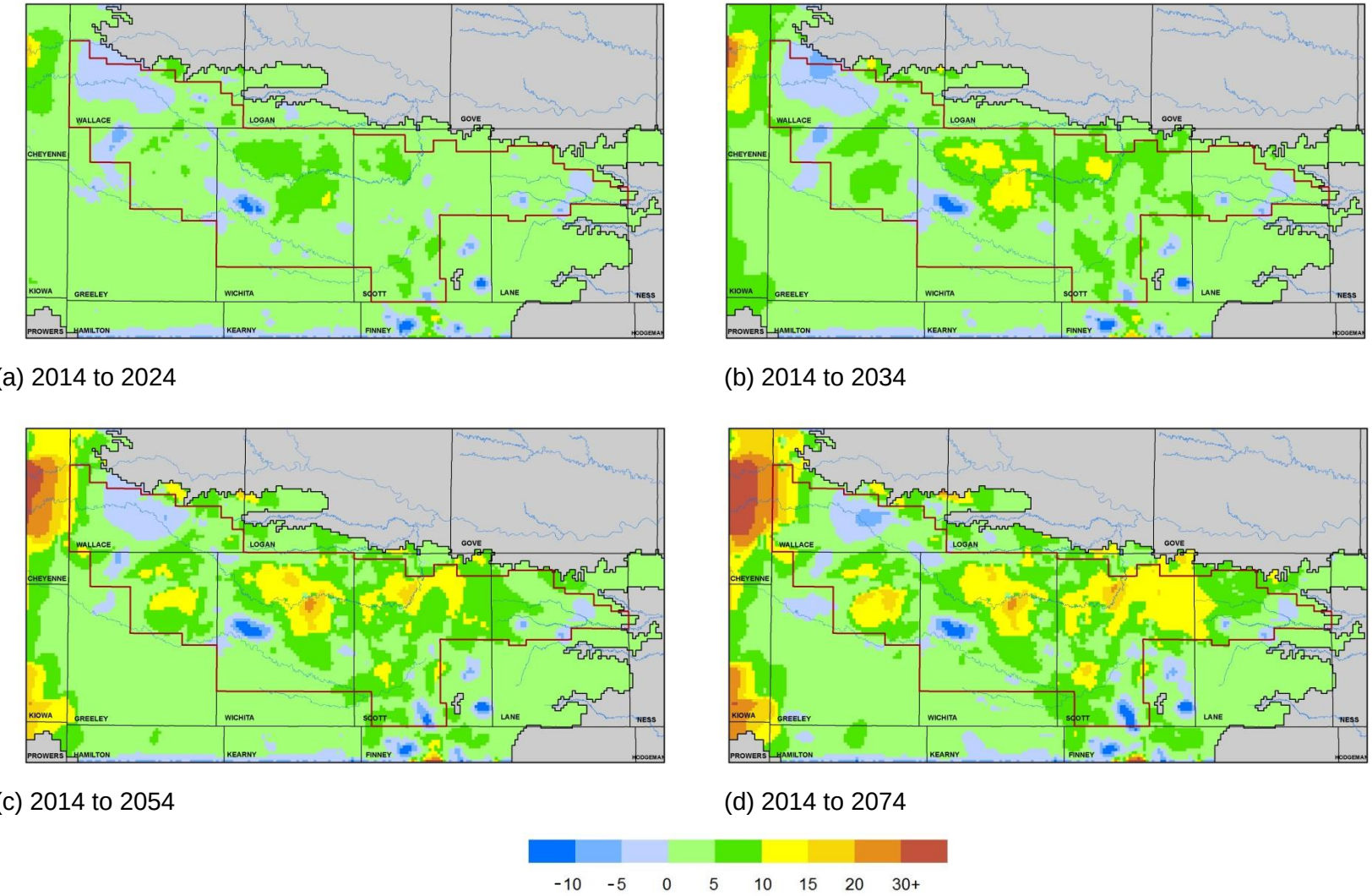

(a) 2014 to 2024

(b) 2014 to 2034

(c) 2014 to 2054

(d) 2014 to 2074

Figure 80. Simulated water-level change, in feet, for the 20% GMD1 irrigation pumping reduction scenario.

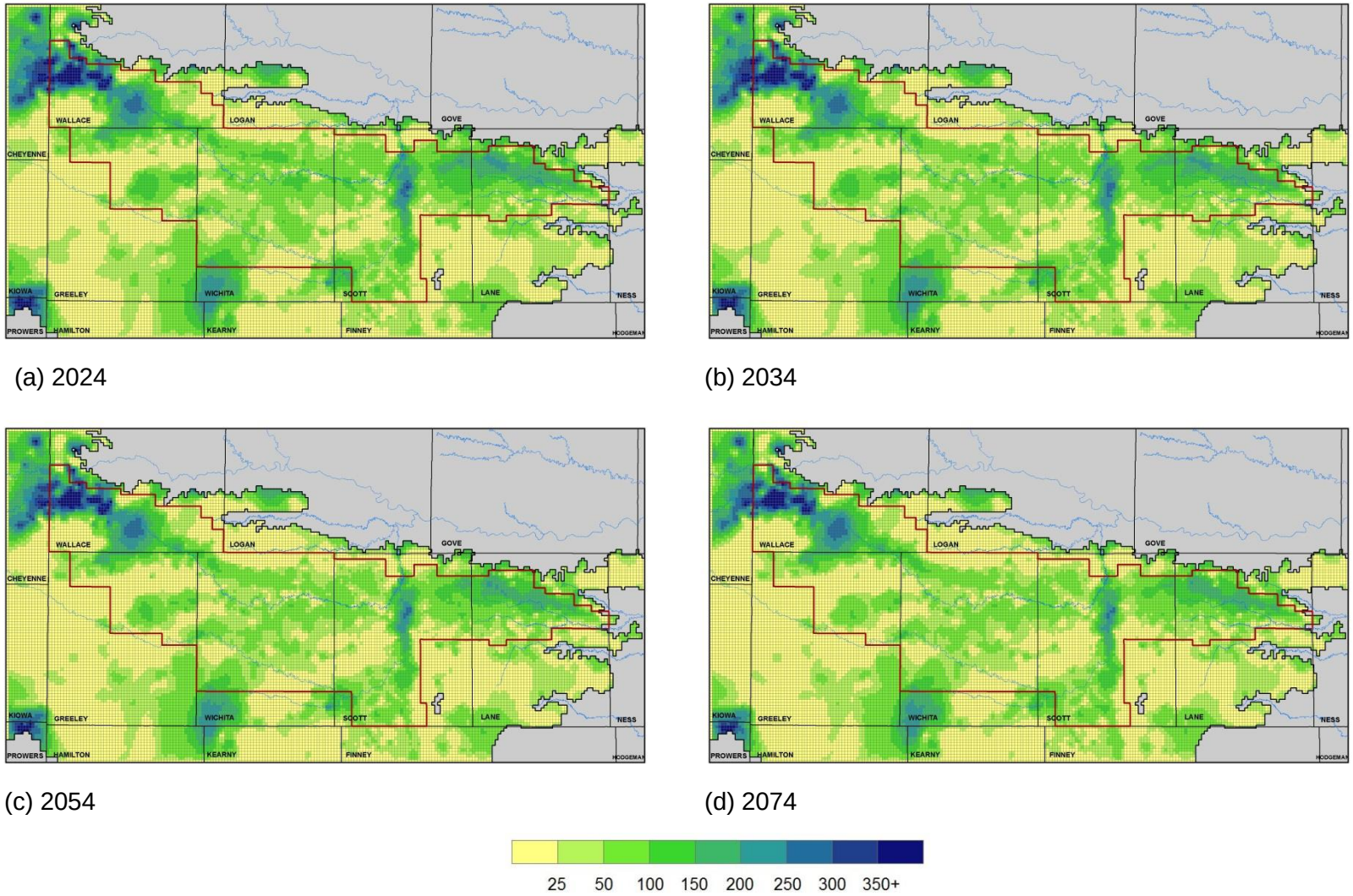

Figure 81. Spatial distribution of simulated aquifer storage (in 100 acre-ft) for the 20% GMD1 irrigation pumping reduction scenario.

To further evaluate the effects of different water-use scenarios on aquifer conditions, fig. 82 shows the cumulative change in aquifer storage with time for the GMD1 area for all three scenarios. Although the annual difference in the aquifer storage between the continued and 20% reduction in irrigation pumping is not substantial initially, the accumulative difference becomes increasingly significant with time. However, a larger reduction in pumping would be needed to keep the aquifer storage at 2013 levels.

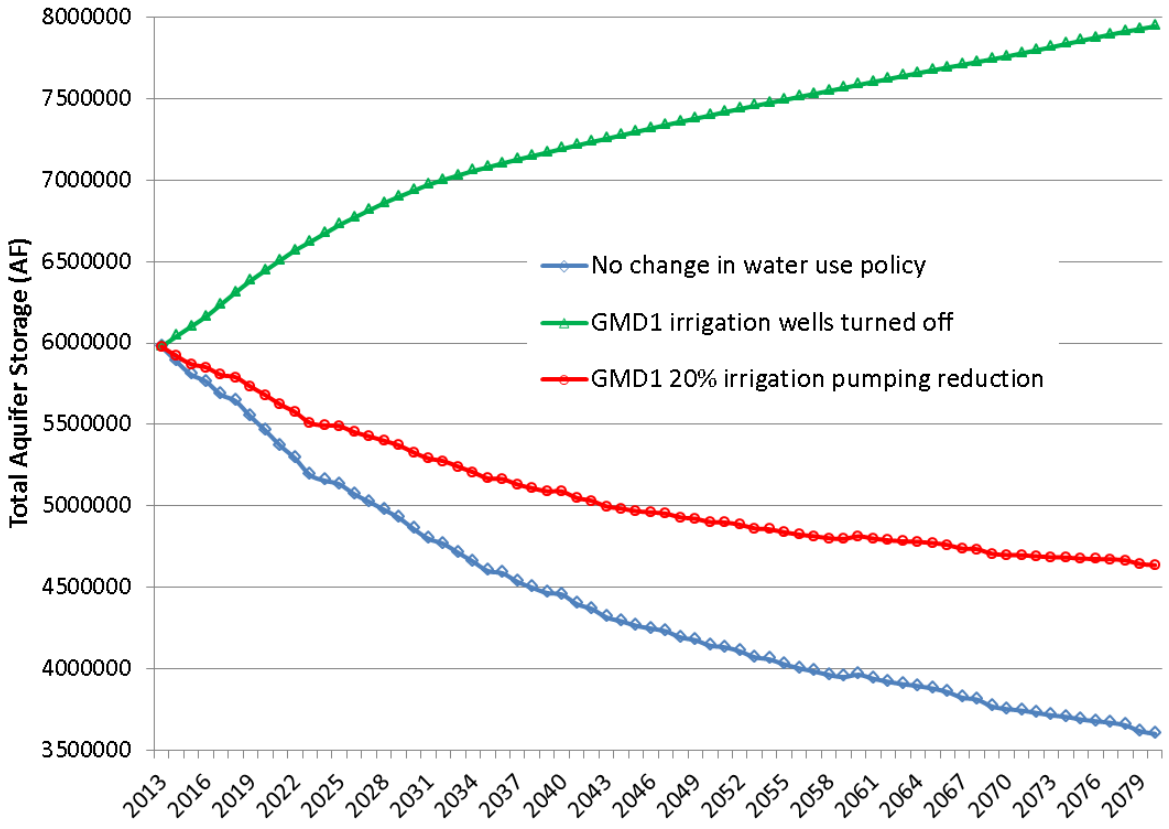

Figure 82. Change in GMD1 aquifer storage for all three future scenarios.

Figure 83 compares the GMD1 aquifer storage between the 20% reduction in GMD1 irrigation pumping scenario and the no change in future water-use policy scenario. During the first two decades (2013–2023), the 20% reduction in irrigation pumping reduces the rate of storage loss by an average rate of almost 32,000 acre-ft/year, with a total aquifer savings of more than 300,000 acre-ft. Over the remaining future years this reduction in the rate of storage loss begins to gradually decrease, a reflection of declining aquifer yield with time (Figure 67) (the magnitude of the 20% reduction of pumping thus becomes smaller with time). At the end of future simulation (2080), the annual aquifer savings is about 8,550 AF/year. The total aquifer savings from 2013 to 2080 by the 20% reduction of pumping is about 1,034,900 AF.

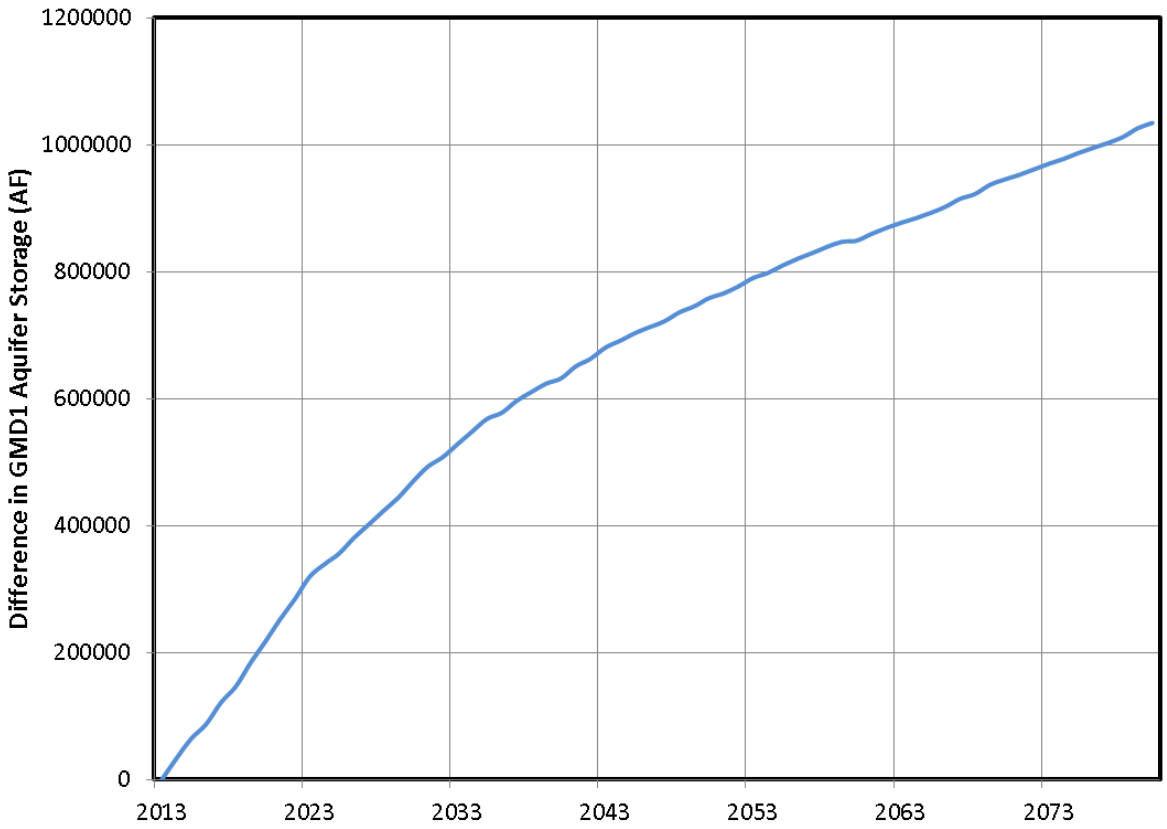

Figure 83. GMD1 aquifer storage difference between the 20% reduction in GMD1 irrigation pumping scenario and the no change in future water-use policy scenario. Values are calculated by subtracting the cumulative GMD1 storage in the no change in water-use policy scenario from that in the 20% reduction in GMD1 irrigation pumping scenario.

Acknowledgments

The KGS modeling team acknowledges the funding support of the Kansas Water Office (and the State Water Plan fund) and Western Kansas GMD #1 for this project. We also recognize KGS staff who contributed to this report. John Woods spent a substantial amount of time reviewing well logs, improving the estimated bedrock surface, and identifying stream elevations along Ladder and Whitewoman creeks. We are grateful for the contribution of Dustin Fross to the HyDRA project in reviewing the quality of drillers' logs. We also thank Julie Tollefson, KGS editor, who reviewed the final report.

The authors recognize the help of Kyle Spencer and Diane Knowles who served as the primary contacts for GMD1 and the KWO, respectively. We appreciate the active involvement of the GMD1 Board—Greg Graff, Bob Hoeme, Alan James, Arla Peters, and Danny Welsh—for their local insight and recommendations. We also recognize the model advisory group of Chris Holovach, Mark Jones, Frank Mercurio, Bo Parkinson, Jim Rowton, Alan Schlegel, and Mike Todd for volunteering their time. Finally, we appreciate the assistance Jan King (former GMD1 Manager) and Susan Stover (formerly of the KWO).

REFERENCES

Becker, M. F., 1999, Digital map of predevelopment water levels for the High Plains aquifer in parts of Colorado, Kansas, Nebraska, New Mexico, Oklahoma, South Dakota, Texas, and Wyoming: U.S. Geological Survey, Open-File Report 99-264.

Boettcher, A. J., 1964, Geology and ground-water resources in Eastern Cheyenne and Kiowa counties, Colorado: Geological Survey Water Supply Paper 1779-N, 38 p.

Butler, J. J., Whittemore, D. O., Reboulet, E., Knobbe S., Wilson, B. B., Stotler, R. R., and Bohling, G. C., 2015, High Plains aquifer index well report: Kansas Geological Survey Open-File Report 2015-3, 155 p.

Doherty, J., 2004, PEST—Model-Independent Parameter Estimation. User Manual, 5th Edition.Watermark Numerical Computing, 333 p.

Gutentag, E.D., Heimes, F.J., Krothe, N.C., Luckey, R.R., and Weeks, J.B., 1984, Geohydrology of the High Plains aquifer in parts of Colorado, Kansas, Nebraska, New Mexico, Oklahoma, South Dakota, Texas, and Wyoming. U.S. Geological Survey Professional Paper 1400-B, 63 p.

Harbaugh, A. W., Banta, E. R., Hill, M. C., and McDonald, M. G., 2000, MODFLOW-2000, the U.S. Geological Survey modular ground-water model—User guide to modularization concepts and the Ground-Water Flow Process: U.S. Geological Survey, Open-File Report 00-92, 121 p.

Hodson, W. G., 1963, Geology and ground-water resources of Wallace County, Kansas. Kansas: Kansas Geological Survey, Bulletin 161, 108 p.

Hodson, W.G., Wahl, K. D., 1960, Geology and ground-water resources of Gove County, Kansas. Kansas Geological Survey, Bulletin 145, 126 p.

Krieger, R. A., 1957, Ground-water resources of the Ladder Creek area in Kansas: Kansas Geological Survey, Bulletin 126, 194 p.

Latta, B. F., with analyses by Holmes, E. O., 1944, Geology and ground-water resources of Finney and Gray counties, Kansas: Kansas Geological Survey, Bulletin 55, 272 p.

Liu, G., Wilson, B. B., Whittemore, D. O., Wei Jin, W., Butler, J. J., Jr., 2010, Ground-water model for Southwest Kansas Groundwater Management District No. 3: Kansas Geological Survey, Open-File Report 2010-18, 106 p.

Luckey, R.R., Gutentag, E.D., Heinmes, F.J., Weeks, J.B., Digital simulation of ground-water flow in the High Plains Aquifer in parts of Colorado, Kansas, Nebraska, New Mexico, Oklahoma, South Dakota, Texas, and Wyoming, U.S. Professional Paper 1400-D, 57 p.

Ludvigson, G. A., Sawin, R. S., Franseen, E. K., Watney, W. L., West, R. R., and Smith, J. J, 2009, A review of the stratigraphy of the Ogallala Formation and revision of Neogene ("Tertiary") nomenclature in Kansas; *in*, Current Research in Earth Sciences: Kansas Geological Survey, Bulletin 256, part 2. (http://www.kgs.ku.edu/Current/2009/Ludvigson/index.html, accessed September 2010).

Macfarlane, P.A., Wilson, B.B., and Bohling, G., 2005, Practical saturated thickness of the Ogallala in two small areas of southwest Kansas Groundwater Management District 3: Kansas

Geological Survey, Open-File Report 2005-29, 27 p.

Macfarlane, P. A., and Wilson, B. B., 2006, Enhancement of the bedrock-surface map beneath the Ogallala portion of the High Plains aquifer, western Kansas: Kansas Geological Survey, Technical Series Report 20, 28p.

Macfarlane, P.A., and Schneider, N., 2007, Distribution of the permeable fraction and practical saturated thickness in the Ogallala portion of the High Plains aquifer in the Southwest Kansas Groundwater Management District 3: Kansas Geological Survey Open-file Report, 2007-28, 70 p.

McLaughlin, T. G., with analyses by Holes, E. O., 1943, Geology and ground-water resources of Hamilton and Kearny counties, Kansas: Kansas Geological Survey, Bulletin 49, 220 p.

National Water Information System (NWIS), United States Geological Survey, http://waterdata.usgs.gov/nwis, accessed July 2013.

Niswonger, R. G., Panday, S., and Ibaraki, M., 2011, MODFLOW-NWT, A Newton formulation for MODFLOW-2005: U.S. Geological Survey Techniques and Methods 6–A37, 44 p.

Prescott, G. C., Jr., 1951, Geology and ground-water resources of Lane County, Kansas: Kansas Geological Survey, Bulletin 93, 126 p.

Prescott, G. C., Jr., Branch, J. R., and Wilson, W. W., 1954, Geology and ground-water resources of Wichita and Greeley counties, Kansas: Kansas Geological Survey, Bulletin 108, 134 p.

PRISM Climate Group, Oregon State University, http://prism.oregonstate.edu, accessed May, 2014.

Prudic, D.E., Konikow, L.F., Banta, E.R., 2004, A New Streamflow-Routing (SFR1) Package to Simulate Stream-Aquifer Interaction with MODLFOW-2000; U.S. Geological Survey, Open-File Report 2004-1042, 104 p.

Waite, H. A., 1947, Geology and ground-water resources of Scott County, Kansas: Kansas Geological Survey, Bulletin 66, 216 p.

Water Information Management and Analysis System (WIMAS): Kansas Geological Survey, Kansas Department of Agriculture, http://hercules.kgs.ku.edu/geohydro/wimas/index.cfm, accessed July 2013.

Water Information Storage and Retrieval Database (WIZARD): Kansas Geological Survey, http://www.kgs.ku.edu/Magellan/WaterLevels/index.html, accessed July 2013 and May 2015.

Water Well Completion Records Database (WWC5): Kansas Geological Survey, http://www.kgs.ku.edu/Magellan/WaterWell/index.html, accessed July 2013.

Whittemore, D. O., Sophocleous, M. A., Butler, J. J., Wilson, B. B., Tsou, M. S., Zhan, X., Young, D. P., McGlashan, M., 2006, Numerical model of the middle Arkansas River subbasin: Kansas Geological Survey, Open-File Report 2006-25, 122 p.

Whittemore, D. O., Macfarlane, P. A., Wilson, B. B., 2014, Water resources of the Dakota aquifer in Kansas: Kansas Geological Survey, Bulletin 260, 68 p.

Wilson, B. B., and Bohling, G. C., 2003, Assessment of reported water use and total annual precipitation, State of Kansas: Kansas Geological Survey, Open-File Report 2003-55C, 39 p.

Wilson, B. B., Liu, G., Whittemore, D. O., Butler, J. J., 2008, Smoky Hill River ground-water model: Kansas Geological Survey, Open-File Report 2008-20, 99 p.

Supplements

A. County results for the no change in future water use scenario

Figures SA1, SA3, SA5, SA7, and SA9 show the annual aquifer budget for Wallace, Greeley, Wichita, Scott, and Lane counties for the no change in future water use scenario. Figures SA2, SA4, SA6, SA8, and SA10 show different recharge components for these counties. Figure SA11 compares the absolute aquifer storage between different counties. Assuming no change in future water use, Scott and Wichita counties have the most storage loss, followed by Wallace County. For all GMD1 counties, the most significant storage loss occurred between the 1960s and 2010s.

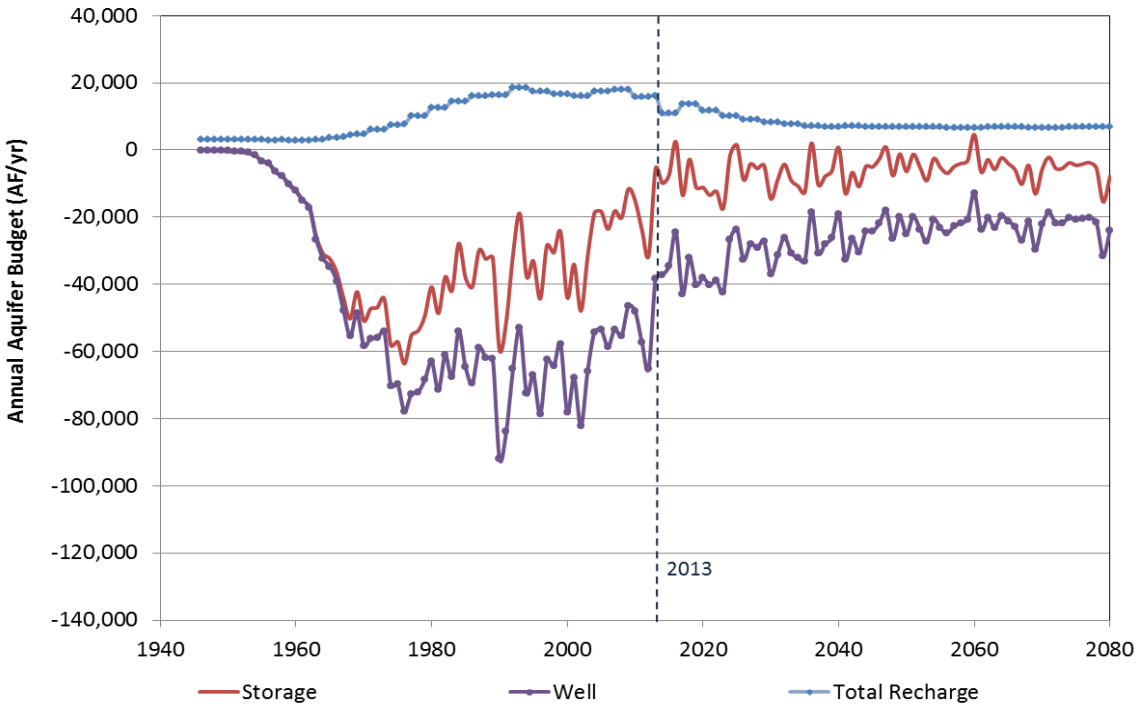

Figure SA1. Annual aquifer budget for Wallace County for the no change in future water use scenario.

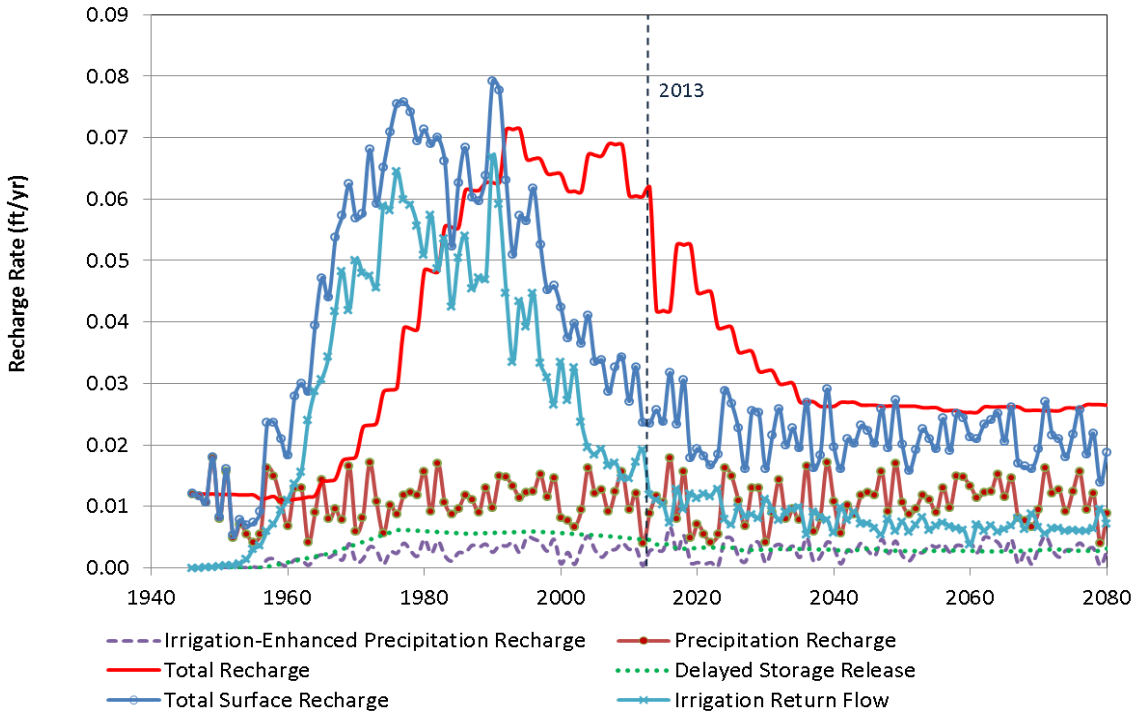

Figure SA2. Different recharge components for Wallace County for the no change in future water use scenario.

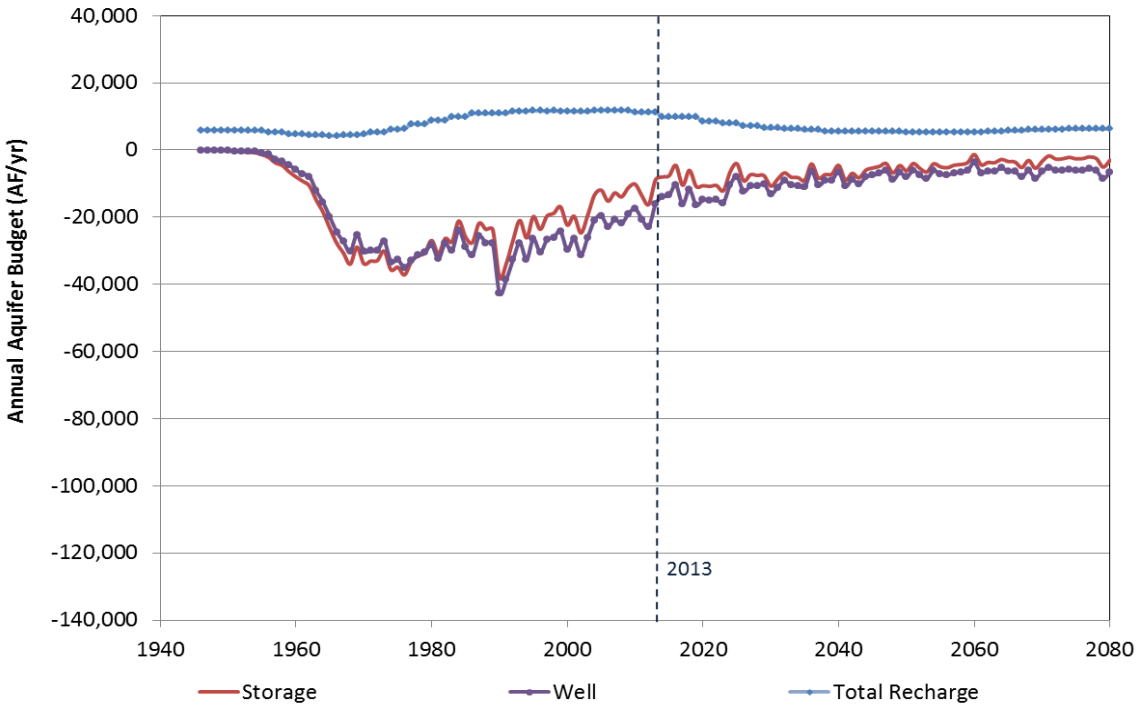

Figure SA3. Annual aquifer budget for Greeley County for the no change in future water use scenario.

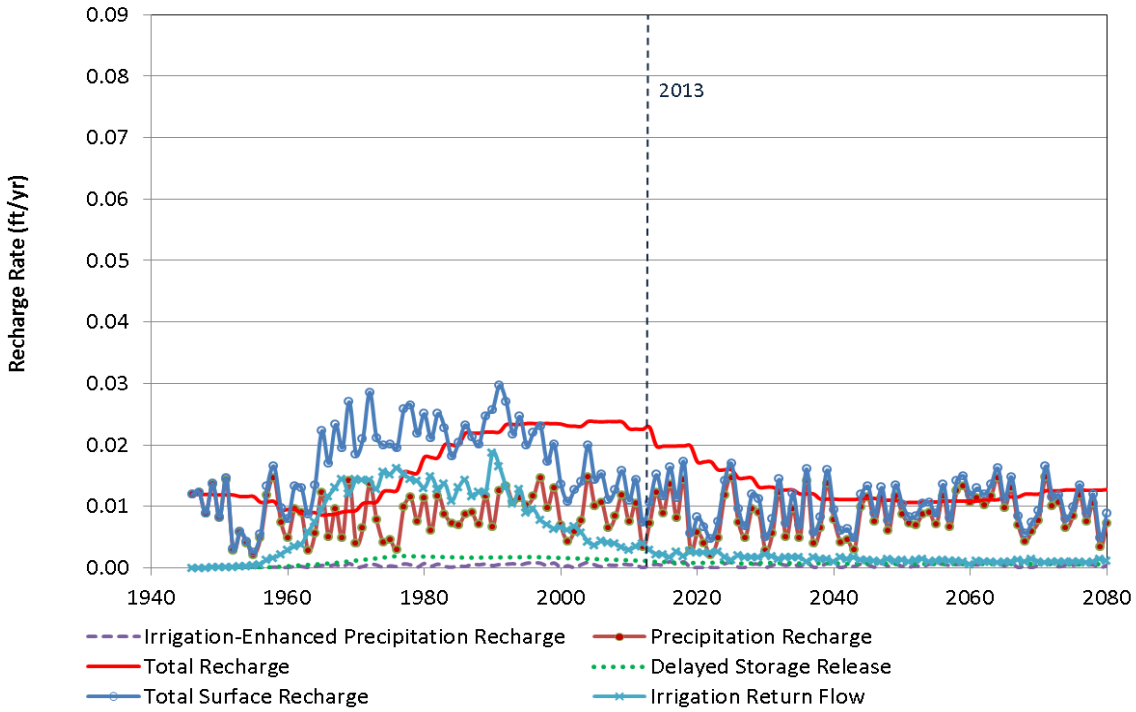

Figure SA4. Different recharge components for Greeley County for the no change in future water use scenario.

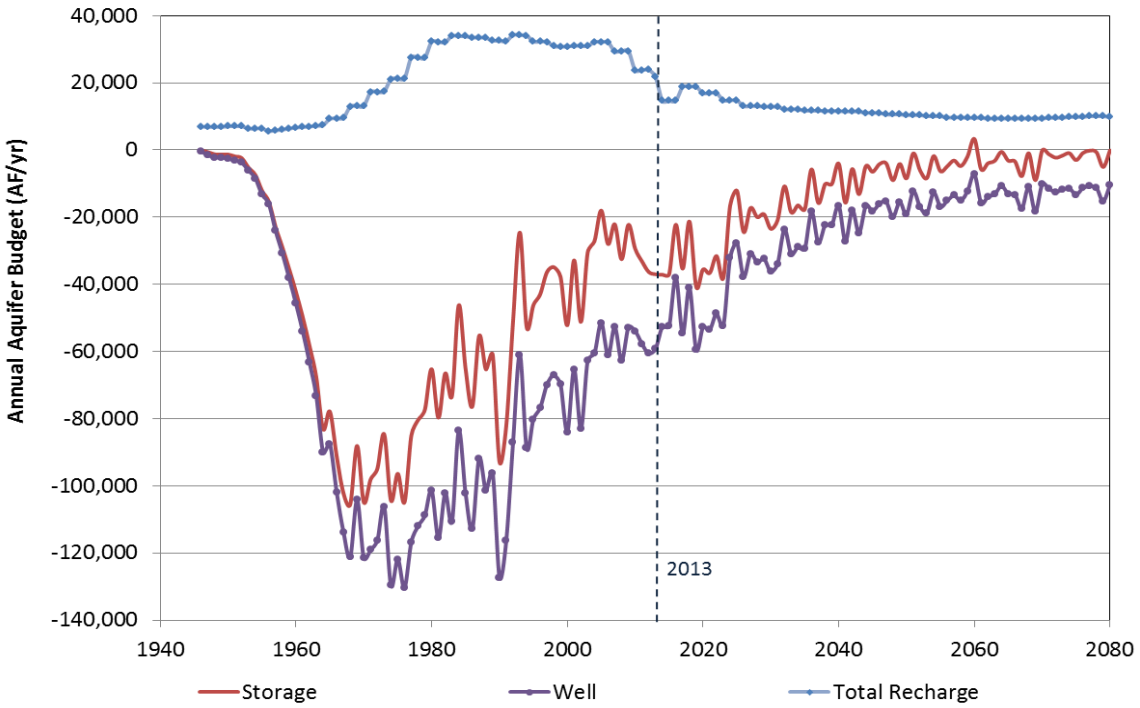

Figure SA5. Annual aquifer budget for Wichita County for the no change in future water use scenario.

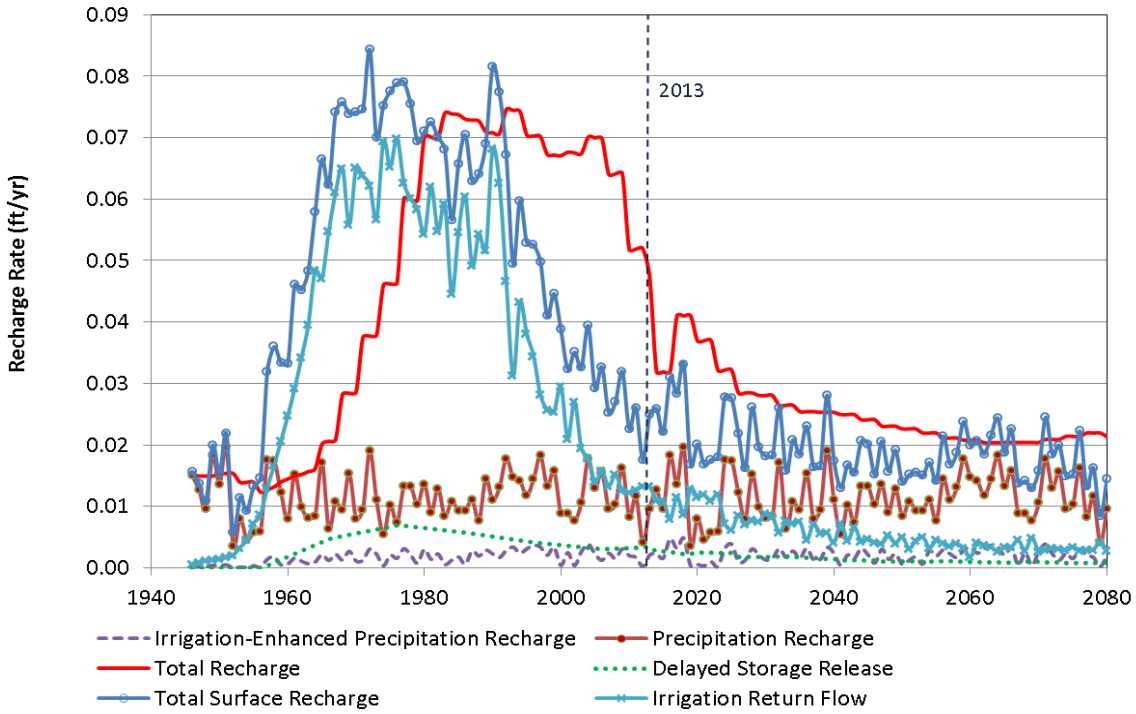

Figure SA6. Different recharge components for Wichita County for the no change in future water use scenario.

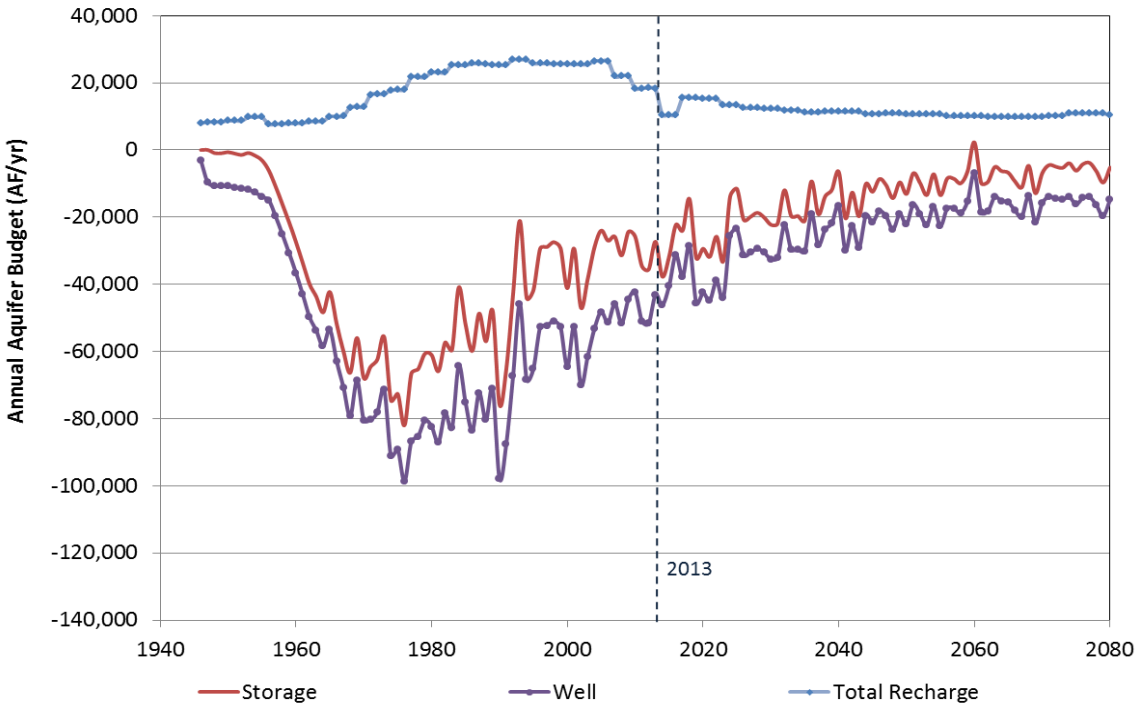

Figure SA7. Annual aquifer budget for Scott County for the no change in future water use scenario.

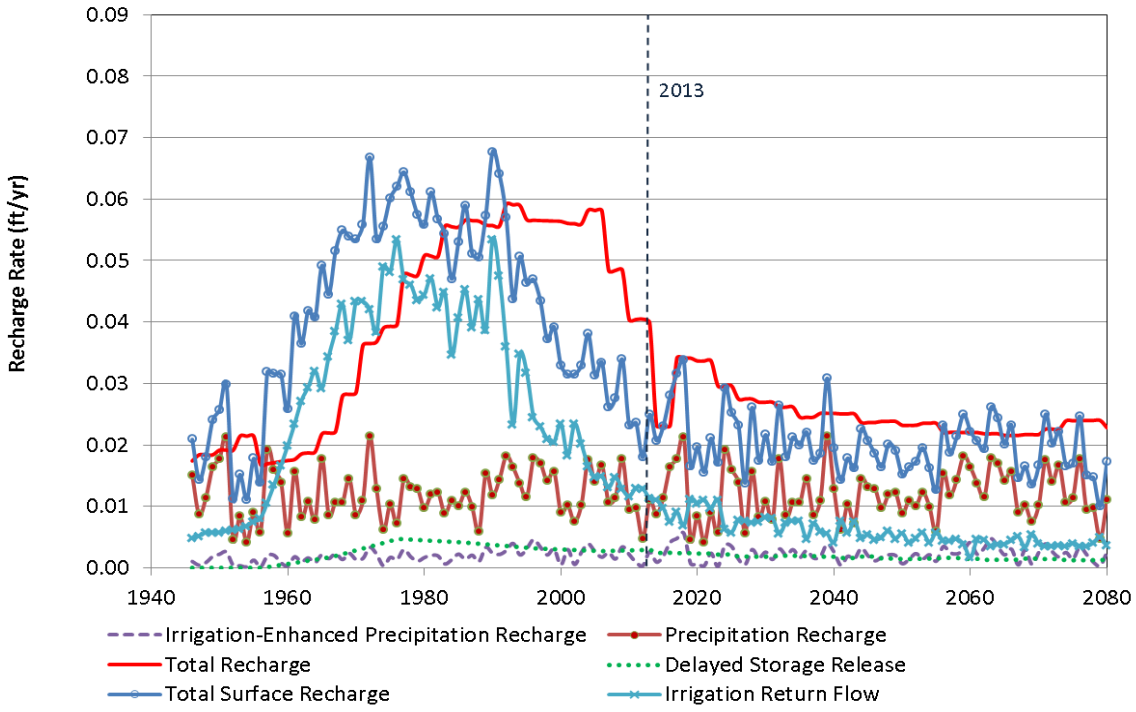

Figure SA8. Different recharge components for Scott County for the no change in future water use scenario.

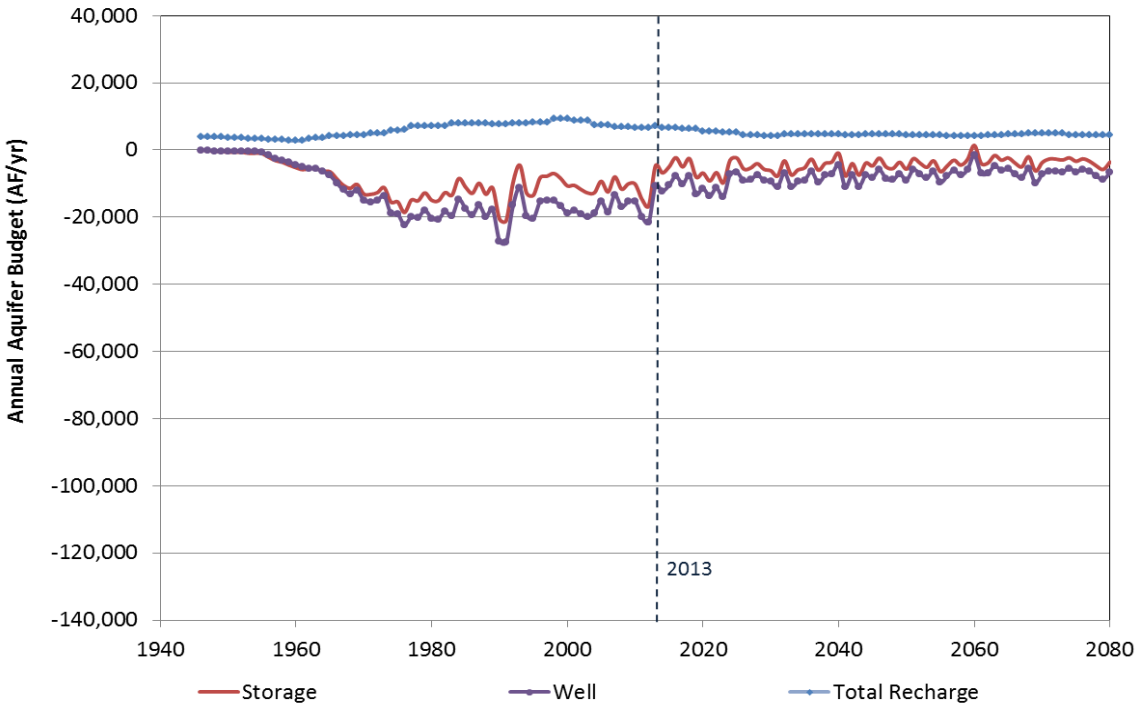

Figure SA9. Annual aquifer budget for Lane County for the no change in future water use scenario.

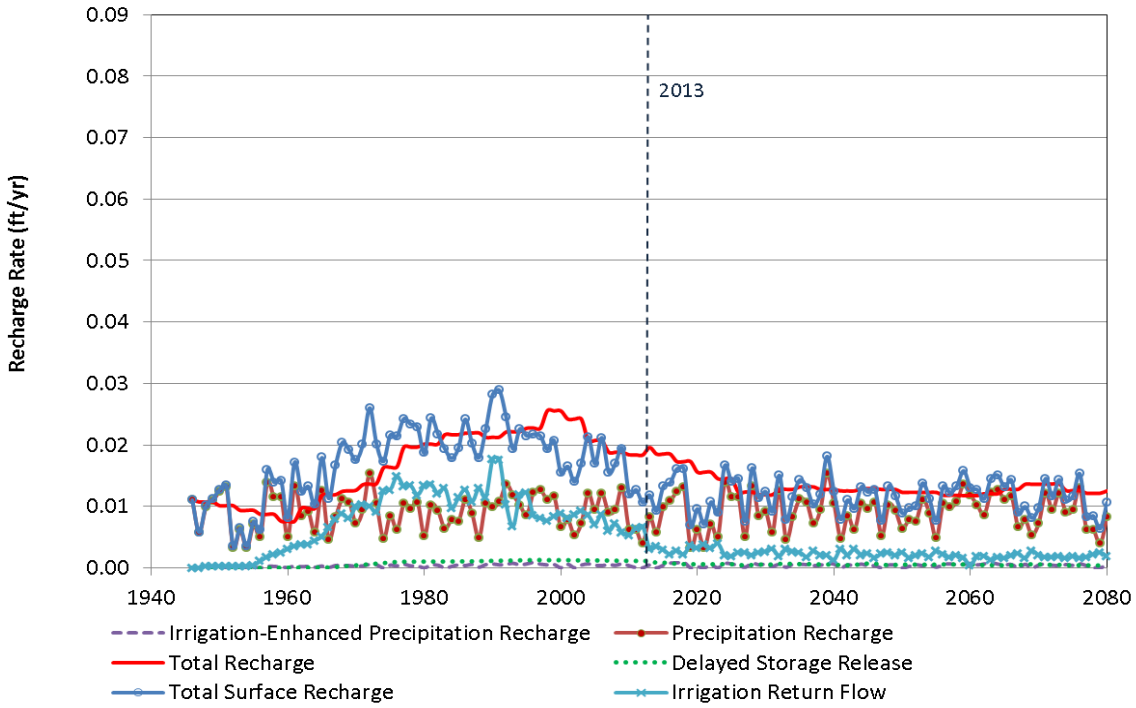

Figure SA10. Different recharge components for Lane County for the no change in future water use scenario.

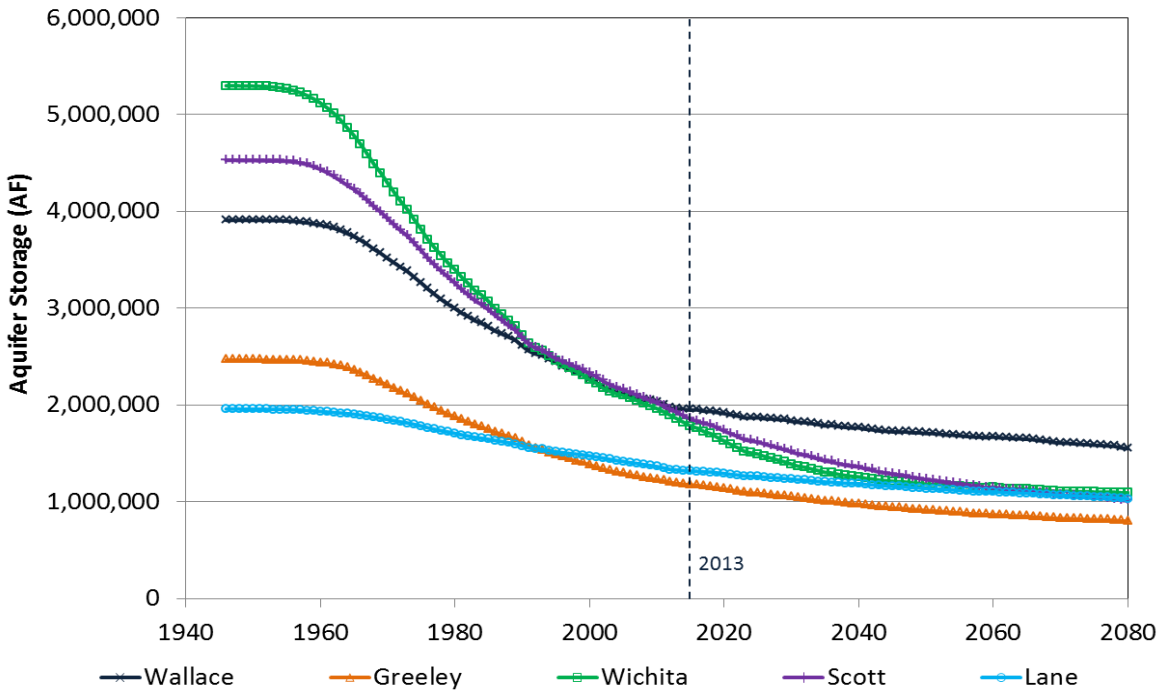

Figure SA11. Aquifer storage for different counties in GMD1 for the no change in future water use scenario.

B. County results for the no irrigation pumping in GMD1 scenario

Figures SB1, SB3, SB5, SB7, and SB9 show the annual aquifer budget for Wallace, Greeley, Wichita, Scott, and Lane counties for the no irrigation pumping in GMD1 scenario. Figures SB2, SB4, SB6, SB8, and SB10 show different recharge components for these counties. Figure SB11 compares the absolute aquifer storage between different counties.

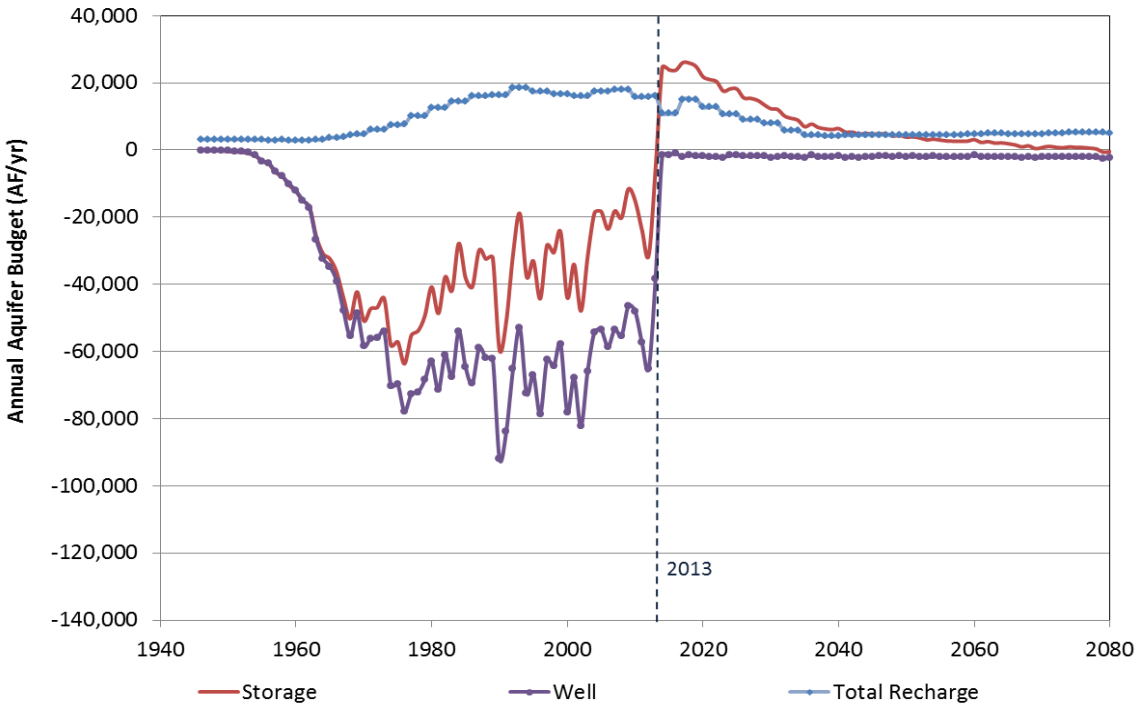

Figure SB1. Annual aquifer budget for Wallace County for the no irrigation pumping in GMD1 scenario.

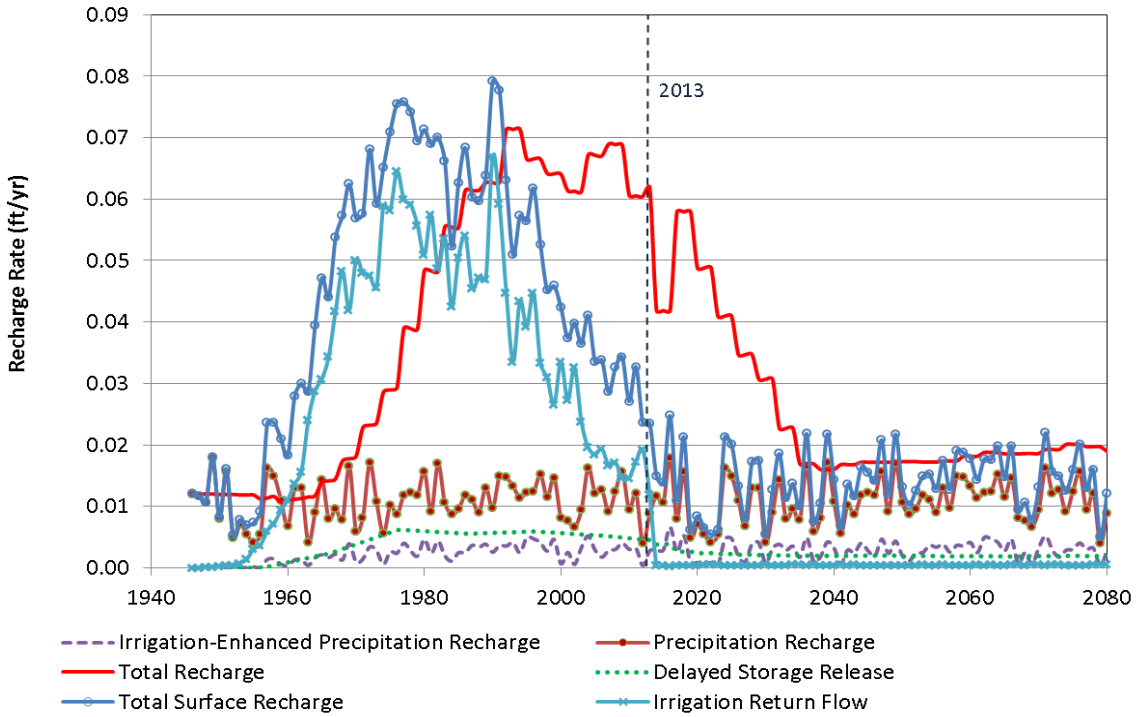

Figure SB2. Different recharge components for Wallace County for the no irrigation pumping in GMD1 scenario.

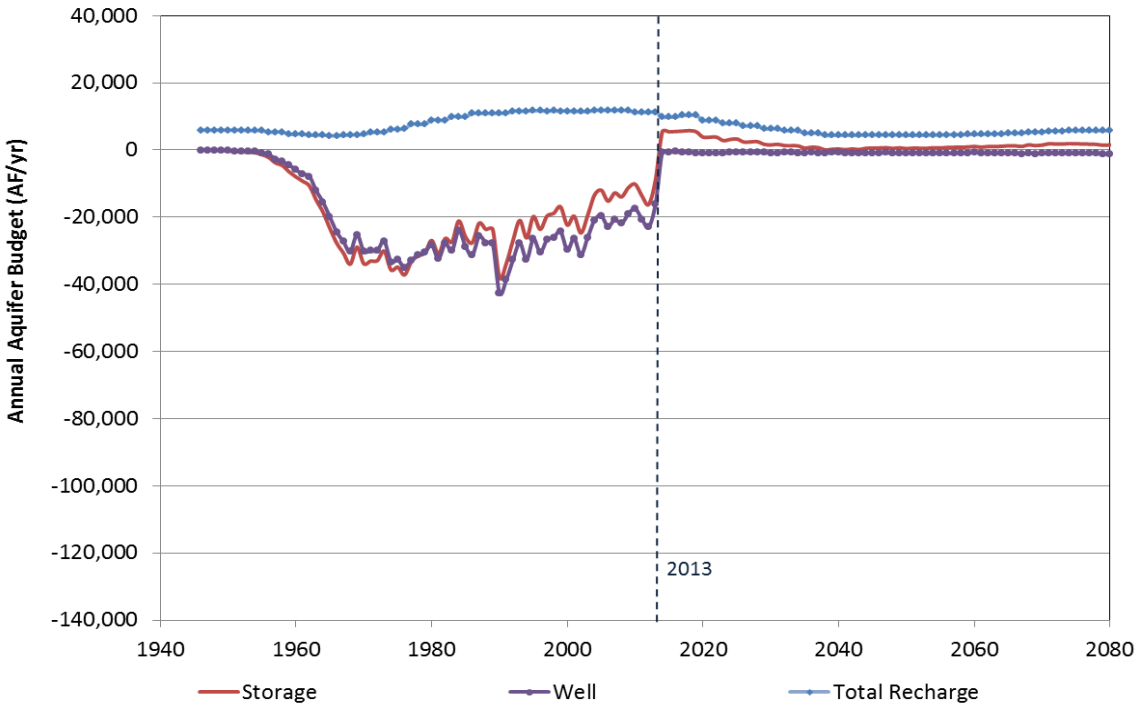

Figure SB3. Annual aquifer budget for Greeley County for the no irrigation pumping in GMD1 scenario.

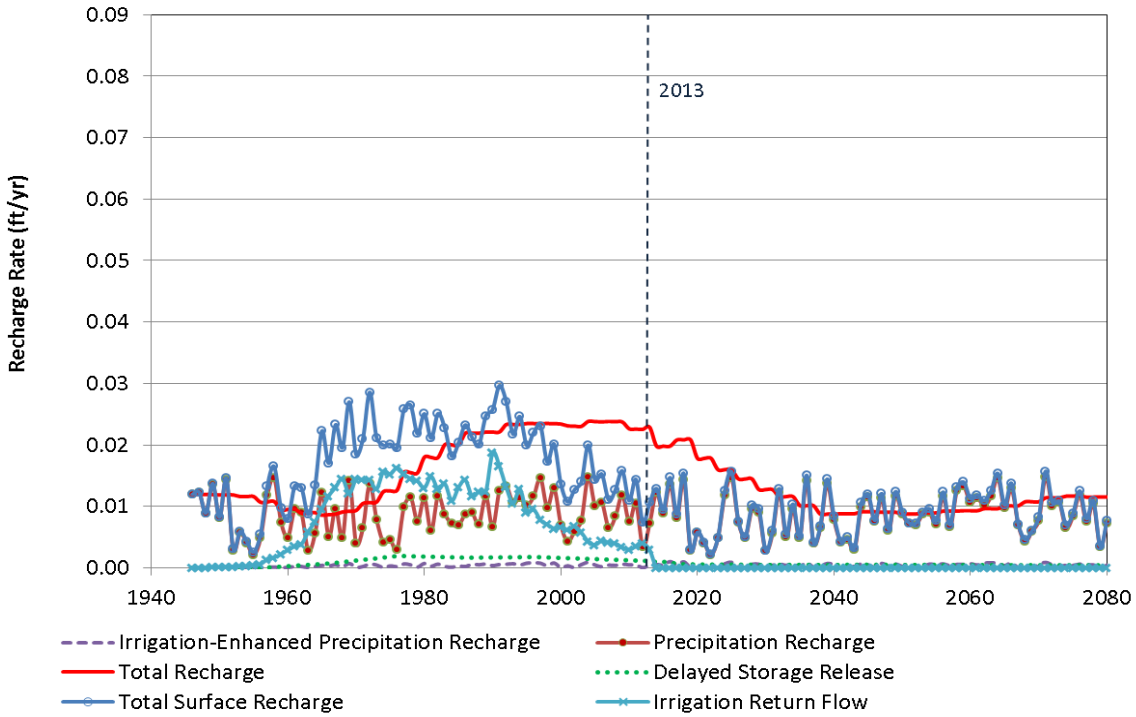

Figure SB4. Different recharge components for Greeley County for the no irrigation pumping in GMD1 scenario.

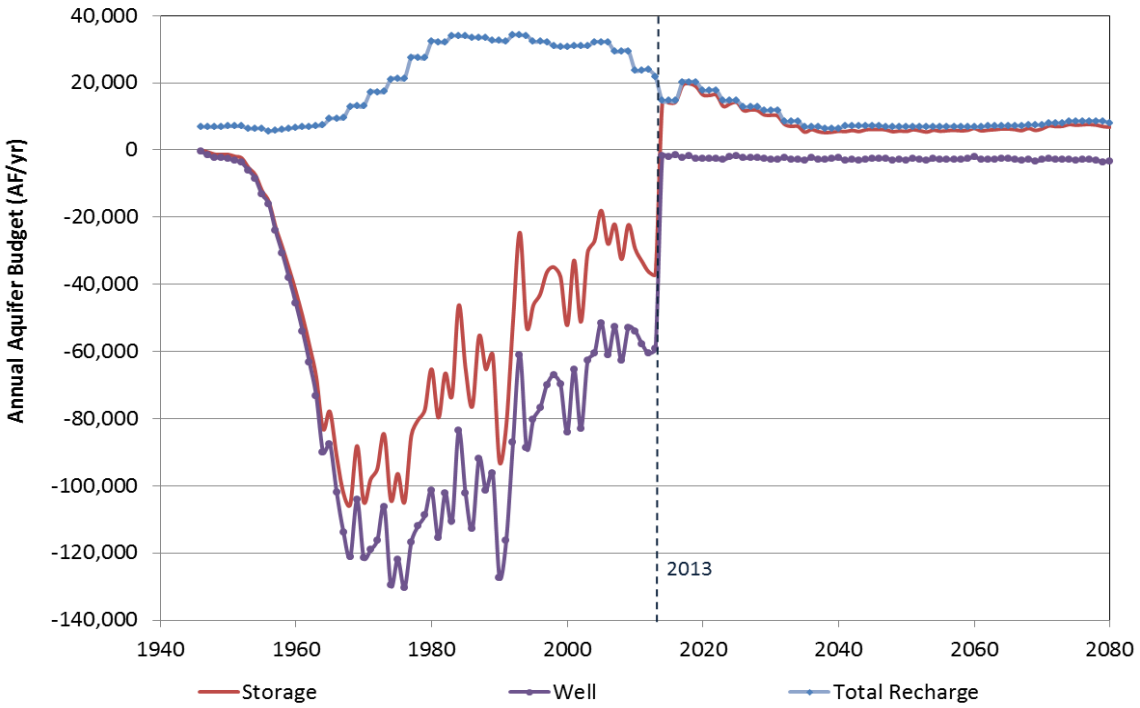

Figure SB5. Annual aquifer budget for Wichita County for the no irrigation pumping in GMD1 scenario.

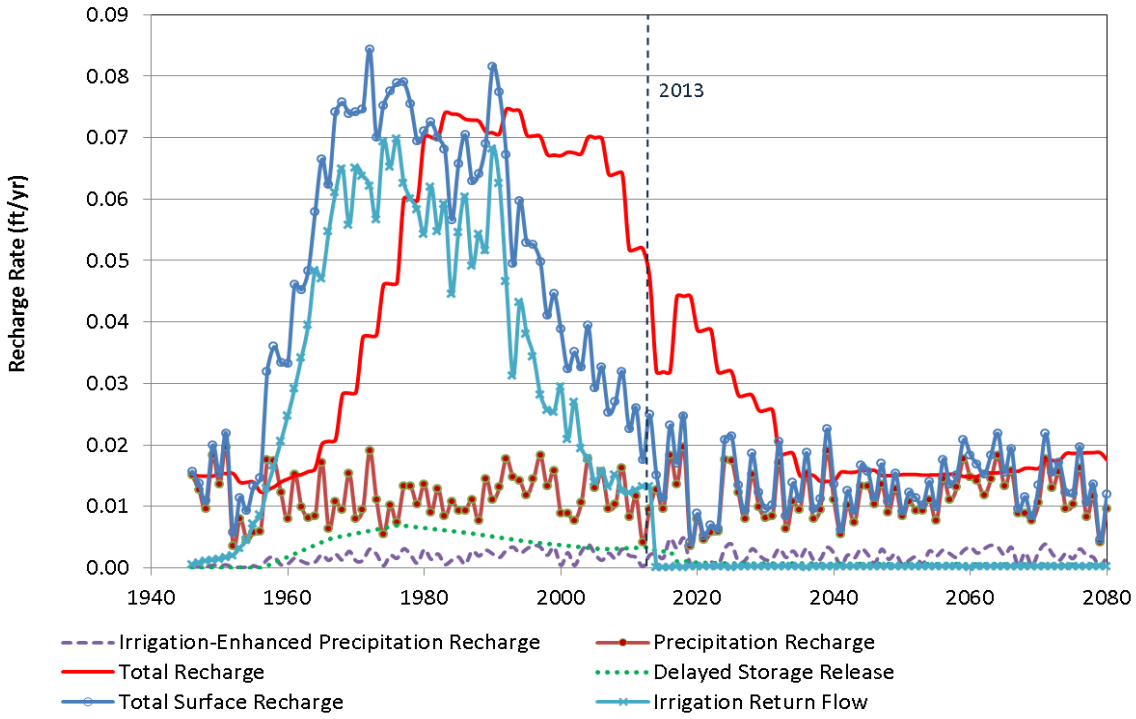

Figure SB6. Different recharge components for Wichita County for the no irrigation pumping in GMD1 scenario.

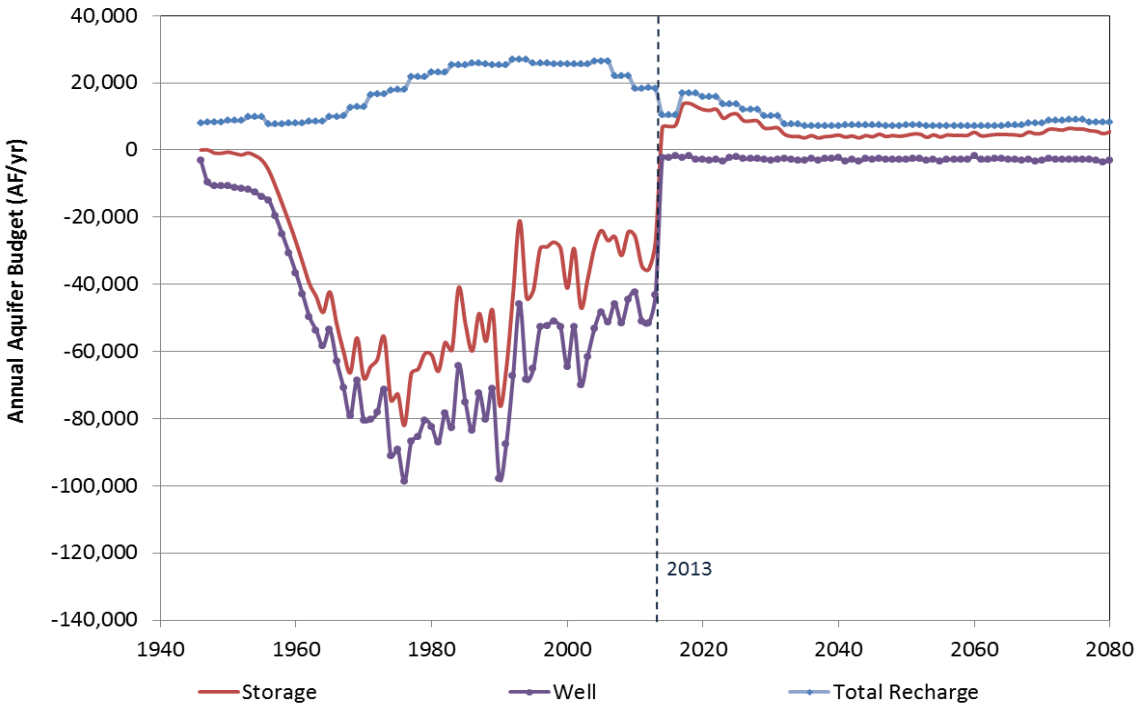

Figure SB7. Annual aquifer budget for Scott County for the no irrigation pumping in GMD1 scenario.

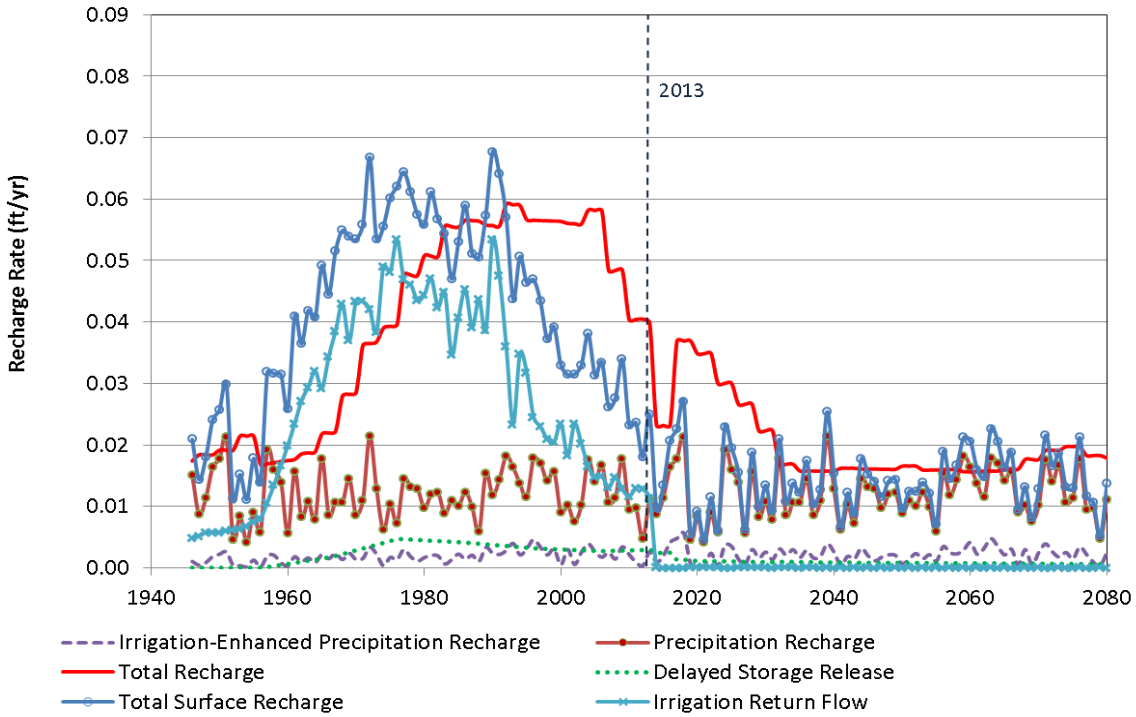

Figure SB8. Different recharge components for Scott County for the no irrigation pumping in GMD1 scenario.

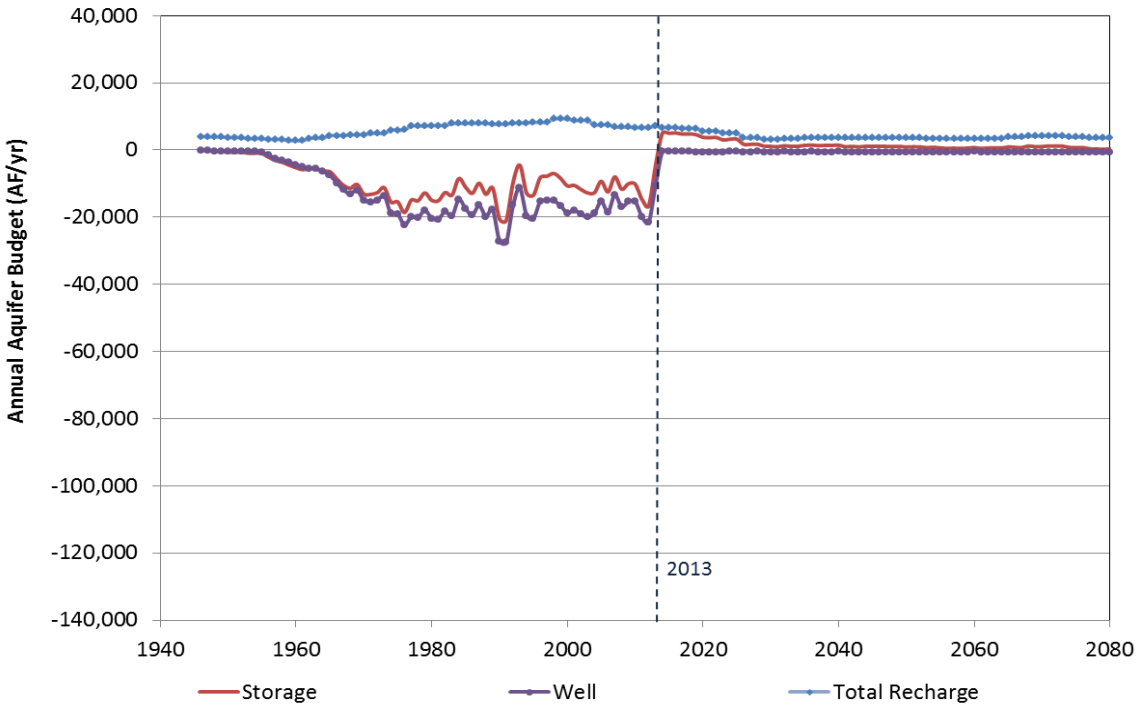

Figure SB9. Annual aquifer budget for Lane County for the no irrigation pumping in GMD1 scenario.

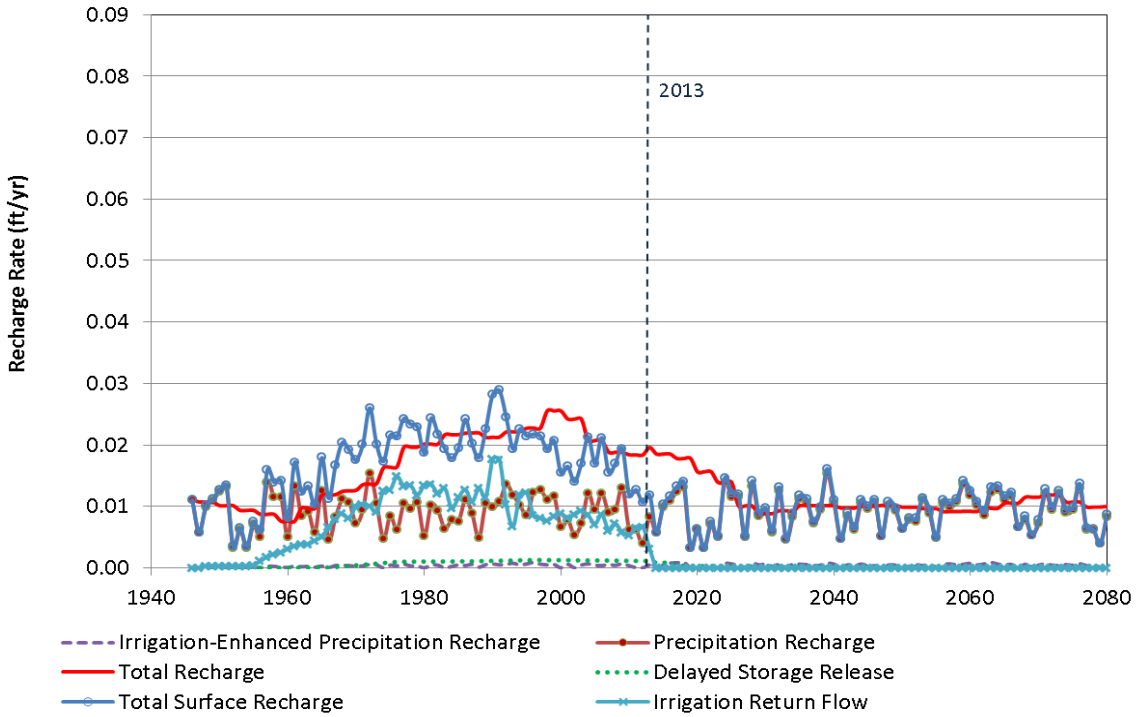

Figure SB10. Different recharge components for Lane County for the no irrigation pumping in GMD1 scenario.

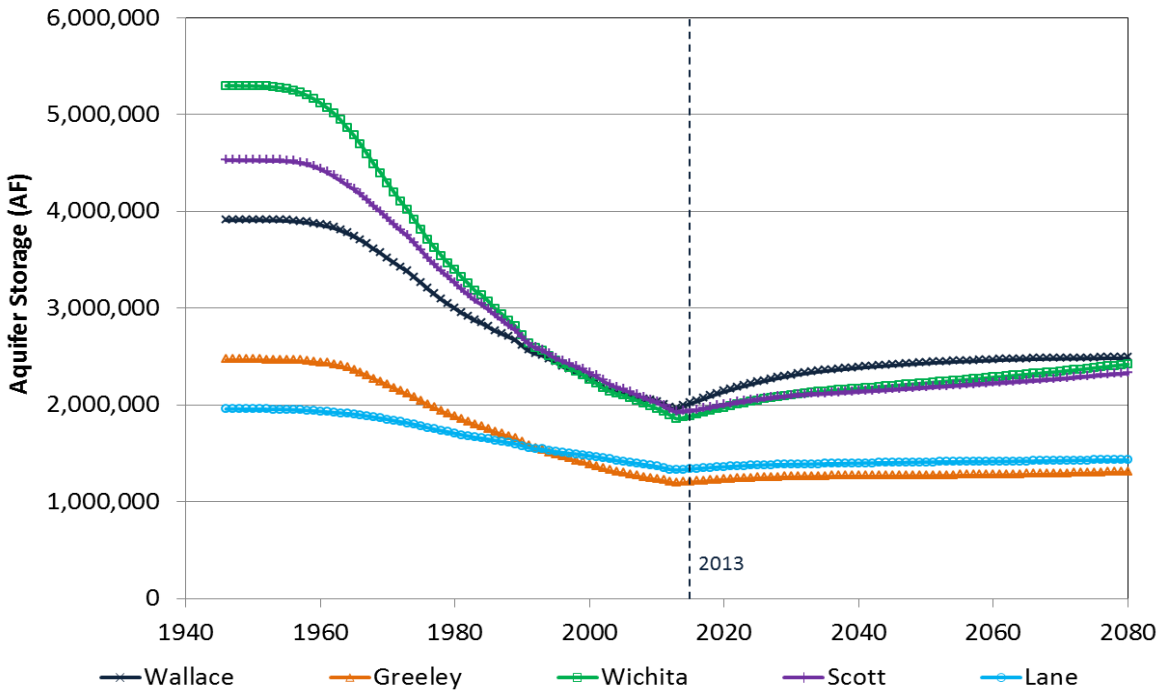

Figure SB11. Aquifer storage for different counties for the no irrigation pumping in GMD1 scenario.

C. County results for the 20% GMD1 irrigation pumping reduction scenario

Figures SC1, SC3, SC5, SC7, and SC9 show the annual aquifer budget for Wallace, Greeley, Wichita, Scott, and Lane counties for the 20% GMD1 irrigation pumping reduction scenario. Figures SB2, SC4, SC6, SC8, and SC10 show different recharge components for these counties. Figure SC11 compares the absolute aquifer storage between different counties.

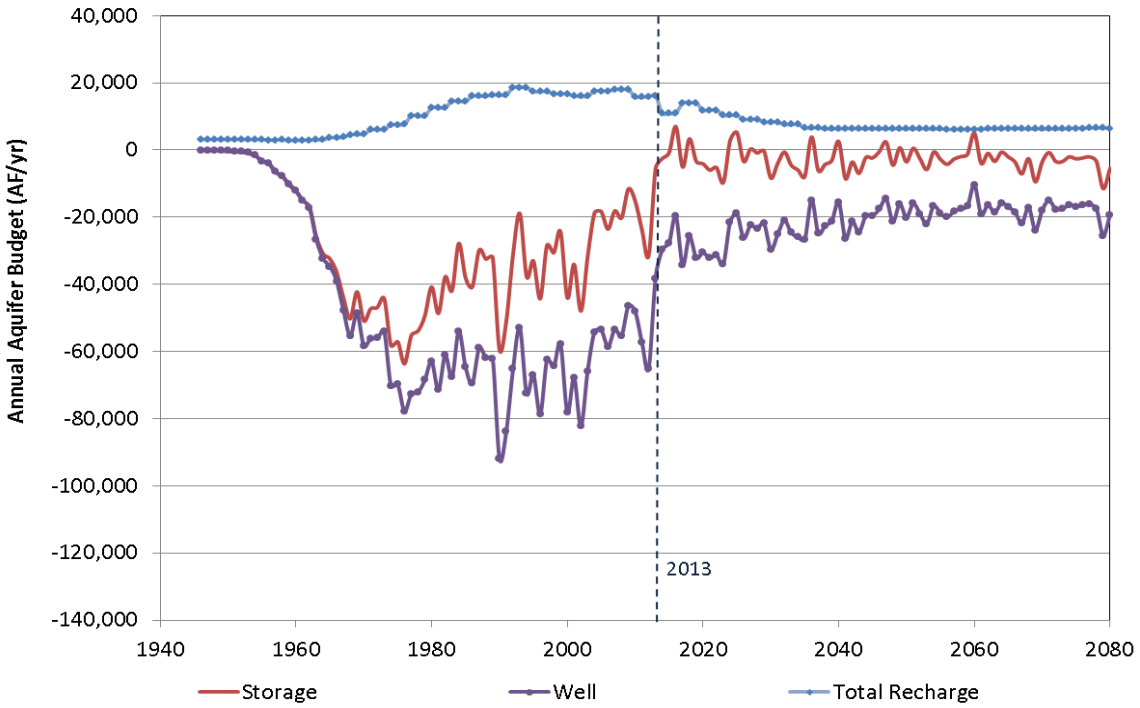

Figure SC1. Annual aquifer budget for Wallace County for the 20% GMD1 irrigation pumping reduction scenario.

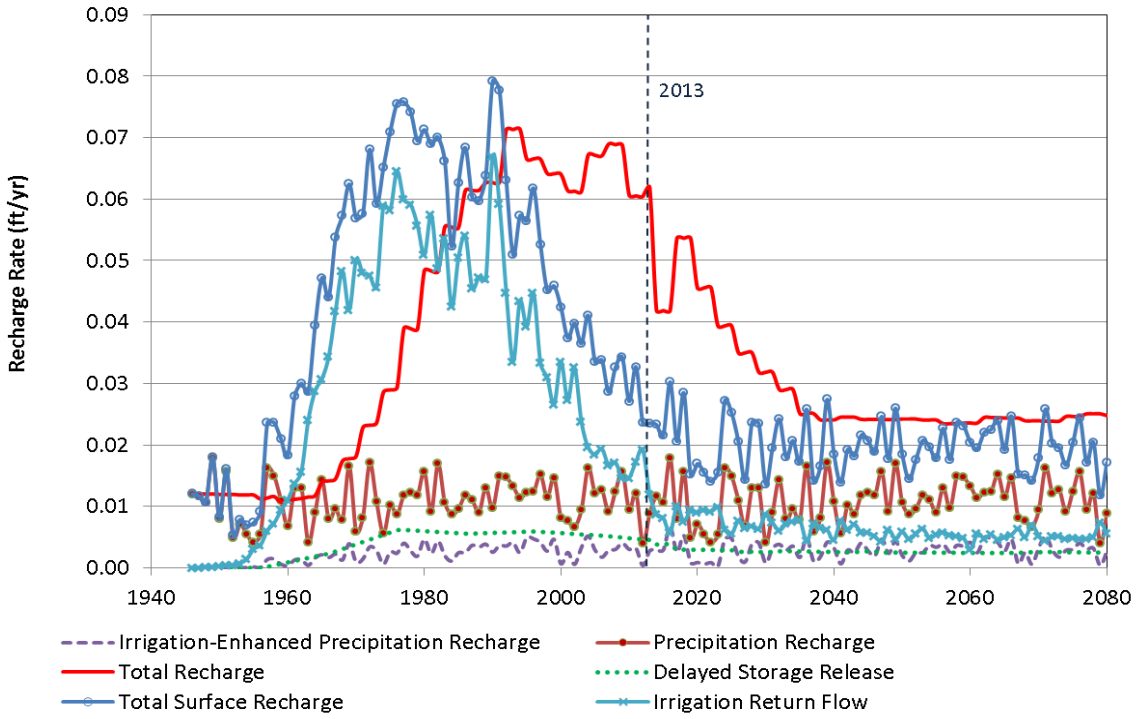

Figure SC2. Different recharge components for Wallace County for the 20% GMD1 irrigation pumping reduction scenario.

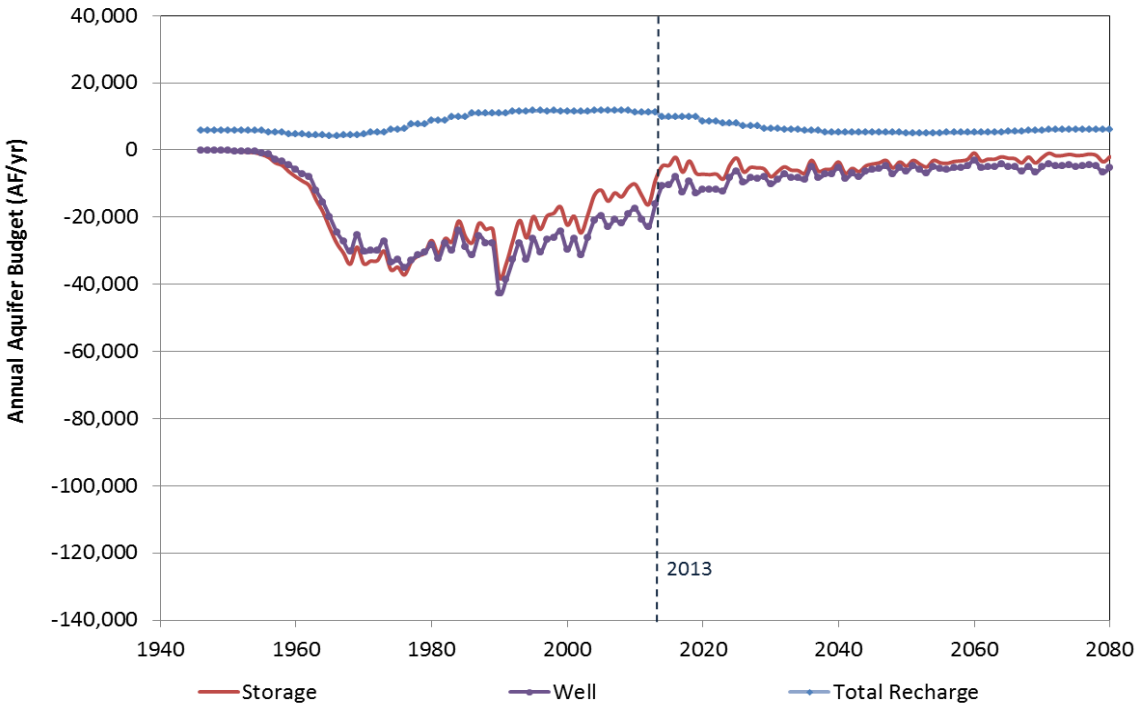

Figure SC3. Annual aquifer budget for Greeley County for the 20% GMD1 irrigation pumping reduction scenario.

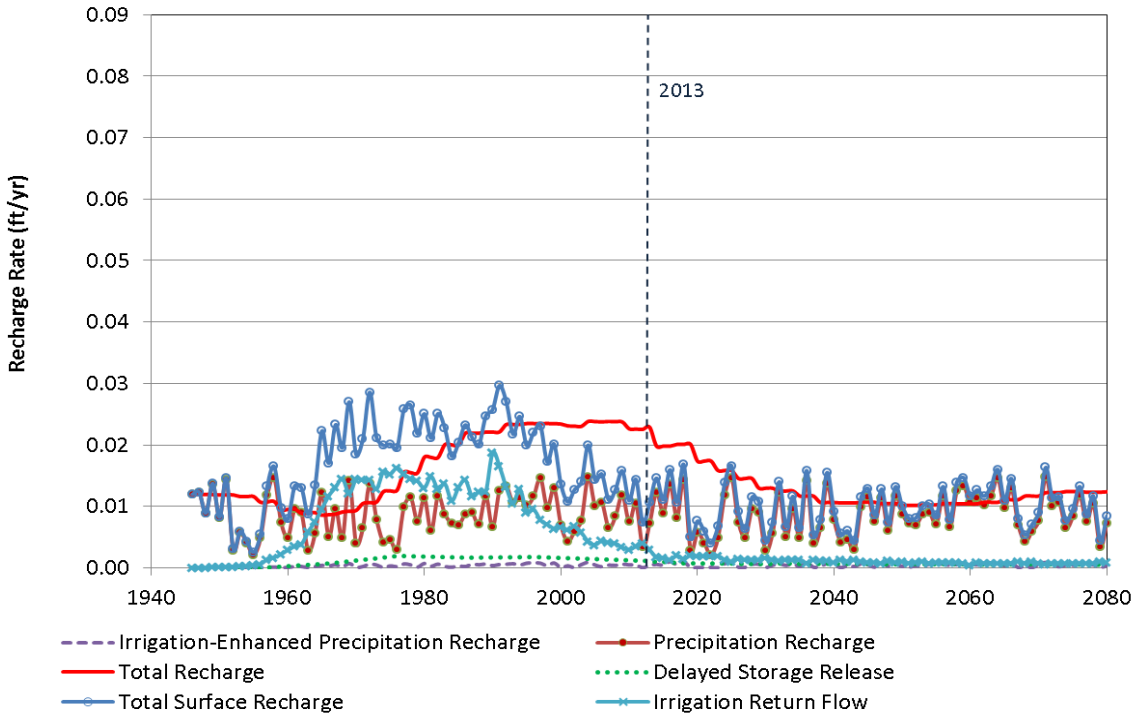

Figure SC4. Different recharge components for Greeley County for the 20% GMD1 irrigation pumping reduction scenario.

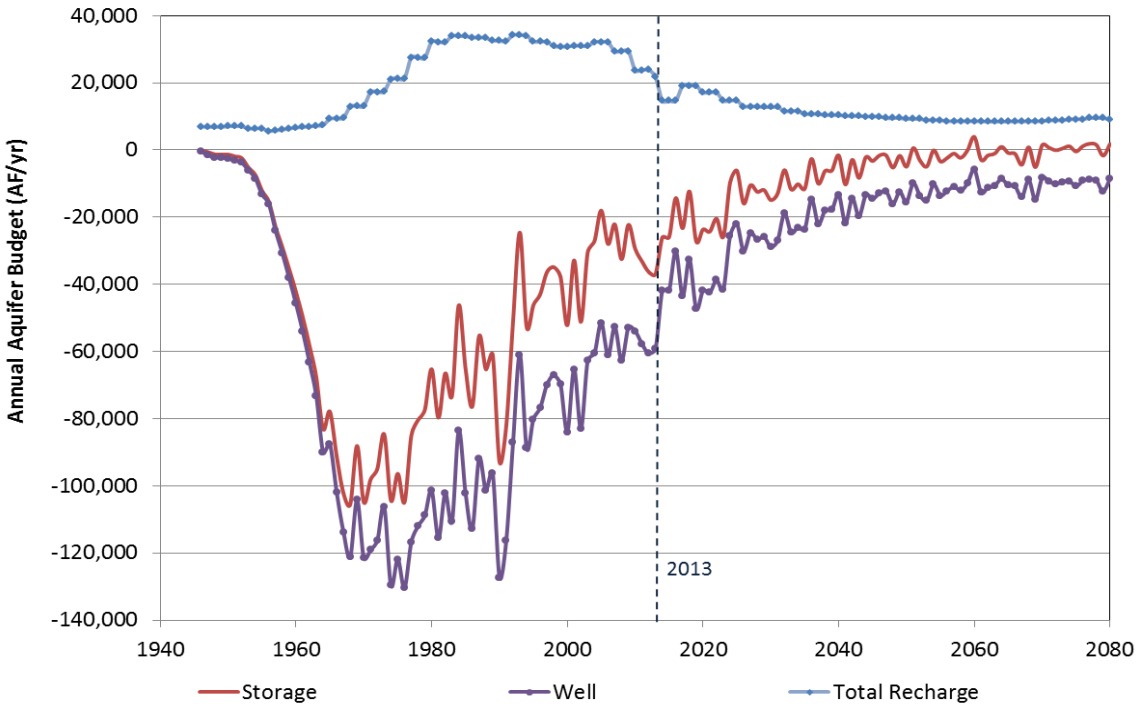

Figure SC5. Annual aquifer budget for Wichita County for the 20% GMD1 irrigation pumping reduction scenario.

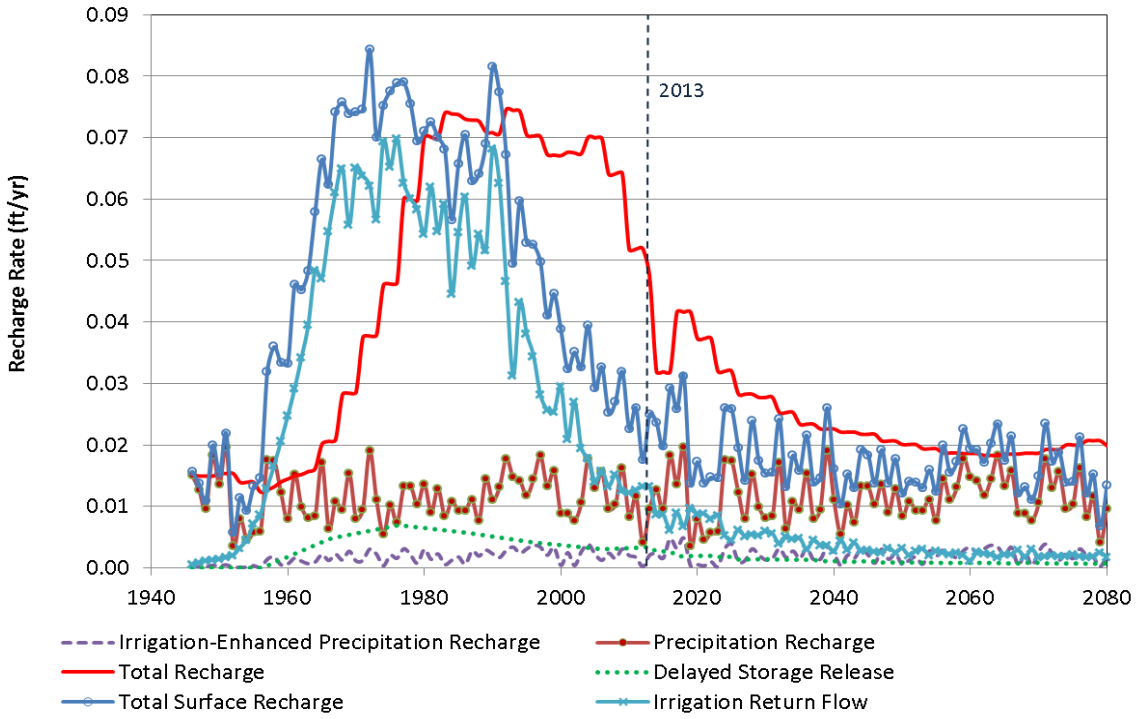

Figure SC6. Different recharge components for Wichita County for the 20% GMD1 irrigation pumping reduction scenario.

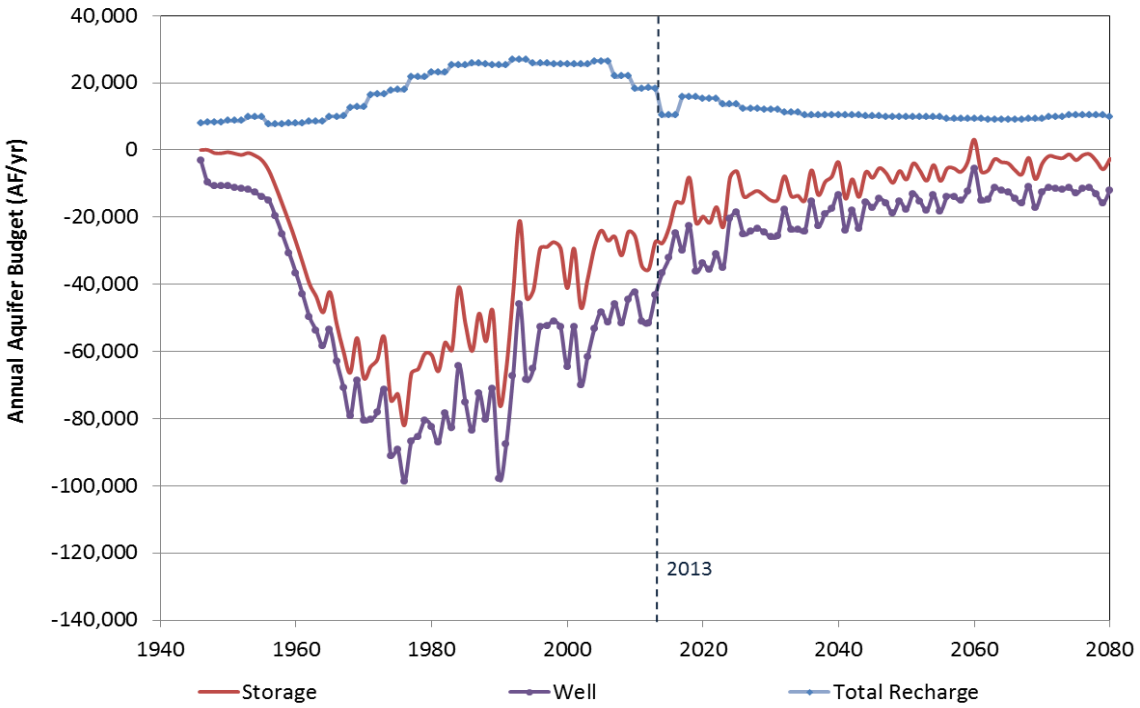

Figure SC7. Annual aquifer budget for Scott County for the 20% GMD1 irrigation pumping reduction scenario.

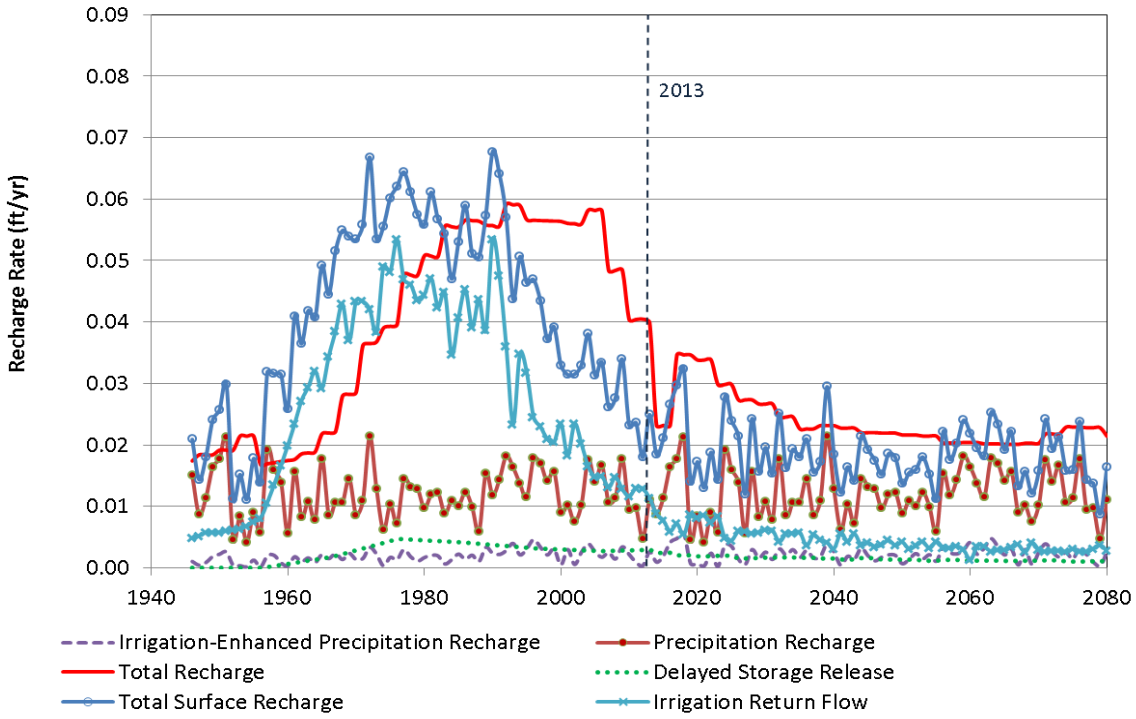

Figure SC8. Different recharge components for Scott County for the 20% GMD1 irrigation pumping reduction scenario.

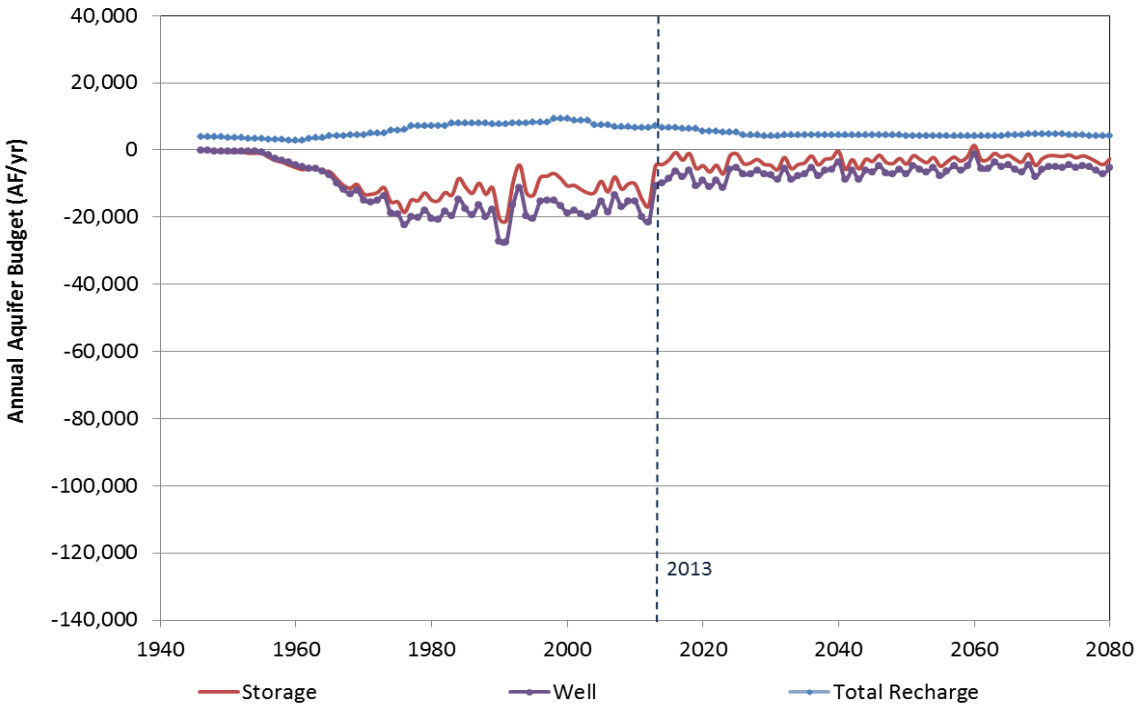

Figure SC9. Annual aquifer budget for Lane County for the 20% GMD1 irrigation pumping reduction scenario.

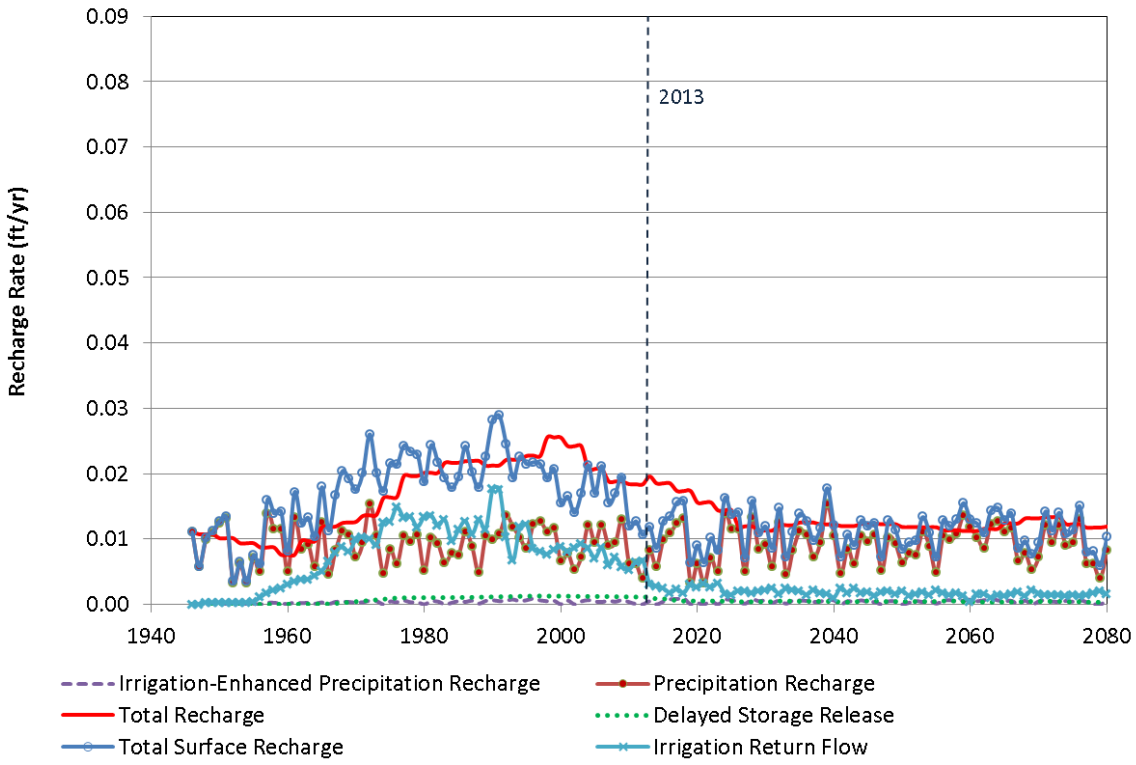

Figure SC10. Different recharge components for Lane County for the 20% GMD1 irrigation pumping reduction scenario.

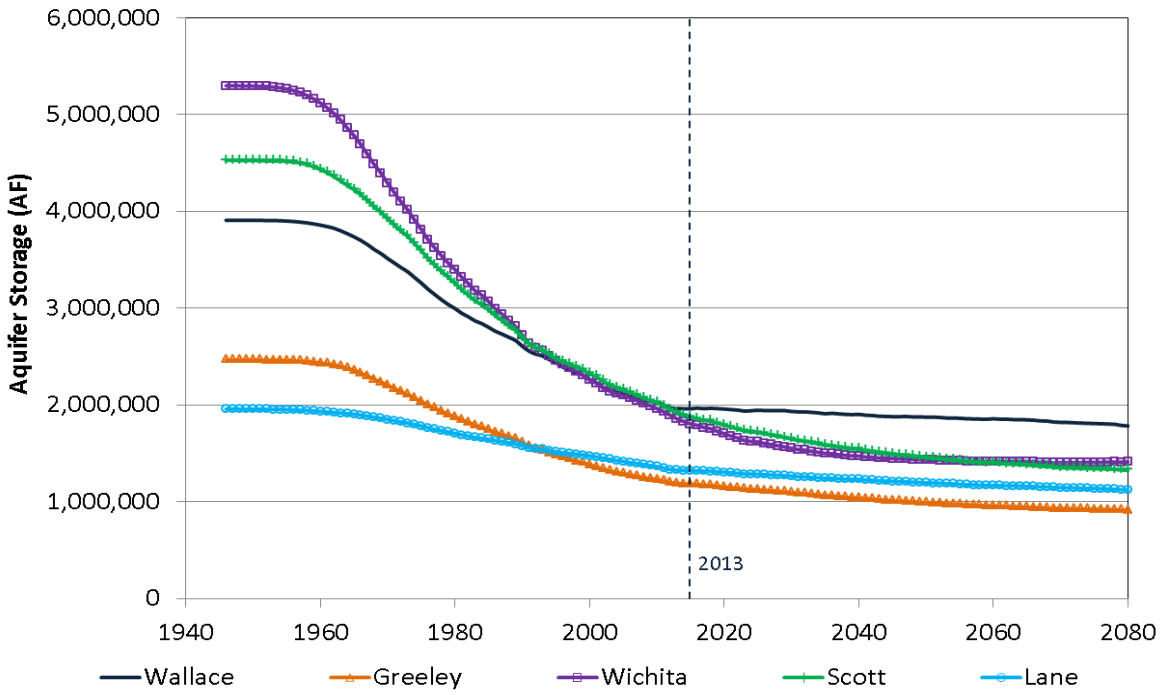

Figure SC11. Total aquifer storage for different counties for the 20% GMD1 irrigation pumping reduction scenario.

D. County comparisons scenario

Figures SD1 through SD5 compare the aquifer storage of all three future scenarios for each GMD1 county.

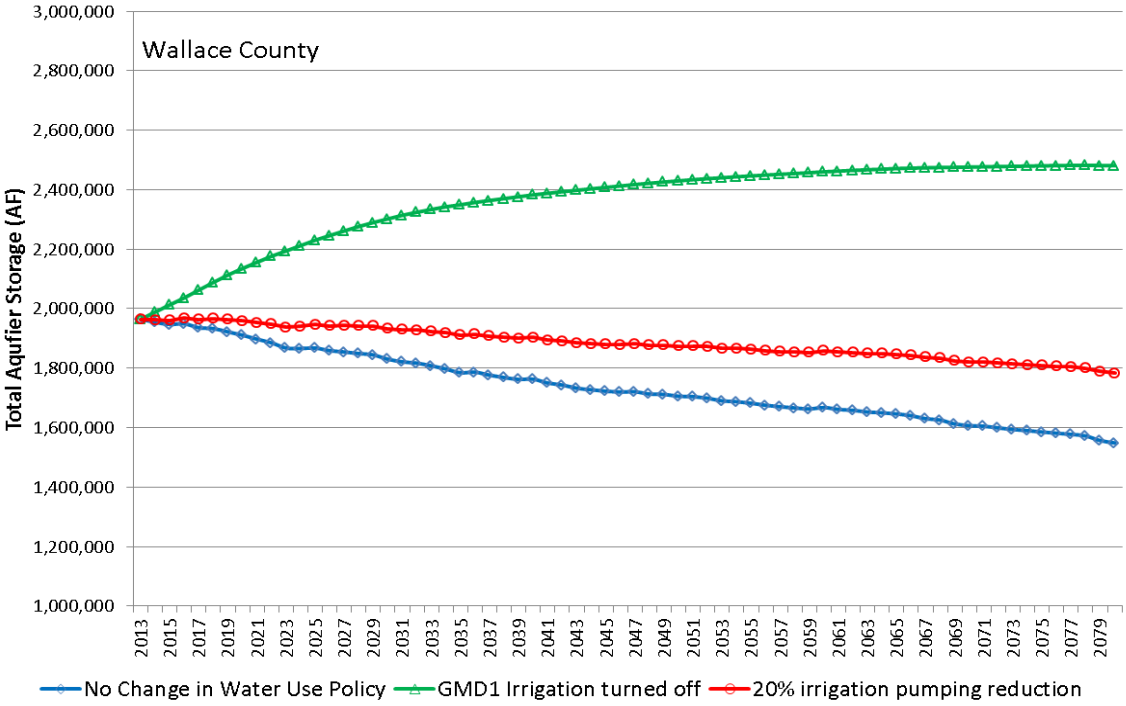

Figure SD1. Comparison of total aquifer storage for all future scenarios, Wallace County.

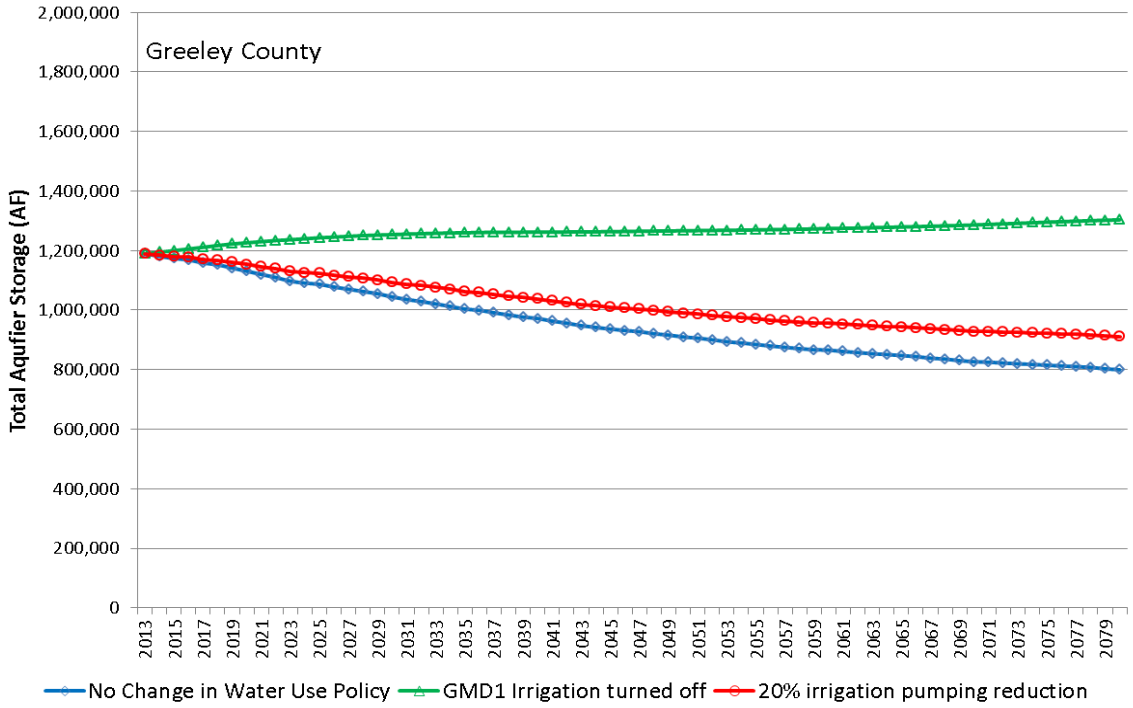

Figure SD2. Comparison of total aquifer storage for all future scenarios, Greeley County.

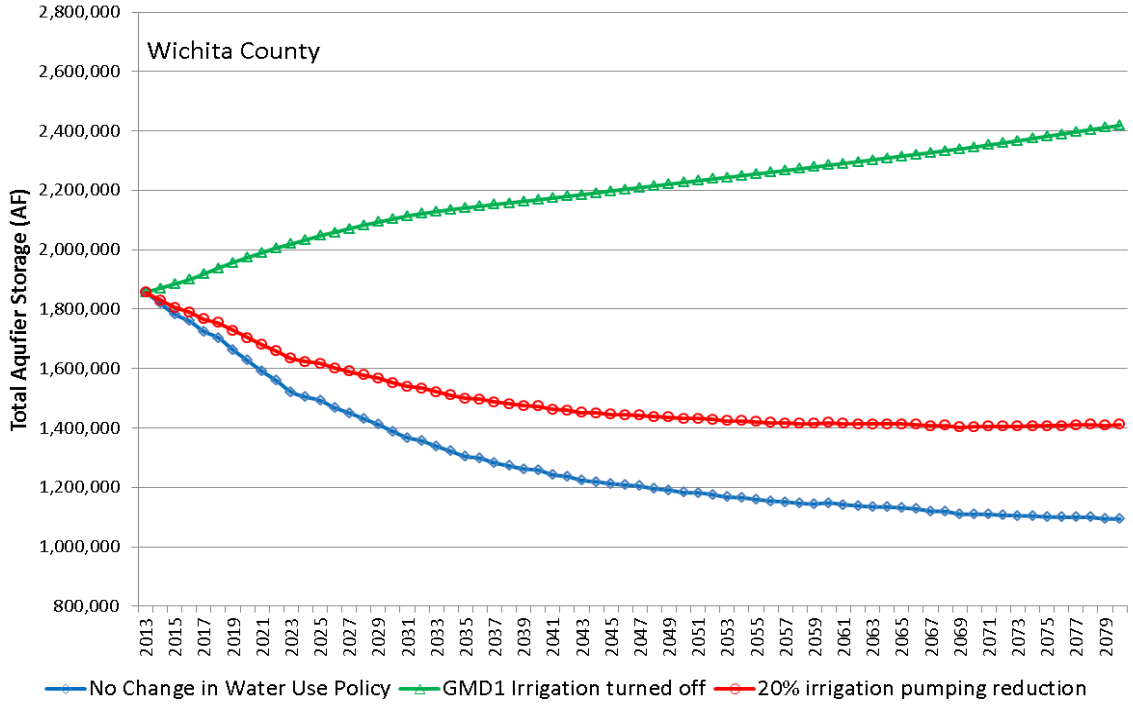

Figure SD3. Comparison of total aquifer storage for all future scenarios, Wichita County.

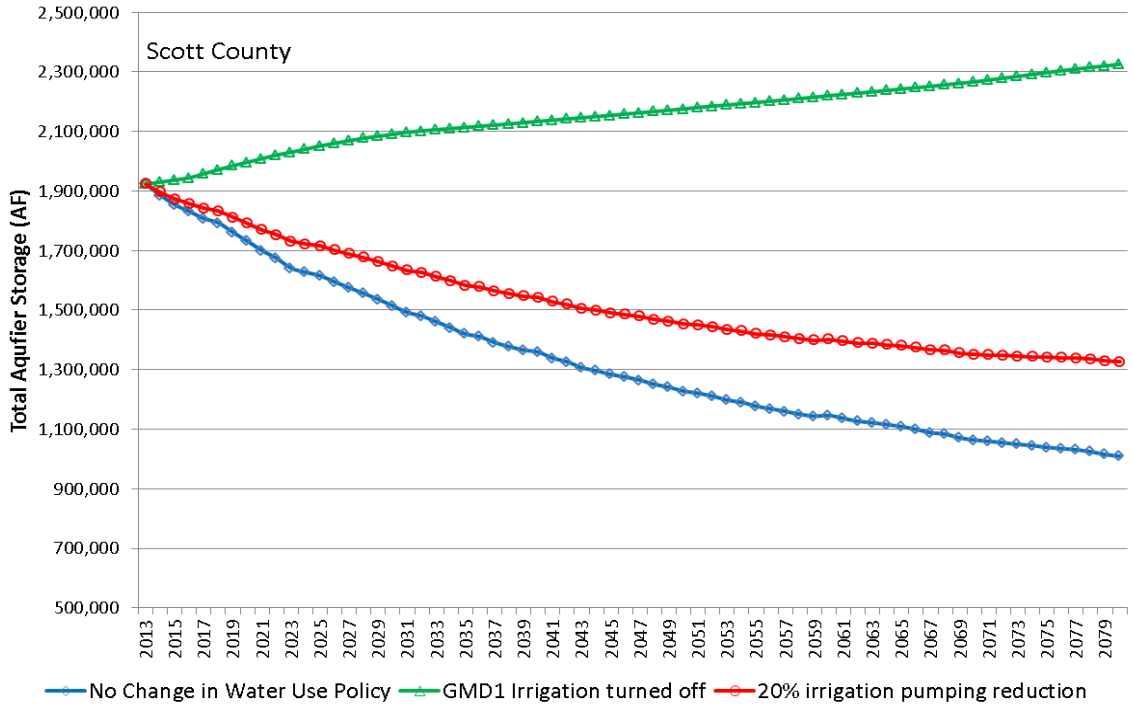

Figure SD4. Comparison of total aquifer storage for all future scenarios, Scott County.

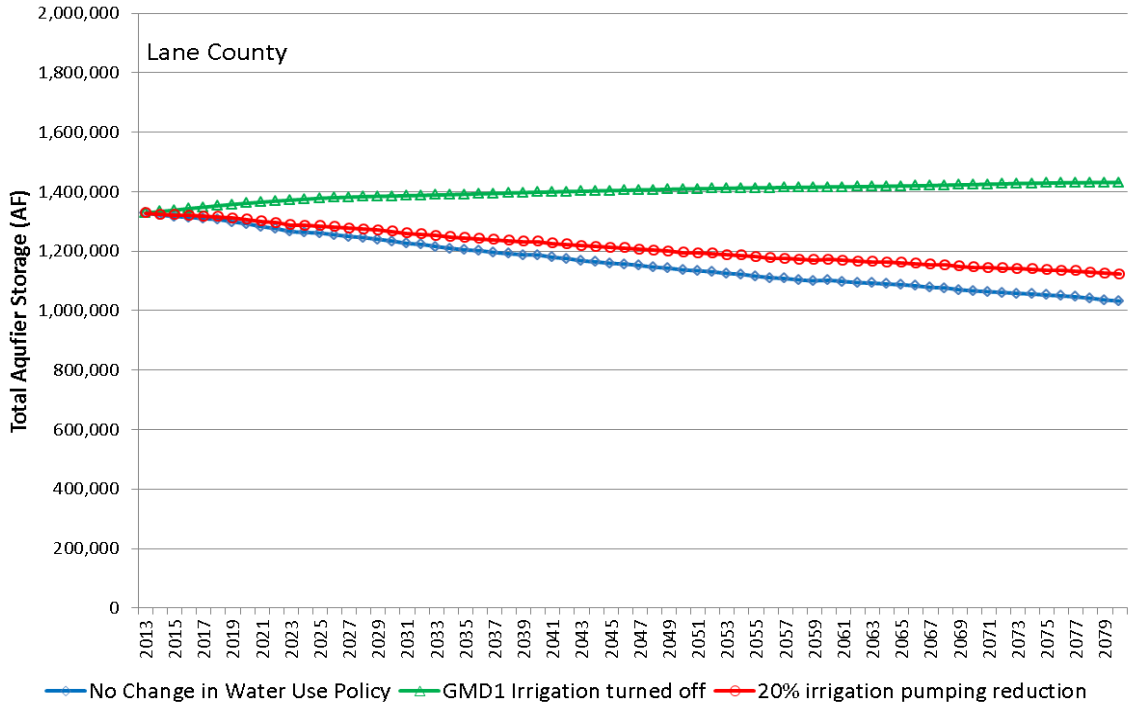

Figure SD5. Comparison of total aquifer storage for all future scenarios, Lane County.